Springer Theses
Recognizing Outstanding Ph.D. Research

Alastair J. J. Lennox

Organotrifluoroborate Preparation, Coupling and Hydrolysis

Springer

Springer Theses

Recognizing Outstanding Ph.D. Research

For further volumes:
http://www.springer.com/series/8790

Aims and Scope

The series "Springer Theses" brings together a selection of the very best Ph.D. theses from around the world and across the physical sciences. Nominated and endorsed by two recognized specialists, each published volume has been selected for its scientific excellence and the high impact of its contents for the pertinent field of research. For greater accessibility to non-specialists, the published versions include an extended introduction, as well as a foreword by the student's supervisor explaining the special relevance of the work for the field. As a whole, the series will provide a valuable resource both for newcomers to the research fields described, and for other scientists seeking detailed background information on special questions. Finally, it provides an accredited documentation of the valuable contributions made by today's younger generation of scientists.

Theses are accepted into the series by invited nomination only and must fulfill all of the following criteria

- They must be written in good English.
- The topic should fall within the confines of Chemistry, Physics, Earth Sciences, Engineering and related interdisciplinary fields such as Materials, Nanoscience, Chemical Engineering, Complex Systems and Biophysics.
- The work reported in the thesis must represent a significant scientific advance.
- If the thesis includes previously published material, permission to reproduce this must be gained from the respective copyright holder.
- They must have been examined and passed during the 12 months prior to nomination.
- Each thesis should include a foreword by the supervisor outlining the significance of its content.
- The theses should have a clearly defined structure including an introduction accessible to scientists not expert in that particular field.

Alastair J. J. Lennox

Organotrifluoroborate Preparation, Coupling and Hydrolysis

Doctoral Thesis accepted by
the University of Bristol, UK

Springer

Author
Dr. Alastair J. J. Lennox
School of Chemistry
University of Bristol
Bristol
UK

Supervisor
Prof. Dr. Guy Lloyd-Jones
School of Chemistry
University of Bristol
Bristol
UK

ISSN 2190-5053 ISSN 2190-5061 (electronic)
ISBN 978-3-319-01133-2 ISBN 978-3-319-01134-9 (eBook)
DOI 10.1007/978-3-319-01134-9
Springer Cham Heidelberg New York Dordrecht London

Library of Congress Control Number: 2013942478

Printed on acid-free paper

Springer is part of Springer Science+Business Media (www.springer.com)

Parts of this thesis have been published in the following journal articles:

1. M. Butters, J. N. Harvey, J. Jover, A. J. J. Lennox, G. C. Lloyd-Jones, P. M. Murray, *Angew. Chem. Int. Ed.* **2010**, *49*, 5156–5160.
2. A. J. J. Lennox, G. C. Lloyd-Jones, *Isr. J. Chem.* **2010**, *50*, 664–674.
3. A. J. J. Lennox, G. C. Lloyd-Jones, *J. Am. Chem. Soc.* **2012**, *134*, 7431–7441.
4. A. J. J. Lennox, G. C. Lloyd-Jones, *Angew. Chem. Int. Ed.* **2012**, *51*, 9385–9388.

Supervisor's Foreword

Due to their unique reactivity characteristics and convenient physical properties, potassium organotrifluoroborate reagents have enjoyed a huge increase in use in recent years. However, despite numerous synthetic advances, mechanistic understanding of these reagents, particularly under the aqueous conditions often employed for engendering the selective and efficient reaction, have lagged behind.

Alastair set out to identify the mode of action of organotrifluoroborates in their most commonly utilised reaction; the "Suzuki–Miyaura coupling". This cross-coupling methodology is employed in the synthesis of pharmaceuticals, agrochemicals, LCDs and organic LEDs, and was subject of a share of the Nobel Prize in Chemistry (Suzuki, 2010). They are often found to be highly advantageous replacements for the boronic acid, which until recently has been the more traditionally employed reagent. Carefully designed heteronuclear NMR, kinetic, and isotopic labelling experiments, and meticulous experimental technique allowed Alastair to identify a range of processes that slowly release the boronic acid and thereby elucidate how a number of major side reactions are suppressed. This led on to the development of predictive models that were able to ensure consistency in their behaviour and predict how other organotrifluoroborates reacted under Suzuki–Miyaura coupling conditions, with hydrolytic half-lives spanning minutes to months.

By way of a range of ^{19}F NMR experiments, Alastair also identified that the practical issues associated with the preparation of organotrifluoroborates, for example isolation and purification via repeated extraction, as well as the use of KHF_2, a corrosive reagent that causes glassware etching, might be solved via design of alternative reagents and conditions. He thus developed a new, safe and scalable, route for their preparation, avoiding the extensive etching of reactor vessels and employing a simple and facile work-up method; this procedure is already being applied industrially.

Alastair's work was published in four papers in the premier journals in the field, attracting extensive international attention and being highlighted in Chemical and Engineering News and Chemistry World. All four papers elicited exceptional peer review commentary, for example "This contribution is bound to be a classic, filled with remarkable details and analysis that explains much that defied prior

explanation". Moreover, Alastair's discovery and explanation of the effect of vessel shape on the efficacy of the cross-coupling reactions has allowed reactions previously conducted in medicinal chemistry discovery to be repeated, this time resulting in successful product isolation and thus biological testing.

I hope that Alastair's thesis will prove a useful and lasting resource for the many researchers working in the field of organoboron reagents or cross-coupling.

Bristol, May 2013 Guy C. Lloyd-Jones

Acknowledgments

I would like to first thank my supervisor, Guy Lloyd-Jones, whose patience and careful guidance through my Ph.D. has been indescribable. It has been very exciting working with Guy, whose passion for chemistry is very infectious, and as such, has allowed my confidence and passion for the subject to grow. He has given the project a tremendous amount of time, which I have acknowledged and appreciated throughout the 4 years of working with him. I have also both enjoyed, and learnt an awful lot from the unique working mentality he has installed within the group, which allows freedom to "follow ones nose" in the exploration of interesting results.

I would like to thank Dr. Paul Murray and Dr. Mike Butters, previously of *AstraZeneca,* for helping to finance my Ph.D. I have collaborated with a number of people in the School of Chemistry which I would like to acknowledge, including Prof. Jeremy Harvey and Dr. Jesus Jover, Paul Cogswell, Nina Ursinyova, Ryan Beattie, Ben Mills, Tom Hornsby and Tom Carter. Being one of the heaviest users, my gratitude deeply extends to the amazing NMR facility which is run at the department. Special thanks have to go to Paul Lawrence who has always willingly aided my urgent NMR and mass spec needs. In addition I am grateful to Des Davis who turns round samples for elemental analysis at lightning speed.

I would like to move on to thanking the whole of the GCL-J group who have made my time in the lab a very enjoyable experience. In no particular order I would like to thank Joe Tate, Rob Cox, Gareth Owen-Smith, Ruth Dooley, Carl Poree, Tomas Racys, Nick Taylor, Sophie Purser, Paz Munoz, Bertram Ong and Liam Ball. However in my first year, I would like to especially thank Joe Renny, Dave Sale and Louise Evans who were exceptionally helpful in answering all my questions. All three were overly generous with their time in getting me up to standard with the chemistry, advising on my project and teaching me the workings of the lab. In my second year I would like to acknowledge Waldemar Czaplik, who, as well as becoming a great friend of mine, I learnt a huge amount from during many hours spent discussing all aspects of the subject. Finally, Vincent Brunet and Alvaro Gordillo were both excellent at answering and discussing problems I had in my third year.

On a deeper note, I would like to thank everyone who has helped me to get where I am now. Of the many people to whom I should mention, four people stand out. First I feel I owe a lot to Dr. Ian Watt (*University of Manchester*) who really sparked my interest for physical organic chemistry, and because of working with him decided to undertake a Ph.D. Second, my parents have given me unrelenting support and guidance throughout my life, which is impossible to accurately describe in one sentence, as is my sincere appreciation for it. Lastly, I would like to thank Juliet Burke, who generally makes my life very happy. She has been selflessly and consistently accommodating of the daily aftermaths of this high-tempo Ph.D., and therefore, it is her to whom I dedicate this thesis.

Contents

Abbreviations

BHT	Butylhydroxytoluene
dan	Diaminonaphthylene
DBU	1,8-Diazabicycloundec-7-ene
DEA	Diethanolamine
EDG	Electron donating group
EWG	Electron withdrawing group
GSK	GlaxoSmithKline
LG	Leaving group
MIDA	N-Methylimidodiacetic acid
MOPS	3-(N-morpholino)propanesulfonic acid
P_4-*t*Bu	1-tert-Butyl-4,4,4-tris(dimethylamino)-2,2-bis[tris(dimethylamino)-phosphoranylidenamino]-catenadi(phosphazene)
SM	Suzuki-Miyaura
TBAF	Tetrabutylammoniumfluoride
TBATB	Tetraammonium tribromide
TCICA	Trichloroisocyanuric acid
THF	Tetrahydrofuran
TMS	Trimethylsilyl
TRIS	Tris(hydroxymethyl)aminomethane

Chapter 1
General Introduction

1.1 Potassium Organotrifluoroborate Salts

Potassium organotrifluoroborate (R-BF_3K) salts (**1**) were discovered in 1960 by Chambers [1], but the following three decades saw them appearing in only a handful of publications. However, since the mid 1990s their application has grown as they have rapidly become a hugely important and widely used class of reagent, Fig. 1.1 [2–4]. In a seminal 1995 publication, Vedejs outlined an efficient preparation of the salts [5], where it was stated they were "not appreciably hygroscopic and could be stored in air for many months without significant decomposition." Indeed, R-BF_3K salts exhibit favourable physical characteristics of being free-flowing crystalline solids, which tend to melt only at very high temperatures, and are stable to air and moisture. This renders them easy reagents to handle, unlike, for example, certain boronic acids (**2**), e.g. some alkylboronic acids decompose in air [6], or organoboronic acid pinacol esters (**4**), many of which are liquids or low melting solids. This superior stability has aided their growing popularity as nucleophilic 'R-group' synthons, for many varied retrosynthetic pathways.

The major areas of chemical reactivity and applicability of R-BF_3K salts can be classed into four categories: firstly for precursors to difluoroboranes (**11**), secondly as intermediates for a range of synthetic pathways, thirdly as precursors for ionic liquids and electrolytes, and lastly as nucleophilic partners in metal-catalysed cross-coupling reactions.

1.1.1 Difluoroborane Precursors

Organodifluoroboranes (R-BF_2, **11**) can be revealed upon the addition of a strong Lewis base to R-BF_3K salts, which provides a safe and stable route to these highly reactive and unstable species. Indeed, the main incentive for Vedejs in developing the efficient route to R-BF_3K salts was for their use as precursors to $ArBF_2$, therefore removing the need to handle the corrosive trivalent boron reagents. The

A. J. J. Lennox, *Organotrifluoroborate Preparation, Coupling and Hydrolysis*, Springer Theses, DOI: 10.1007/978-3-319-01134-9_1,

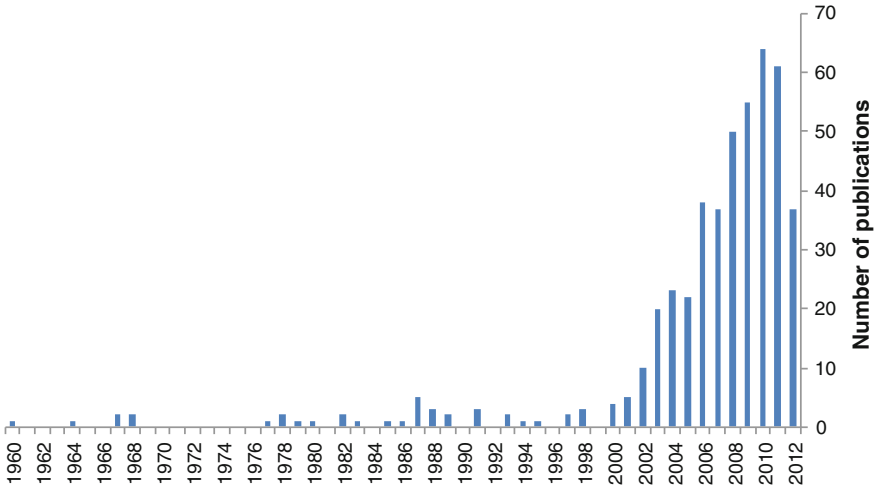

Fig. 1.1 A SciFinder search containing the concept of "trifluoroborate"; showing the 463 examples in chronological order

Lewis acidic aryldifluoroborane compounds were exploited in the preparations of oxazaborolidinones from amino acid derivatives [7]. The generation of the anionic "ate" species, instead of employing Lewis base precursors, e.g. $BH_3.SMe_2$, was pursued due to the exceptional bench-top stability exhibited by R-BF_3K salts.

Batey [8, 9] developed crotylation reactions of aldehydes with R-BF_3K salts to generate homoallylic alcohols in excellent yields and diastereomeric ratios. Only a catalytic quantity of BF_3.OEt is required, to generate the reactive difluoroborane, which coordinates to the aldehyde facilitating a Zimmerman-Traxler transition state, Scheme 1.1. Batey [10] also developed convenient phase-transfer catalysed (PTC), biphasic conditions, for the transformation to occur, which negated the necessity for the presence of a Lewis acid, Scheme 1.1. Due to the observed diastereoselectivity it was proposed that the undetected difluoroborane must form, *via* KF dissociation, to participate in a Zimmerman-Traxler transition state. Slow reaction occurred in a purely organic medium and the addition of fluoride (KF and TFAB) attenuated the reaction; thus confirming the equilibrium driven dissociative mechanism of activation [10]. Finally, fluorophilic Montmorillonite K10 was found to effect the transformation in the biphasic system to an expanded substrate scope, which included forming homo-allylic alcohols from the less reactive ketones [11].

Batey [12, 13] successfully demonstrated the crotylation methodology on imines to generate homoallylic amines. Under similar conditions to those employed for the aldehydes, BF_3.OEt was found to catalyse the allylation of *N*-tosylimines. The *N*-tosyl protecting group was found to engender sufficient electrophilicity for the imine to accept the allyl fragment, and also induce enough

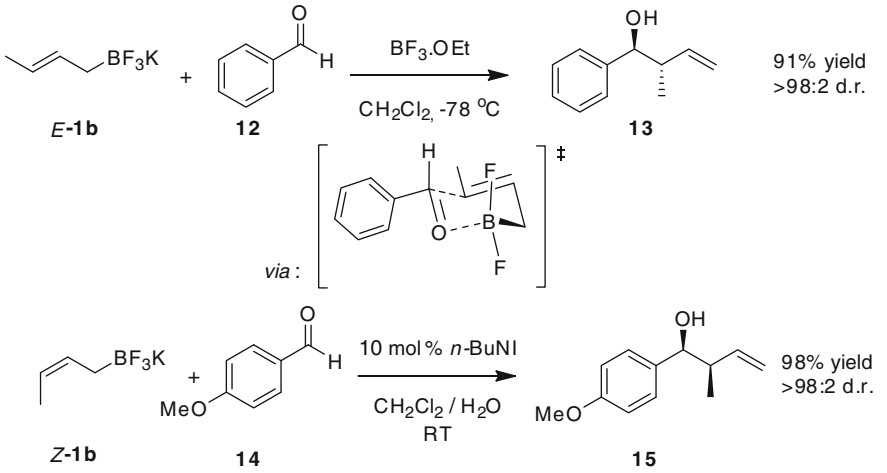

Scheme 1.1 Example crotylation reactions of aldehydes with R-BF_3K salts under Lewis acid and PTC conditions

stability towards hydrolysis, unlike for example, when simple imines (PhCH = NPh) were employed.

The Petasis or Boronic Mannich reaction, is a multi component coupling between an aldehyde, amine and, traditionally, a boronic acid [14]. More recently however, R-BF_3K salts have been shown to be useful partners for the reaction, after treatment with one equivalent of TMS-Cl [15] or BF_3.OEt [16], Scheme 1.2, to reveal the corresponding difluoroborane (**11**).

Lastly, R-BF_3K salts have been employed in this context for the formation of dialkyl ethers; [17, 18] thus providing an alternative route to the Williamson protocol, which can be highly functional group intolerant due to the presence of strongly basic nucleophiles. Rather than forming a C–O bond, the strategy involves the formation of a C–C bond through a coupling between the *in situ* generated difluoroborane and an acetal, Scheme 1.3.

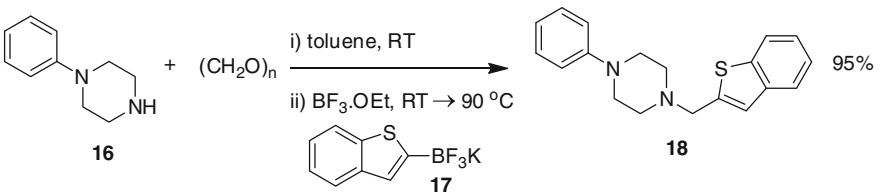

Scheme 1.2 R-BF_3K application in the Boronic Mannich reaction between **16**, **17** and *para*-formaldehyde

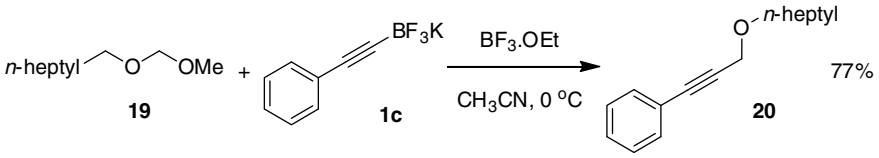

Scheme 1.3 Dialkyl ether preparation employing R-BF_3K salts

1.1.2 Intermediates for Synthetic Pathways

R-BF_3K salts are used as intermediates for a range of synthetic pathways; popularised by the stability exhibited towards distal manipulation of various functional groups, Scheme 1.4.

Resistance of R-BF_3K salts to common synthetic transformations include Swern/Dess Martin oxidations [19], ozonolysis [20], Wittig and Horner-Wadsworth-Edmonds olefinations [21], condensation reactions [22], and 1,3-dipolar cycloadditions ("click" chemistry) [23]. However, for certain transformations, e.g. reductive amination [24] and lithium-halogen exchange [25], KHF_2 was employed during work up, implying that the trifluoroborate functionality was not maintained throughout the procedure. Moreover, the greatest disadvantage to R-BF_3K salts is in their instability to silica-gel, in addition to their insolubility in many apolar solvents. Nonetheless, they are easily purified through crystallisation techniques, which can be beneficial, especially on scale-up.

Trans-ligation of the fluoride to give organoboronic acids is readily effected under aqueous fluorophilic conditions. This transformation is especially pertinent to pinacol ester hydrolyses [26], whereby proceeding *via* the R-BF_3K salt, avoids the recombination of the diol and boronic acid that renders the direct hydrolysis very difficult indeed. Typical preparative hydrolysis routes employ a fluorophile, e.g. silica-gel [27], iron (III) chloride [28] or alumina [29], in combination with

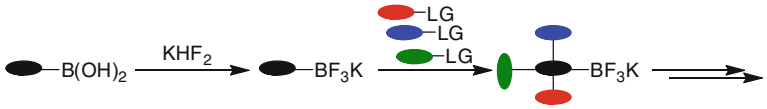

Scheme 1.4 Stability of the trifluoroborate functionality to various common transformations. *Oval shapes* are unspecified organic fragments

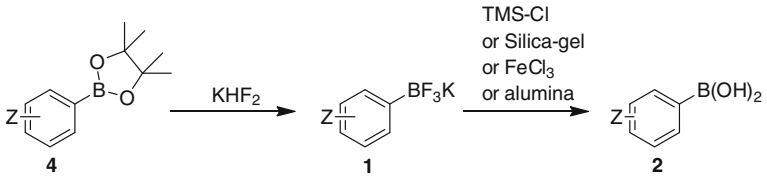

Scheme 1.5 Hydrolysis of pinacol esters to boronic acids *via* R-BF_3K salts

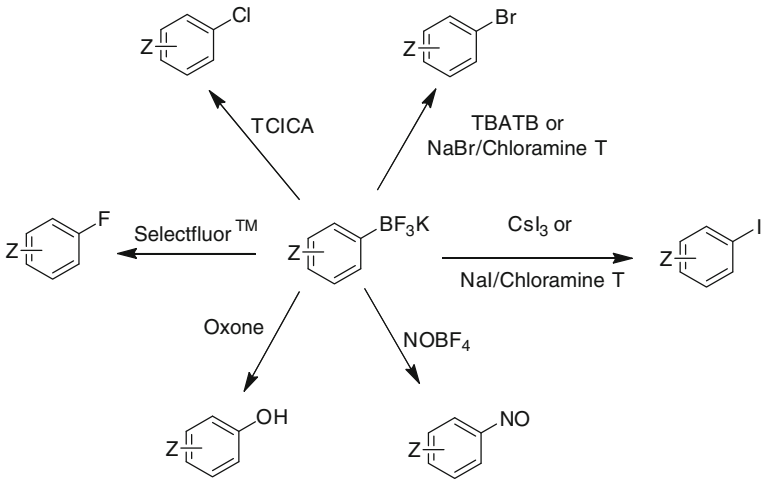

Scheme 1.6 Functional group interconversion of the trifluoroborate functionality

water, to convert the R-BF_3K salt back to the organoboronic acid, which can then undergo further condensations or other manipulations if required, Scheme 1.5. Pinanediol boronic esters, which exhibit useful chiral induction properties, can also be deprotected in this way [30].

Functional group interconversion of the trifluoroborate functionality expands the realm of application accessed in these reagents. Switching the "R-group synthon" from being nucleophilic to electrophilic is readily achieved by transformation to an organohalide. This halodeboronation has been demonstrated with the use of electrophilic sources of iodide [31], chloride [32], bromide [33, 34] and fluoride [35]. In addition, it has been shown that R-BF_3K salts are oxidised to phenols [36], and nitrosated at the *ipso* position [37], from which a whole plethora of chemical transformations are available, Scheme 1.6.

1.1.3 Ionic Liquids

In a less synthetic context, (perfluoro) [38] alkyl and alkenyl [39] trifluoroborate salts are found to be facile precursors for ionic liquids, Fig. 1.2, which show desirable properties including low melting points, high thermal stabilities, high conductivities and have wide electrochemical windows. As such, they have

Fig. 1.2 Ionic liquid prepared from $KBF_3C_3F_6$

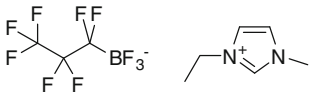

21

potential for use as electrolytes in high energy storage devices. Of particular note is the low viscosity (26–77 cP at 25 °C) that the R-BF_3^- based ionic liquid inherits, possibly due to the many degrees of freedom within the ion, which lowers the electrostatic attraction to the cation.

1.1.4 Metal Catalysed Cross-Coupling Reactions

The widest application of R-BF_3K salts is in their use as nucleophilic coupling partners in metal catalysed cross-coupling reactions, the most of which are catalysed by copper, rhodium, nickel or palladium. Their relative stability towards many side reactions often makes them more favourable than boronic acids. However, it is not clear whether direct transmetalation of the R-BF_3K salt is occurring in all contexts or whether a hydrolytic derivative is the active transmetalating species.

Copper(II) catalysed etherification of phenols with arylboronic acids was first realised by Evans [40]. However Batey [41] was able to employ Ar-BF_3K salts to couple with unactivated aliphatic alcohols under mild and essentially neutral conditions. The optimised conditions employed 2 equivalents of R-BF_3K salt with 1 equivalent of alcohol in the presence of $Cu(OAc)_2$, DMAP, and 4 Å molecular sieves (Scheme 1.7). The reaction proceeds well at room temperature under an atmosphere of O_2 for 24 h. When a boronic acid was substituted for the R-BF_3K salt, lower yields resulted, due to a competing oxidative homocoupling side reaction. Similarly, without the molecular sieves, only traces of the ether were detected; thereby confirming the importance of the non-solvolytic conditions to ensure integrity of the R-BF_3K partner.

The Miyaura-Hayashi reaction, the asymmetric 1,4-addition of boron reagents to enones, is conveniently catalysed by rhodium(I), in conjunction with a chiral ligand. Batey [42] established that R-BF_3K salts effected the aryl or alkenyl addition to enones in a superior manner to boronic acids, but did not report any asymmetric examples. Genet, however, developed conditions which generated excellent stereoselectivity for the arylation of various enones [43, 44] and alkenyl esters [45]. The chirality was induced through the use of (*S*)-binap ligand, with the rhodium(I) precursor, Scheme 1.8. Interestingly, the enantioselectivity of the product was found to be sensitive to the quantity of water present in the medium, where the enantiomeric excess increased with the addition of up to 2.5 equivalents. When boronic acids are employed, water is required for protonation of the latent enolate, which can affect the yield, but there are no reports of it effecting the enantioselectivity. Unfortunately no rationale was provided for the enantiomeric necessity of water when specifically employing R-BF_3K salts.

Rhodium can also catalyse the arylation[42, 46] and alkylation [47] of aldehydes (1,2-addition). Aggarwal has demonstrated an elegant protocol for the addition of secondary and tertiary benzylic trifluoroborate salts to aldehydes, in moderate to excellent isolated yields, Scheme 1.9. There was no evidence for

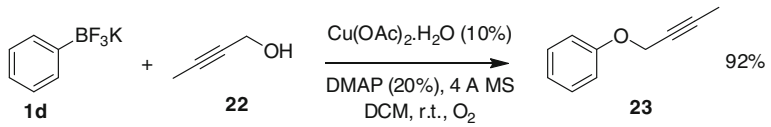

Scheme 1.7 Copper(II) catalysed ether formation between unactivated alkyl alcohol **22** and **1d**

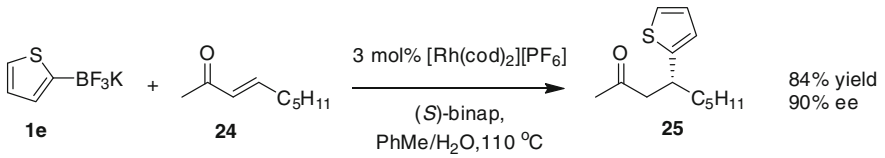

Scheme 1.8 Rhodium-catalysed asymmetric conjugate addition of aryltrifluoroborate **1e** to enone **24**

β-hydride elimination of the benzyltrifluoroborate salt, which was able to transmetalate the organic moiety to the aldehyde with excellent stereo-retention. Complete stereo-retention was even maintained when the tertiary trifluoroborate salts were employed, thus leading to perfectly stereo-defined quaternary centres. Only limited reactivity, of the addition to the aldehyde, was observed when coupling with a benzylic pinacol ester. The yield could be improved under anhydrous conditions but substantial racemisation occurred in both cases. It was also reported [42] in the 1,2-arylation of aldehydes that the use of R-BF_3K salts led to superior outcomes to the use of boronic acids

The asymmetric synthesis of chiral α-branched amines is important in the preparation of therapeutic agents. Ellman [48] demonstrated that rhodium (I) conveniently catalysed the alkenylation of aromatic and aliphatic *N-tert*-butanesulphinyl imines (**27**) in good to excellent yields, and with remarkable diastereoselectivity. The *N-tert*-butanesulfinyl chiral auxiliary protecting group is especially appealing in this regard due to its ease in preparation and subsequent acidic removal to give the hydrochloride salt of the amine. Although the conditions optimised are hydrolytic (basic/aqueous), R-BF_3K salts gave superior outcomes to when boronic acids were employed. However, when the *N*-methyliminodiacetic acid (MIDA) boronates (**28**) were directly compared to the R-BF_3K salts [49]

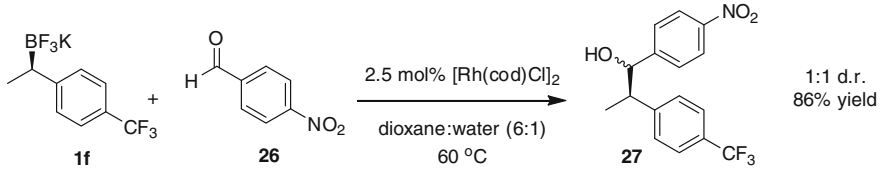

Scheme 1.9 Rhodium-catalysed 1,2-addition of benzyltrifluoroborate **1f** to aldehyde **26**. Complete transfer of stereochemical information from **1f** is observed

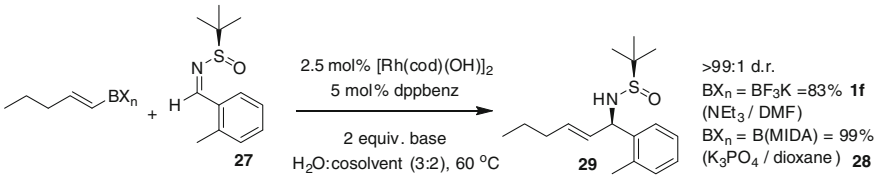

Scheme 1.10 The diastereoselective 1,2-addition of alkenyltrifluoroborate salt **1f** and MIDA boronate **28** to *N*-**tert**-butanesulphinyl imine **29**

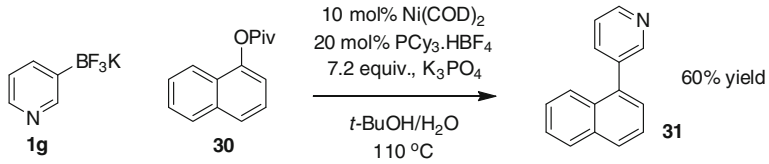

Scheme 1.11 Nickel-catalysed cross-coupling between arylpivalate **30** and heteroaryltrifluoroborate salt **1g**

further improvements in the yield were observed; even under conditions which have been shown [50] to effect hydrolysis of the reagent to the boronic acid itself, Scheme 1.10.

The transmetalation of R-BF_3K salts, or a species derived from it, with nickel(II) complexes has been shown to be effective for the cross-coupling with phenol derivates, such as mesylates and pivalates [51]. As palladium is particularly poor at the C–O activation of the ester based nucleofuges, e.g. pivalate or carbamate, cross-coupling of these functionalities demonstrates the broad range of coupling partners available to R-BF_3K cross-coupling. Potassium heteroaryl and aryl trifluoroborates were coupled with a range of phenol-derived electrophiles in reasonable to excellent yields, in 4 h at 110 °C, Scheme 1.11.

Finally, palladium catalysed Suzuki–Miyaura (SM) reactions are possibly what R-BF_3K salts are most renowned for [52]. A huge plethora of organic moieties have been successfully coupled, and in many cases do so in a superior way to boronic acids. This area forms the subject of this thesis.

References

1. R.D. Chambers, H.C. Clark, C.J. Willis, J. Am. Chem. Soc. **82**, 5298–5301 (1960)
2. S. Darses, J.-P. Genet, Chem. Rev. **108**, 288–325 (2007)
3. J.-P. Genet, S. Darses, Eur. J. Org. Chem., 4313–4327 (2003)
4. H.A. Stefani, R. Cella, A.S. Vieira, Tetrahedron **63**, 3623–3658 (2007)
5. E. Vedejs, R.W. Chapman, S.C. Fields, S. Lin, M.R. Schrimpf, J. Org. Chem. **60**, 3020–3027 (1995)
6. D.G. Hall, *Structure, Properties, and Preparation of Boronic Acid Derivatives. Overview of Their Reactions and Applications* (Wiley, Weinheim, 2005)

7. E. Vedejs, S.C. Fields, S. Lin, M.R. Schrimpf, J. Org. Chem. **60**, 3028–3034 (1995)
8. R.A. Batey, A.N. Thadani, D.V. Smil, Tetrahedron Lett **40**, 4289–4292 (1999)
9. R.A. Batey, A.N. Thadani, D.V. Smil, A.J. Lough, Synthesis **2000**, 990–998 (2000)
10. R.A. Batey, A.N. Thadani, Org. Lett. **4**, 3827–3830 (2002)
11. F. Nowrouzi, A.N. Thadani, R.A. Batey, Org. Lett. **11**, 2631–2634 (2009)
12. T.R. Ramadhar, R.A. Batey, Synthesis, 1321–1346 (2011)
13. S.-W. Li, R.A. Batey, Chem. Commun. 1382–1383 (2004)
14. N.A. Petasis, I. Akritopoulou, Tetrahedron Lett. **34**, 583–586 (1993)
15. N. Schlienger, M.R. Bryce, T.K. Hansen, Tetrahedron Lett. **41**, 1303–1305 (2000)
16. J.-P. Tremblay-Morin, S. Raeppel, F. Gaudette, Tetrahedron Lett. **45**, 3471–3474 (2004)
17. T.A. Mitchell, J.W. Bode, J. Am. Chem. Soc. **131**, 18057–18059 (2009)
18. C.-V.T. Vo, T.A. Mitchell, J.W. Bode, J. Am. Chem. Soc. **133**, 14082–14089 (2011)
19. G.A. Molander, D.E. Petrillo, J. Am. Chem. Soc. **128**, 9634–9635 (2006)
20. G.A. Molander, D.J. Cooper, J. Org. Chem. **72**, 3558–3560 (2007)
21. G.A. Molander, R. Figueroa, J. Org. Chem. **71**, 6135–6140 (2006)
22. G.A. Molander, W. Febo-Ayala, L. Jean-Gérard, Org. Lett. **11**, 3830–3833 (2009)
23. G.A. Molander, J. Ham, Org. Lett. **8**, 2767–2770 (2006)
24. G.A. Molander, D.J. Cooper, J. Org. Chem. **73**, 3885–3891 (2008)
25. G.A. Molander, N.M. Ellis, J. Org. Chem. **71**, 7491–7493 (2006)
26. C.A. Hutton, A.K.L. Yuen, Tetrahedron Lett. **46**, 7899–7903 (2005)
27. G.A. Molander, L.N. Cavalcanti, B. Canturk, P.-S. Pan, L.E. Kennedy, J. Org. Chem. **74**, 7364–7369 (2009)
28. D.W. Blevins, M.-L. Yao, L. Yong, G.W. Kabalka, Tetrahedron Lett. **52**, 6534–6536 (2011)
29. G.W. Kabalka, V. Coltuclu, Tetrahedron Lett. **50**, 6271–6272 (2009)
30. S.R. Inglis, E.C.Y. Woon, A.L. Thompson, C.J. Schofield, J. Org. Chem. **75**, 468–471 (2010)
31. G.W. Kabalka, A.R. Mereddy, Tetrahedron Lett. **45**, 343–345 (2004)
32. G.A. Molander, L.N. Cavalcanti, J. Org. Chem. **76**, 7195–7203 (2011)
33. G.W. Kabalka, A.R. Mereddy, Organometallics **23**, 4519–4521 (2004)
34. M.-L. Yao, M.S. Reddy, L. Yong, I. Walfish, D.W. Blevins, G.W. Kabalka, Org. Lett., 700–703 (2010)
35. N.A. Petasis, A.K. Yudin, I.A. Zavialov, G.K.S. Prakash, G.A. Olah, Synlett **1997**, 606–608 (1997)
36. G.A. Molander, L.N. Cavalcanti, J. Org. Chem. **76**, 623–630 (2011)
37. G.A. Molander, L.N. Cavalcanti, J. Org. Chem. **77**, 4402–4413 (2012)
38. Z.-B. Zhou, H. Matsumoto, K. Tatsumi, Chem. Eur. J. **12**, 2196–2212 (2006)
39. Z.-B. Zhou, H. Matsumoto, K. Tatsumi, ChemPhysChem **6**, 1324–1332 (2005)
40. D.A. Evans, J.L. Katz, T.R. West, Tetrahedron Lett. **39**, 2937–2940 (1998)
41. R.A. Batey, T.D. Quach, Org. Lett. **5**, 1381–1384 (2003)
42. R.A. Batey, A.N. Thadani, D.V. Smil, Org. Lett. **1**, 1683–1686 (1999)
43. J.-P. Genet, M. Pucheault, S. Darses, Tetrahedron Lett. **43**, 6155–6157 (2002)
44. M. Pucheault, S. Darses, J.-P. Genêt, Eur. J. Org. Chem., 3552–3557 (2002)
45. L. Navarre, M. Pucheault, S. Darses, J.-P. Genet, Tetrahedron Lett. **46**, 4247–4250 (2005)
46. M. Pucheault, S. Darses, J.-P. Genet, Chem. Commun, 4714–4716 (2005)
47. A. Ros, V.K. Aggarwal, Angew. Chem. Int. Ed. **48**, 6289–6292 (2009)
48. K. Brak, J.A. Ellman, J. Am. Chem. Soc. **131**, 3850–3851 (2009)
49. K. Brak, J.A. Ellman, J. Org. Chem. **75**, 3147–3150 (2010)
50. E.P. Gillis, M.D. Burke, J. Am. Chem. Soc. **129**, 6716–6717 (2007)
51. G.A. Molander, F. Beaumard, Org. Lett. **12**, 4022–4025 (2010)
52. G.A. Molander, B. Canturk, Angew. Chem. Int. Ed. **48**, 9240–9261 (2009)

Chapter 2
Organotrifluoroborate Preparation

2.1 Introduction

2.1.1 Preparation of R-BF_3K Salts

2.1.1.1 Initial Reports

The first report of an organofluoroborate salt was in 1940 by Fowler and Krauss [1], who prepared tetramethyl/butylammonium triphenylfluoroborate (**33a/b**) from an amine-borane complex **32** with tetramethyl/butylammonium fluoride, Scheme 2.1.

It took a further twenty years before a potassium organotrifluoroborate (**1**) appeared in the literature. In 1960, Chambers [2] prepared potassium (trifluoromethyl)trifluoroborate (**1h**) by treatment of (trifluoromethyl)trimethylstannane (**34**) with BF_3 gas followed by a work-up with aqueous potassium fluoride, Scheme 2.2. The barium and ammonium salts were also prepared *via* this method but showed inferior stability to the potassium salt, which was described as being 'thermally stable and non-hygroscopic'.

This strategy, of boron displacement of tin to form the C–B bond, was further developed by Stafford [3] in 1963, who synthesised the first potassium vinyl and methyltrifluoroborates. Shortly after, Chambers and Chivers [4] prepared potassium pentafluoro phenyl trifluoroborate, and Chivers [5] in 1970 synthesised potassium 2-(trifluoromethyl) phenyl trifluoroborate.

The alternative strategy involves heteroatom/fluoro exchange on boron, which was first realised by Kaufmann [6] in 1988. A dibromoborane camphenyl derivative **35** was treated with potassium fluoride to give isopinocamphenyl trifluoroborate salt **1i** in good yield, Scheme 2.3, although this was the only example reported.

A. J. J. Lennox, *Organotrifluoroborate Preparation, Coupling and Hydrolysis*, Springer Theses, DOI: 10.1007/978-3-319-01134-9_2,

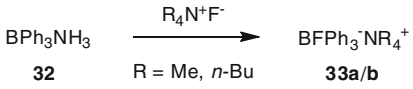

Scheme 2.1 First report of an organofluoroborate salt

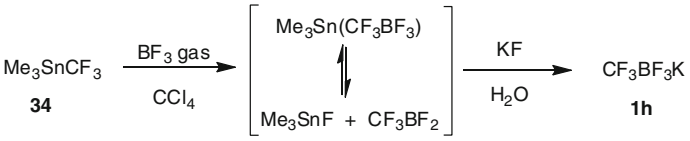

Scheme 2.2 First preparation of a potassium organotrifluoroborate salt by C–B bond formation

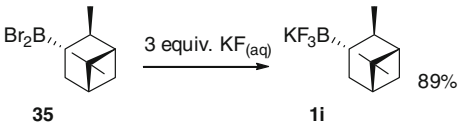

Scheme 2.3 Preparation of isopinocamphenyl trifluoroborate salt **1i** by B–F bond formation

2.1.1.2 Introduction of KHF_2

Intermediate preparation of the exceptionally reactive and unstable dihaloboranes, in combination with the toxicity associated with gaseous boron trifluoride and tin reagents, did not make any of the preparative routes thus far, ideal for the chemistry of organotrifluoroborate salts to flourish. In 1995 an elegant procedure was published by Vedejs [7], who demonstrated that potassium bifluoride was an efficient fluorinating agent for organoboronic acids. Inspiration was taken from a publication by Umland and Thierig in 1967 [8], who employed KHF_2 to transform Ph_2BOH to the tetravalent KPh_2BF_2 salt. They proceeded to report that $PhBF_3K$ could be produced by further heating of KPh_2BF_2 in glacial acetic acid. Their paper contained no experimental information, spectral data, or yields; so Vedejs developed the method, with the incentive of preparing stable precursors for organodifluoroboranes, Sect. 1.1.1 *vide supra*. A saturated aqueous solution of KHF_2, added to the organoboronic acid (**2**) in methanol, was also found to convert any boroxines, or boronic acid dimers present in commercial samples, to the organotrifluoroborate salt (**1**), Scheme 2.4. Isolation of pure product was then achieved by evaporation of all solvents, followed by multiple extractions with acetone.

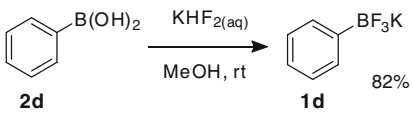

Scheme 2.4 KHF_2 as a fluorinating agent for the preparation of **1d** from **2d**

The scope of this reaction is evidently vast due to the availability and wide spread use of organoboronic acids, and, as such, they have become the primary starting materials for the preparation of R-BF_3K salts.

Organoboronic acid pinacol esters (**4**) are important building blocks in organic synthesis, and are important precursors for R-BF_3K salts. Aside from cost and atom-economy, the monomeric nature and stability towards silica-gel of pinacol esters renders them advantageous in many contexts when compared to boronic acids. Their applications are diverse, ranging from direct use in SM cross-coupling reactions [9] to the generation of enantiopure tertiary alcohols [10]. Pinacol esters are conveniently prepared *via* the Miyaura borylation; a palladium catalysed conversion of an organohalide to the corresponding boronic ester [11]. The transformation is highly functional group tolerant and uses cheap, commercially available starting materials, allowing access to a wide substrate variety. Iridium has recently been found to catalyse the C–H activation of 3, 5-bis-substituted arenes, thus bypassing the requirement for inclusion of a halide leaving group [12]. Treatment of the pinacol ester with KHF_2, and purification from residual pinacol, yields pure R-BF_3K salt, Scheme 2.5.

Direct conversion from pinacol esters to the more Lewis acidic boronic acid is problematic, due to difficulties in separation and subsequent recombination of the boronic acid and diol. This problem can be averted by the intermediate preparation and hydrolysis of the organotrifluoroborate salt [13]. Thus, boronic ester conversion to R-BF_3K salts, becomes a key transformation, widely used throughout academic research and industrial application.

Organoboronic acid methyl (**37**)/isopropyl (**38**) esters are another class of important intermediates for the generation of organotrifluoroborate salts (**1**). Primarily they are generated *in situ* from, (***i***) lithium-halogen exchange *via* treatment of an organohalide with BuLi, or (***ii***) *via* deprotonation of a suitably acidic proton, e.g. of a terminal alkyne, followed by workup with $B(OMe)_3$ or $B(O\textit{i}\text{-Pr})_3$. Genet [14] demonstrated these could be taken through in a "one-pot" process to the corresponding potassium organotrifluoroborate by direct treatment with KHF_2, Scheme 2.6. Grignard reagents, (***iii***), e.g. vinylmagnesium bromide, are also suitable nucleophiles for the borylation/fluorination protocol, allowing moieties such as ethynyl and vinyl to be incorporated into the growing repertoire of known R-BF_3K salts, Scheme 2.6.

Finally, treatment of boronic esters with KHF_2, which have been prepared from the hydroboration of alkynes, forms an important route to alkenyltrifluoroborate

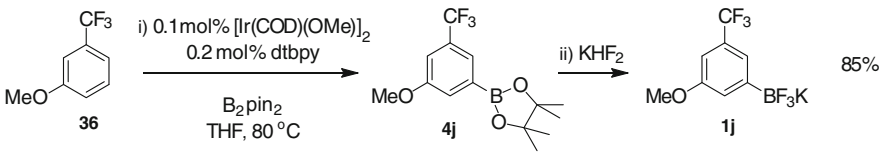

Scheme 2.5 Iridium-catalysed C–H activation for the borylation of arene **36** and subsequent "one-pot" transformation to organotrifluoroborate salt **1j**

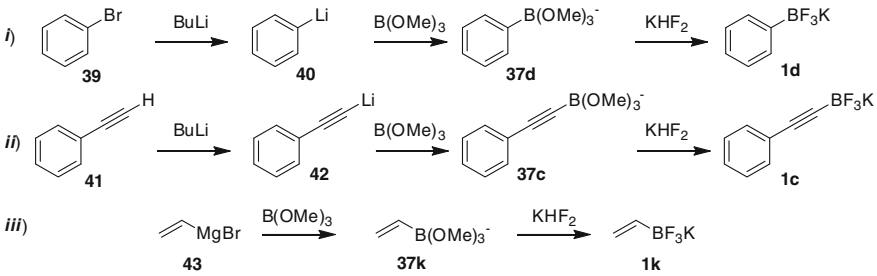

Scheme 2.6 Organotrifluoroborate (**1d**, **1c** and **1k**) preparation from the generation of intermediate boronic esters **37d**, **37c** and **37k**

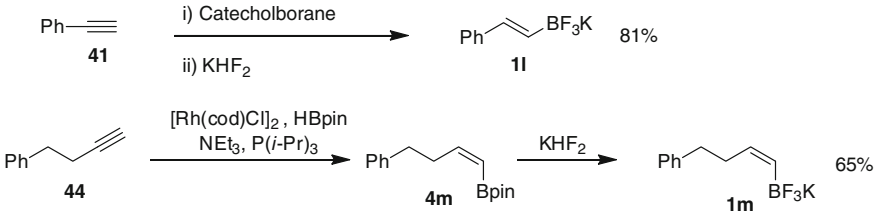

Scheme 2.7 Preparation of organotrifluoroborate **1l** and **1m** *via* the hydroboration of alkynes **41** and **44**

salts. The *E* stereoisomers can be conveniently prepared *via* syn hydroboration [15], Scheme 2.7. Preparation of the *Z* stereoisomer is achieved *via* isolation of the intermediate pinacol ester, obtained from rhodium catalysed hydroboration of alkynes [16], followed by treatment with KHF_2 [17], Scheme 2.7.

A wide range of potassium organotrifluoroborates have since been synthesised using KHF_2 as the fluorinating agent, including potassium alkyl [18, 19], alkenyl [15], alkynyl [14], allyl [20, 21], perfluoroalkyl [22] /alkenyl [23], acyl [24] and amino [25, 26] trifluoroborates. However, addition of $HF_{(aq)}$ in conjunction with KHF_2, is still required for the perfluorinated examples [22], presumably due to the greater stability of the alkoxo-ligated boron intermediates.

2.1.2 *Preparation of R-BF_3^- Salts with Different Counter Cations*

The counter cation of organotrifluoroborate salts, not only dictates the physical properties of the compound, but also the solubility characteristics in which it inherits. Therefore, it is possible to tune the solubility of the reagent to a particular process. The potassium salts have generated the most attention, due to their free-flowing crystalline physical properties and ease in preparation, through the

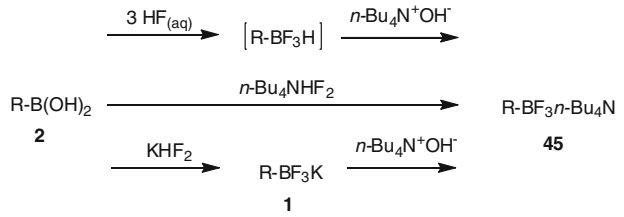

Scheme 2.8 Preparation of the tetrabutylammonium organotrifluoroborate salt **45** from **2**

commercial availability of KHF_2. Other salts of organotrifluoroborates have been isolated, including other alkali metals and tetraalkylammonium, *e.g.* tetrabutylammonium (n-Bu_4N^+) [27].

Tetrabutylammonium organotrifluoroborate salts (**45**) offer a greater range of solubility in apolar solvents, but they suffer in their physical handling properties, as they are often oils or low melting solids. The n-Bu_4N^+ salts are prepared from the organoboronic acid by either treatment with tetrabutylammonium hydroxide and $HF_{(aq)}$ [27], or more conveniently with preformed tetrabutylammonium bifluoride; [28] an alternative procedure employs a cation exchange protocol on the corresponding potassium salt, Scheme 2.8 [27].

Along with the potassium salt, Batey [27] was able to prepare a range of metal salts with the HF/MOH methodology, Scheme 2.8, including lithium, sodium and cesium. However this was only demonstrated on a single substrate ($PhB(OH)_2$), with little experimental details or spectroscopic evidence. Matteson [29] reported on the preparation of cesium alkyltrifluoroborate salts (**5**) from pinanediol boronic esters (**46**). This was developed after attempts to form the potassium salt were complicated by difficulties in purification from free pinanediol and KHF_2 in solution; the cesium salt was preferred as it readily precipitated from Et_2O. Primary and secondary alkyltrifluoroborates were prepared in good to excellent yields, by treatment of the boronic ester with a premixed solution of $HF_{(aq)}$ and CsF, Scheme 2.9.

The cesium salt has an increased cost disadvantage in comparison to the potassium salt, but it does provide a difference in its solubility properties, which allows a broader range of applications for organotrifluoroborate salts in general. As $CsHF_2$ is not commercially available, Matteson's HF/CsF methodology forms the primary way to prepare the cesium salts. The toxicity and associated handling problems of $HF_{(aq)}$, has therefore meant the chemical applications of the cesium salts have not grown as rapidly as their potassium analogous.

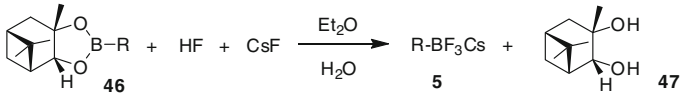

Scheme 2.9 Matteson's preparation of cesium alkyltrifluoroborate salts (**5**) from **46**; an excess of HF with CsF forms $CsHF_2$ *in situ*

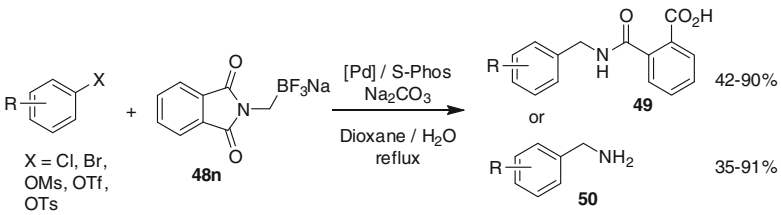

Scheme 2.10 Tanaka's cross-coupling of sodium phthalimidoylmethyltrifluoroborate (**48n**) to give amides **49** and benzylic amines **50**

There are fewer reports on the preparation and utility of sodium organotrifluoroborate salts (**48**). Although $NaHF_2$ is commercially available and cheaper than KHF_2, this may be due to a lower stability that the harder counter cation induces. However, Batey [27] claimed the phenyl moiety induced sufficient stability and a large number of aromatic examples do exist in the patent literature. Additionally, Tanaka [30] recently reported on the SM coupling of sodium phthalimidoylmethyl trifluoroborate (**48n**) with aryl halides. Unfortunately, no rationale is given to their preference for employing the sodium over the potassium salts, but their couplings achieve good to excellent yields, Scheme 2.10, implying there is little disadvantage in their use.

2.1.3 Problems and Proposals

The KHF_2 method avoids many of the handling problems associated with employing $HF_{(aq)}$ or BF_3 gas, but it still comes at a practical cost due to the severe etching effect of glassware it exerts. The damage from the *in situ* release of HF on a small scale may be relatively insignificant compared to the costs of reagents or substrates; however, on an industrial scale this damage can be tremendously costly, rendering the process undesirable. Moreover, current procedures employ a large excess of KHF_2, (2–6 equivalents), which provokes further waste concerns. The isolation and purification is laborious, requiring separation of the RBF_3K salt from the mixture of potassium salts ($KF/KOH/KHF_2$) remaining after the removal of methanol/water *in vacuo*. Often the removal of solvents requires high vacuum for long periods of time, e.g. overnight, and the isolation of R-BF_3K salts sometimes necessitates multiple extractions at different temperatures [14] or Soxhlet extraction [31], which is impractical on a large scale.

Due to the wide ranging and ever increasing applications of organotrifluoroborate salts, an improved methodology is required to deal with the issues stated above: a fluorinating agent that does not involve the *in situ* generation of HF will suppress glassware etching, and an operationally simple workup and isolation to give pure R-BF_3K is desired.

2.2 Preparation of R-BF_3K Salts from Boronic Acids

2.2.1 Optimisation

In Vedejs' pioneering publication [7], potassium fluoride was found to be ineffective at forming Ph-BF_3K salts from boronic acids, as "the fluoride exchange did not take place when KF was used in place of KHF_2". However preliminary studies in our hands showed (^{19}F and ^{11}B NMR) complete consumption of 4-fluorophenylboronic acid (**2a**) upon treatment with 4 equivalents of potassium fluoride in methanol, Fig. 2.1. The exact identity of the partially methoxylated/hydroxylated/fluorinated 'ate' product **51a** was unknown, but integration of the ^{19}F NMR peaks suggested two fluorine atoms were ligated to boron; and due to the very much greater concentration of methanol to water, a methoxyl ligand was likely to have displaced hydroxide. Consistent with Vedejs' observations, equilibrium was established, and no potassium 4-fluorophenyltrifluoroborate (**1a**) was detected.

From studies on the hydrolysis of organotrifluoroborates (**1**) (Sect. 4.2, *vide infra*) to boronic acids (**2**), it was demonstrated that the transformation can be catalysed by a specific acid pathway, and thus microscopic reversibility infers the forward reaction should also be catalysed by acid. Additionally, in order to push the equilibrium in favour of the trifluoroborate, KOH sequestration is required, which can in principle be achieved by the addition of stoichiometric quantities of acid. Therefore, by replacing HF in KHF_2, with a weak acid (HA) in the presence of KF, it was envisaged that complete conversion to the trifluoroborate would take place, under HF-free, non-etching conditions, Scheme 2.11.

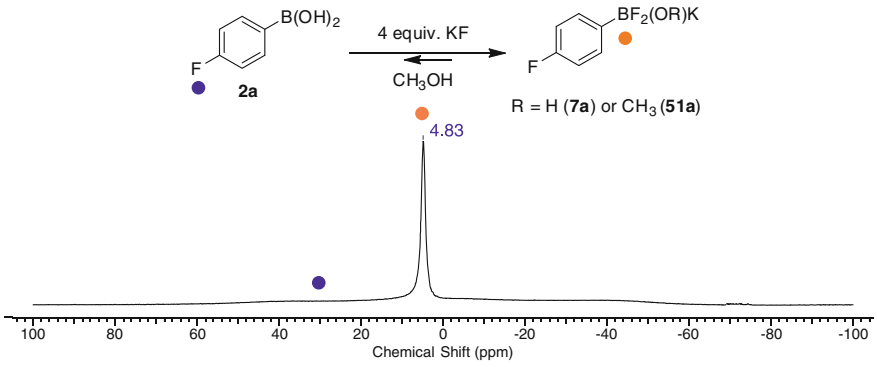

Fig. 2.1 ^{11}B NMR spectrum of the 'ate' species formed after the addition of KF to **2a**. Baseline due to background borosilicate glass signals

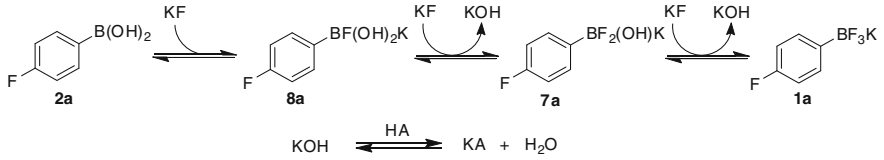

Scheme 2.11 Mechanistic proposal for the non-etching preparation of **1a** from **2a**

2.2.1.1 Methanol and Acetic Acid

Acetic acid was initially chosen due to its low cost and high availability, and 4-fluorophenylboronic acid (**2a**) was employed as a test substrate due to the ease of *in situ* reaction monitoring offered by ^{19}F NMR. To explore the system, the loadings of potassium fluoride and acetic acid were varied in a solution of **2a** in methanol. It was found the conversion to **1a** was dependent on both KF and acetic acid concentrations, requiring over 30 equivalents of the latter to reach a satisfactory conversion, Table 2.1.

2.2.1.2 Solvent Study

With the proof of principle established, the solvent was studied in order to find a suitable system, which would give the most operationally facile procedure, combined with the highest yields and purities. Ideally, either the product **1a**, or co-products (KA), would precipitate out of solution, thus requiring only a simple filtration and evaporation to isolate pure R-BF_3K.

Unfortunately, methanol dissolved all reactants and products thereby rendering it less than ideal. A range of alternative solvents were tested, where unsurprisingly, the relatively nonpolar solvents e.g. THF, toluene and DCM gave 0 % conversion,

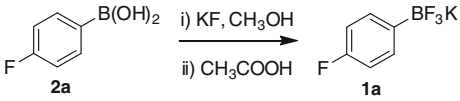

Table 2.1 Initial investigations into the use of acetic acid and KF in the preparation of **1a**

Entry	Acetic acid/equiv.	KF/equiv.	Conversion (→ 1a)/ %[a]
1	2	3	44
2	3	3	47
3	5	3	57
4	5	4	68
5	14	3	87
6	32	3	98

[a] % **1a** ($\delta_F = -118.8$ and -141 ppm) by ^{19}F NMR

presumably due to the poor solubility of the KF. Although KF was initially insoluble in most solvents tested, upon the addition of acetic acid in some solvents e.g. acetone, EtOAc, CH_3CN and Et_2O, it subsequently dissolved and gave good conversions to **1a**, Table 2.2.

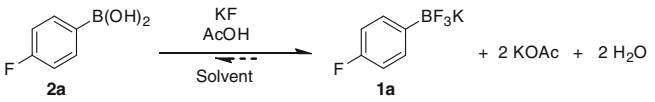

Table 2.2 Variation of the solvent in the preparation of **1a** from **2a**

Entry	Solvent	Acetic acid/equiv.	KF/equiv.	Conversion (→ 1a)/ %[a]
1	CH_3OH	50	3	98
2	DCM	50	3	0
3	THF	50	3	0
4	Toluene	50	3	0
5	Et_2O	50	3	81[b]
6	Acetone	50	3	99
7	EtOAc	50	3	75
8	CH_3CN	30	4	99

[a] % **1a** ($\delta_F = -118.8$ to -119.7 and -140 to -142 ppm) by ^{19}F NMR
[b] **1a** isolated, due to precipitation from solution

For reasons currently not understood, diethyl ether gave satisfactory conversions when other non-polar solvents did not. The R-BF_3K salt precipitated out of solution, which was initially promising due to the ease in isolation it offered. But when performed on a preparative (0.71 mmol) scale, only 64 % of **1a** could be isolated. Product was lost during purification from the co-precipitated KOAc and KF, and acetic acid contamination, which was difficult to remove under reduced pressure. Switching to acetone, in which the conjugate base, KOAc, and KF were not soluble, but **1a** was, also gave a 64 % isolated yield (0.71 mmol scale). However, purification was again required due to the acetic acid contamination.

2.2.1.3 Acid Study

Evidently the acetic acid contamination was problematic due to the large excesses (20–50 equivalents) required. A stoichiometric acid which would allow facile isolation of pure **1a** by precipitation of all co-products would thus be beneficial. The use of formic acid effected good conversions (99 %) in methanol, but still required an excess (30 equivalents) and thus gave rise to similar problems as acetic acid. The use of a strong acid such as $HCl_{(aq)}$ (2 N) gave only traces of **1a**, possibly due to a competing acid catalysed protodeboronation degradation of **2a**, or intermediates **7a** and **8a**. Eventually, L-(+)-tartaric acid (**3**) was identified as fitting the criteria: not only is it a safe, easily handled and cheap solid, but it could be

used stoichiometrically (2 equivalents) as the conjugate base, potassium bitartrate (cream of tartar, **52**), is extremely insoluble in all common organic solvents.

2.2.1.4 Flocculating Agent

Initial optimisations of **2a**–**1a** with tartaric acid (**3**) were undertaken (0.15 mmol scale) in methanol, and employing stoichiometric quantities of KF (3 equiv.) and **3** (2 equiv.). Although 75 % conversion was reached, potassium bitartrate (**52**) precipitated out of solution as a very fine suspension, thus causing significant problems during the filtration of the co-products. On a small test scale (0.15 mmol) filtration of **52** was found to be slow, however, when moving to a large scale it was envisaged that efficient filtration would become impossible.

Attempts were made at controlling the precipitation rate of potassium bitartrate (**52**) to increase the particle size through slow addition of tartaric acid (**3**), however, no long lasting effect was observed. Additionally the use of low temperature, slow diffusion with layering, seeding and increasing the concentration, all had no influence on the suspension. A suitable flocculating agent, to agglomerate the fine suspension, was sought. A range of inorganic salts were screened, *via* addition to a solution of **52** in methanol, Table 2.3.

Few salts had any initial effect, with the exception of KOH and brine. The strong basicity of the former hampered the inertness of an ideal flocculating agent, but use of the latter was more encouraging. Unfortunately, when the procedure was performed on a larger scale (0.5 mmol) and brine was used to flocculate the suspension, isolation of pure **1a** still proved difficult, due to contamination with

Table 2.3 Inorganic salts tested for the flocculation of potassium bitartrate in methanol

Entry	Salt	Initial effect[a]	Longer term effect[b]
1	$MgSO_4$	Nil	Slight flocculation
2	KCl	Nil	Nil
3	K_2CO_3	Nil	Slow flocculation
4	KOAc	Nil	Slight flocculation
5	$NaHCO_3$	Nil	Slight flocculation
6	KI	Nil	Nil
7	KBF_4	Nil	Slow flocculation
8	KOCN	Nil	Nil
9	KBr	Nil	Nil
10	Na_2SO_4	Nil	Nil
11	NH_4Cl	Nil	Nil
12	$CaCl_2$	Nil	Nil
13	KOH	Rapid flocculation	Flocculation
14	NaCl	Nil	Nil
15	$NaCl_{(aq)}$	Rapid flocculation	Flocculation

[a] Initial observation after 1–2 min
[b] Upon standing for 1–2 h

NaCl. Interestingly, the addition of a larger volume of pure water also effected this physical change, however it was slow, and too much water remained after filtration, raising concerns over its removal *in vacuo,* and the instability of some of R-BF_3K salts to an aqueous medium.

2.2.1.5 Water as a Flocculating Agent

Although water was found to successfully flocculate the suspension, a further problem experienced in methanol was the formation of small quantities of a stable partially methoxylated/fluorinated 'ate' species **51a** detected (^{11}B, ^{19}F NMR) *in situ*. This warranted efforts into sourcing an alternative solvent system where the level of methanol in the mixture could be reduced.

Various ratios of methanol/THF were tested in the formation of **1a** from **2a**, followed by the use of water to flocculate the bitartrate. Increasing proportions of methanol led to increasing quantities of **51a**; but increasing proportions of THF led to the insolubility of KF, which caused the reaction to take longer to proceed to completion. However, it was noted under these 'low methanol conditions' that the addition of smaller quantities of water could effect flocculation of bitartrate **52** more efficiently. It was speculated that the flocculation mechanism involved water forming a strong hydrogen bonded network to **52**, which forced the suspension to coagulate. A single crystal X-ray structure of **52**, recrystallised from water, confirmed the solid could contain a high proportion of water. Consequently, a large excess of methanol would easily disturb this structure and slow down flocculation.

The solvent system needed to accommodate all R-BF_3K salts, which are generally only soluble in very polar solvents, yet avoid the use of protic alcohol solvents, which disturb flocculation of bitartrate **52**. Naturally acetonitrile was chosen because of the solubility it offers to R-BF_3K salts and partially to KF. However, a proportion of THF (16.7 %) was still required to dissolve the tartaric acid, which exhibited no solubility in acetonitrile. Under these conditions the loadings of KF and tartaric acid were varied, and 4 and 2.05 equivalents respectively gave the most reliable results. The conversion of **2a**–**1a** generally proceeded in 2 h (*in situ* ^{19}F NMR), with the KF dissolution being the rate-limiting process. Following the addition of water to flocculate **52**, filtration and evaporation of the filtrate, good yields of high purity **1a** were achieved. To test the methodology, a range of electron poor and electron rich arylboronic acids were tested (0.75 mmol scale; 0.2 M), Table 2.4.

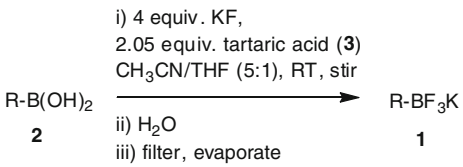

Table 2.4 A range of R-BF_3K salts prepared with KF/tartaric acid in CH_3CN/THF (5:1)

Entry	Substrate		Isolated yield/ %[a]	Time/hr[b]	Added H_2O/mL[c]
1	4-F-C_6H_4	**2a**	99 (99)[d]	2	0.1
2	*E*-*β*-styryl	**2 l**	82	3	0.1
3	4-MeO-C_6H_4	**2o**	64	3	0
4	1-naphthyl	**2p**	96	3	0.1
5	3,5-$(CF_3)_2$-C_6H_3	**2q**	0	4	0.1
6	4-NO_2-C_6H_4	**2r**	58	3	0.3
7	3-Cl-C_6H_4	**2 s**	0	3	0
8	4-CN-C_6H_4	**2t**	64	4	0.1
9	3-MeCO-C_6H_4	**2u**	88	3	0.1
10	4-CHO-C_6H_4	**2v**	51	3	0
11	*cyclo*-hexyl	**2w**	43	4	0.1

[a] Isolated yield of pure (^1H, ^{11}B and ^{19}F NMR) R-BF_3K (**1**)
[b] Reaction completion monitored by ^{19}F and ^{11}B NMR
[c] 0.1 mL initially added to the suspension and stirred for 5 min. If insufficient flocculation resulted, further aliquots of 0.1 mL were added
[d] 35 mmol scale

Aside from two exceptions, the yields were average to excellent, especially on scale-up (35 mmol), where **2a** gave 7.07 g (<99 %) of **1a**. However, variations in the water required to flocculate the bitartrate, the yield, and the time required for complete conversion of **2**, still rendered the current process less than ideal in comparison to the KHF_2 method.

Two possible problems remained: firstly, the entropically favoured dehydration of boronic acids to form linear or cyclic boroxines under the dry reaction conditions of CH_3CN/THF (5:1), possibly stabilised the boronic acid towards fluoride exchange. This problem is avoided in the KHF_2 procedure, due to the large excesses of water present that readily rehydrate the boroxines. Secondly, the time taken for each of the reactants (boronic acid/KF/tartaric acid) to dissolve is responsible for the extended and variable reaction times. Therefore, through the addition of water from the start, and ensuring all reactants are initially dissolved, both problems could be averted: KF could be conveniently added as an aqueous solution, and tartaric acid as a solution in THF.

2.2.2 The Optimised Procedure

Pleasingly, on a number of test substrates, when KF (aq) was added to the boronic acid in acetonitrile followed by the addition of tartaric acid (**3**) in THF,

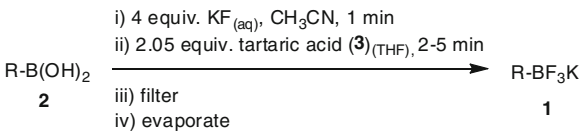

Scheme 2.12 Preparation of R-BF_3K salts with $KF_{(aq)}$ and tartaric $acid_{(THF)}$

Scheme 2.12, this improved methodology proceeded well; giving **1a** from **2a** in a 99 % isolated yield. Flocculation of bitartrate **52** occurred rapidly and generally without the need for additional water. The stoichiometry of both KF and tartaric acid were again screened, and found that 4 and 2.05 equivalents respectively gave the most reliable results. It was found that the increasing concentrations of $KF_{(aq)}$, lead to increasing rates of flocculation. This is likely due to an increase in the volume of the aqueous biphase formed from the excess $KF_{(aq)}$ in acetonitrile. **52** is drawn into this bilayer, which initiates the hydrogen bonded network and subsequent rapid coagulation and flocculation. The excess KF additionally aides fluoride complexation to the Lewis acidic **2a**. The small excess in **3** would reliably accommodate the variations in stoichiometry arising from boroxine anhydrides in commercial samples of boronic acids.

After the addition of KF in water (ca. 10 M) to **2** in acetonitrile, the biphasic mixture was stirred until complete dissolution of **2**. Hydration of all boroxines and precomplexation by fluoride, as confirmed by ^{11}B and ^{19}F NMR, occurred at this point. The mixture was stirred rapidly as **3** in THF (ca. 1.4 M) was added dropwise. **52** precipitated, and rapidly flocculated before the solution was filtered, washed through with further acetonitrile, and evaporated to give the pure R-BF_3K salt. Under these conditions, a number of boronic acids were cleanly converted to the corresponding R-BF_3K salts, Table 2.5.

Electron poor and electron rich aryl systems, heteroaryl, vinylic and alkyl systems were all reliably accommodated by the methodology. Reaction times were almost instantaneous, requiring less than 20 min, from start to finish to isolate pure (^1H, ^{13}C, ^{11}B, ^{19}F NMR, elemental analysis) R-BF_3K salts, using commercial grade solvents at room temperature.

A number of substrates initially did not undergo complete conversion (unreacted boronic acid detected by ^1H, ^{19}F and ^{11}B NMR). By employing a slight excess protocol (4.5 equiv. KF, 2.5 equiv. **3**) conversions increased. However, it was found that recrystallisation of the starting material **2** from water, improved yields and purities of the final product **1** when the original protocol (4 equiv. KF, 2.05 equiv. **3**) was reemployed. It is likely that these commercial samples contained large proportions of boroxines, thus causing problems in establishing the correct stoichiometry for the reaction. The recrystallisation avoided these problems by ensuring all were hydrolysed to the boronic acid **2**.

However, for the reaction of electron-poor boronic acids **2q**, **2aa**, **2af** and **2ah** recrystallisation from water was not enough to improve the conversions when reemploying the regular quantities (4 equiv. KF, 2.05 equiv. **3**) and therefore the excess (4.5 equiv. KF, 2.5 equiv. **3**) protocol was still required. Analysis (^1H, ^{19}F

Table 2.5 The preparation of a range of R-BF_3K salts using the optimised conditions, Scheme 2.12

R-BF_3K (1)	R =	Isolated yield[a] /%	R-BF_3K (1)	R =	Isolated yield[a] /%
1a	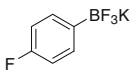	>99 / 96[b]	**1y**		57[d]
1d	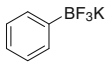	90	**1z**	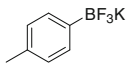	89
1l	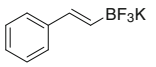	90	**1aa**	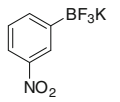	87[d]
1o	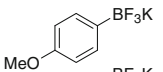	84	**1ab**	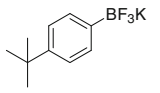	98
1p	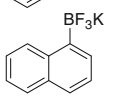	96 (>99)[c]	**1ac**	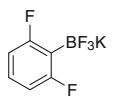	78
1q	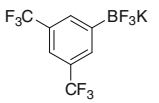	96[d]	**1ad**	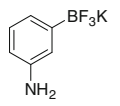	76
1r	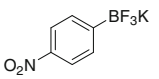	78	**1ae**	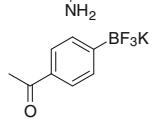	57
1s	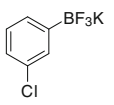	93	**1af**	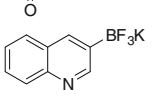	69[d,e,f]
1t	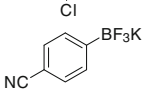	88	**1ag**	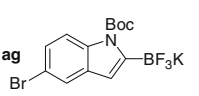	90
1u	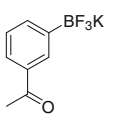	82 (95)[c]	**1ah**	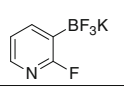	85[d,e]
1x		70[d]			

[a] Isolated yield of analytically pure R-BF_3K (**1**)
[b] Average of 30 runs
[c] Value in parenthesis:18-fold scale-up
[d] 4.5 equiv. KF and 2.5 equiv. tartaric acid
[e] CH_3OH/CH_3CN (1:1), dilute with CH_3CN
[f] Putilised, due to the lowerroduct refined with K_2CO_3 in acetone

and ^{11}B NMR) of the isolated material indicated the presence of an intermediate mixed species of the type **7** or **8**, suggesting incomplete conversion. Interestingly, although observed *in situ* in reactions involving boronic acid **2a**, these mixed species are not stable enough to be isolated and characterised, thus suggesting a greater induction of stability from very electron poor moieties.

For the reaction of heteroaryl boronic acids **2af** and **2ah**, the solvent system optimised for pinacol esters, Sect. 2.3.1 *vide infra*, was utilised, due to the lower solubility of heteroaryl boronic acids in acetonitrile. The proportion of methanol present successfully facilitates fluoride complexation to **2**, thereby ensuring its complete conversion upon addition of **3**. Due to the basic nitrogen, **2af** was initially isolated as a mixture of the potassium salt and the internal salt (quinoliniumtrifluoroborate), as confirmed by elemental analysis. Treatment with K_2CO_3 (acetone, room temp, 10 min) readily deprotonated any internal salts to the desired product.

Upon increasing the scale 18 fold (18 mmol), **2p** and **2u** were cleanly converted to trifluoroborates **1p** and **1u** in an improved 95 % (3.9 g) and >99 % (4.2 g) yield respectively. This demonstrates the potential utility of this new procedure towards industrial application. Furthermore, as isolation *via* filtration is preferred on large scale, rather than evaporation of the filtrate, an anti-solvent e.g. Et_2O, can be slowly added to crystallise the R-BF_3K salt from the filtrate.

To confirm that precipitation of bitartrate **52** was responsible for the stoichiometric requirement of tartaric acid (**3**), *o*-iodobenzoic acid (**53**) was titrated into a solution of **2a** in acetonitrile and $KF_{(aq)}$ (4 equiv.). **53** exhibits a similar p*K*a (2.9) to **3** (3.0), but the conjugate base (potassium *o*-iodobenzoate **54**) was expected to be more soluble than potassium bitartrate (**52**) in the reaction medium. Indeed, the use of this acid required 4 equivalents to reach complete conversion, thus supporting the conclusion that a precipitation-driven equilibrium is in operation.

2.2.3 Purity Comparison

To check inorganic (e.g. KF or KHF_2) contamination, the purity of **1aa** was compared with samples prepared *via* the KHF_2 route, KF/tartaric acid route and with commercial material. To reach complete conversion, this substrate required a larger excess of KF (4.5 equiv.) and tartaric acid (**3**; 2.5 equiv.) thereby providing the worst case scenario in terms of possible contaminants. The KHF_2 and KF/tartaric acid methods were run in parallel, gave isolated yields of 86 and 87 % respectively, and were assessed by elemental analysis. All samples being compared were close to that calculated; however, pleasingly the KF/tartaric acid method gave the purest product in the best yield, Table 2.6.

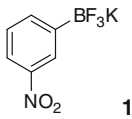

1aa

Table 2.6 Comparison of the purity of **1aa** prepared from the two routes

	Found C	Found H	Found N
Commercial	30.19	1.84	5.73
KHF_2	31.90	1.79	5.93
KHF_2[a]	31.31	1.80	5.67
KF/Tartaric acid	31.64	1.78	5.98
	Calc'd C	Calc'd H	Calc'd N
$C_6H_4BF_3KNO_2$	31.47	1.76	6.12

[a] From Ref. [32]

2.2.4 Glassware Etching

The newly developed KF/tartaric acid procedure avoids the *in vacuo* removal of large volumes of water and the often laborious series of acetone extractions necessary in the KHF_2 method to isolate the pure R-BF_3K salts. Furthermore, the use of KHF_2 is notorious for the etching it effects on regular glassware, producing irreversible damage. To test how the KF/tartaric acid methodology and the KHF_2 method compared in this regard, **1a** was repeatedly prepared (0.75 mmol scale) by each method in two brand new 25 mL round bottomed flasks. The KHF_2 method was repeated 20 times and the KF/tartaric acid method 30 batch times, Figs. 2.2 and 2.3.

There was no trace of clouding in the glass of the round bottomed flask from reactions undertaken using the KF/tartaric acid method, Figs. 2.2 and 2.3. In contrast, the flask used for the KHF_2 method was severely etched. When each method was compared *in situ* (^{19}F NMR), in PTFE vessels so as to not consume

Fig. 2.2 The *left* hand flask has had 30 batch reactions using the KF/tartaric acid method to synthesise **1a** from **2a**, and the *right* hand flask has had 20 batch runs using the KHF_2 method to synthesise **1a** from **2a**

Fig. 2.3 The *left* hand flask has had 30 batch reactions using the KF/tartaric acid method to synthesise **1a** from **2a**, and the *right* hand flask has had 20 batch runs using the KHF_2 method to synthesise **1a** from **2a**

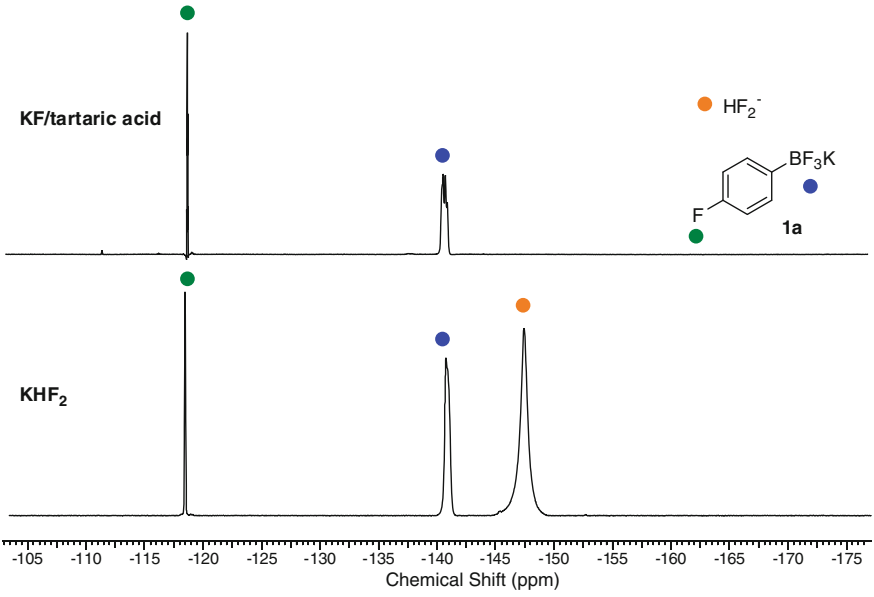

Fig. 2.4 ^{19}F NMR spectra of the *in situ* preparation of **1a** *via* the KF/tartaric acid and KHF_2 methods conducted in PTFE. HF_2^- is clearly observed ($\delta_F = -147$ ppm) in solution in the KHF_2 method but is absent in the KF/tartaric acid method. The chemical shift (δ_F) of KHF_2 is highly dependent on the water content of the solution and ranges, in our hands, from −180 to 139 ppm

any HF by glass, a large peak was observed for the HF_2^- anion in the KHF_2 method, but not the KF/tartaric acid method, Fig. 2.4.

When KF is subjected to an acidic medium it will form KHF_2 *in situ,* Scheme 2.13. But due to the complexation of fluoride to boronic acid and the slow addition of tartaric acid (**3**) to push the equilibrium to the right, this process is

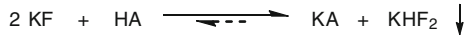

Scheme 2.13 The *in situ* formation and precipitation of KHF_2 in acetonitrile/THF

avoided. However, any excess KF (1 equiv.) and **3** (5 %) will combine to form KHF_2 (5 %).

Under the optimised solvent system (CH_3CN/THF) any KHF_2 generated was shown to precipitate out of solution, Scheme 2.13, as is indicated by ^{19}F NMR analysis of the filter cake, and is therefore considered to be unproblematic. Whilst **1a** was prepared from **2a** *via* the KHF_2 route, it was observed that the aqueous stock solution of KHF_2 was considerably more etching than the overall reaction in methanol containing **2a**. In contrast, aqueous stock solutions of KF and **3** in THF are both completely non-etching.

2.3 Preparation of R-BF_3K Salts from Boronic Esters

2.3.1 Pinacol Esters

2.3.1.1 Optimisation

The conditions optimised for boronic acids (4 equiv. $KF_{(aq)}$, 2.05 equiv. $\mathbf{3}_{(THF)}$, CH_3CN) were employed for the conversion of 4-fluorophenylboronic acid pinacol ester **4a**–**1a**. Although the desired product was synthesised, nearly a stoichiometric amount of pinacol remained after filtration and evaporation. When KHF_2 is employed for the preparation of R-BF_3K salts, there are two general methods to purify the product from pinacol: firstly, Hartwig [12] demonstrated that it could be 'sublimed' (6 mTorr, 60 °C) from a mixture containing R-BF_3K (which melt or decompose at temperatures greater than 250 °C). Secondly, Aggarwal [33] demonstrated that pinacol forms an azeotrope with methanol/water, and by the repetitive addition and evaporation of the solvents, it can be removed from a mixture containing the R-BF_3K salt and excess KHF_2. The number of cycles varied from 1 to 9 and depended on the substrate and precise make-up of the azeotrope.

The Aggarwal procedure was initially tested, by the repetitive addition and evaporation of methanol/water (4:1), to the concentrated filtrate, containing only a mixture of pure R-BF_3K and pinacol. However, due to the solvolytic conditions, hydrolysis to boronic acid **2a** occurred, which condensed with pinacol to reform the starting material. Under the KHF_2 conditions, refluorination of hydrolysed boronic acid by the excess KHF_2 present, results in complete conversion to the R-BF_3K salt as pinacol is slowly removed. Hartwig's 'sublimation' procedure was more effective, as the anhydrous, non-solvolytic conditions left only pure R-BF_3K salt. However, contrary to the original report, pinacol was observed to melt, then

Table 2.7 Variation of the equivalents of added KF and tartaric acid (**3**) in the reaction of **4a** to **1a**

Entry	KF/equiv.	Tartaric acid/equiv.	Conversion (→ 1a)/ %[a]
1	4	2.05	84
2	5	3	95
3	5.5	3.5	85

[a] % **1a** ($\delta_F = -118.8$ and -141 ppm) by ^{19}F NMR

evaporate and condense as a liquid, rather than a solid; therefore 'evaporation' not 'sublimation' is a more precise description of the process. Aggarwal reported the Hartwig procedure did not work in the presence of KHF_2, implying that strong hydrogen bonding between KHF_2 and pinacol attenuated its thermolytic removal.

With the purification method established, the loadings of KF and **3** were screened in the conversion of **4a**–**1a** (0.25 mmol scale) under the conditions optimised for boronic acids, Table 2.7.

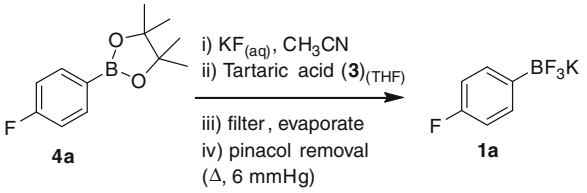

An increase in the stoichiometry of KF and **3** did not directly correlate with an increase in the conversion to **1a**. When the methodology, employing 5.5 equiv. KF and 3.5 equiv. **3**, was scaled up (1 mmol scale), incomplete conversion (82 %) again resulted, highlighting the capriciousness of the current protocol.

Analysis (^{19}F and ^{11}B NMR) of a solution of boronic ester **4a** containing 4 equiv. $KF_{(aq)}$ in CH_3CN indicated no complexation of fluoride to **4a**. By comparison, fluoride complexation to the more Lewis acidic boronic acid **2a** was observed, Fig. 2.5, under the same conditions. The greater Lewis acidity must aid fluoride transfer from the aqueous biphase, Fig. 2.6.

Under these non-complexing conditions of **4a**, the addition of tartaric acid (**3**) is likely to generate/precipitate KHF_2 out of solution, thus leading to the decreased conversions. It was also observed that the bitartrate (**52**) precipitate was more physically defined by the aqueous biphase and thus less mobile in the stirred reaction vessel. This latter problem will further restrict the solubility of KF in the organic phase due to the loss of water to the bitartrate/KHF_2 cluster. Therefore, bringing the KF into solution by moving to a more homogeneous solvent system would alleviate these issues.

Analysis (^{19}F and ^{11}B NMR) of **4a** treated with 4 equiv. $KF_{(aq)}$ in pure methanol indeed showed complete consumption of the starting material to give two unknown 'ate' species. Returning to the loadings of KF (4 equiv.) and tartaric acid (2.05 equiv.) employed for boronic acids, but switching the solvent system to methanol,

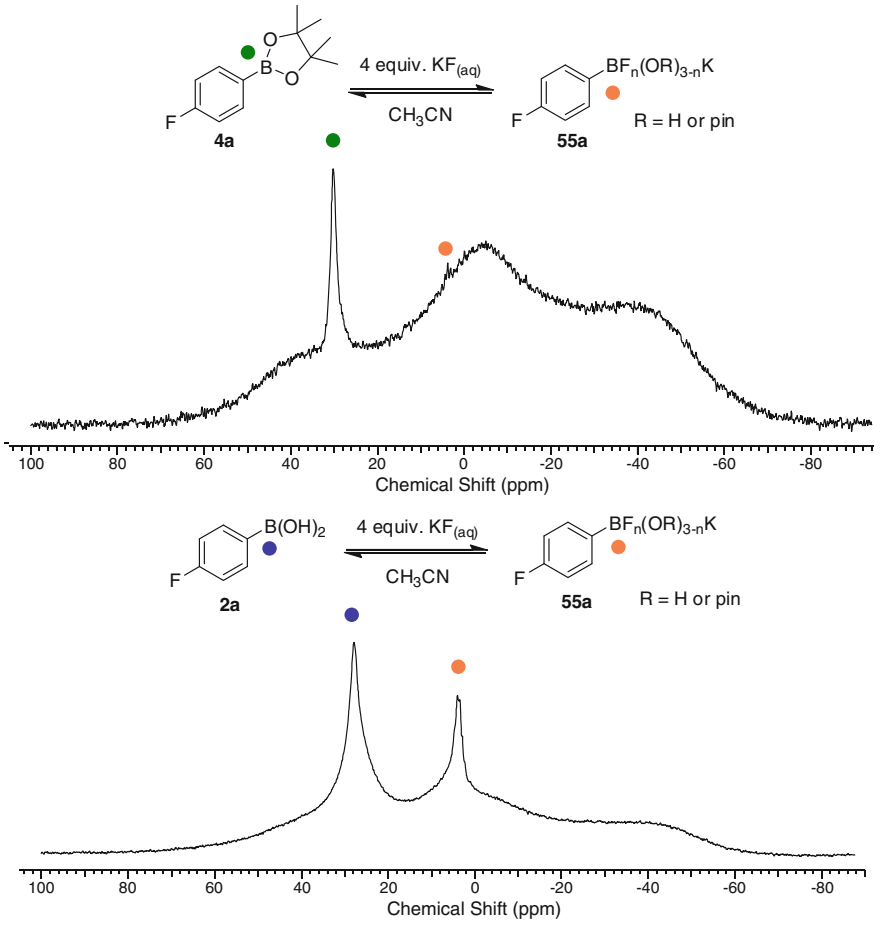

Fig. 2.5 Upper ^{11}B NMR spectrum: KF addition to pinacol ester **4a** in CH_3CN, indicating no significant complexation of fluoride. Lower ^{11}B NMR spectrum: KF addition to boronic acid **2a** in CH_3CN, indicating complexation of fluoride to form mixed fluoro/pinacol ester **55a**. Baseline due to background borosilicate glass signals

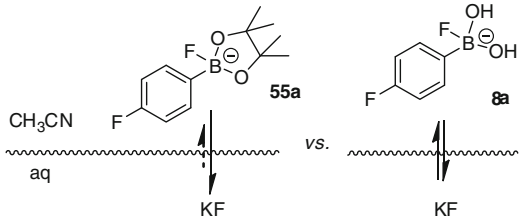

Fig. 2.6 The increased Lewis-acidity of boronic acid **2a** aids complexation of F^- from the aqueous biphase to form mixed fluoro/hydroxy species **8a**

gave 87 % conversion to product **1a** from **4a**. Unfortunately, as previously noted, problems associated with the flocculation of bitartrate **52** in methanol occurred, but was found to improve with substantial dilution with CH_3CN. In addition, generation of stable methoxylated 'ate' species (**51a**) hampered complete conversions; therefore a balance between CH_3CN and CH_3OH was clearly sought

Partial complexation of fluoride to **4a** was observed (^{19}F NMR, ^{11}B NMR) in a 9:1 CH_3CN:CH_3OH system. However, when test reactions were scaled up to (1 mmol,) 4-acetylphenylboronic acid pinacol ester (**4ae**) was again incompletely converted (80 %) to the corresponding trifluoroborate salt **1ae**. This was due to problems of **52** precipitations leading to KHF_2 generation/precipitation. A ratio of 3:1 CH_3CN:CH_3OH was tested only to exhibit a better, but similar outcome.

2.3.1.2 Optimised Procedure for the Preparation of R-BF_3K Salts from Pinacol Esters

A mixture of 1:1 CH_3CN:CH_3OH, allowed for fluoride complexation of **4a** to give two species (^{11}B NMR), Fig. 2.7, and complete conversion to **1a** was observed upon addition of 2.05 equiv. **3**. Subsequent dilution with CH_3CN aided flocculation and effected precipitation of all co-products and excess reagents.

The conditions were tested on alkyl, allylic and electron rich and poor aryl systems, which were all cleanly converted to the corresponding R-BF_3K salts, Table 2.8. Reactions were instantaneous, allowing isolation of the R-BF_3K/pinacol mixture less than 20 min. The majority (>90 %) of the pinacol could be evaporated in 5 min (6 mmHg, gentle heat), but a further 15–20 min heating was found to be necessary to ensure good purity.

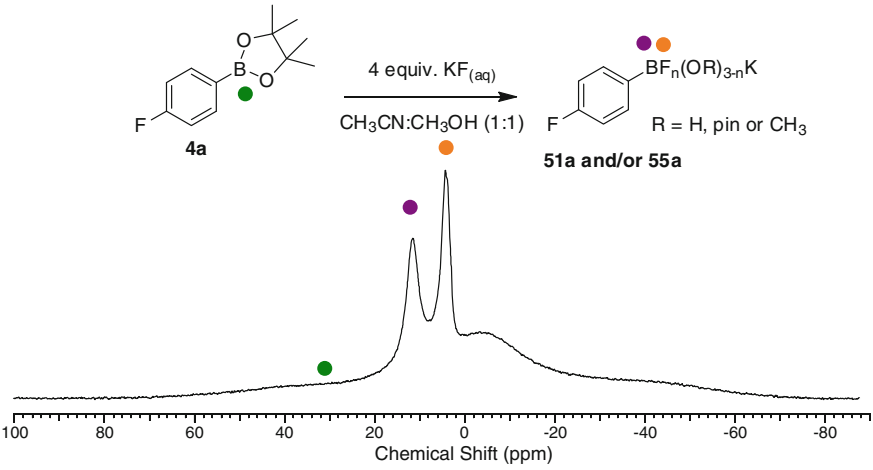

Fig. 2.7 ^{11}B NMR spectrum of KF addition to **4a** in CH_3CN:CH_3OH (1:1), showing its complete consumption to form two mixed species (**51a** and/or **55a**). Baseline due to background borosilicate glass signals

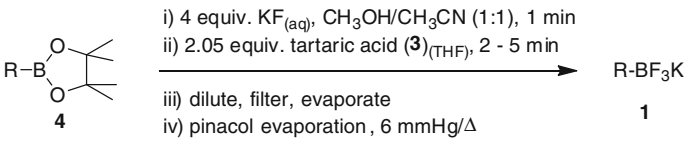

Table 2.8 The preparation of a range of R-BF_3K salts from pinacol esters

R-BF_3K (1)	R =	Isolated yield[a] /%	R-BF_3K (1)	R =	Isolated yield[a] /%
1a	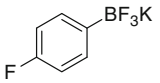	94	**1ab**	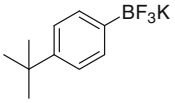	95
1w	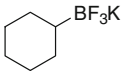	83	**1ai**	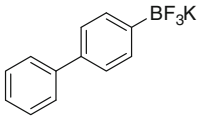	72
1aa	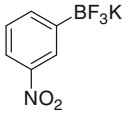	89	**1aj**	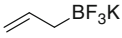	75

[a] Isolated yield of analytically pure R-BF_3K

2.3.2 *Methyl/Isopropyl Esters Prepared In Situ*

Application of the KF/tartaric acid methodology to the *in situ* generated methyl (**37**) or isopropyl (**38**) boronate esters, Scheme 2.6, would provide another useful route to R-BF_3K salts. To ensure ease of isolation, the lithium/magnesium salts would ideally co-precipitate with potassium bitartrate (**52**), thus leaving a simple filtration to yield pure R-BF_3K salt. As protonation of the additional alkoxy ligand on the intermediate boronate ester is required, the stoichiometry in tartaric acid (**3**) necessitated adjustment; the loadings of both KF (5 equiv.) and **3** (3.05–3.5 equiv.) were thus increased.

Unfortunately, all attempts at preparing potassium vinyltrifluoroborate (**1k**) from vinyl magnesium bromide (**43**) failed, Scheme 2.14. Possible explanations include the instability of the intermediate fluorinated 'ate' species towards **3**, or alternatively, possible magnesium interference with fluoride (MgF_2 generation). More encouraging was the formation of potassium phenyltrifluoroborate (**1d**) from phenyllithium (**40**), but purification *via* recrystallisation was required, which reduced the yield. Finally, phenylacetylene (**41**) was smoothly converted to potassium phenylethynyl trifluoroborate (**1c**) in a reasonable 48 % yield,

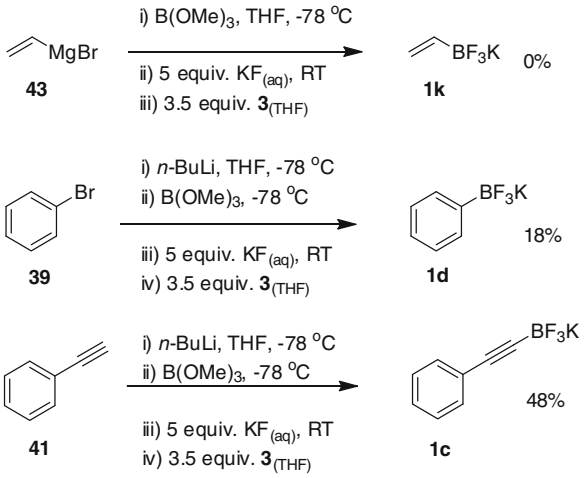

Scheme 2.14 Preparation of R-BF_3K salts from *in situ* generated boronate esters

Scheme 2.14. For comparison, the KHF_2 method generated the product in a 32 % yield, possibly inferring complications in the formation of the intermediate boronate ester **37c**, rather than the organotrifluoroborate salt **1c**.

These unoptimised results clearly demonstrate the potential for the process, but presently, further investigation is required in warranting it a useful procedure.

2.4 Preparation of R-BF_3^- Salts with Different Counter Cations

2.4.1 Cesium Salts

2.4.1.1 Prepared from Boronic Acids

As noted above, the solubility of organotrifluoroborate salts can be manipulated and tuned to a process by modification of the counter cation. Cesium salts in particular offer the same free-flowing crystalline physical properties as potassium but dissolve more readily into apolar solvents. By switching KF for CsF it was envisaged that the corresponding cesium organotrifluoroborate salt (**5**) could be formed. Pleasingly, on three substrates of varying electron demands, good to excellent isolated yields of pure (elemental analysis) **5** were observed, Table 2.9. Cesium bitartrate (**56**, identity confirmed by ^1H NMR and elemental analysis) was found to be equally insoluble under the reaction conditions, which drives the equilibrium, Scheme 2.11, towards **5**.

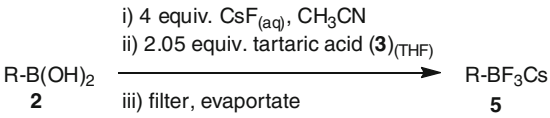

Table 2.9 The preparation of R-BF_3Cs salts from boronic acids

R-BF_3Cs (5)	R =	Isolated yield[a] /%
5p	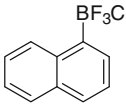	87
5r	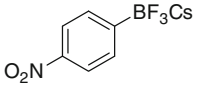	84
5z	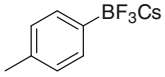	94

[a] Isolated yield of analytically pure R-BF_3Cs

2.4.1.2 Prepared from Pinacol Esters

Preparation of cesium organotrifluoroborate salts (**5**) from boronic acid pinacol esters (**4**) would demonstrate the wider application of the KF/tartaric acid methodology. The same procedure (CH_3CN:CH_3OH, 1:1, followed by dilution with CH_3CN) employed for the generation of **1a** from **4a**, was initially attempted. Pleasingly, complete conversion was achieved, although the increased solubility of CsF in CH_3CN:CH_3OH (1:1) caused it to contaminate the R-BF_3Cs salt (**5a**), after concentration of the filtrate. A reduction in the proportion of methanol (9:1 CH_3CN:CH_3OH) was found to successfully avert CsF contamination, whilst still enabling complexation of fluoride to **4a** to ensure complete conversion, Scheme 2.15. Analogous to the preparation of **1a** from **4a**, when solely CH_3CN was employed, incomplete conversions resulted.

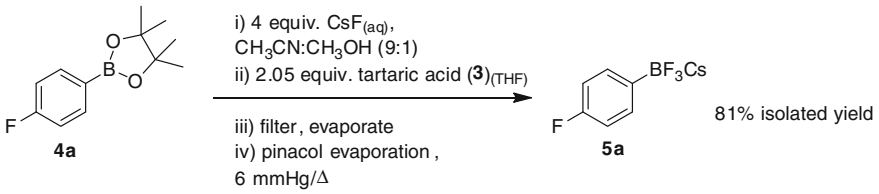

Scheme 2.15 Preparation of **5a** from **4a** using the newly developed KF/tartaric acid methodology

2.4.2 Sodium Salts

2.4.2.1 Prepared from Boronic Acids

In a similar vein to the cesium organotrifluoroborate salts (**5**), sodium organotrifluoroborates (**48**) have a characteristically different solubility to their potassium analogues. By switching KF for NaF in the general procedure, Scheme 2.12, it was envisaged that the sodium salt could be isolated *via* sodium bitartrate (**57**) precipitation/filtration.

Studies were conducted using 1-naphthyl boronic acid (**2p**), $NaF_{(aq)}$ (4 equiv.) in acetonitrile followed by treatment with tartaric acid (**3**) in THF. Upon the addition of 2 equivalents of tartaric acid (**3**), only naphthalene (**58**) was isolated. It was proposed that disodium tartrate formed, thus necessitating only 1 equivalent of **3**. Unfortunately, although *in situ* analysis (^{19}F and ^{11}B NMR) indicated formation of sodium 1-naphthyl trifluoroborate (**48p**), with one equivalent of **3**, **48p** could not be isolated in pure form. Elemental analysis of the precipitate was not indicative of either mono or disodium tartrate, suggesting significant contamination by NaF, possibly through poor solubility in the organic phase. Although various sodium organotrifluoroborate salts (**48**) have been prepared [27, 30], there are no specific reports on the stability of **48p**. Alternatively, if the sodium cation is not sufficiently soluble in the organic phase, then a hydronium cation could be neutralising the naphthyl trifluoroborate anion, as observed (^{19}F and ^{11}B NMR) *in situ*. The hydronium coordinated organotrifluoroborate salts (**59**) are known to be unstable upon isolation [27].

2.5 Summary

A new methodology for the preparation of potassium (**1**) and cesium (**5**) organotrifluoroborates has been developed, employing KF and tartaric acid (**3**) in a completely non-etching and operationally simple manner. Boronic acids (**2**) and pinacol esters (**4**) are accommodated as starting materials in the procedure, which is rapid and can be conducted at room temperature with bench grade solvents. A wide range of organic moieties proceeded well, giving good to excellent isolated yields of pure R-BF_3K/Cs. The procedure was shown to scale-up proficiently, proving its potential for both academic and industrial application.

References

1. D.L. Fowler, C.A. Kraus, J. Am. Chem. Soc. **62**, 1143–1144 (1940)
2. R.D. Chambers, H.C. Clark, C.J. Willis, J. Am. Chem. Soc. **82**, 5298–5301 (1960)
3. S.L. Stafford, Can. J. Chem. **41**, 807–808 (1963)

4. R. D. Chambers, T. Chivers, D. A. Pyke, J. Chem. Soc. 5144–5145 (1965)
5. T. Chivers, Can. J. Chem. **48**, 3856–3859 (1970)
6. D. Kaufmann, G. Bir, W. Schacht, J. Organomet. Chem. **340**, 267–271 (1988)
7. E. Vedejs, R.W. Chapman, S.C. Fields, S. Lin, M.R. Schrimpf, J. Org. Chem. **60**, 3020–3027 (1995)
8. D. Thierig, F. Umland, Naturwiss. Unterr. Chem. **54**, 563 (1967)
9. M. Shimizu, C. Nakamaki, K. Shimono, M. Schelper, T. Kurahashi, T. Hiyama, J. Am. Chem. Soc. **127**, 12506–12507 (2005)
10. J.L. Stymiest, V. Bagutski, R.M. French, V.K. Aggarwal, Nature **456**, 778–782 (2008)
11. T. Ishiyama, M. Murata, N. Miyaura, J. Org. Chem. **60**, 7508–7510 (1995)
12. J.M. Murphy, C.C. Tzschucke, J.F. Hartwig, Org. Lett. **9**, 757–760 (2007)
13. C.A. Hutton, A.K.L. Yuen, Tetrahedron Lett. **46**, 7899–7903 (2005)
14. J.-P. Genet, S. Darses, G. Michaud, Eur. J. Org. Chem. 1875–1883 (1999)
15. N.A. Petasis, A.K. Yudin, I.A. Zavialov, G.K.S. Prakash, G.A. Olah, Synlett **1997**, 606–608 (1997)
16. T. Ohmura, Y. Yamamoto, N. Miyaura, J. Am. Chem. Soc. **122**, 4990–4991 (2000)
17. G.A. Molander, L.A. Felix, J. Org. Chem. **70**, 3950–3956 (2005)
18. G.A. Molander, T. Ito, Org. Lett. **3**, 393–396 (2001)
19. G.A. Molander, P.E. Gormisky, J. Org. Chem. **73**, 7481–7485 (2008)
20. R.A. Batey, A.N. Thadani, D.V. Smil, A.J. Lough, Synthesis **2000**, 990–998 (2000)
21. R.A. Batey, A.N. Thadani, D.V. Smil, Tetrahedron Lett. **40**, 4289–4292 (1999)
22. H.J. Frohn, V.V. Bardin, Z. Anorg. Allg. Chem. **627**, 15–16 (2001)
23. H.-J. Frohn, V.V. Bardin, Z. Anorg. Allg. Chem. **627**, 2499–2505 (2001)
24. A.M. Dumas, J.W. Bode, Org. Lett. **14**, 2138–2141 (2012)
25. G.A. Molander, J. Ham, Org. Lett. **8**, 2031–2034 (2006)
26. G.A. Molander, P.E. Gormisky, D.L. Sandrock, J. Org. Chem. **73**, 2052–2057 (2008)
27. R.A. Batey, T.D. Quach, Tetrahedron Lett. **42**, 9099–9103 (2001)
28. G. K. S. Prakash, F. Pertusati, G. A. Olah., Synthesis, 292–302 (2011)
29. D.S. Matteson, D. Maliakal, P.S. Pharazyn, B.J. Kim, Synlett 2006, 3501–3503 (2006)
30. N. Murai, M. Miyano, M. Yonaga, K. Tanaka, Org. Lett. **14**, 10–13 (2012)
31. G.A. Molander, S.L.J. Trice, S.D. Dreher, J. Am. Chem. Soc. **132**, 17701–17703 (2010)
32. G.A. Molander, B. Biolatto, J. Org. Chem. **68**, 4302–4314 (2003)
33. V. Bagutski, A. Ros, V.K. Aggarwal, Tetrahedron **65**, 9956–9960 (2009)

Chapter 3
Organotrifluoroborate Coupling

3.1 Introduction

3.1.1 Suzuki–Miyaura Cross-Coupling

Metal-catalysed cross-coupling reactions have revolutionised organic synthetic application by providing simple solutions to complex retrosynthetic problems. The ease and practical utility of conjoining different building blocks *via* a carbon–carbon bond has many advantages over more traditional approaches. Palladium is particularly primed for this type of reactivity, and stands out from all metals under this regard, due to its facile access to useful oxidation states. In addition, the propensity for palladium(0) to undergo oxidative addition with cheap, commercially available, electrophilic organohalides has provided numerous avenues for the development of nucleophilic partners, therefore establishing a vast array of cross-coupling opportunities. These include organometallic reagents such as Kumada's Grignard reagents [1], Negishi's [2] use of organozinc reagents and organotin reagents developed by Stille [3]. Alternatively, the electron rich unsaturation of olefins, as developed by Heck [4, 5], are sufficiently nucleophilic, as is Sonogashira's [6] exploitation of basic terminal alkynes. Finally, organometalloid compounds such as Hiyama's [7] organosilanes and Suzuki's [8] organoboronic acid's undergo facile cross-coupling, Scheme 3.1. Recognition of the importance of this area was made recently in awarding three influential pioneers, Heck, Negishi and Suzuki, the 2010 Nobel Prize for chemistry.

Of the range of palladium-catalysed cross-coupling reactions available, Scheme 3.1, the Suzuki–Miyaura (SM) coupling reaction is arguably the standout transformation. This is primarily due to its exceptional functional group tolerance and its mild, cheap, scalable and environmentally benign nature, unlike, for example, the Stille reaction which generates toxic tin by-products. It has become the "gold standard" for biaryl construction, which has arguably resulted in the ubiquity of this moiety in modern medicinal chemistry [9]. In particular, heteroatomic biaryls appear in many "blockbuster" drug molecules, Fig. 3.1.

A. J. J. Lennox, *Organotrifluoroborate Preparation, Coupling and Hydrolysis*, Springer Theses, DOI: 10.1007/978-3-319-01134-9_3,

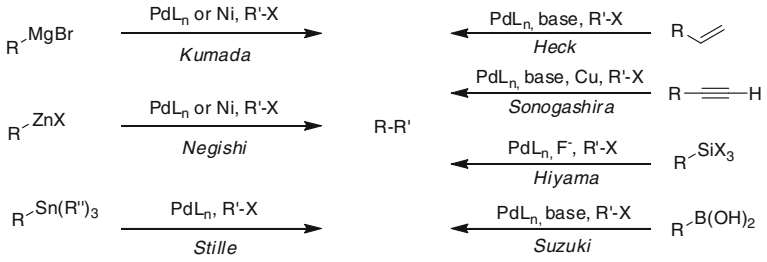

Scheme 3.1 Palladium-catalysed cross-coupling reactions

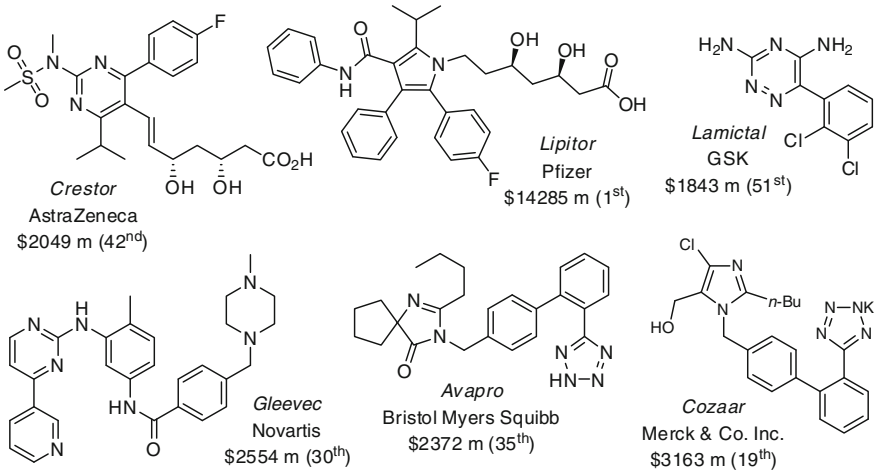

Fig. 3.1 "Blockbuster" drugs with biaryl moieties. Figures in *brackets* are overall rank based on stated revenue in 2006

The SM coupling reaction has undoubtedly passed the test of time, unlike many of its contempories e.g. the Stille coupling [10]. However that is not to say it has stagnated since its discovery, indeed quite the opposite has occurred. A vast array of developments have occurred, from expansion of the substrate scope to include unactivated aryl chlorides [11] and sterically demanding substrates [12], to reducing the catalyst loadings [13] to "homeopathic" [14] levels and lower reaction temperatures [15, 16].

3.1.1.1 Mechanism of SM Coupling

The mechanism of the Suzuki–Miyaura coupling reaction is one of the simplest exhibited by a catalytic organometallic reaction. The three major events are: an oxidative addition followed by transmetalation and reductive elimination, which

Scheme 3.2 The generally accepted SM coupling catalytic cycle

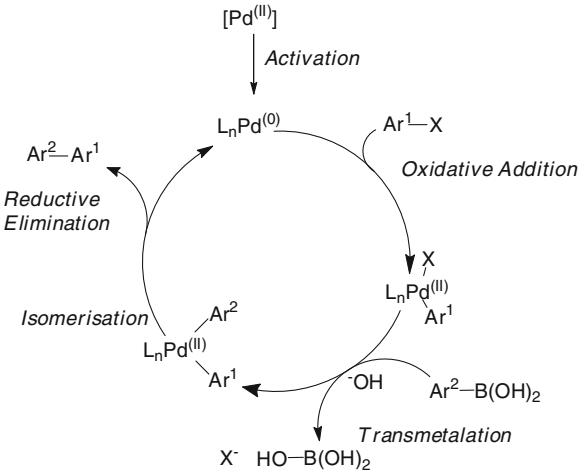

gives the cross-coupled product and recycles the active palladium(0) catalyst, Scheme 3.2.

The storage of active palladium(0) complexes often leads to catalyst decomposition *via* ligand oxidation. Therefore, the active metal species is generally reduced *in situ*, from a more stable palladium(II) precatalyst. This generates a free coordination site on the more electron rich metal centre, which can then participate in an oxidative addition event with an organohalide or pseudohalide, e.g. OTf. The ease of insertion into the polarised covalent bond is proportional to the bond dissociation enthalpy, therefore I > OTf > Br ≫ Cl. Electron withdrawing groups in a conjugated system, e.g. arylhalide, can also facilitate this process by removing electron density from the halide, thereby weakening the bond. Inductively this effect can also aid association to the electron rich metal centre. Oxidative addition is frequently considered to be turnover limiting; therefore the use of very electron rich ligands, such as trialkylphosphines [11], can be used to promote this step. In this way, organochlorides [11], which are the cheapest but least reactive organohalide (with the exception of organofluorides), can participate in cross-coupling reactions.

Organoboronic acids containing electron rich moieties undergo the subsequent transmetalation with the oxidised palladium(II), more readily than electron poor moieties. Base is essential for efficient turnover, but mechanistically its precise role in transmetalation is ambiguous, and has been the subject of much debate [17, 18]. It is known that hydroxide can act as a μ-bridge to guide the organic group towards the palladium centre. However, preceding this facilitation, discussion surrounds whether the hydroxide activates the boronic acid (***I***, Scheme 3.3), through coordination to give a more nucleophilic boronate species, or, the metal (***II***, Scheme 3.3), *via* exchange of the halide on the palladium(II) centre to generate an oxo-palladium species, Scheme 3.3.

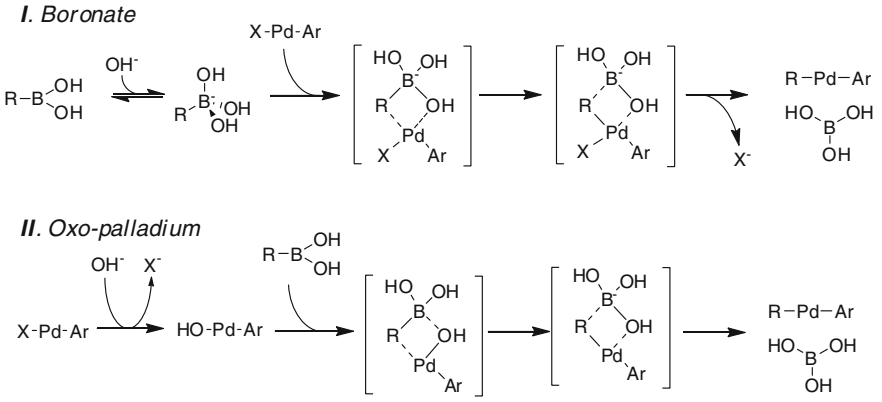

Scheme 3.3 Two possible pathways of transmetalation

An understanding of these conflicting mechanisms would naturally aid optimisation; by tuning the conditions to facilitate the correct pathway. However, this elucidation is not straightforward: Suzuki [18] and Miyaura [7] have independently stated that either pathway is possible, although they acknowledge from Linear Free Energy Relationship (LFER) analysis that the 'boronate' pathway is more likely. Matos and Soderquist's [19] kinetic study similarly concluded transmetalation could proceed *via* both pathways depending on the affinity of hydroxide to boron. Through DFT calculations of each route, Maseras [20] found the '*boronate*' pathway was more favourable on a model reaction. However, three independent studies from the groups of Jutand [21], Hartwig [22] and Schmidt [23] have all recently concluded that the '*oxo-palladium*' pathway is *kinetically* the most likely. Jutand optimised conditions for the kinetic analysis (cyclic voltammetry) of the redox reactions of various on-cycle intermediates, and concluded the base played two roles in transmetalation: firstly, through halide exchange with the product of oxidative addition (Ar-Pd-X) to form the active Ar-Pd-OH species, and secondly, in the deceleration of transmetalation *via* formation of inactive aryl trihydroxyboronate (**60**). Hartwig's [22] and Schmidt's [23] independent kinetic studies drew the same conclusions; that a neutral boronic acid reacts with an oxo-palladium species.

A further study on the transmetalation event from Jutand [24] demonstrated that the counter-cation, which is inevitably added with the anionic base, has a decelerating affect on the overall rate. This was proposed to be due to a deactivating coordination to Ar-Pd-OH; whereby the least coordinating anion led to the greatest rate: $NBu_4^+ > K^+ > Cs^+ > Na^+$. Finally, an analogous study was performed on the effect of fluoride in the system under anhydrous conditions, which verified it could exhibit similar reactivity to hydroxide [25].

Post-transmetalation, the complex undergoes a series of ligand dissociation and association events to isomerise the *trans* complex to *cis,* which can then undergo reductive elimination. Typically reductive elimination is rapid, especially with

bulky ligands which sterically enhance the step. Jutand [21] elucidated an interesting and important role of the base in reductive elimination: it was found to accelerate the step *via* formation of a penta co-ordinated intermediate, Scheme 3.4, thus by-passing the requirement for a formal isomerisation of ligands, *via* Berry pseudorotation.

The coordinatively unsaturated palladium(0) complex is recycled and is available to undergo further catalytic cycles.

Scheme 3.4 Hydroxide promoted reductive elimination

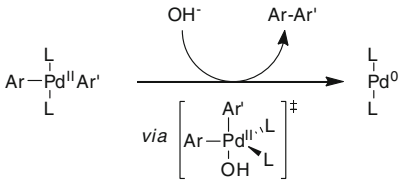

3.1.2 Potassium Organotrifluoroborates as Substrates

3.1.2.1 Organotrifluoroborates Verses Organoboronic Acids

Potassium organotrifluoroborate ($R\text{-}BF_3K$) salts have generated considerable interest in the last two decades as substrates in SM coupling reactions [26–29]. Their advantages over the traditionally used boronic acids come in both their physical and chemical nature. Physically, they are crystalline, free-flowing powders or solids, which are stable to air and moisture, unlike certain boronic acids. Due to the quarternisation at the boron centre, side reactions associated with Lewis base coordination to a Lewis acidic trivalent boron centre, are avoided. This additional stability gives them an advantage over boronic acids in that they are amenable to being "carried" through a synthetic sequence, (Sect. 1.1.2, *vide supra*). The Lewis acidity of boronic acids render them vulnerable functional groups and thus incompatible with many common reagents, as well as undergoing numerous side reactions under the typical conditions of SM couplings. Chemically, $R\text{-}BF_3K$ salts are all monomeric in nature in comparison to boronic acids that readily dehydrate to form cyclic anhydrides, known as boroxines (**61**), Scheme 3.5.

Under the aqueous conditions of a typical SM coupling reaction, any anhydrides present will be hydrolysed, thus reverting back to the boronic acid. However, it is not a straightforward task in determining the levels of boroxines present in solid commercial or prepared material, thereby causing difficulties in establishing the correct stoichiometry for the reaction. Considering these uncertainties, along with the boronic acid vulnerability, it is common place to use an excess of the reagent, which provokes obvious waste related issues.

Scheme 3.5 Dehydration of boronic acids (**2**) to form cyclic boroxines

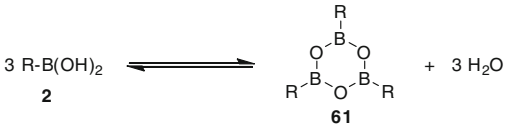

3.1.2.2 Cross-Coupling with Arenediazonium Salts

Genet and Darses were the first to discover that R-BF_3K salts were viable substrates in SM coupling reactions [30]. Their investigations into arenediazonium salts as effective electrophiles in SM coupling reactions initially employed boronic acids as coupling partners [31]. Interestingly, unlike all other reported SM conditions, the use of diazonium salts negates the requirement for base in the reaction. Indeed the addition of base actually caused the diazonium functionality to be reduced, which significantly dropped the yields. Under these base-free conditions it was then shown that successful cross-coupling of the arenediazonium salts with aryl or alkenyl trifluoroborate salts gave superior outcomes to those observed with boronic acids [30]. Under the non-solvolytic conditions of anhydrous dioxane that was employed, direct transmetalation from the more nucleophilic (R-BF_3K > R-$B(OH)_2$) organic group was proposed as being responsible for the enhanced reactivity. Reactions were conducted under mild conditions at room temperature in both cases, Scheme 3.6.

Oxidative addition was chemoselective towards the diazonium moiety when in the presence of other potential bond insertions, e.g. C–Br. Surprisingly it was found to be even more reactive than the very polarisable C–I bond; however, conditions for the SM coupling of organohalide electrophiles do require the use of base.

Frohn extended this methodology in the cross-coupling of the perfluorinated trifluoroborate salts, such as trifluoroethylene and pentafluorophenyl [32] trifluoroborate, with arenediazonium salts. Yields were moderate but conditions were mild for these inherently difficult to couple, electron poor substrates.

3.1.2.3 Iodonium Salts

Chen [33] demonstrated that hypervalent iodonium salts, such as diaryliodonium tetrafluoroborate (**64**), smoothly cross-coupled with aryltrifluoroborate salts under

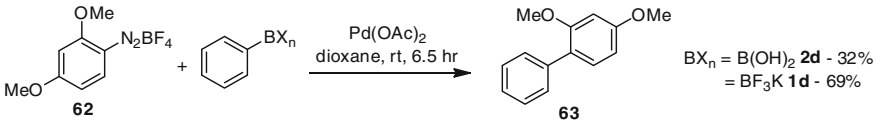

Scheme 3.6 Palladium-catalysed cross-coupling of arenediazonium salt **62** with boronic acid **2d** and trifluoroborate **1d** to give biaryl **63**

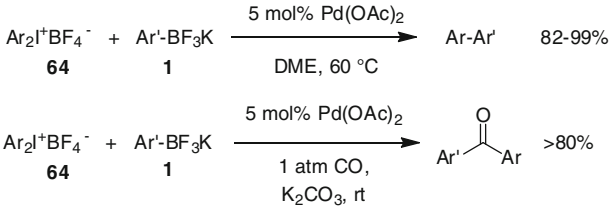

Scheme 3.7 Cross-coupling and carbonylative cross-coupling of iodonium salt **64** with R-BF_3K salts

base-free conditions, Scheme 3.7. The reaction was robust, accommodating various solvents and catalyst precursors, affording high yields in most cases. In the presence of a CO atmosphere and base, a carbonylative coupling predominated. Base was found to be required, to suppress direct coupling, Scheme 3.7. Additionally the tetrafluoroborate anion was shown to play a role in the reaction, but gave better outcomes than chloride or tosylate anions.

3.1.2.4 Organohalides or Triflates

Undoubtedly, due to the ease of preparation and commercial availability, organohalides or pseudo halides, have generated the most interest as electrophilic partners in cross-coupling chemistry. In combination with boronic acids, these reagents cross-couple efficiently, albeit under basic conditions unlike those required for diazonium or iodonium salts. Molander has developed and optimised conditions for a large range of potassium (organo)trifluoroborate/organo halide cross-couplings, including: (aryl)/aryl [34], (heteroaryl)/heteroaryl [35], (aryl)/alkenyl [36], (aryl)/benzyl [37], (alkenyl)/aryl [38], (alkynyl)/aryl [39], (vinyl)/aryl [40], (alkenyl)/alkenyl [41], (alkyl)/aryl [42], (alkyl)/alkyl[43] and (alkyl)/alkenyl [44]. In most cases conditions worked well for a range of substrates, including the electronically demanding combinations of electron rich organo halides with electron poor organotrifluoroborates. The successful couplings of a wide range of heteroaryl halides and organotrifluoroborates facilitate important transformations in medicinal chemical synthesis [35].

These couplings have also been incorporated into a number of different natural product syntheses, including the elegant preparation of Trityrosine (**65**) [45] and Oximidine II (**66**) [46], Fig. 3.2. In both of these examples organotrifluoroborates demonstrated significant advantages in selectivity and yield over the corresponding organoboronic acids.

The transmetalation of alkenyltrifluoroborate salts was found to proceed with retention of configuration when a THF:water mixture was employed [47]. Interestingly, when the solvent was switched to an alcohol, with a different catalyst precursor, this stereoselectivity was attenuated. Unfortunately no rationale was provided into the underlying mechanistic reasons behind these observations.

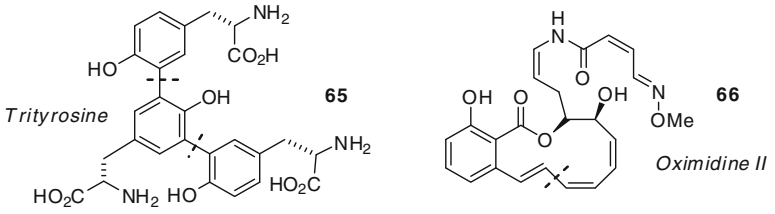

Fig. 3.2 R-BF_3K salts have been used in cross-coupling (*dashed lines*), for the syntheses of natural products **65** and **66**

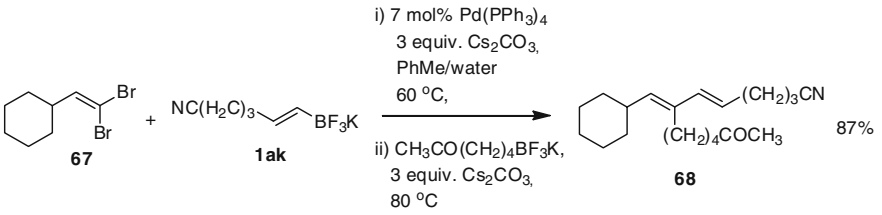

Scheme 3.8 Stereoselective trisubstituted alkene **68** preparation from **67** and **1ak**

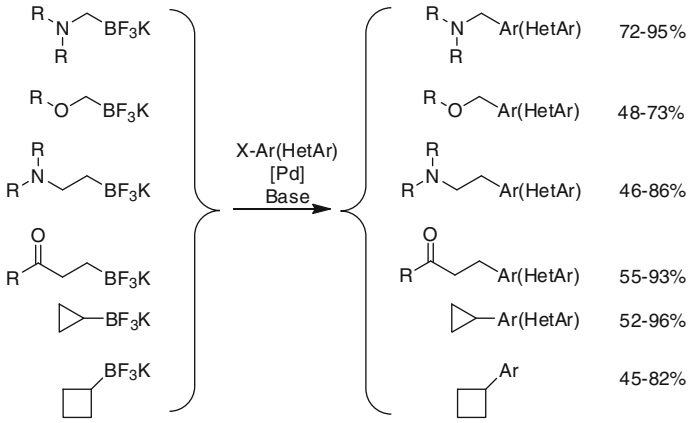

Scheme 3.9 SM coupling of pharmacologically important alkyl moieties

Molander exploited this selective transmetalation, and the stereo-preference of oxidative addition for *E*-alkenylbromides, in the sequential cross-coupling of 1,1-dibromoalkenes [48]. Excellent yields of stereo-defined conjugated dienes were achieved in "one-pot", Scheme 3.8.

The cross-coupling of sp [3] systems has always been problematic due to an inherently slower transmetalation, instability towards protodeboronation, and a competitive β-hydride elimination side reaction. Employing R-BF_3K substrates,

which show relative resistance to protodeboronation, and a suitable catalyst system, to outcompete β-hydride elimination with reductive elimination, these problems could be attenuated, and a number of successes have been show-cased. For example, the pharmacologically important aminomethyl [49] and alkoxymethyl [50] motifs were found to be suitable nucleophilic partners for couplings with a range of aryl/heteroaryl bromides and chlorides. Additionally, conditions for the incorporation of aminoethyl [51], 3-oxoalkyl [52] and cyclobutyl/propyl [53] functionalities have been optimised, Scheme 3.9.

3.1.3 Mechanistic Investigations

3.1.3.1 Chemical Superiority of R-BF_3K Reagents

Considering the physical contributions R-BF_3K salts provide as reagents, they have great potential of becoming standard reagents in SM coupling if their chemical utility is greater than their competitors. As previously noted, Genet described their increased reactivity with arenediazonium salts under non-solvolytic conditions [30]. However, under the basic conditions, typical of SM couplings with organohalides, there are also a number of reports where the R-BF_3K salt achieved higher yields than the corresponding boronic acid or ester. For example, in the preparation of trityrosine (**65**) [45], Fig. 3.2, all attempts made employing pinacol esters resulted in failure, in contrast to those made with R-BF_3K salts, which were successful. In addition, homocoupling of indolylboronic acids is prevalent and causes low yielding cross-couplings. With a switch to an indolyltrifluoroborate salt, Sekine et al. [54] were able to improve yields of their coupling with a heteroaryliodide from 37 to 60 %. Likewise, Meggers et al. [55] observed improved yields in their switch to a R-BF_3K salt, Scheme 3.10.

Therefore, in addition to the monomeric nature of R-BF_3K salts, they appear to be the superior SM coupling reagent due to the reported higher yields and cleaner reactions [27]. In 1,2 and 1,4 rhodium-catalysed conjugate additions, Batey [56] has also reported a greater reactivity of the organotrifluoroborates compared to the boronic acids. Higher yields and a greater tolerance of functional groups were also noted.

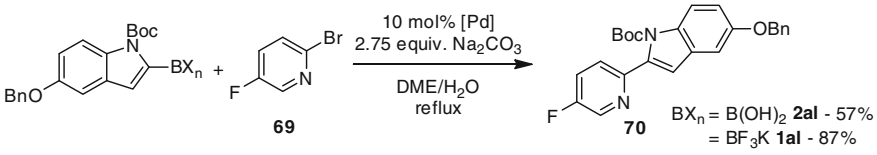

Scheme 3.10 Superior cross-coupling of indolyltrifluoroborate **1al** with **69**, in comparison to when **2al** is coupled with **69**

3.1.3.2 Elucidations of the Active Species

A 1994 report by Wright [57] on SM couplings of boronic acids with added fluoride, proposed that an organotrifluoroborate was being generated *in situ*, and was the active transmetalating species. However, two further investigations since proved this not to be the case: Fu [15] conducted two parallel reactions in the cross-coupling of 4-bromo-*N,N*-dimethylaniline (**71**) with either *o*-tolyl-BF_3K (**1am**) (THF, no base) or *o*-tolylboronic acid (**2am**) (THF, 3.3 equiv. KF). **1am** yielded no cross-coupled product after 12 h, in which time **2am** gave 91 %, Scheme 3.11. This carefully designed experiment challenged Wright's predictions in two ways: firstly that KF addition to a boronic acid does not mediate R-BF_3K salt formation, and secondly that the R-BF_3K salt cannot be the active species.

A similar investigation was conducted by Batey [58] who compared the cross-coupling of cesium phenyltrifluoroborate (**5d**) (no base) with phenylboronic acid (**2d**) (3 equiv. CsF). Similar to the Fu investigation, **5d** gave no product, however, after the addition of Cs_2CO_3, comparable yields to that gained from **2d** resulted. Batey therefore speculated that a mixed tetra-coordinated hydroxy/fluoro boronate, such as R-$BF_2(OH)^-$ (**7**) or R-$BF(OH)_2^-$ (**8**), was the superior transmetalating species.

Many reports exist on the important requirement of water being present in the SM couplings of R-BF_3K salts. In addition, alcoholic solvents work well in SM couplings without added water [34]. Although the degree of dryness is not stated, it has been observed that bench grade solvents give better outcomes than anhydrous alcohols [59]. In either case, base is required for turnover, implying alkoxy ($^-$OR) ligands coordinate to boron in alcoholic solvents, rather than hydroxy.

Molander [34] and Hutton [60] have used spectroscopic methods to find evidence for the proposed active mixed hydroxy/fluoro boronates. Hutton [60] titrated base (LiOH) into an aqueous solution of Ph-BF_3K (**1d**), and observed (^{19}F NMR) a mixed species (Ph-$BF_2(OH)^-$ **7d**/Ph-$BF(OH)_2^-$ **8d**) upon the addition of substoichiometric quantities. The observed broad peak is characteristic of **7d** and **8d** in equilibrium. In methanol, upon the addition of 1 equiv. of base to **1d**, **7d** was

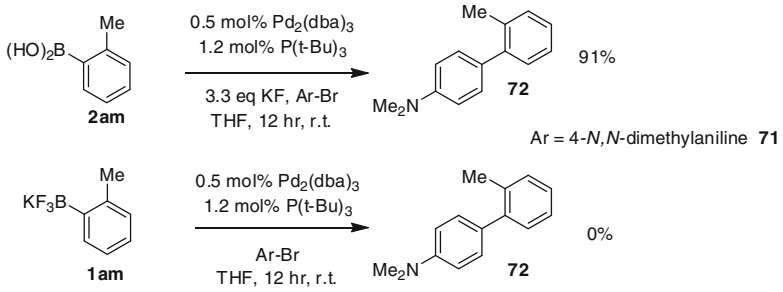

Scheme 3.11 Fu's investigations into the effect of fluoride ion on the cross-coupling of **2am** with **71** and **1am** with **71**

observed (MS–ESI$^-$) along with Ph-BF_2(OMe)$^-$ (**51d**). These observations confirm the presence of these species under aqueous or methanolic conditions, but do not give any evidence for their activity in the catalytic cycle. Molander [34] also analysed (^{19}F and ^{11}B NMR) the treatment of **1d** with different amounts of base with heating. The more base added, the more of an "ate" species was produced "with no fluorines attached", which matched that generated when **2d** was employed in place of **1d**. No conclusions were drawn from these experiments but they noted that, rather confusingly, C_6F_5-BF_3K (**1an**) underwent cross-coupling in dry THF with dry *i*-Pr_2NEt, which they proposed to be evidence for direct transmetalation.

3.1.4 Introducing the Project

The majority of research undertaken on R-BF_3K reagents has been upon optimising conditions of their coupling and applying it to the synthesis of novel compounds or new synthetic methods. Efforts into deciphering their reactivity have been slow and sparse, possibly inferring the potential difficulties of the task. Indeed there are many research groups promoting organotrifluoroborates and therefore it is difficult to find negative comparisons, even with high yielding boronic acid examples. However, an understanding of whether organotrifluoroborates are simply a protected form of boronic acids, or whether there is something unique about their transmetalation, is seminal to the future use and development of these reagents. With a greater understanding of the mechanisms, efficient optimisations can be applied more effectively to the reaction. A detailed, systematic and in depth study into the reactivity of these reagents in the Suzuki–Miyaura cross-coupling reaction is required.

The two important issues which need to be elucidated are:

1. Firstly, that of identifying the active species in transmetalation when organotrifluoroborates salts are employed in SM coupling.
2. Secondly, if, and then why, and under what conditions, do organotrifluoroborates give higher yields than boronic acids.

3.2 Initial Investigations

3.2.1 Substrates and Conditions

A simple biaryl coupling was selected due to the contextual importance of the transformation. Either potassium 4-fluorophenyltrifluoroborate (**1a**) or potassium phenyltrifluoroborate (**1d**) along with the activated 3,5-bis(trifluoromethyl)bromobenzene (**6**) were employed as model substrates for the investigation. Both R-BF_3K

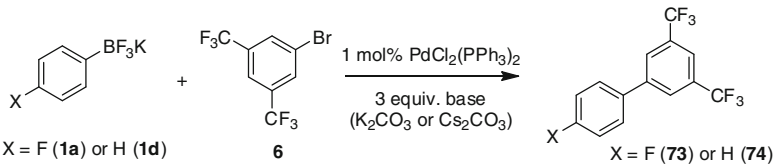

Scheme 3.12 SM coupling conditions of **1a** or **1d** with ArBr **6** initially used for the study

salts are cheap, simple, commercially available and gave the desired unsymmetrical biaryl, **73** or **74**, Scheme 3.12, in reasonable reaction times. The advantage of **1a** over **1d** arises from the additional information gained from *in situ* ^{19}F NMR analysis of the *para*-fluorine, whose chemical shift was found to be sensitive to substitution about the γ-position, and the ligation surrounding boron.

The precise optimised SM coupling conditions vary considerably within the reports published by Molander [27] and depend on the functionality of the cross-coupling partners. Three equivalents of either potassium or cesium carbonate is favoured along with the expected use of a protic solvent or an aqueous/organic solvent mixture. However, the precise solvent varies from toluene/water, THF/water, CPME/water, *t*-BuOH/water and dioxane/water in a range of ratios, as well as the single solvent systems, ethanol or methanol. The palladium precursor varies considerably, but appears to vary chronologically, as well as being dependent on the cross-coupling substrates. For example, reports published *circa* 2002 tend to use catalysts based on PPh_3 or dppf ligands, whereas those published after *circa* 2006 utilise the more powerful, formally monodentate, *o*-biaryl Buchwald ligands.

The reported advantages of employing R-BF_3K salts over boronic acids were confirmed by ^{19}F NMR of two typical reactions starting from **1a** and **2a** in THF:water (10:1). Although the reaction starting from boronic acid **2a** had not reached completion, large proportions of side-products were clearly observed. In contrast, a clean reaction was observed when starting from trifluoroborate **1a**, Fig. 3.3.

3.2.2 Solvent Study

Under the conditions of Scheme 3.12 (K_2CO_3), the kinetics of the SM coupling of phenyltrifluoroborate salt **1d** with ArBr **6** in a range of solvents were investigated, Fig. 3.4. Gas Chromatography (GC) was used for the analysis, due to the associated ease of sampling and generation of data. Plotted conversions are those of the Ar-Br **6** to the cross-coupled product **74**.

No reaction was observed in dry toluene after 35,000 s, a solvent system not employed by Molander. However, when in combination with water (3:1, toluene:water), a more commonly used solvent, 40 % conversion was reached, thereby

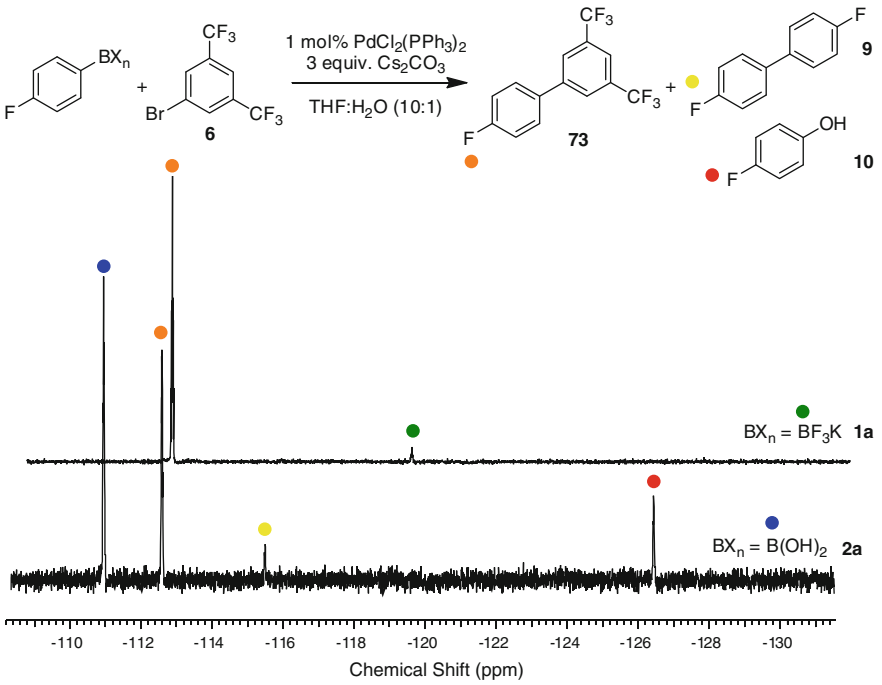

Fig. 3.3 Offset ^{19}F NMR spectra of parallel SM coupling reactions of **1a** and **2a** with **6**, showing a clean reaction when starting from **1a** (*upper spectrum*), in contrast to when starting from **2a** (*lower spectrum*)

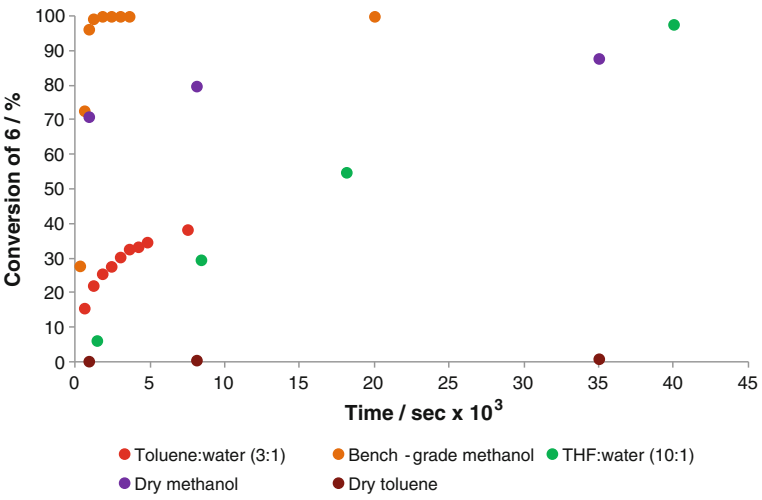

Fig. 3.4 Time *vs* conversion of **6** for the SM coupling of **1d** with **6** in various solvents systems

confirming the hydrolytic requirement of **1d.** Similarly, bench grade methanol, which contains small proportions of water, reached complete conversion in less than 30 min, in comparison to anhydrous methanol which reached 90 % conversion in 9 h. Initial rates were greater than toluene or THF media containing water, but were retarded during the latter stages of reaction. Protonation/decarboxylation of the carbonate base potentially provides a source of water under the anhydrous methanol conditions. Alternatively, methoxy ligands could behave like hydroxy ligands in a μ-bridged transmetalation transition state, Scheme 3.3 *vide supra*. A more homogeneous mixture of THF:water (10:1), commonly used by Molander, achieved high conversions over a longer period of time. This kinetic analysis confirms the importance of water and/or protic medium in (aryl)/aryl couplings.

3.3 Incomplete Conversions Study

3.3.1 Toluene:Water (3:1)

3.3.1.1 Reagent Degradation

The toluene:water (3:1) system was subjected to further study, to elucidate what was responsible for the low conversions of ArBr **6**. Analysis (GC-FID) at the end of reaction confirmed the residual presence of **6**, therefore either the catalyst or trifluoroborate salt **1d** was undergoing competitive decomposition before the reaction reached completion. Further additions of both palladium catalyst and **6** were made to two separate reactions which had ceased turning over, Fig. 3.5.

Although a minor increase in product formation was observed upon the further addition of catalyst, the addition of **1d** caused a substantial increase in conversion, in a similar kinetic profile to the first addition. This confirmed the longevity of the catalyst, and the rapid deactivation of the boron containing species.

3.3.1.2 ^{19}F NMR *In Situ* Monitoring

By monitoring (^{19}F NMR) the SM coupling *in situ*, Scheme 3.13, the fate of the R-BF_3K salt and the mechanisms leading to its decomposition could be elucidated. Proportionally sized samples were removed from both the organic and aqueous layers throughout the SM coupling of **1a** with **6**, cooled to 0 °C and analysed by ^{19}F NMR (25 °C, 128 scans), Figs. 3.6 and 3.7. A control sample left at 0 °C for 4 h showed <1 % conversion, verifying it to be an adequate quench technique. The chemical shifts of all possible side-products were corroborated by spiking synthetic samples into previously analysed NMR samples.

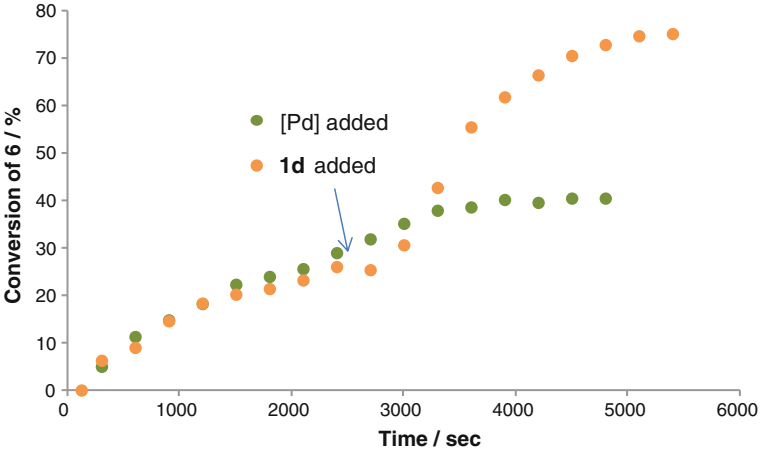

Fig. 3.5 Additional catalyst ([$PdCl_2(PPh_3)_2$]) and **1d** added to two separate reactions, where only the addition of **1d** made any significant contribution to the conversion of **6**

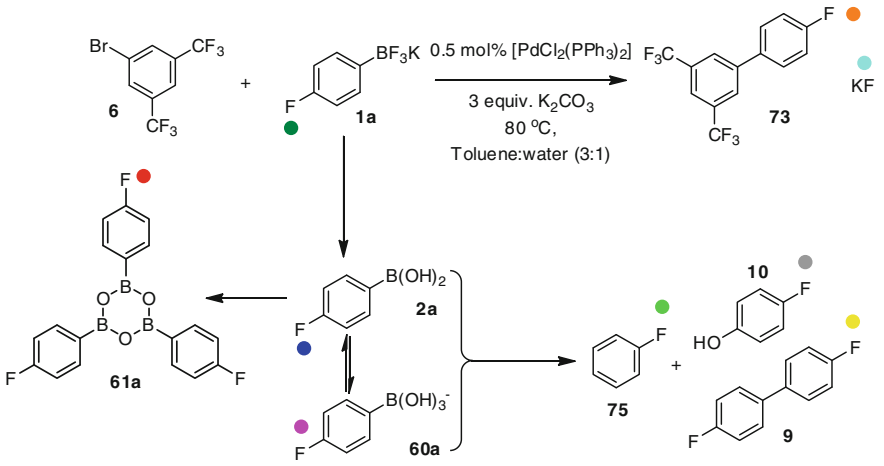

Scheme 3.13 SM coupling of **1a** with **6** in toluene:water (3:1), showing all species detected

Upon addition of the precatalyst to a stirred solution of the reactants at 80 °C, all of **1a** ($\delta_F = -115$ ppm, aqueous layer) had been consumed. Due to the greater solubility of **1a** in the aqueous layer and its ensuing hydrolytic propensity under the highly basic conditions, as confirmed from aqueous base titrations, Sect. 3.4.2 *vide infra*, this was unsurprising. The three equivalents of F^- liberated from this hydrolysis were clearly visible (^{19}F NMR) as KF ($\delta_F = -121$ ppm) in the aqueous layer.

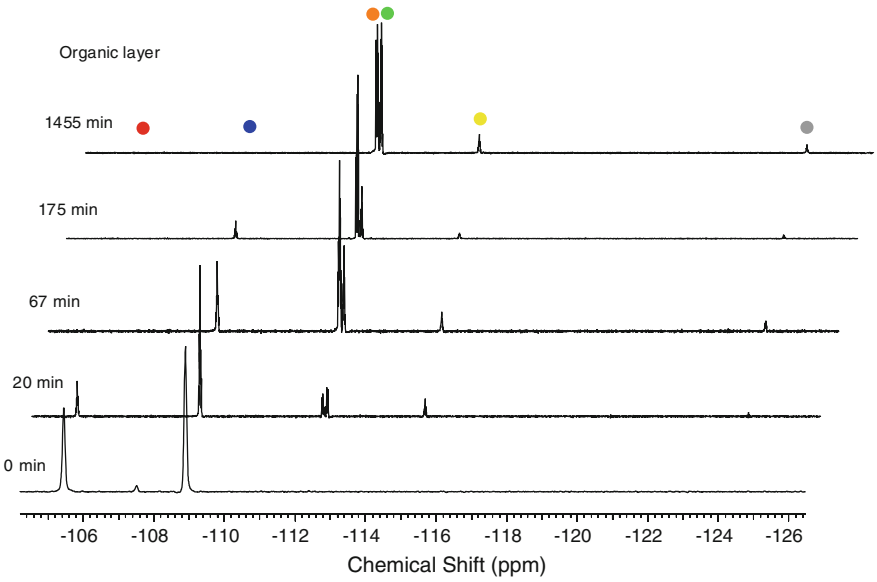

Fig. 3.6 Offset ^{19}F NMR spectra from the toluene layer of the SM coupling between **1a** and **6** under the conditions of Scheme 3.13

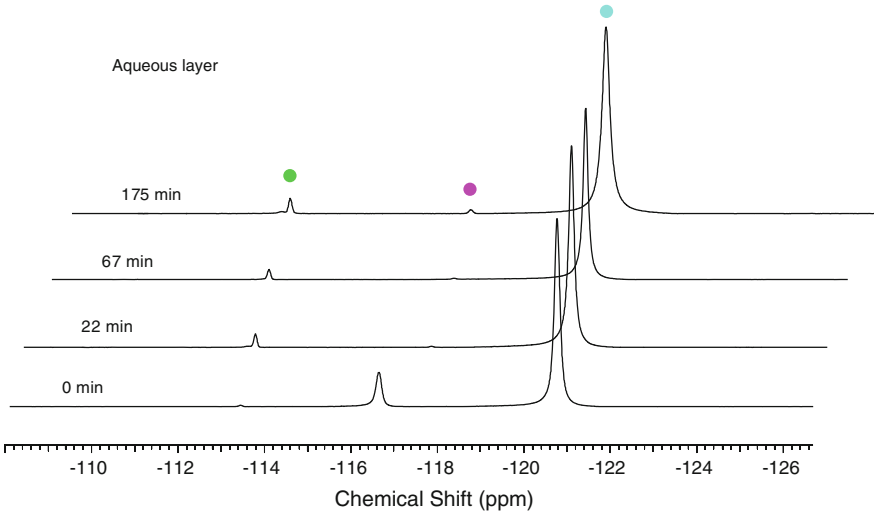

Fig. 3.7 Offset ^{19}F NMR spectra from the aqueous layer of the SM coupling between **1a** and **6** under the conditions of Scheme 3.13

Complete conversion of **1a** to the trihydroxyboronate **60a** ($\delta_F = -118$ ppm) was observed in the aqueous layer, from which, diffusion of the less polar boronic acid **2a** ($\delta_F = -110$ ppm) into the less polar organic layer followed. Under the

drier toluene conditions, **2a** dehydrated to give small quantities of boroxine **61a** ($\delta_F = -106$ ppm).

The cross-coupled product **73** ($\delta_F = -113.7$ ppm) was formed in the organic layer throughout the reaction, but only 32 % of the arylbromide **6** was converted to **73**, due to boron reagent decomposition. No homo-coupling of ArBr **6** was observed, in contrast to the steady build up of 4,4-difluorobiphenyl (**9**, $\delta_F = -116$ ppm) and 4-fluorophenol (**10**, $\delta_F = -126$ ppm) in the organic layer. Both **9** and **10** are known to be generated *via* a palladium peroxo complex [61], presumably formed through incomplete degassing of solvent or the ingress of air during sampling. However, the dominating side reaction, responsible for the decreased yields, was a base-catalysed protodeboronation of **60a** in the aqueous layer. Fluorobenzene (**75**, $\delta_F = -113.9$ ppm) was observed as a metastable dispersion in this phase, which migrated to the organic phase and ultimately accounted for the 55 % of consumed **1a**.

For R-BF_3K salts susceptible to rapid hydrolysis and base-catalysed protodeboronation, biphasic systems (toluene:water 3:1) are inefficient and should be avoided, consistent with the observations made by Molander [34].

3.3.1.3 Protodeboronation

Kuivila [62] proposed that base-catalysed protodeboronation proceeds *via* the trihydroxyboronate species (**60**). In an attempt to understand why protodeboronation was so prevalent under these biphasic conditions, but undetectable under the conditions of THF:water (10:1), Fig. 3.3, the effect of increasing proportions of THF on homogenous aqueous solutions of **60a** was studied, Scheme 3.14. **60a** was generated from **1a** *in situ* with 4 equivalents of K_2CO_3 in water.

By establishing δ_F for **2a** and **60a**, analysis of $\Delta\ \delta_F$ was used to calculate the mol % of **60a** in the equilibrium (**2a/60a**). As the water concentration was reduced from 55 M (100 % D_2O) to 0 M (100 % THF) the equilibrium population shifted from being ≥98 % boronate **60a** to ≥98 % boronic acid **2a**, Fig. 3.8. In THF:water 10:1, where the equilibrium contains 95 % boronic acid **2a**, protodeboronation was negligible over 12 days at room temperature, Fig. 3.9. In contrast, a 47 M water sample containing 80 % boronate **60a**, left for the same time period and

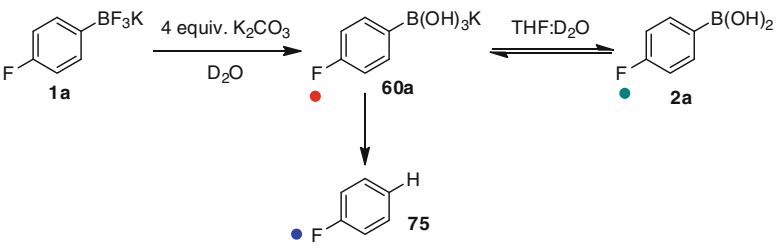

Scheme 3.14 Protodeboronation of **1a** *via* **60a** as proposed by Kuivila, in THF:water

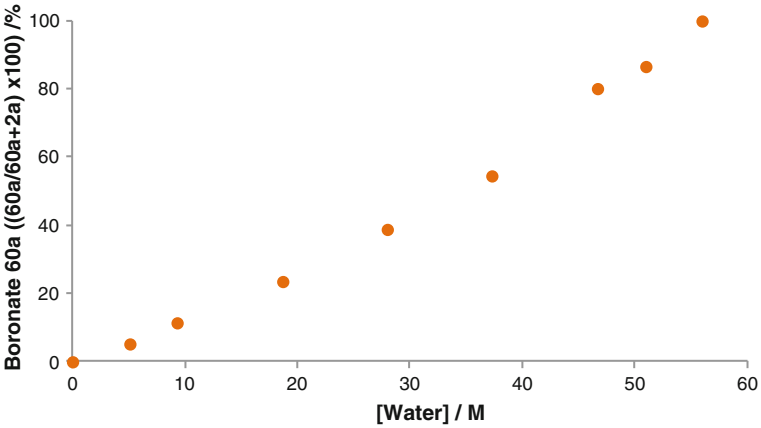

Fig. 3.8 The dependency of equilibrium proportions of **2a** and **60a** on water concentration

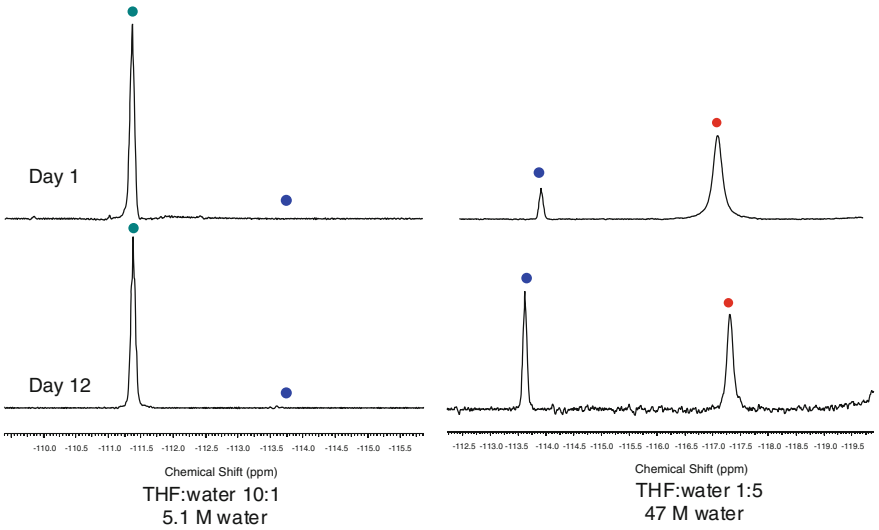

Fig. 3.9 ^{19}F NMR spectra of two reaction mixtures (**1a** + 4 equiv. K_2CO_3) at high and low water concentrations. A high water concentration gave substantial quantities of protodeboronation after 12 days at room temperature, whereas no protodeboronation could be detected at low water concentrations. Coloured dots refer to species in Scheme 3.14

temperature underwent 46 % protodeboronation. Therefore, the equilibrium population of **60**, which is determined by the concentration of water under basic homogenous conditions, is directly related to the rate of protodeboronation, consistent with that proposed by Kuivila [62].

3.4 Organotrifluoroborate Activation

In the studies directed towards the elucidation of the active transmetalating species in the SM coupling of **1a**, three solvent systems were studied; toluene:water (3:1), water, and THF:water (10:1).

3.4.1 Toluene:Water (3:1)

Close inspection of a SM coupling between **1d** and **6** in toluene:water (3:1), Scheme 3.12, taking many time points during the initial stages, indicated an induction period (100 s) in product **74** formation when **1d** was added last. This could be avoided by stirring **1d** in toluene:water (3:1) at 70 °C for 10 min before the other reactants were added; consistent with the hypothesis of an activation to form a mixed fluoro/hydroxy boronate species (**7d/8d**) for transmetalation, Fig. 3.10, as previously proposed [58], Sect. 3.1.3, *vide supra*.

The effect of additional fluoride on the SM coupling of **1d** with **6** was tested, as it was reasoned that it would give an increase in the concentration of mixed species **7d** or **8d**. Consistent with this hypothesis, when 3.5 equiv. KF was added, a rate increase was observed, providing 70–80 % conversion of the Ar–Br **6**, Fig. 3.11.

Although this rate enhancing effect supports the proposed hypothesis, KF is often used as a base in SM coupling reactions and could therefore be adjusting the pH of the medium, leading to a more efficient transmetalation. Alternatively, an increase in the ionic strength of the aqueous medium could aid solubility of the active species in the organic phase. However, this effect was later deemed unlikely as neither the addition of CsF (3.5 equiv.) nor KI (3.5 equiv.) exhibited any significant rate enhancements.

Partitioning analysis (^{19}F NMR) of all species between the organic and aqueous layers unsurprisingly demonstrated the KF to reside in the aqueous layer. Therefore, by studying the effect of increasing concentrations of KF on boronic acid **2d** in a purely aqueous medium, it was hoped that this enhancing effect could be elucidated. If the fluoride affinity for boronic acid was high then the equilibrium, Scheme 3.15, would favour the tetra-coordinated boronate **8d** ($\delta_B \approx 5$ ppm, identity assumed over **7d**). Alternatively, if it was low then the equilibrium would favour boronic acid ($\delta_B = 29$ ppm).

The equilibrium position, Scheme 3.15, was represented as a time-averaged ^{11}B NMR peak, Fig. 3.12, where the mol % **8d** could be monitored by the $\Delta\delta_B$. The affinity of fluoride for **2d** in water is evidently low, as the addition of 3.5

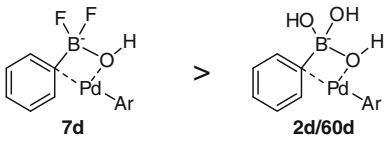

Fig. 3.10 Proposed faster transmetalation from mixed fluoro/hydroxy species **7d**

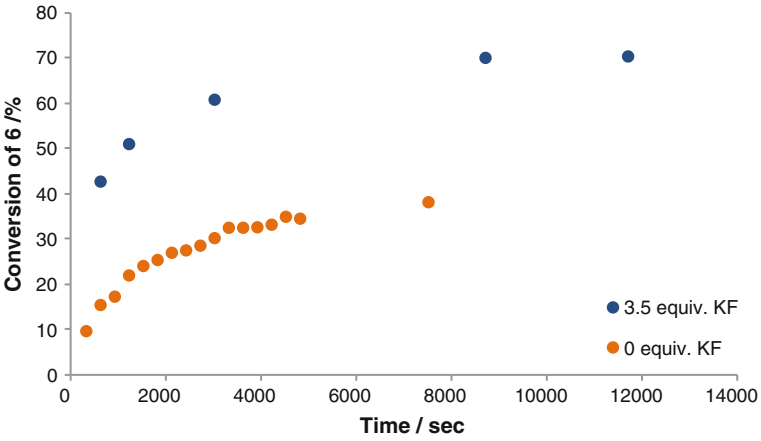

Fig. 3.11 SM coupling of **1d** with **6** under the conditions of Scheme 3.12 in toluene:water (3:1) at 80 °C with additional KF (3.5 equiv.)

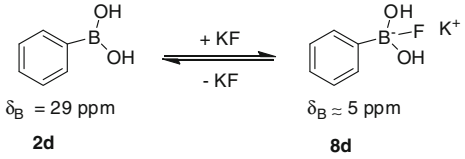

Scheme 3.15 Fluoride affinity for boronic acid **2d** as monitored by ^{11}B NMR

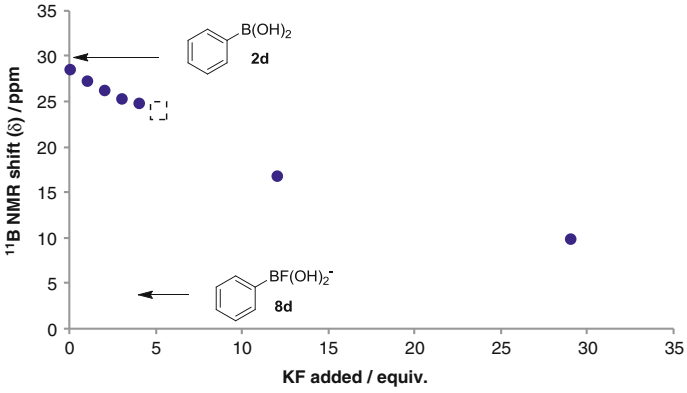

Fig. 3.12 KF titration of boronic acid **2d** in water, showing a poor affinity for fluoride over the concentrations present during SM couplings of **1d.** Dashed box indicates fluoride content in the fluoride enhanced SM coupling, Fig. 3.11

equiv. of KF only effected <10 % change in the position of the equilibrium. However, in a polar organic solvent, fluoride was shown to efficiently complex to boronic acid **2a**, (CH_3OH—Sect. 2.2.1, CH_3CN—Sect. 2.3.1, *vide supra*). This may arise from a deactivating hydration sphere surrounding the potassium cation under the aqueous conditions tested herein.

The rate enhancement observed upon the addition of 3.5 equiv. KF, Fig. 3.11, is therefore unlikely to be due to an increased concentration of mixed species **8d**. Plausible explanations include either, an advantageous slight rise in the pH induced by the KF, or that KF can inhibit protodeboronation, e.g. by inhibiting the formation of trihydroxyboronate **60d**.

3.4.2 Water

3.4.2.1 Base Titrations

Water and base are both necessary for the activation of organotrifluoroborate salts for transmetalation, therefore the effect of increasing quantities of base on **1a** in water was examined, Scheme 3.16, similar to experiments performed by Hutton [60].

Potassium carbonate was added to a solution of **1a** in D_2O in half equivalent amounts up to a total of 4, followed by further additions of 2 and 4 equivalents, at room temperature and without inertion. Each sample was analysed by ^{11}B and ^{19}F NMR spectroscopy, Figs. 3.13 and 3.14.

As K_2CO_3 is added, **1a** is rapidly consumed, leading to a time averaged ^{19}F and ^{11}B NMR shift for the equilibrium between boronic acid **2a** and trihydroxyboronate **60a,** Figs. 3.13, 3.14 and Scheme 3.17.

When employing boronic acid **2a** directly, the K_2CO_3 titration induced an identical equilibrium shift, after consideration of the three equivalents of HF to be sequestered (1.5 equiv. K_2CO_3) when starting from **1a**, Fig. 3.15. Therefore, 1.5 equivalents of dibasic carbonate were required to completely consume **1a**, before any considerable shift in the equilibrium between **2a** and **60a** occurred; an important consideration during SM coupling optimisations.

Analogous base titrations of **1a** were performed with Cs_2CO_3 and KOH in water. There was no meaningful difference observed between K_2CO_3 and Cs_2CO_3, however as KOH is mono-basic, the demand was doubled to effect the same sequestration of liberated HF. Therefore, complete conversion of **1a** to **60a** necessitated approximately 3 equivalents of dibasic Cs_2CO_3 or K_2CO_3 and 6 equivalents of monobasic KOH.

An initially unidentified peak ($\delta_F = -143$ ppm) in the ^{19}F NMR spectra, Figure 3.14, which was later recognised as being that of $BF_3(OH)$, formed upon

Scheme 3.16 Base titration of **1a** in water

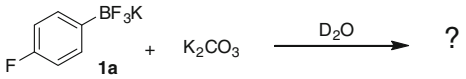

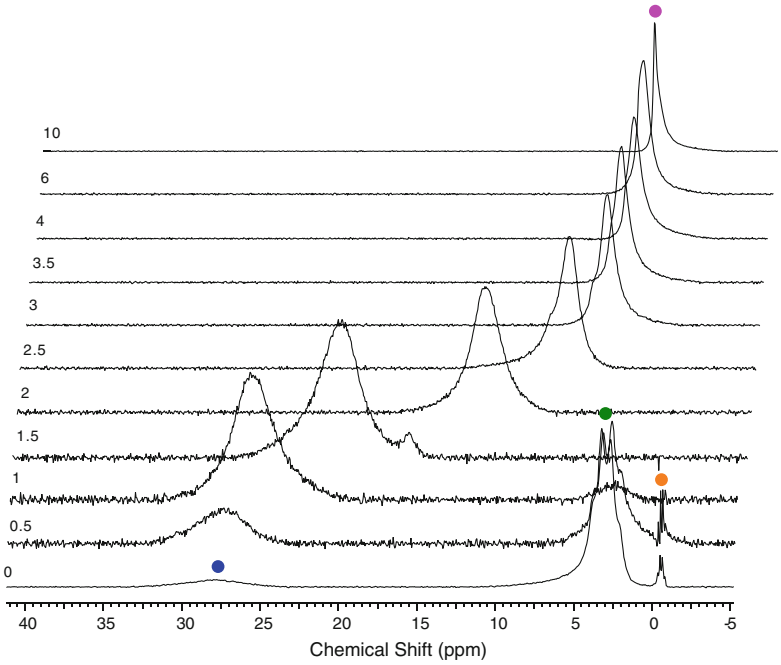

Fig. 3.13 Offset ^{11}B NMR spectra of the K_2CO_3 titration of **1a** in water; left-hand numbers are equivalents of K_2CO_3 added. Coloured dots refer to species in Scheme 3.17

the addition of 0–0.5 equiv K_2CO_3, but was rapidly consumed upon further additions of base. This species had to be either generated from protodeboronation of **1a** or from the borosilicate glass surface of the reaction vessel. To test this [^{10}B]-**2a** was prepared and subjected to 0.5 equiv. K_2CO_3 in water. The observed superimposed quartet and septet arising from natural abundance boron (^{11}B 80 %, spin = 3/2, and ^{10}B 20 % spin = 3) was indicative of that coming from the glass surface. The origin of the species, as coming from the glass surface, was confirmed by the absence of the signal when the experiment was conducted in a PTFE vessel.

Interestingly, when a base titration (0.5–4 equiv. K_2CO_3) of **1a** was performed in THF:water (10:1), the equilibrium position (95 % boronic acid **2a**/5 % boronate **60a**) was found to be completely base independent. No change was observed (^{11}B NMR) upon the addition of up to 4 equivalents of K_2CO_3. The origins of this phenomenon are discussed later, Sect. 4.2.5 vide infra.

3.4.2.2 Effect of Fluoride on Base Titrations

Additional fluoride (4, 8 and 12 equiv. KF) added to **1a** in water caused partial hydrolysis to form a mixed species **7a/8a**, presumably encouraged by the generation of stable KHF_2, Scheme 3.18. However, upon sequential addition of K_2CO_3,

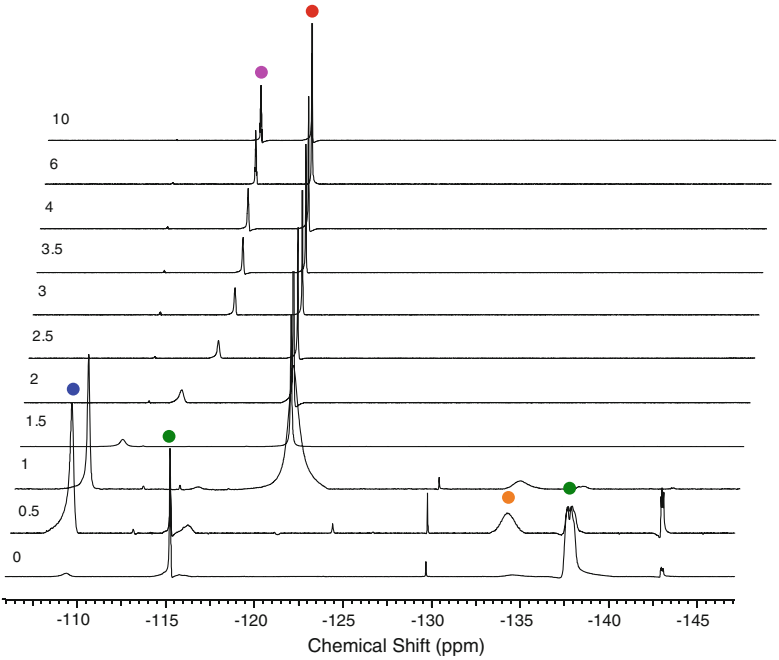

Fig. 3.14 Offset ^{19}F NMR spectra of the K_2CO_3 titration of **1a** in water; left-hand numbers are equivalents of K_2CO_3 added. Coloured dots refer to species in Scheme 3.17

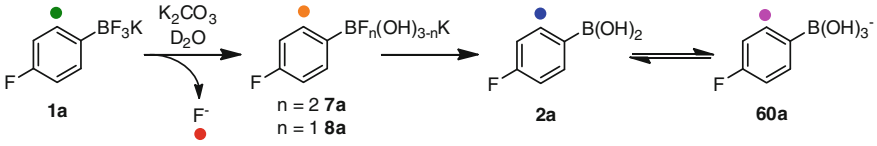

Scheme 3.17 Base titration of **1a** to give boronic acid **2a** which proceeds to form trihydroxyboronate **60a** upon the addition of increasing quantities of base

this species was rapidly consumed, in parallel with **1a**. The greater concentration of fluoride had a small effect on the overall outcome of the equilibrium between **2a** and **60a**, Fig. 3.16. Due to the slight increase in pH associated with aqueous KF, at low concentrations of K_2CO_3 an increase in the proportion of **60a** was observed. However, a difference was observed in the proportion of boronate between 0 and 4 equivalents of KF (ca. 10 %), at the concentrations of base employed for SM coupling (3 equiv.), Fig. 3.16. This may account for the suppression of protodeboronation, upon addition of KF (3.5 equiv.) to an SM coupling in a toluene:water (3:1) biphase, Fig. 3.11.

Attempts were made to extract binding isotherms (K_a) from the base titrations with additional KF, Fig. 3.16. However, due to the series of complex equilibria

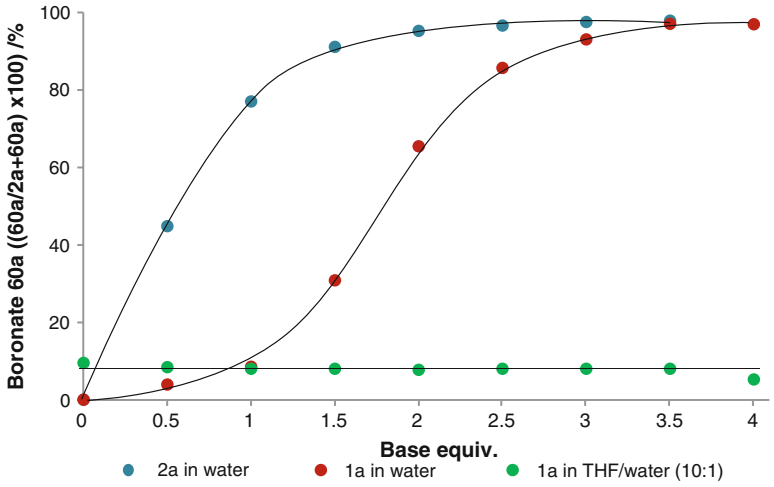

Fig. 3.15 Proportion of **60a** from **2a** versus equivalents of added base, in the base titrations of **1a** and **2a**

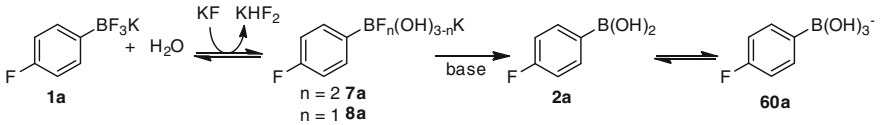

Scheme 3.18 The effect of additional KF on **1a** to give **7a/8a**, followed by its consumption by base leading to the equilibrium between **2a** and **60a**

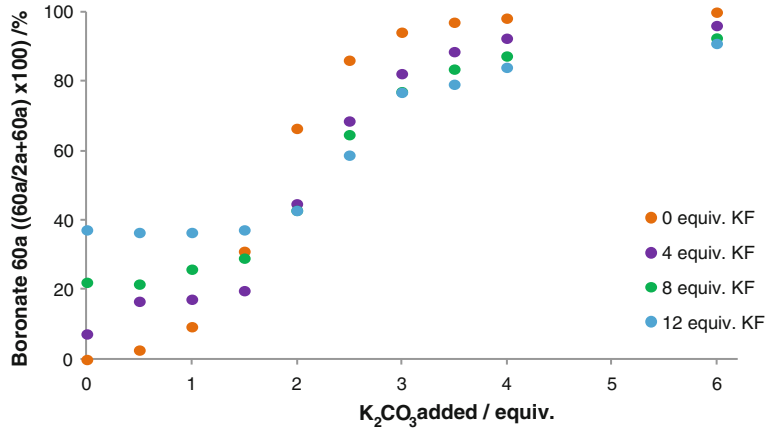

Fig. 3.16 The effect of added fluoride on K_2CO_3 titrations of **1a**

involved, Scheme 3.18, each possessing their own K_a, it was not possible to successfully deconvolute them from the simplified model that was assumed. Even when the data in the HF sequestration region (0–1.5 equivalents) was not taken into account, the error margins of each K_a were bigger than any trends that could be predicted.

3.4.2.3 Mixed Species

Preliminary efforts into the synthesis and isolation of a mixed species, of the type 4-F-Ph-BF_2(OH)K (**7a**) and 4-F-Ph-BF(OH)$_2$K (**8a**), were undertaken, for comparisons of transmetelation rates with a stoichiometric palladium complex. **1a** was treated with 1 equivalent of TMS-Cl to reveal difluoroborane **11a** [63], followed by the addition of 1 equivalent of KOH. The product **7a** could be observed *in situ* (^{19}F NMR), however its instability was clear, as only mixtures containing predominately boronic acid **2a** could then be isolated.

No chromatographic or spectroscopic (GC, ^{19}F, ^{11}B NMR) evidence existed for mixed species **7a** and **8a** during SM coupling in either toluene:water (3:1) or THF:water (10:1). However, under primarily aqueous conditions, with substoichiometric quantities of base, they were observed ($\delta_F = 116.0, 134.5$ ppm). The intermediate reached a maximum (8 % of the total Ar–B species) when 0.5 equivalents of K_2CO_3 was added in a THF:water (1:10, 45 M water) solution. From integration of the two broadened fluorine peaks (*para*-F *vs* B–F) it was tentatively assigned as **7a**. Under these conditions ^{19}F EXSY NMR demonstrated it to be in rapid equilibrium (τ = 20–40 ms) with boronic acid **2a** and free KF, but not with trifluoroborate **1a**, Fig. 3.17. This suggested that, under these predominately aqueous conditions, regeneration of **1a** is energetically unfavourable.

3.4.3 THF:Water (10:1)

3.4.3.1 Kinetics of SM Coupling

Returning to the conditions pertinent to SM coupling, the activation of **1a** was studied in THF:water 10:1, due to its frequent use in Molander's optimised conditions. Additionally, it avoids the major biphasic issues associated with the use of toluene:water 3:1, thus aiding kinetic analysis. However, a small, concentration dependent biphase does exist in THF:water (10:1), the problems of which were predominately reduced by employing a low reaction concentration (8 mM). In the toluene:water (3:1) system it was difficult to track substrates between the phases, whereas in THF:water (10:1, 8 mM) all substrates were easily monitored (^{19}F NMR). The volatile product of protodeboronation, fluorobenzene (**75**), evaporated out of the system in reactions conducted at 80 °C in toluene:water (3:1). In order to limit this, the temperature was reduced (55 °C) and experiments were initially

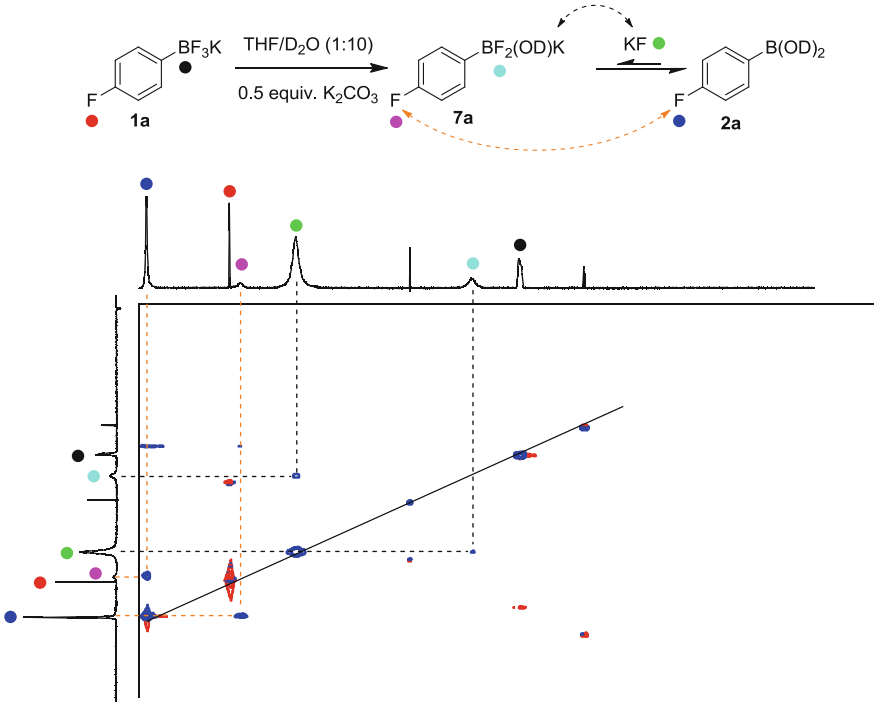

Fig. 3.17 ^{19}F EXSY NMR ($\tau = 40$ ms) of a reaction mixture (**1a**, 0.5 equiv. K_2CO_3 in THF:water (1:10)) containing mixed species **7a**, which is shown to be in exchange (*dashed lines*) with KF and **2a**

performed in a closed system, i.e. Young's tap NMR tube. Frequent monitoring could be achieved by using a time delayed array directly in the *Varian 500 MHz* spectrometer probe. Although no differences had been observed between K_2CO_3 and Cs_2CO_3, the latter was chosen due to the more frequent use in Molander's optimised conditions.

Under the conditions of Scheme 3.19, a clean SM coupling was observed, Fig. 3.18, with no spectroscopic evidence for mixed species **7a** and **8a**, or protodeboronation product **75**.

Complete hydrolysis of **1a** to **2a** occurred rapidly, followed by a slow build-up of the cross-coupled product **73**. Control reactions for the hydrolysis of **1a** to **2a** illustrated that the rate did not depend on the catalyst precursor, or **6**. Interestingly in the absence of any Cs_2CO_3, **1a** was shown to efficiently hydrolyse to **2a** in THF:water (10:1) at 55 °C. This rate was found to be dependent on the glass surface area, Scheme 3.20, with a faster first order decay observed in an NMR tube than in a Schenk tube, Fig. 3.19, while no reaction occurred in a PTFE vessel. It is known that R-BF_3K salts are sensitive to silica-gel [64] or other "fluorophiles" such as alumina [65]. This is, therefore, consistent with the hypothesis that the glass surface provides a fluoride sink for the liberated fluoride by forming a strong

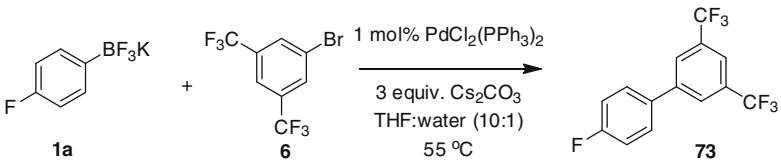

Scheme 3.19 Conditions used the SM coupling of **1a** with **6** in THF:water (10:1)

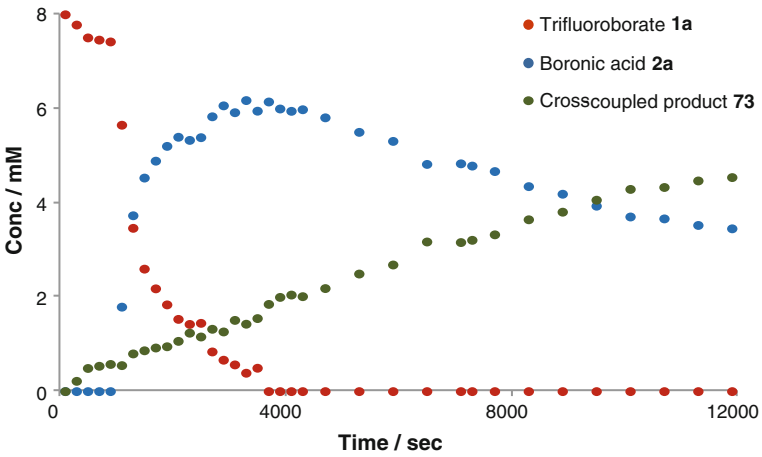

Fig. 3.18 Kinetic rate profile of the SM coupling of **1a** with **6** in THF:water 10:1

Si–F bond. Additionally, the phase transfer of fluoride provides an explanation as to why it is not detected by ^{19}F NMR *in situ*.

The apparent "burst" in cross-coupled product **73** formation in the first 1,000 s, Fig. 3.18, before any appreciable build up of boronic acid, was thought to be the rapid transmetalation of a very active mixed species **7a** or **8a**, consistent with that previously proposed [58, 60]. By increasing the catalyst loading, this "burst" should proportionally increase as it can "catch" more of **7a** or **8a** when **1a** hydrolyses to **2a**, Scheme 3.20. However, when the loading was increased 5–15 fold, there was no detectable initial rate enhancement.

3.4.3.2 Reverse Hydrolysis

The use of [^{2}H$_4$]-**2a**, prepared *via* the *para*-bromination of [^{2}H$_5$]-fluorobenzene ([^{2}H$_4$]-**75**) followed by lithiation and borylation, was very informative. The isotope shift ($\Delta\delta_F = 0.55$ ppm) of the *para*-fluorine in ^{19}F NMR, induced by the aromatic deuteration, made it possible to distinguish the origin of the observed species. In this way, reversible generation of trifluoroborate **1a** was confirmed: smooth

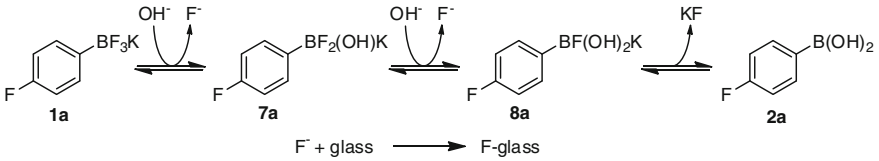

Scheme 3.20 Hydrolysis of **1a** to **2a** *via* mixed species intermediates **7a** and **8a**, through sequestration of fluoride by glass

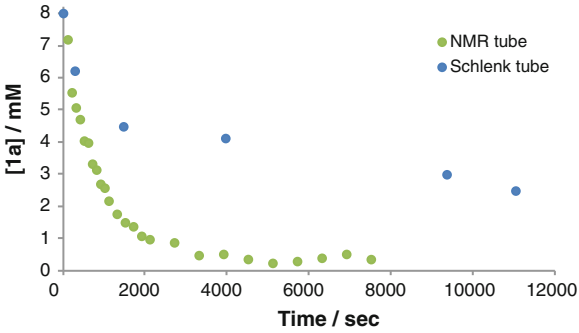

Fig. 3.19 Hydrolysis of **1a** to **2a**, without Cs_2CO_3 in THF:water (10:1) at 55 C in an NMR tube and a Schlenk tube, showing the faster rate of hydrolysis coming from the system with a greater glass surface area

equilibration occurred between [$^2H_4$]-**2a** and [$^2H_0$]-**1a** (1:1) to give [$^2H_0$]-**2a** and [$^2H_4$]-**1a** at 55 °C in THF:water (10:1). In the absence of any fluorophilic glass, i.e. in PTFE, this equilibration was very obvious by the generation of significant quantities of [$^2H_0$]-**2a** and [$^2H_4$]-**1a**, Fig. 3.20. However, even in the presence of glass during the SM coupling of [$^2H_4$]-**2a** and [$^2H_0$]-**1a** with **6**, small quantities of these cross-over species were detected (^{19}F NMR) before the complete sequestration of fluoride.

The observed reversibility between **1a** and **2a** thus validates the prolonged existence of intermediate mixed species **7a** and **8a** in very low, undetectable concentrations (≤60 μM). Rapid disproportionation to the more stable fully fluorinated or non-fluorinated species therefore dominates.

3.4.3.3 DFT Calculations

Having detected the mixed species, albeit in extremely low concentrations, during SM coupling reactions, it was evident that they would therefore have to be exceptionally reactive to make any impact on the overall catalysis. To assess this quandary, DFT calculations (B3LYP/6-31G*,lacv3p) were performed by Dr. J. Jover and Prof. J. N. Harvey (University of Bristol), on the phenyl transfer of $[Ph\text{-}BX_3]^-$ (X = F or OH) to $[Pd(Br)Ph(PPh_3)_n]$ (n = 1 or 2), generated by oxidative addition of PhBr to $[Pd(PPh_3)_2]$, in a THF continuum, Fig. 3.21.

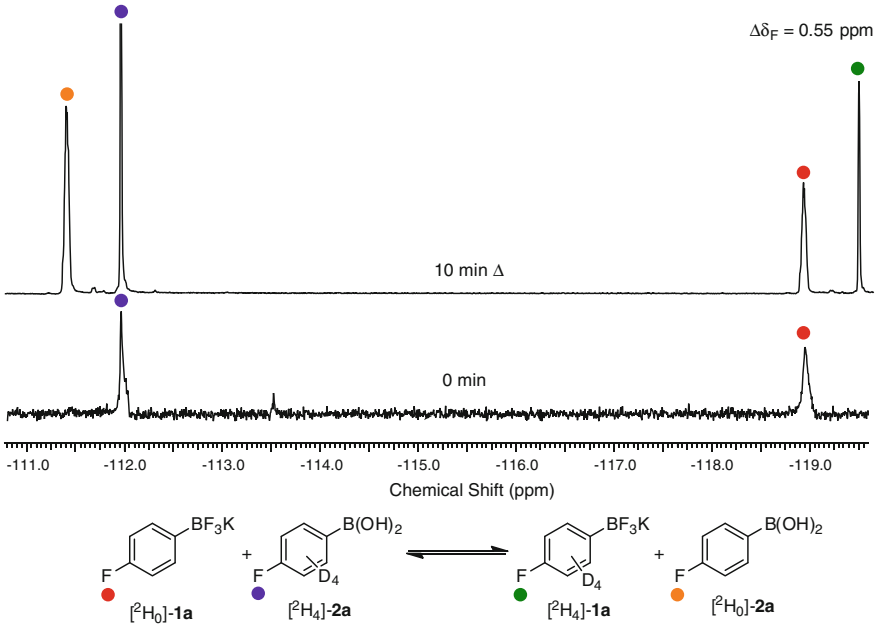

Fig. 3.20 Equilibration between [$^2H_0$]-**1a** and [$^2H_4$]-**2a** in THF:water (10:1) in a PTFE tube

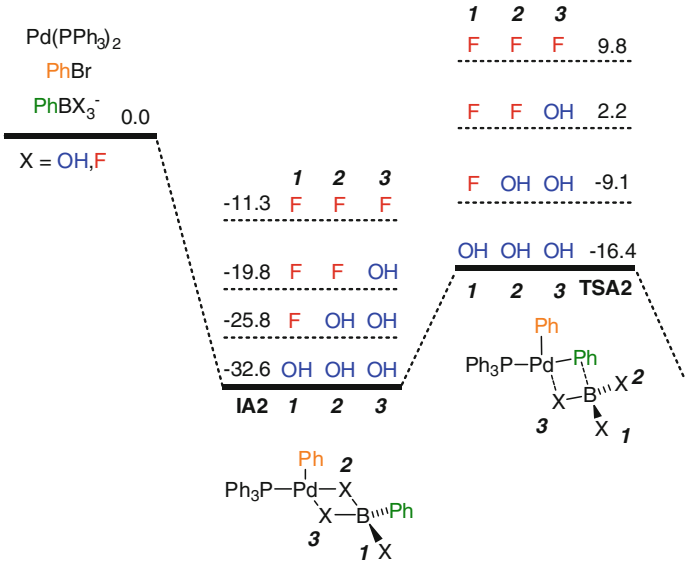

Fig. 3.21 Energy levels of DFT calculated intermediate (**IA2**) and transition state (**TSA2**) for the transmetalation of $PhBX_3^-$ (X = F or OH) with [$Pd(PPh_3)BrPh$]

The lowest energy barrier for the transmetalation of phenyl from $[Ph\text{-}BX_3]^-$ (X = F or OH) to the mono-ligated $[Pd(Ph)BrPPh_3]$, is given when boron is wholly ligated by hydroxide (X = OH) (16.2 kcalmol^{-1} (3 OH) > 16.7 kcalmol^{-1} (2 OH, 1 F) > 22.0 kcalmol^{-1} (1 OH, 2 F) > 21.1 kcalmol^{-1} (3 F)), Fig. 3.21. This pattern is similarly mirrored, although 20 kcal mol^{-1} higher in energy, in the transmetalation of $[Ph\text{-}BX_3]^-$ (X = F or OH) with the bis-phosphine ligated complex, $[Pd(Ph)Br(PPh_3)_2]$. As the fluoride ligation increases, the ability of the boron reagent to coordinate to palladium decreases (increasing **IA2**). Equally, electron density around the boron centre is reduced, thus decreasing the nucleophilic ability to transfer the phenyl moiety to palladium (increasing **TSA2**). Therefore, catalytic flux is expected to proceed almost exclusively through aryl transfer from Ar–$B(OH)_2$ (**2**) to $[Pd(OH)(Ar)PPh_3]$, or Ar–$B(OH)_3^-$ (**60**) to $[Pd(Ar)PPh_3]^-$ with no contribution from either of the mixed species (**7**/**8**) or trifluoroborate **1**.

3.4.3.4 Boronic Acid/Trifluoroborate Competition

In order to investigate this reactivity experimentally, [$^2H_4$]-**2a** and [$^2H_0$]-**1a** were competed for limiting Ar-Br **6**. Five different proportions (10:90, 30:70, 50:50, 70:30, 90:10; [$^2H_4$]-**2a** :[$^2H_0$]-**1a**) of each reagent were co-reacted in five separate experiments, Scheme 3.21. The isotope shift ($\Delta\delta_F$) in the cross-coupled product **73** could determine how the proportions of each aryl ring, nominally from each reagent, were incorporated.

Catalytic turnover proceeded in parallel to hydrolytic equilibration between [$^2H_4$]-**2a** and [$^2H_0$]-**1a**, but the initial isotope ratio employed always matched the final isotope ratio of the cross-coupled product **73**, Scheme 3.21. However, prior to full equilibration the evolving isotope ratio of **73** throughout catalytic turnover reflected that of the most reactive species, Fig. 3.22.

During the initial stages of reaction, cross-coupled product **73** generation was predominately [$^2H_4$] labelled, Fig. 3.22, originating from boronic acid [$^2H_4$]-**2a**. Even when the mixture only contained 10 % of [$^2H_4$]-**2a**, the rate of transmetalation from this reagent was so superior that after only 15 % conversion to **73**, 60 % of it was [$^2H_4$] labelled. As the reaction progressed, the [$^2H_4$] label became diluted in the pool of reactive species; leading to **73** containing the initial isotopic

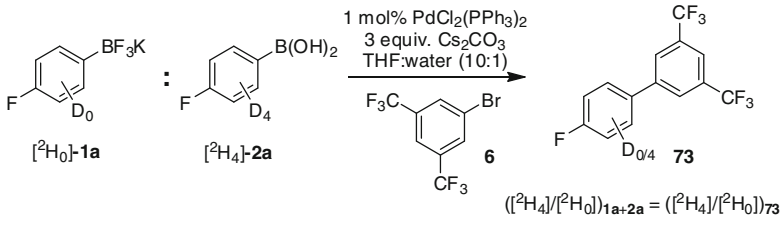

Scheme 3.21 Conditions for the SM coupling competition between **1a** and **2a** for **6**

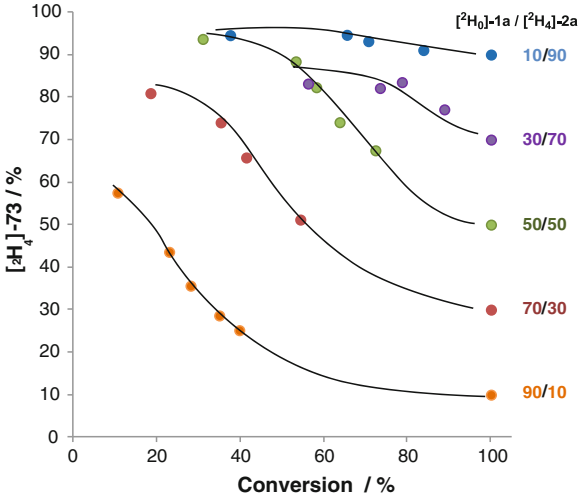

Fig. 3.22 [$^2H_4$] incorporation into the cross-coupled product **73** versus total conversion to **73**, showing high levels of [$^2H_4$] during the early stages of the reaction even when the concentration of the [$^2H_4$] label is low. Lines through data are solely a guide to the eye

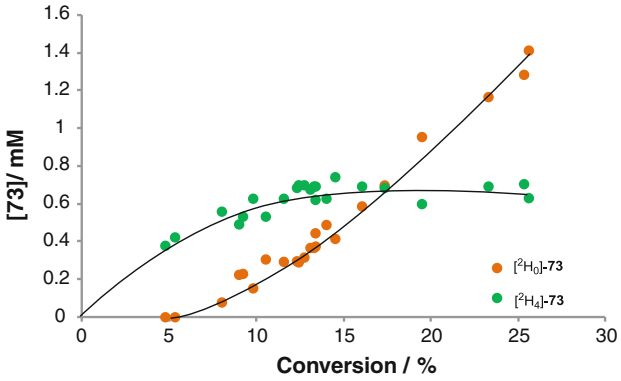

Fig. 3.23 Concentration of cross-coupling product **73** versus total conversion to **73**, in the SM coupling of 90 % [$^2H_0$]-**1a** and 10 % [$^2H_4$]-**2a** with **6**, showing the generation of [$^2H_4$]-**73** in advance of [$^2H_0$]-**73**. *Lines* through data are solely a guide to the eye

mixture of the starting materials. Conversely, when the boronic acid [$^2H_4$]-**2a** was the major species (90 %), [$^2H_4$] incorporation in **73** was very high, and only until the latter stages of reaction did it dilute down to 90 %. The evolving isotope ratio of the product therefore reflects that of the boronic acid **2a** and not of the trifluoroborate **1a** or anything derived from it. If catalytic flux predominately came from a mixed species **7a** or **8a**, the isotope signature of **73** would not be as biased towards incorporation of the [$^2H_4$] label.

Monitoring the same set of reactions in the NMR probe made it possible to study the very early stages of reaction through the collection of many data points. The most informative example contained only 10 % [$^2H_4$]-**2a**, but the [$^2H_4$]-**73**

generation was well in advance of [$^2H_0$]-**73**, Fig. 3.23, indicating its superior reactivity over [$^2H_0$]-**1a**.

These experiments reinforce the conclusion that trifluoroborate **1a** serves as a reservoir for the more active **2a**, which undergoes transmetalation and not either of the mixed species **7a** or **8a**.

3.5 Side Product Study

Under the conditions of Scheme 3.19 in THF:water 10:1, employing trifluoroborate **1a** generated fewer side products than employing boronic acid **2a**, Fig. 3.3. This study revealed that up to 40 % of side products could be generated when using **2a**, compared to <2 % with **1a**, a trend that was paralleled even when the reactions were run in air. Whilst it has been established that both reactions transmetalate *via* the boronic acid **2a**, the difference, therefore, must not be in the generation of a more efficient transmetalation but in differences to each individual side-reaction. Indeed, reactions starting from **2a** proceeded to completion faster than those from **1a**, due to the slow and often variable hydrolysis rate which limits the rate of catalytic turnover.

As the rate of protodeboronation of **1a** in aqueous THF is negligible, Sect. 3.3 *vide supra*, the side-products that differentiate the two reagents are the homo-coupled product **9** and phenol **10**. Under the routine synthetic conditions used during SM couplings, i.e. solvents or reagents that have not been rigorously purified, these are rapidly generated at the start, followed by a progressive build-up throughout the reaction. They were found to come from three separate processes, Scheme 3.22: a pre-catalytic activation (***I***) gives **9** at the start of the reaction, an oxidation (***II***) produces **10** also at the start, followed by an oxidative homocoupling (***III***) throughout the reaction to give both **9** and **10**. In all three cases, the use of trifluoroborate **1a** suppressed these side-reactions compared to the use of boronic acid **2a**.

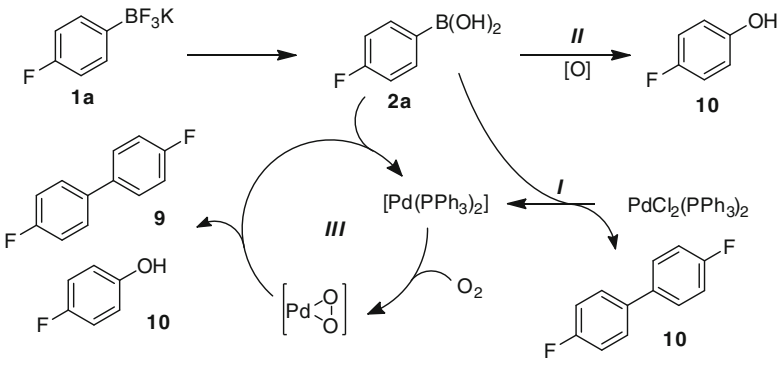

Scheme 3.22 Three side-reactions of boronic acid **2a**, which are attenuated when employing **1a**

3.5.1 Precatalyst Activation (I)

When the more stable palladium(II) precatalysts are employed for SM couplings, an *in situ* reduction process must occur before the onset of oxidative addition. This reductive activation generally proceeds *via* a two stage transmetalation/reductive elimination to give palladium(0), whilst consuming two boronic acid molecules to yield a homo-coupled product, Scheme 3.23.

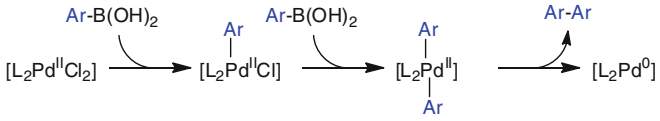

Scheme 3.23 Precatalyst activation *via* a double transmetalation/reductive elimination

In reactions starting from boronic acid **2a**, $[PdCl_2(PPh_3)_2]$ underwent activation *via* this mechanism, as confirmed by the detection (^{19}F NMR) of homo-coupled product **9** immediately after turnover began, Figs. 3.24 and 3.25. As expected, the

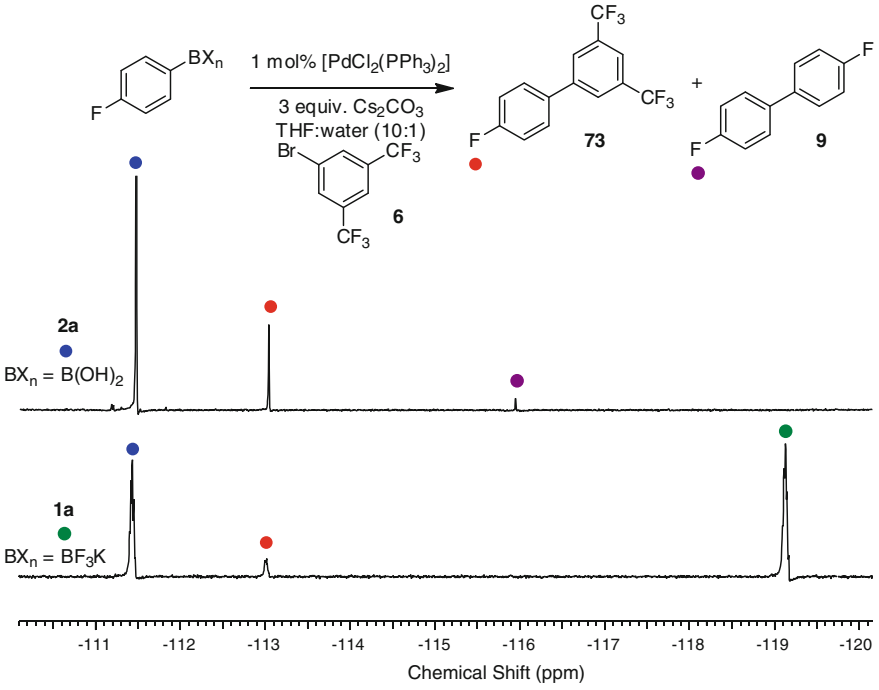

Fig. 3.24 ^{19}F NMR of a SM coupling of **2a** (*upper spectrum*) with ArBr **6**, showing the precatalyst activation product **9**, in contrast to a SM coupling of **1a** (*lower spectrum*) with **6** where this side product is completely absent

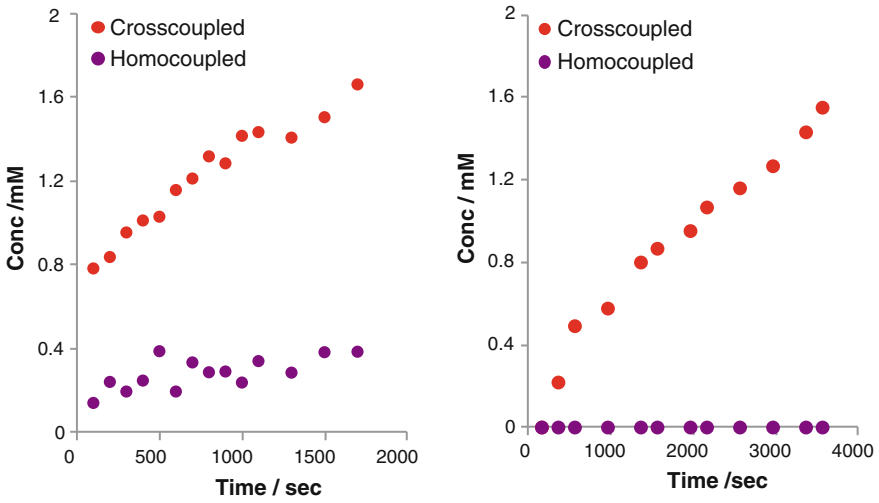

Fig. 3.25 Concentration vs time for the SM coupling between **2a** (*left plot*) with ArBr **6** and **1a** (*right plot*) with **6**. The plots clearly illustrate the generation of **9** only when **2a** is employed, despite both reactions containing an active catalyst

extent of homo-coupling was found to be in direct proportion to the catalyst loading. However, in reactions employing trifluoroborate **1a**, which generates **2a** *in situ*, there was no trace of **9** (<0.1 %), Figs. 3.24 and 3.25, even in the presence of high catalyst loadings (15 mol %).

2a build up from **1a** proceeded after the first 20–30 catalytic turnovers, implying an alternative, very efficient reductive activation was taking place. The rates of each activation process were compared by competing **2a** with **1a** and monitoring (^{19}F NMR) the extent of homocoupling. It required as much as 50 % of **2a** in a mixture with **1a** to restore the regeneration of **9** *via* the transmetalation/reductive elimination manifold, Scheme 3.23.

Verkade et al. [66] reported a fluoride-catalysed hydrolytic reduction of palladium(II) using tetrabutylammonium fluoride (TBAF). Fluoride attack on the phosphine ligand causes a shift in the electron density around the palladium(II) centre. This results in the donation of the phosphine based electron pair to palladium, thereby effecting its reduction to a mono-phosphine palladium(0) complex. A fluorophosphonium species (**76**) is liberated which is rapidly hydrolysed to phosphine oxide (**77**), Scheme 3.24.

In order to ascertain whether the fluoride liberated on the hydrolysis of **1a** could similarly mediate this reduction, isotopically enriched [^{18}O] (70 %) water was employed, Scheme 3.24. The label would be transferred to the triphenylphosphine oxide (**77**) under the fluoride-catalysed manifold but not under the double transmetalation/reductive elimination.

Isolated triphenylphosphine oxide (**77**) was compared between the SM coupling of **1a** and **2a** with **6** under the conditions of Scheme 3.19. Substantially higher

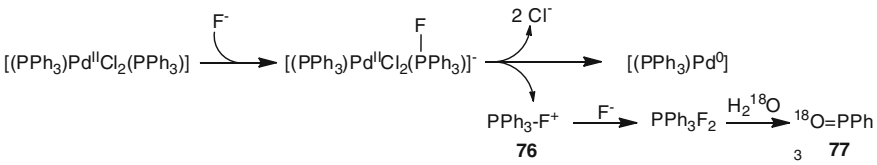

Scheme 3.24 Verkade's fluoride-catalysed hydrolytic reduction of palladium(II) to palladium(0)

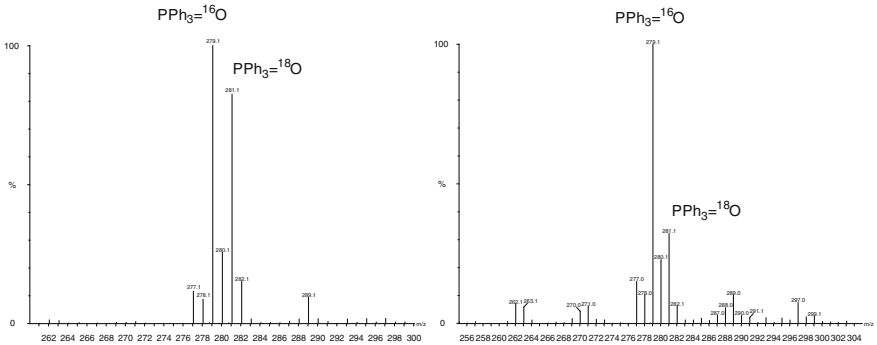

Fig. 3.26 MS (CI) of the isolated triphenylphosphine oxide (**77**) from a SM coupling of **1a** with **6** (*left spectrum*) and **2a** with **6** (*right spectrum*), clearly indicating an increase in the level of [^{18}O]-**77** (*m/z* = 281) when **1a** is employed

levels of ^{18}O incorporation were observed (MS–CI, *m/z* = 281) from reactions starting from **1a**, providing strong evidence for the Verkade mechanism in operation, Scheme 3.24. The isolation method utilised induced aerobic oxidation of the other phosphine ligand, which is responsible for the observed neighbouring peak (*m/z* = 279), (Fig. 3.26).

However, when the reaction was analysed by ^{31}P NMR *in situ*, the two isotopologues could be distinguished by an isotope shift ($\Delta\delta_P = 0.04$ ppm), and gave ratios characteristic of the initial enrichment in the water (70:30 ^{18}O:^{16}O), Fig. 3.27. The isotopic signature of the phosphine oxide was confirmed to be stable and not subject to exchange, as there was no difference detected when phosphine oxide **77** (0.12 mM, 32 % ^{18}O) was stirred overnight under the reaction conditions (55 °C, THF:water 10:1, 3 equiv. Cs_2CO_3).

^{31}P NMR, however, illustrated that both systems were phosphine deficient by the detection of phosphine oxide in reactions starting from **2a**. As the catalysis was shut down in each system upon the addition of a mercury droplet, this heterogeneous catalysis test infers, but not defines, the possibility of nano-particular catalysis. However, control reactions confirmed there was no difference in the coupling rates or outcomes, when catalysts prepared from either manifold were used in conjunction with the other substrate (**1a** or **2a**).

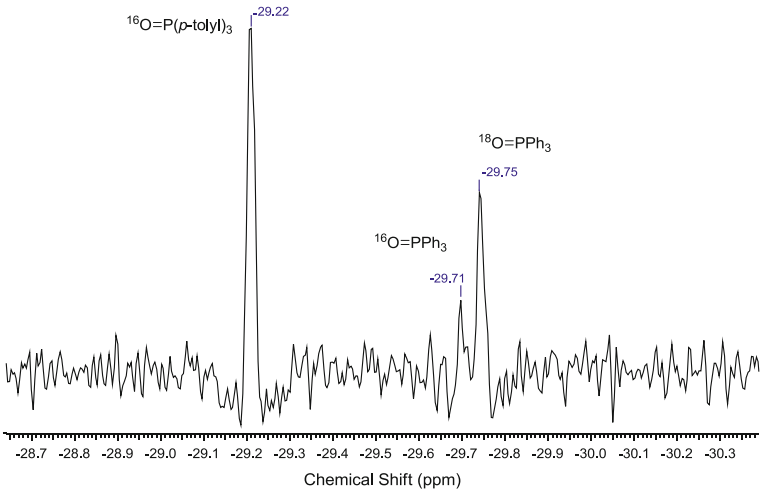

Fig. 3.27 ^{31}P NMR spectrum of the *in situ* SM coupling between **1a** and **6**, showing the isotope ratio of liberated **77** reflecting that of the water [$^{18}O_{0.7}$]. Tri-*p*-tolylphosphine oxide was used as an internal standard

It was additionally found that in the absence of any fluoride, and if boronic acid **2a** was in very low concentration, the aqueous basic THF effected a slower hydrolytic reduction of palladium(II), thus also bypassing the generation of **9**.

3.5.2 THF Hydroperoxide (II)

Phenol **10** was rapidly formed at the beginning of SM coupling reactions when boronic acid **2a** was employed, in quantities that depended on the purity of the THF. THF derived oxidants readily form *in situ* when free from inhibitors such as BHT. Commonplace purification techniques, such as distillation from sodium/benzophenone ketyl, remove these stabilisers, thereby rendering the solvent vulnerable to oxidation, if in contact with light and O_2.

The mechanism of the oxidation of **2a** presumably proceeds *via* a 1,2-rearrangement of a Lewis acid/Lewis base adduct (**79**$_{OH}$) to an electron deficient oxygen, Scheme 3.25.

This rapid oxidation was absent in reactions employing **1a** as the coupling partner. Indeed, R-BF_3K salts may be resistant to this decomposition pathway due to their enhanced stability; however the lack of ensuing oxidation, even upon liberation of **2a**, demonstrated that the quenching of the THF hydroperoxide (**78**) preceded the hydrolysis of **1a**.

To test the observations, "oxidising THF" was purposefully prepared by bubbling air through a sample of inhibitor-free THF under a light. Starch iodine

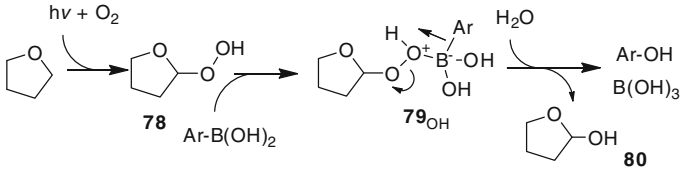

Scheme 3.25 Oxidation of arylboronic acid **2** by THF hydroperoxide (**78**) *via* $\mathbf{79}_{OH}$

paper would colourise when solutions were sufficiently oxidising, but the process was often variable in its outcomes and irreproducible, with ideal conditions unknown.

When [$^2H_4$]-**2a** was added to a solution of "oxidising THF", rapid oxidation to [$^2H_4$]-**10** was observed (^{19}F NMR). However, if the solution was pre-mixed with trifluoroborate [$^2H_0$]-**1a**, then a decisive drop in oxidation of [$^2H_4$]-**2a** was detected, thus confirming the quenching effect.

Fluoride has been shown to consume alkylperoxides in the gas phase, by deprotonation of the α-CH [67]. However, this possibility was eliminated after the same "oxidising THF" was pre-treated with TBAF or KF, where neither exhibited a difference to the level of oxidation of [$^2H_4$]-**2a** in untreated solutions. The effects of base, heat and glass on the reaction were all tested, but none had any effect, thereby confirming the quenching to be specific in **1a**.

The difference in Lewis acidity between boron ligated by fluoride and hydroxide, could induce a mechanistic bifurcation of the intermediate Lewis acid/Lewis base adduct **79**. The increased Lewis acidity of fluoride would lead to a decreased migratory aptitude of the aryl moiety, as well as affecting the polarity of the O–O bond. These factors may contribute to a 1,2-H/CH_2 shift from the THF ring, opening the peroxide bond towards the boron, which, following further hydrolysis, would give boronic acid **2a**, Scheme 3.26.

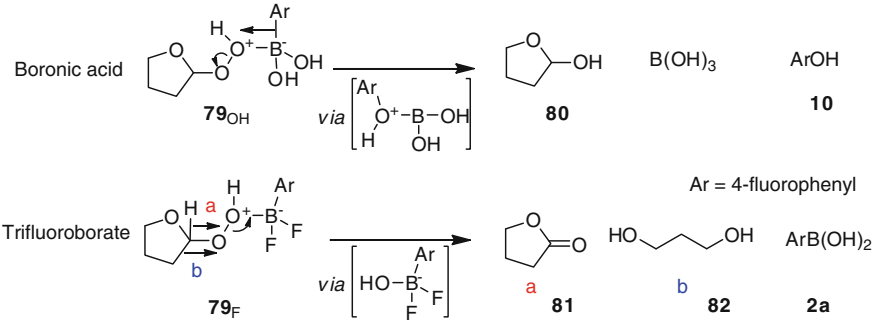

Scheme 3.26 Proposed quenching mechanism from trifluoroborate salts (*lower*) induced by greater Lewis acidity, compared to boronic acids (*upper*) which undergo oxidation

The by-products of both pathways were not easily differentiated (GC–MS, ^{1}H and ^{13}C NMR) from the extremely high concentrations of THF. Nonetheless, γ-butyrolactone (**81**) was observed (^{1}H NMR) upon the use of BF_3.OEt in "oxidising THF", which also pleasingly induced a quenching effect, consistent with an increasing Lewis acidity at boron. The Lewis acidic balance must be very fine as the use of $B(OH)_3$ similarly induced a quenching effect. The low cost and relative inertness of this latter reagent has potential application in the pre-treatment of reactions particularly sensitive to oxidations, e.g. rhodium-catalysed conjugate additions employing boronic acids in highly photooxidisable dioxane [68].

3.5.3 Oxidative Homo-Coupling (III)

In the SM coupling of boronic acid **2a**, incomplete degassing or the ingress of air during sampling can result in the steady production of the homo-coupled **9** and phenol **10**, Scheme 3.27. These side-products are formed in a 1:1 ratio throughout catalytic turnover. The mechanism of their formation, elucidated by Amatore and Jutand [61], involves a key palladium peroxy species, formed from O_2 and palladium(0). This species consumes two molecules of boronic acid to form **9** and perboric acid, $B(OH)_2OOH$, oxidises a third, to form **10**, Scheme 3.27.

The generation of side products **9** and **10** throughout the reaction was completely absent when **1a** was employed, even though catalytic turnover proceeds *via* boronic acid **2a**. To study the system further, SM coupling reactions were conducted in air, Scheme 3.28, to keep the level of O_2 constant, but primarily to exaggerate the process to aid in the elucidation. Reactions rarely went to completion due to catalytic degradation under these oxidising conditions; however, enough conversion was reached (30–70 %) to gain meaningful data.

The ratio between the cross-coupled product (**73**) and the total side products (**9** + **10**) for reactions employing **1a** as the nucleophilic partner was 3.6, in comparison to when **2a** was employed, it was observed to be 1.6. These experiments confirmed the difference between the systems, even under the forcing oxidative conditions.

In reference to the preceding hydrolysis necessary for **1a** to participate in catalytic turnover, three differences between the systems (**1a** and **2a**) were tested:

1. Due to the neutralisation of liberated HF, 1.5 equivalents of Cs_2CO_3 are consumed, Sect. 3.4.2, *vide supra*, in reactions starting from **1a**. Therefore, as both

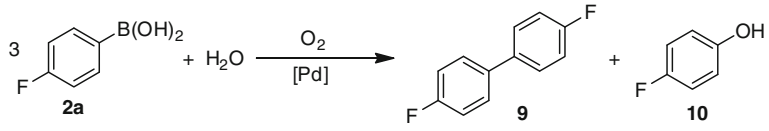

Scheme 3.27 Palladium-catalysed oxidative homocoupling of boronic acid **2a**

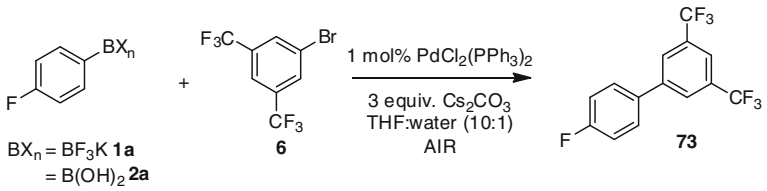

Scheme 3.28 SM coupling conditions of **1a** and **2a** with **6** in air

systems (**1a** and **2a**) employ 3 equivalents, there will be a lower loading of active base in couplings of **1a**. The concentration of base was varied in the SM coupling of **2a** with **6** in air, but the ratio (**73/9** + **10**) showed no dependence on this variable.

2. It has been shown, Sect. 3.4 *vide supra*, that the glass surface sequesters the liberated HF, and vessels with a higher surface area induced a faster rate of hydrolysis of **1a**. If the glass surface played a role in the oxidative homo-coupling then changes to the glassware may be significant. A Schlenk tube, which had not been washed after the SM coupling of **1a** with **6**, was used directly for the coupling of **2a** with **6** in air. However, no difference in the ratio (**73/9** + **10**) was observed in comparison to a control reaction.
3. Finally, the remaining salts from hydrolysis/base consumption of HF/KHF_2 were considered. **2a** was allowed to completely hydrolyse to **1a** under the basic (Cs_2CO_3) THF:water (10:1) conditions, before the addition of the coupling partner **6** and palladium precatalyst. No difference in the ratio (**73/9** + **10**) was again observed in comparison to a control reaction, this being consistent with fluoride not inhibiting oxidative homo-coupling [69].

It was also proposed that phenol could ligate to palladium and increase the rate of oxidative homo-coupling, but its addition to a SM coupling between **2a** and **6** showed this to be incorrect.

Considering the conjoined mechanisms for SM coupling and oxidative homo-coupling through the palladium(0) intermediate, suggests it to be partitioned between oxidative addition with Ar-Br and addition of O_2 to form the peroxo intermediate, Scheme 3.29.

The competition for the palladium(0) intermediate between Ar-Br **6** and O_2 was confirmed by the resulting linear relationship when increasing the concentration of **6** led to an increase in the ratio of **73/9** + **10**, Fig. 3.28.

Due to the concentration of **6** being the same in both systems, this analysis is not relevant in explaining the observed differences in side product generation between employing **1a** and **2a.** However, the concentration of the active boronic acid **2a** is not the same in each system. Careful analysis of the published homo-coupling mechanism from Amatore and Jutand [61], suggests that the addition of O_2 to palladium(0) is not reversible, thereby implying no concentration dependency of **2a** on the partitioning of the processes. That is, after the oxidation of

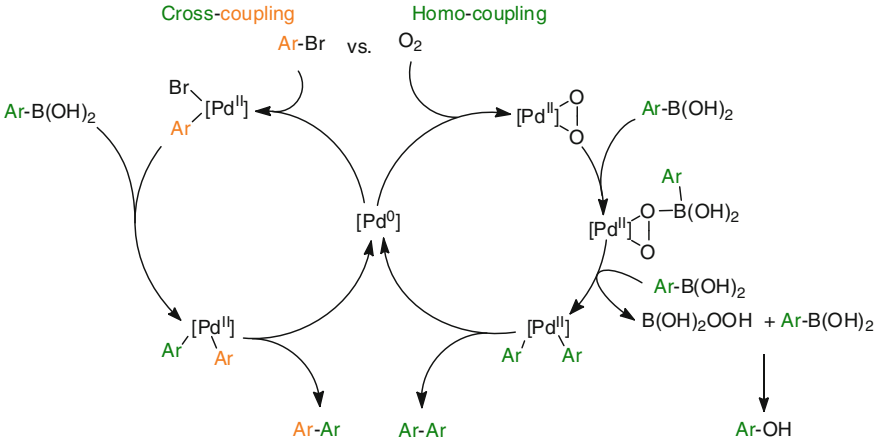

Scheme 3.29 The fused mechanisms of cross-coupling and homo-coupling, partitioned by palladium (0)

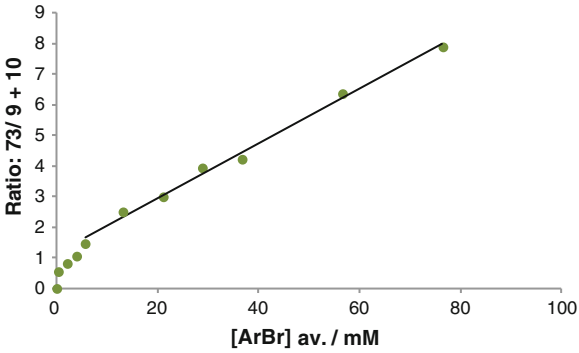

Fig. 3.28 The linear relationship between the average ArBr **6** concentration and the ratio of cross-coupled/homo-coupled + phenol (**73**/**9** + **10**). Higher concentrations of **6** engender a more efficient SM coupling by out-competing O_2 for [Pd^0]

palladium(0) to palladium(II), from either ArBr or O_2, no manipulation of either catalytic intermediate is possible before recycling the palladium(0) complex, Scheme 3.29. However, when the initial concentration of boronic acid **2a** was varied in the SM coupling with **6** in air, Scheme 3.28, different ratios of cross-coupled **73** to homo-coupled **9** + phenol **10** were observed. Two different concentrations of Ar-Br were tested, and the same trend was repeated, Fig. 3.29.

In contrast to that proposed, this concentration dependency therefore implies reversibility of the O_2 addition to palladium(0), Scheme 3.30. This contradiction may be due to differences in the ligation surrounding palladium, as the published homo-coupling mechanism focused on a bis-phosphine complex [61], whereas the observations reported herein are made from a phosphine deficient system. This side-product dependence on the concentration of **2a** may imply that the turnover limiting step shifts from that of oxidative addition to transmetalation. Therefore, when **2a** is low in concentration, the resting state becomes the product of the

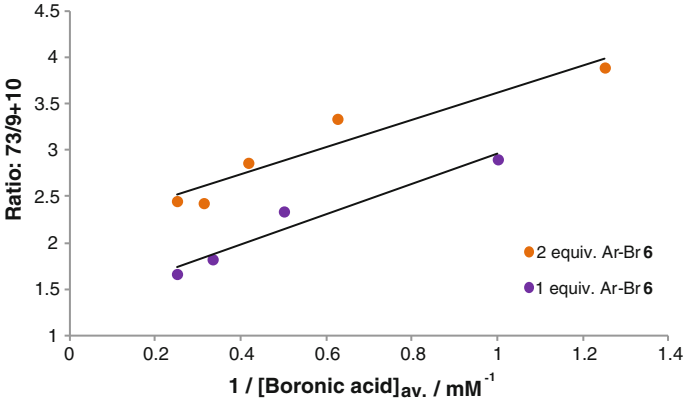

Fig. 3.29 The dependency of average boronic acid **2a** concentration on the ratio of cross-coupled/homo-coupled + phenol (**73/9** + **10**). Lower **2a** concentrations engender a more efficient SM coupling

halide/hydroxide metathesis following oxidative addition, [Pd(Ar)(OH)]. An alternative explanation can be provided by a boronic acid assisted O_2 addition to palladium(0); whereby the lower concentrations of **2a** would inhibit this step in the process, thus favouring cross-coupling, Scheme 3.30.

The high sensitivity of the boronic acid **2a** concentration to the balance in manifolds is key to the efficient cross-coupling of trifluoroborate **1a**. The trifluoroborate serves as an inert reservoir for **2a**, releasing it slowly and keeping its concentration low. This conclusion was tested by the slow, syringe-pump addition (0.2 μMs^{-1}) of boronic acid **2a** + Cs_2CO_3 in THF:water (10:1), to an SM

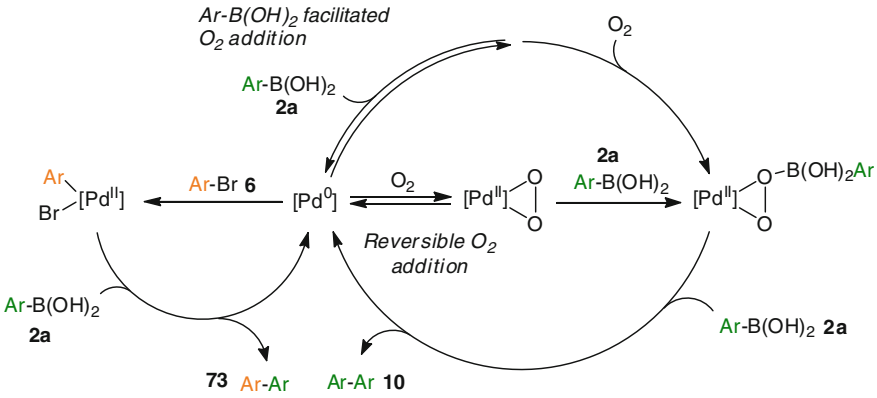

Scheme 3.30 Proposed alteration of the published[61] mechanism for oxidative homo-coupling, to include either a reversible O_2 addition to [Pd^0] or a boronic acid assisted addition, which is coupled to an irreversible oxidative addition of ArBr. Numbers refer to when Ar (*green*) = 4-fluorophenyl, Ar (*orange*) = 3,5-bis(trifluoromethyl)benzene

coupling with **6**, under air. The effect was substantial, as the ratio (**73/9** + **10**) increased to >9.5; compared to 3.6 when **1a** was directly employed. This "slow-release" reactivity in R-BF_3K salts is additionally postulated to be applicable in the attenuation of protodeboronation for substrates that are more sensitive to this side reaction.

3.6 Summary

The reactivity of trifluoroborate **1a** in the SM coupling with ArBr **6** has been studied in toluene:water and THF:water. Reactions in toluene:water (3:1) did not reach high conversions due to a competing base-catalysed protodeboronation pathway. A series of base titrations in water demonstrated that, under the biphasic conditions, **1a** hydrolysed instantly.

Protodeboronation was attenuated in the lower water concentrations of THF:water (10:1), due to a lower concentration of trihydroxyboronate **60a**. There was no evidence of the presence of any mixed species **7a** or **8a**, though it was shown they must exist in very low concentrations. Through DFT calculations of the transmetalation event and an isotopically labeled kinetic competition, it was shown that catalytic flux proceeds predominantly or solely, through the boronic acid **2a**.

1a led to cleaner SM coupling reactions than **2a**, *via* the suppression of three side reactions: precatalyst activation giving homo-coupled biaryl **9**, oxidation from a THF derived oxidant to give phenol **10** and palladium-catalysed oxidative homocoupling which gives **9** and **10**. The endogenous fluoride liberated, and the slow release of **2a** from **1a**, were both important features that contributed to the attenuation of side reactions.

References

1. M. Kumada, K. Tamao, K. Sumitani, J. Am. Chem. Soc. **94**, 4374–4376 (1972)
2. E. Negishi, A.O. King, N. Okukado, J. Org. Chem. **42**, 1821–1823 (1977)
3. J.K. Stille, Angew. Chem. Int. Ed. **25**, 508–524 (1986)
4. R.F. Heck, J.P. Nolley, J. Org. Chem. **37**, 2320–2322 (1972)
5. I.P. Beletskaya, A.V. Cheprakov, Chem. Rev. **100**, 3009–3066 (2000)
6. R. Chinchilla, C. Najera, Chem. Rev. **107**, 874–922 (2007)
7. Y. Hatanaka, T. Hiyama, J. Org. Chem. **53**, 918–920 (1988)
8. N. Miyaura, A. Suzuki, Chem. Rev. **95**, 2457–2483 (1995)
9. T.W.J. Cooper, I.B. Campbell, S.J.F. Macdonald, Angew. Chem. Int. Ed. **49**, 8082–8091 (2010)
10. D. Milstein, J.K. Stille, J. Am. Chem. Soc. **100**, 3636–3638 (1978)
11. A.F. Littke, G.C. Fu, Angew. Chem. Int. Ed. **41**, 4176–4211 (2002)
12. G. Altenhoff, R. Goddard, C.W. Lehmann, F. Glorius, J. Am. Chem. Soc. **126**, 15195–15201 (2004)

13. J.P. Wolfe, R.A. Singer, B.H. Yang, S.L. Buchwald, J. Am. Chem. Soc. **121**, 9550–9561 (1999)
14. A. Alimardanov, L. Schmieder-van de Vondervoort, A.H.M. De Vries, J.G. De Vries, Adv. Synth. Catal. **346**, 1812–1817 (2004)
15. G.C. Fu, A.F. Littke, C. Dai, J. Am. Chem. Soc. **122**, 4020–4028 (2000)
16. D. Zim, A.S. Gruber, G. Ebeling, J. Dupont, A.L. Monteiro, Org. Lett. **2**, 2881–2884 (2000)
17. N. Miyaura, J. Organomet. Chem. **653**, 54–57 (2002)
18. A. Suzuki, J. Organomet. Chem. **576**, 147–168 (1999)
19. K. Matos, J.A. Soderquist, J. Org. Chem. **63**, 461–470 (1998)
20. A.A.C. Braga, N.H. Morgon, G. Ujaque, F. Maseras, J. Am. Chem. Soc. **127**, 9298–9307 (2005)
21. C. Amatore, A. Jutand, G. Le Duc, Chem. Eur. J. **17**, 2492–2503 (2011)
22. B.P. Carrow, J.F. Hartwig, J. Am. Chem. Soc. **133**, 2116–2119 (2011)
23. A.F. Schmidt, A.A. Kurokhtina, E.V. Larina, Russ. J. Gen. Chem. **81**, 1573–1574 (2011)
24. C. Amatore, A. Jutand, G. Le Duc, Chem. Eur. J. **18**, 6616–6625 (2012)
25. C. Amatore, A. Jutand, G. Le Duc, Angew. Chem. Int. Ed. **51**, 1379–1382 (2012)
26. S. Darses, J.-P. Genet, Chem. Rev. **108**, 288–325 (2007)
27. G.A. Molander, B. Canturk, Angew. Chem. Int. Ed. **48**, 9240–9261 (2009)
28. G.A. Molander, N. Ellis, Acc. Chem. Res. **40**, 275–286 (2007)
29. F. Bellina, A. Carpita, R. Rossi, Synthesis **2004**, 2419–2440 (2004)
30. S. Darses, J.-P. Genêt, J.-L. Brayer, J.-P. Demoute, Tetrahedron Lett. **38**, 4393–4396 (1997)
31. S. Darses, T. Jeffery, J.-P. Genet, J.-L. Brayer, J.-P. Demoute, Tetrahedron Lett. **37**, 3857–3860 (1996)
32. H.-J. Frohn, N.Y. Adonin, V. V Bardin, V. F. Starichenko. J. Fluorine Chem. **117**, 115–120 (2002)
33. Z.-C. Chen, M. Xia, Synth. Commun. **29**, 2457–2465 (1999)
34. G.A. Molander, B. Biolatto, J. Org. Chem. **68**, 4302–4314 (2003)
35. G.A. Molander, B. Canturk, L.E. Kennedy, J. Org. Chem. **74**, 973–980 (2009)
36. G.A. Molander, T. Fumagalli, J. Org. Chem. **71**, 5743–5747 (2006)
37. G.A. Molander, M.D. Elia, J. Org. Chem. **71**, 9198–9202 (2006)
38. G.A. Molander, C.R. Bernardi, J. Org. Chem. **67**, 8424–8429 (2002)
39. G.A. Molander, B.W. Katona, F. Machrouhi, J. Org. Chem. **67**, 8416–8423 (2002)
40. G.A. Molander, A.R. Brown, J. Org. Chem. **71**, 9681–9686 (2006)
41. G.A. Molander, M.R. Rivero, Org. Lett. **4**, 107–109 (2002)
42. G.A. Molander, C.-S. Yun, M. Ribagorda, B. Biolatto, J. Org. Chem. **68**, 5534–5539 (2003)
43. V. Colombel, F. Rombouts, D. Oehlrich, G.A. Molander, J. Org. Chem. **77**, 2966–2970 (2012)
44. G.A. Molander, J. Ham, D.G. Seapy, Tetrahedron **63**, 768–775 (2007)
45. C.A. Hutton, O. Skaff, K.A. Jolliffe, J. Org. Chem. **70**, 7353–7363 (2005)
46. G.A. Molander, F. Dehmel, J. Am. Chem. Soc. **126**, 10313–10318 (2004)
47. G.A. Molander, L.A. Felix, J. Org. Chem. **70**, 3950–3956 (2005)
48. G.A. Molander, Y. Yokoyama, J. Org. Chem. **71**, 2493–2498 (2006)
49. G.A. Molander, P.E. Gormisky, D.L. Sandrock, J. Org. Chem. **73**, 2052–2057 (2008)
50. G.A. Molander, B. Canturk, Org. Lett. **10**, 2135–2138 (2008)
51. G.A. Molander, L. Jean-Gérard, J. Org. Chem. **72**, 8422–8426 (2007)
52. G.A. Molander, L. Jean-GeÌrard. J. Org. Chem. **74**, 1297–1303 (2009)
53. G.A. Molander, P.E. Gormisky, J. Org. Chem. **73**, 7481–7485 (2008)
54. M. Mizuta, K. Seio, K. Miyata, M. Sekine, J. Org. Chem. **72**, 5046–5055 (2007)
55. N. Pagano, J. Maksimoska, H. Bregman, D.S. Williams, R.D. Webster, F. Xue, E. Meggers, Org. Biomol. Chem. **5**, 1218–1227 (2007)
56. R.A. Batey, A.N. Thadani, D. V Smil. Org. Lett. **1**, 1683–1686 (1999)
57. S.W. Wright, D.L. Hageman, L.D. McClure, J. Org. Chem. **59**, 6095–6097 (1994)
58. R.A. Batey, T.D. Quach, Tetrahedron Lett. **42**, 9099–9103 (2001)
59. S.L. Buchwald, T.E. Barder, Org. Lett. **6**, 2649–2652 (2004)

60. C.A. Hutton, A.K.L. Yuen, Tetrahedron Lett. **46**, 7899–7903 (2005)
61. C. Adamo, C. Amatore, I. Ciofini, A. Jutand, H. Lakmini, J. Am. Chem. Soc. **128**, 6829–6836 (2006)
62. H.G. Kuivila, J.F. Reuwer Jr, J.A. Mangravite, Can. J. Chem. **41**, 3081–3090 (1963)
63. E. Vedejs, R.W. Chapman, S.C. Fields, S. Lin, M.R. Schrimpf, J. Org. Chem. **60**, 3020–3027 (1995)
64. G.A. Molander, L.N. Cavalcanti, B. Canturk, P.-S. Pan, L.E. Kennedy, J. Org. Chem. **74**, 7364–7369 (2009)
65. G.W. Kabalka, V. Coltuclu, Tetrahedron Lett. **50**, 6271–6272 (2009)
66. J.G. Verkade, M.R. Mason, Organometallics **9**, 864–865 (1990)
67. S.J. Blanksby, G.B. Ellison, V.M. Bierbaum, S. Kato, J. Am. Chem. Soc. **124**, 3196–3197 (2002)
68. T. Hayashi, K. Yamasaki, Chem. Rev. **103**, 2829–2844 (2003)
69. S. Punna, D.D. Díaz, M.G. Finn, Synlett **2004**, 2351–2354 (2004)

Chapter 4
Organotrifluoroborate Hydrolysis

4.1 Introduction

4.1.1 Side Product Formation in Suzuki–Miyaura Couplings

Side reactions are ubiquitous in all organic synthetic transformations of significant scope [1], and the Suzuki–Miyaura (SM) coupling is no exception. Side reactions can include catalyst degradation, such as ligand oxidation or metal reduction to form insoluble stable superstructures, i.e. palladium black. Alternatively the organohalide partner can undergo homocoupling or protodehalogenation and the boron reagent can undergo oxidative homocoupling, oxidation, protodeboronation or dehydration, Scheme 4.1.

As the degradation pathways available to the boronic acid coupling partner are most pertinent to this thesis, only these will be elaborated upon.

Dehydration of the boronic acid to cyclic or linear boroxines, which has already been discussed, Sect. 3.1.2 *vide supra*, is not particularly detrimental to SM coupling. This is due to the aqueous reaction conditions generally employed, under which any boroxines present are hydrolysed to the more reactive boronic acid. However, the uncertainties of boroxine content in prepared or commercially purchased material can affect conversions, as it can be difficult to achieve the precise stoichiometry.

The oxidation processes, direct oxidation and oxidative homocoupling, both of which are common in SM coupling reactions, have also been discussed, Sect. 3.5 *vide supra*.

4.1.1.1 Protodeboronation

Depending on the substrate, protodeboronation can be the most prevalent side-reaction that occurs in SM coupling. Coupling partners at particular risk are those based on heteroaryl [2], vinyl [3], alkyl [3] and polyfluoroaryl [4] boronic acids. This is especially salient in medicinal chemistry where heteroatomic biaryl

A. J. J. Lennox, *Organotrifluoroborate Preparation, Coupling and Hydrolysis*, Springer Theses, DOI: 10.1007/978-3-319-01134-9_4,

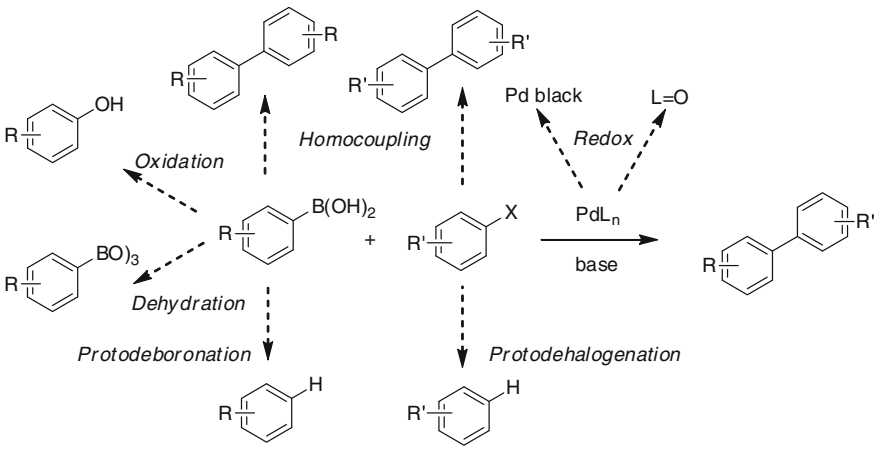

Scheme 4.1 Side reactions in SM coupling

moieties are extremely common motifs, but whose precursors are the most unstable. Considerable research has been directed towards realising the successful cross-coupling of compounds containing a heteroatom adjacent to the carbon bearing the boron atom, e.g. 2-pyridyl [5–8]. Because of its rapid decomposition, the 2-pyridylboronic acid (**2ao**) has become the archetypal unstable coupling partner. The clean reaction of this species is rated as one of the greatest achievements in cross-coupling chemistry, due to the ubiquity of this moiety in natural products and drug molecules.

Surprisingly, very little has been reported on the mechanisms of protodeboronation since a series of publications from Kuivila [9–13] in the early 1960s. From detailed kinetic studies of aqueous protodeboronation Kuivila was able to draw linear-free energy relationships (LFER), which were supported by H/D isotope studies [12]. The effect of metal ions on the system was also explored [9]. Identification of four distinct pathways resulted from the investigations, which included uncatalysed (1), specific base (2) [11], general and specific acid (3) [10] and Cd^{II} (4) [9] catalysed pathways, Fig. 4.1.

The uncatalysed (***i***), or pH independent, mechanism sits at the bottom of the pH well, Fig. 4.1, and is described as such because it exhibits rate constants larger than the sum of the expected contributions of both the acid and base catalysed pathways. The transition state is neutral, with reaction occurring between either a boronic acid (**2**) and water, or a hydronium and boronate (**60**), Scheme 4.2.

The base catalysed reaction (***ii***) occurs above pH 5 and appears to be specific, not general, catalysis, as "an increase in base concentration results in an increase in rate, only when it leads to an increase in the concentration of the boronate anion through an increase in pH" [11]. The transition state is negatively charged and the regular Hammett correlation coefficient ($\rho = -2.32$) suggests a small build up of positive charge. However, the magnitude of this value and the fact that the best

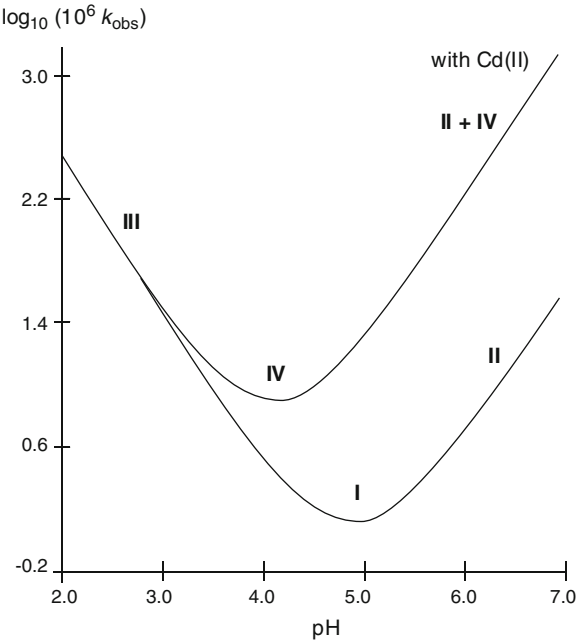

Fig. 4.1 Rate of protodeboronation (log scale) as a function of pH. Summary of each protodeboronation pathway (***i, ii, iii, iv***), as elucidated by Kuivila [9]

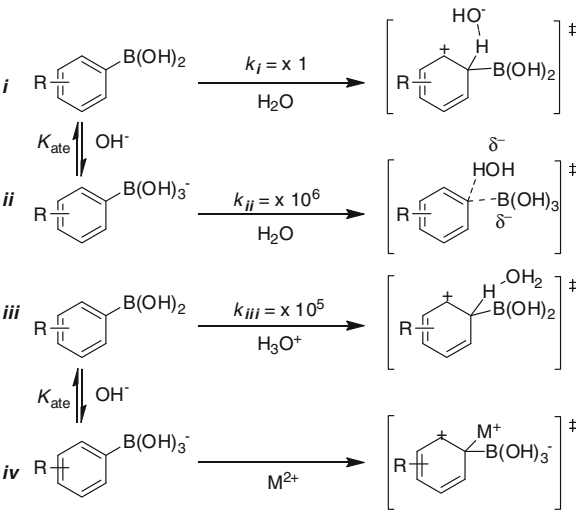

Scheme 4.2 Transition state structures for mechanisms ***i-iv***. The relative rates refer to Ar = 2,6-dimethoxyphenyl at 90 °C in water

correlation originated from regular σ values, not Brown's σ^+ values, implies direct protonolysis rather than *via* the expected Wheland intermediate. Because the two steps (equilibrium generated boronate and rate limiting C–B cleavage, Scheme 4.2) have opposing electronic demand, any substituent in any position has the result of increasing the rate of overall reaction; hence phenyl intriguingly is the slowest and sits slightly off the line of best fit in the Hammett plot [11].

Below pH 5, general acid catalysis predominates, where Brown's σ^+ values give a good correlation to rates ($\rho^+ = -5.0$) [13], implying a Wheland intermediate, Scheme 4.2.

Proficient catalysis in the presence of Cd^{II} ions at higher pH implies the intermediacy of an equilibrium generated trihydroxyboronate (**60**), Scheme 4.2. A whole range of metal ions (Cu > Pb > Ag ≫ Cd > Zn > Co > Mg > Ni) were found to be active although it is not clear whether the same mechanism is operating in all cases. Interestingly, of the group 10 metals, only nickel effected any catalysis; palladium was rapidly reduced, and platinum exhibited no activity. Therefore, under typical SM coupling conditions, it is unlikely that metallodeboronation occurs, although the possibility of catalytically efficient metal contaminants (e.g. Cu) should not be ruled out.

4.1.2 Strategies for the Mitigation of Side Reactions

Boronic acid degradation pathways are inherently linked to the SM coupling cycle through the boronic acid itself. Although mechanistically complex, the system is more readily manipulated than first appears, as the cycle may exhibit variable resting states and saturation kinetics. Attempts to improve conversions and yields in SM couplings have led to a number of different strategies based on the mechanistic manipulation of the SM coupling cycle. Four major categories can be defined: those based on catalyst acceleration (***A***), boron reagent activation (***B***), boron reagent masking (***C***) and slow-release (***D***), Scheme 4.3.

4.1.2.1 Catalyst Acceleration (A)

The use of extremely active catalysts for oxidative addition can increase the concentration of the transmetalating palladium complex, thereby increasing the turnover frequency and suppressing degradation pathways. By tuning the catalyst

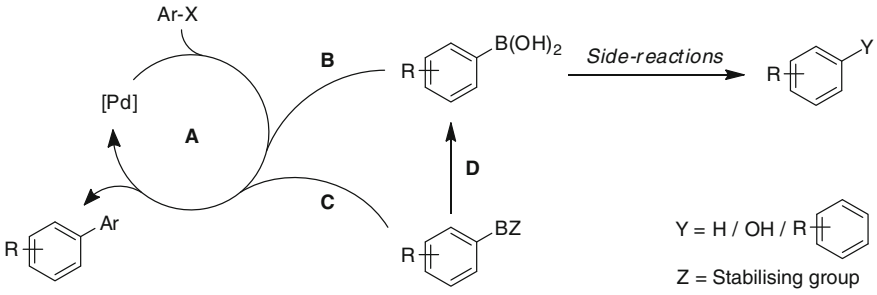

Scheme 4.3 Four major approaches (**A**, **B**, **C** and **D**) for the mitigation of boronic acid side-reactions

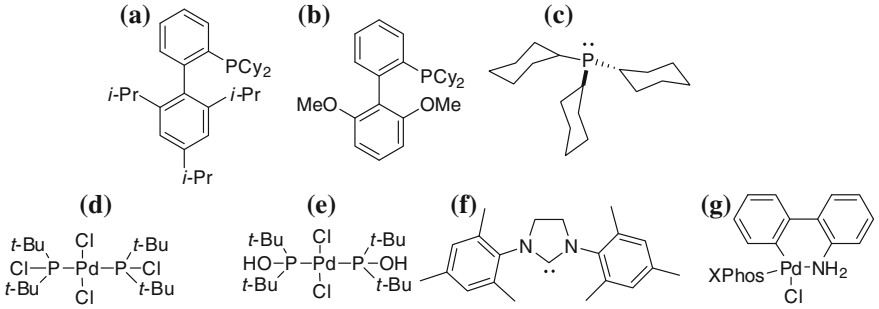

Fig. 4.2 Ligands (**a**, **b**, **c** and **f**) and precatalysts (**d**, **e** and **g**) used in the SM coupling of unstable boronic acids

activity, most commonly through ligand design, the turn-over limiting step may be shifted from oxidative addition to transmetalation. An example which has been successful in this regard comes from Buchwald who has developed dialkyl-*o*-biaryl phosphine ligands to couple heteroaryl boronic acids in excellent yields (70–97 %), ***a***, ***b*** Fig. 4.2 [14, 15]. These ligands are nominally mono-dentate, although evidence exists for palladium stabilisation from the *ortho*-aryl ring or an OMe group. Fu has utilised bulky electron-rich trialkyl phosphines (Cy_3P) to successfully cross-couple troublesome boronic acids, ***c*** Fig. 4.2 [16]. Phosphine chlorides and oxides have been shown [17] to be particularly effective ligands in this context, as have *N*-heterocyclic carbenes for the challenging pentafluorophenyl substrate, ***d***, ***e*** and ***f***, Fig. 4.2 [18]. A slightly different approach in the same category comes again from Buchwald [4], who has developed a precatalyst which is activated under exceptionally mild conditions where rates of protodeboronation are low, ***g***.

4.1.2.2 Boron Reagent Activation (B)

Addition of reagents which enhance the rate of transmetalation can result in catalytic turnover out-competing protodeboronation of the boronic acid. This can occur *via* an assisted transmetalation, for example by the addition of stoichiometric quantities of silver oxide for the coupling of polyfluorophenyl [19–21] or *n*-alkyl boronic acids [22]. Reaction of silver oxide with the isolated palladium complex resulting from oxidative addition of an aryl halide, implied that the role of the additive was to prime the complex for transmetalation by exchanging the halide for hydroxide.

Alternatively, the additive can effect a pre-transmetalation, which then delivers the organic group more efficiently to the palladium centre, thereby reducing protodeboronation. This is exemplified by the use of copper salts in transporting heteroaryl fragments to the palladium complex, Scheme 4.4 [23, 24].

Scheme 4.4 Copper facilitated transmetalation

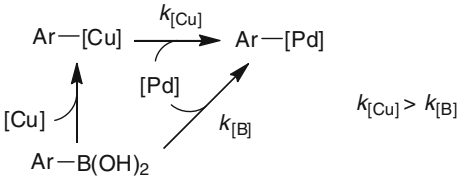

4.1.2.3 Boron Reagent Masking (C)

Protection or stabilisation of the vulnerable boronic acid functionality is a process currently proving very useful in the development of SM coupling reactions. For instance, base-catalysed protodeboronation proceeds *via* the equilibrium generated trihydroxyboronate (**60**) route ***ii*** Scheme 4.2 (see also Sect. 3.3 *vide supra*), which can be attenuated by replacing the boronic acid hydroxide ligands with more electron-donating ligands, thereby reducing the Lewis-acidity of the boron centre (i.e. reduce K_{ate}). Examples include pinacol esters (**4**) [17, 23], and trimethyl dioxaborinanes (**81**) [25], which are especially good reagents for the transfer of vinyl moieties, Fig. 4.3. In these cases it is not clear whether a formal deprotection step is required prior to transmetalation, so the term 'masking' is more appropriate than 'protection'.

The second approach in this category is to block complexation of hydroxide, by generating a comparatively inert anionic species (i.e. reduce k_{ii}) through addition of an alternative Lewis base to the boron centre. Examples include the lithium triisopropoxyboronate complex (**82**) [5], cyclic triolboronates (**83**) [26], and *N*-phenyldiethanolamine boronates (**84**) [7], all of which successfully cross-couple challenging heteroaromatic boronic acids (**2**), Fig. 4.3.

Stabilising the boron centre with a protecting group before a formal deprotection can be useful in some contexts but it is unlikely to aid in the reduction of

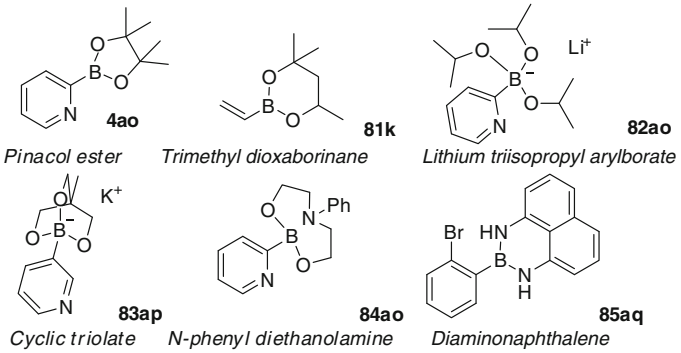

Fig. 4.3 Examples of boron reagent masking

side-reactions. One example is the 1,8-diaminonaphthalene ligated organoboron (**85**) developed by Suginome [27]. Simple acidic deprotection reveals the boronic acid for iterative couplings, Fig. 4.3.

4.1.3 Slow-Release (D)

The final strategy is that based on an inert protecting group from which the reactive boronic acid (**2**) is released *in situ* under the reaction conditions. The concentration of the active species is kept low by its slow release from an inert form, and its rapid consumption by the Pd-complex, thereby avoiding degradation pathways such as protodeboronation or homocoupling. If the release rate is slower than the oxidative addition, the catalyst resting state may shift from the Pd^0 complex to the product of hydroxide/bromide metathesis after oxidative addition, $[Pd^{II}Ar(OH)L]$, thereby rendering the transmetalation turnover limiting. The benefit of this mode of reactivity is that the reaction conditions can be tuned to control the rate of boronic acid release.

Potassium organotrifluoroborate (**1**, R-BF_3K) salts and *N*-methyliminodiacetic acid (**28**, MIDA) boronates are two examples of slow release organoboron reagents that stand out in terms of their broad applicability and growing use in SM cross-coupling reactions. Their popularity has progressed to the point where many examples of each reagent are now commercially available. However, there are a small number of examples in other organometallic cross-coupling reactions where 'slow release' has benefitted the reaction outcome. Nakamura found that slow addition of a Grignard reagent in iron catalysed cross-couplings significantly improved product yields [28]. von Wangelin extended this concept by developing a procedure in which the Grignard reagent was formed *in situ*, thereby keeping the reactive species in low concentration and hence reduced levels of homocoupling [29].

4.1.3.1 MIDA Boronates

MIDA boronates (**28**), pioneered by Burke [30], are stable and safe precursors to boronic acids (**2**). Their cross-coupling, following *in situ* hydrolysis, has been demonstrated in a number of natural product syntheses [31]. Some believe that the future of automated synthesis [32] lies in iterative synthesis; where bifunctional building blocks, with all the functionality and stereochemistry set, are coupled together using only one type of reaction. This is followed by a deprotection of latent functionality, activating it towards further coupling and subsequent repetition. Much development is still required before the concept becomes reality, but MIDA boronates have exhibited strong potential in this regard [33, 34]. They are stable to SM coupling conditions but upon treatment with mild aqueous base, the boronic acid is released for cross-coupling.

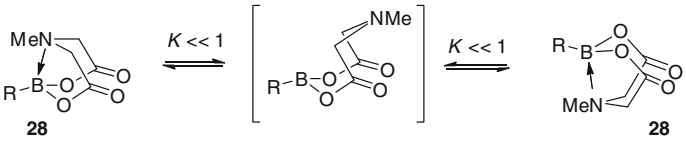

Scheme 4.5 Conformational rigidity exhibited by MIDA boronates (**28**)

MIDA boronates tolerate a large number of reaction conditions, including the harsh Jones oxidation [35] and, as such, can be carried through many synthetic sequences. The coordination of the Lewis basic nitrogen lone pair to the Lewis acidic boron centre pyramidalises boron from the sp^2 to the sp^3 hybridisation state. This renders the MIDA boronates conformationally rigid, and, in contrast to *N*-methyldiethanolamine, conformational flipping is not detected (on the ^1H NMR time scale) [35], Scheme 4.5.

In a seminal publication, Burke reported [3] general conditions under which the hydrolysis of MIDA boronates was slow, but catalytic turn-over of the resulting boronic acids was fast. This strategy was demonstrated for a number of unstable (vinyl (**2 k**), cyclopropyl (**2x**), heteroaryl) boronic acids, with excellent yields (76–99 %) of the cross-coupled product, obtained solely by keeping the boronic acid in low concentration. Under 'fast release' conditions, 2-furyl MIDA boronate (**28ar**) underwent coupling under comparable yield to the corresponding freshly prepared 2-furylboronic acid (**2ar**) (68 % vs. 59 %). Replication of the "slow-release" conditions, by syringe pump addition of boronic acid **2ar** over three hours, restored the yield (94 %) of cross-coupled product **87** to that of when MIDA boronate **28ar** is employed, Scheme 4.6.

This work has climaxed in the team's most recent publication on the subject, in which the 2-pyridyl moiety was successfully (49–96 %) cross-coupled with un-activated aryl chlorides, arguably the most difficult aryl cross-coupling [6]. Clean reaction was achieved by combining the strategies of catalyst activation (***A***), boron reagent activation (***B***) and slow release (***D***) from the 2-pyridyl MIDA boronates. Buchwald's precatalyst system [4], which activates under extremely mild conditions, was used in combination with a substoichiometric copper salt additive, Scheme 4.7. Diethanolamine (DEA) was added in preference to water to take

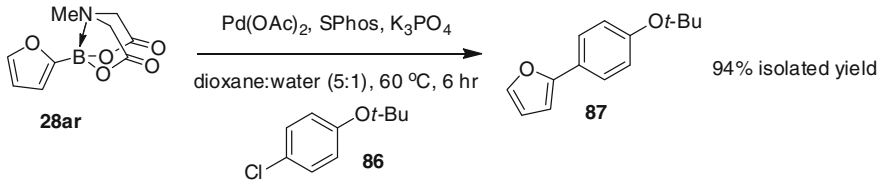

Scheme 4.6 General conditions for the cross-coupling of unstable boronic acids, *via* MIDA boronates. **28ar** efficiently coupled with **86** to give **87** in the same yield that when boronic acid **2ar** was slowly added

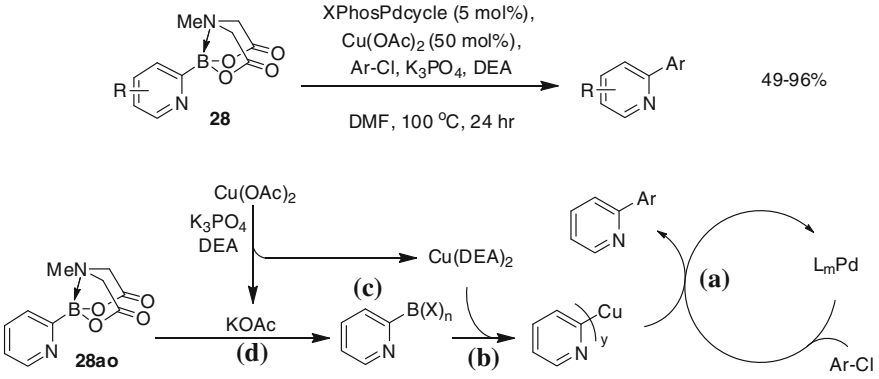

Scheme 4.7 Cross-coupling of the 2-pyridyl moiety utilising strategies ***A***, ***B***, ***D*** and possibly ***C***. DEA = diethanolamine

advantage of strategy (***C***): the diethanolamine boronic ester, which is less Lewis acidic, and therefore, more stable than the boronic acid, would rapidly form after the 'slow release' from the even more stable MIDA boronate. Whilst mechanistic investigations elucidated the role of diethanolamine as being a ligand for copper, the nature of the boron species that pre-transmetalates with copper is not clear, and it was found that *in situ* generated KOAc may be significant in this regard, Scheme 4.7.

4.1.3.2 Potassium Organotrifluoroborates

Potassium organotrifluoroborates (**1**, R-BF_3K) are the other major class of reagent that can operate under the slow-release mode of reactivity, Sect. 3.5 *vide supra*. A survey of reaction conditions used to couple R-BF_3K salts shows that, in contrast to the MIDA boronates, for every class of reagent there is a unique set of optimised conditions. This analysis alone suggests that there is no single mechanistic regime for the hydrolysis to the transmetalating boronic acid (**2**). The optimisation of the reaction temperature, solvent, precatalyst, base and time are thus a careful balance between ensuring the slowest hydrolysis in combination with the fastest turnover. On this basis it appears to be a far more complex system than the MIDA boronates, which could lead to greater difficulties in optimisation. Despite this challenge, a greater diversity of R-BF_3K reagents have been employed and are commercially available. In addition, their preparation is both cheaper and simpler than that of MIDA boronates, making it arguably the more useful class of reagent. Therefore, an appreciation of these complexities would be highly instructive in designing further efficiencies into the system, which is the aim of the present study. Indeed, there are cases where fast release conditions [36] are beneficial, adding to the value that a detailed understanding would provide.

4.2 Hydrolysis of Potassium 4-Fluorophenyltrifluoroborate

Perrin [37] has studied the hydrolysis of potassium aryltrifluoroborates (**1**) under buffered aqueous conditions, which are not relevant to SM couplings. Nonetheless, linear free energy relationship (LFER) analysis supported a rate-limiting loss of KF to give the highly reactive difluoroborane species **11**, prior to a series of exchanges of F^- for OH^-, Scheme 4.8, that ultimately lead to the boronic acid (**2**). Electron poor aromatic systems were highlighted as being especially robust species, as the negativity of the trifluoroborate 'ate' complex is better stabilised. Intermediate species of the type **7** and **8** were not detected, consistent with the observations (Sect. 3.4.3 *vide supra*) made in this study under typical SM coupling conditions. However, under certain conditions they have been detected (^{19}F NMR [38] or ESI MS [39]) *in situ*, for example in a completely aqueous environment or when boronic acids are exposed to fluoride under neutral conditions (Sect. 2.2 *vide supra*).

In order to move the investigation towards the context of SM coupling, the general conditions employed for this study (aqueous THF, Cs_2CO_3, 55 °C) are typical of those used in SM couplings and are prevalent in the reports from Molander [40]. After they were shown not to affect the rate of hydrolysis, the palladium precatalyst and aryl halide were not included in the general conditions. Potassium 4-fluorophenyltrifluoroborate (**1a**) was used as the model substrate, due to the ease in reaction monitoring offered by ^{19}F NMR, Scheme 4.9. The chemical shift (δ_F) of the *para* substituted fluorine atom is usefully sensitive to changes in substitution at the γ-position and to the ligation surrounding the boron centre.

4.2.1 Reaction Vessel Dependency

Kinetics of the hydrolysis of **1a** to **2a** monitored in an NMR tube and in a Schlenk tube showed very contrasting profiles under the otherwise identical conditions of Scheme 4.9. In an NMR tube, the reaction exhibited a rapid but clean pseudo first

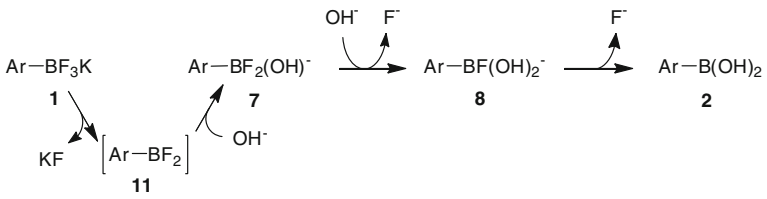

Scheme 4.8 Rate limiting loss of KF followed by F^-/OH^- exchange to give boronic acid (**2**)

Scheme 4.9 General conditions used for the investigation of the hydrolysis of **1a** to **2a**

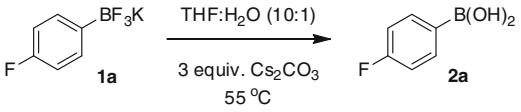

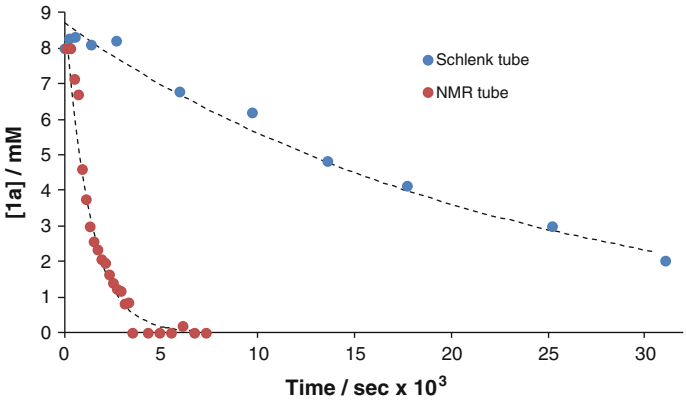

Fig. 4.4 Decay of **1a** under the conditions of Scheme 4.9, in an NMR tube and a Schlenk tube. Dashed lines are first order decays

order decay following an induction period. By comparison, reaction in a Schlenk tube exhibited a considerably slower pseudo first order decay after a much less obvious induction period, Fig. 4.4.

This surprising inconsistency was replicated amongst other reaction vessels, e.g. round bottomed flasks (rbf) and PTFE tubes, and when different stirring rates were used; further emphasising the need for a greater understanding of the hydrolysis. Correlations between vessels and kinetic profiles were not easily drawn from the results, Fig. 4.5, however, raising the stirring rate appeared to increase both $t_{1/2}$ and the induction period (**D** vs. **E**), and the addition of glass appeared to remove the induction period (**F** vs. **G**).

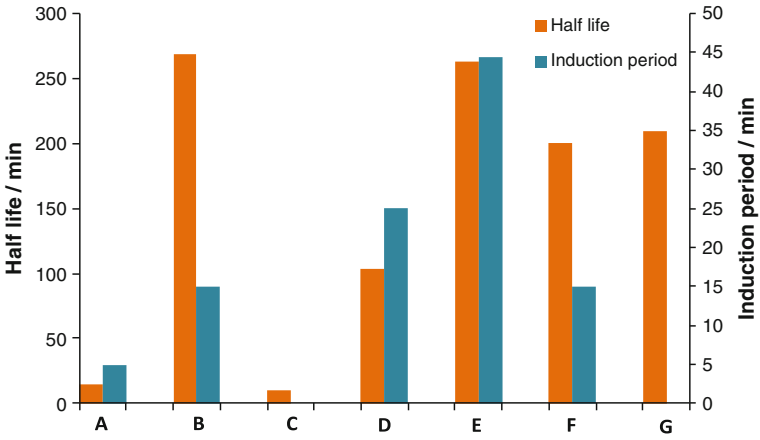

Fig. 4.5 Hydrolysis half lives and inductions periods in various reaction vessels. Where **A** = 5 mm OD NMR tube (20 Hz spin), **B** = 50 mL rbf, **C** = 15 mm Schlenk tube with conical base, **D** = 15 mm Schlenk tube with hemispherical base (100 rpm stirring), **E** = 15 mm Schlenk tube with hemispherical base (500 rpm stirring), **F** = PTFE tube, **G** = PTFE tube with added glass

4.2.2 The Effect of Glass

It is known that R-BF_3K salts are sensitive to silica-gel [41], silyl compounds [39, 42] and alumina; [43] therefore, it was proposed that the glass reaction vessel was sufficiently fluorophilic to actively sequester fluoride from the reaction mixture, Sect. 3.4.3 *vide supra*. By removing the glass and base altogether, equilibrium between **1a** and **2a** was rapidly reached, due to the absence of any mechanism by which to sequester the fluoride (i.e. no exogenous fluorophile such as glass or base). Upon the addition of glass powder to the equilibrated system, a clean pseudo first order decay of **1a** ensued, confirming the role of the fluorophile in net conversion of **1a** to **2a**, Fig. 4.6.

To explore the sensitivity of glass surface area on the system, the kinetics of hydrolysis, under base-free conditions, Scheme 4.10, were performed (by Paul Cogswell (PC) and Nina Ursinyova (NU), University of Bristol) by varying the mass of glass powder added to a Schlenk tube (PC), and the grade of glass powder added to a PTFE tube (NU).

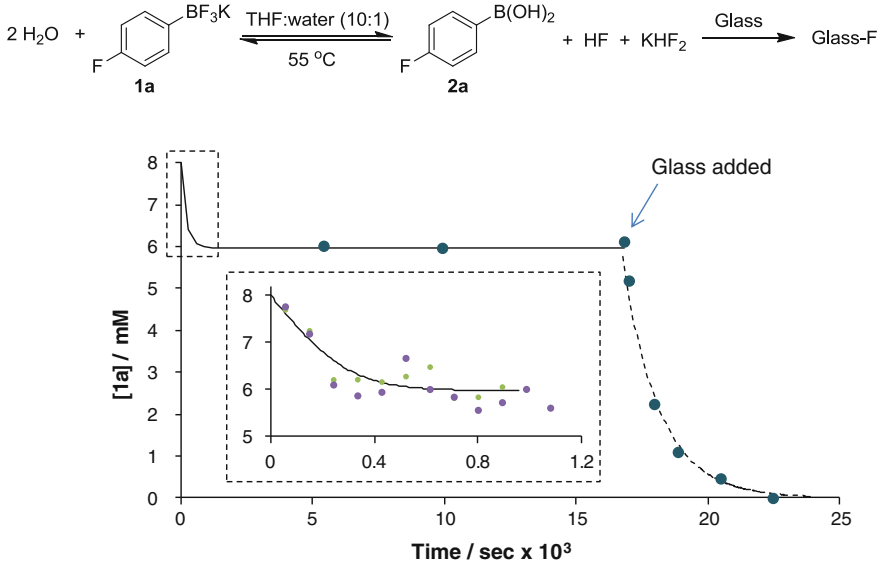

Fig. 4.6 Equilibration between **1a** and **2a** with no fluorophile, followed by the addition of glass—inducing full conversion to **2a**. Inset showing the rapid establishment of equilibrium. *Solid lines* are modelled data, Scheme 4.11 *vide infra*, and *dashed lines* are first order decays

Scheme 4.10 Conditions used to study the effect of glass powder

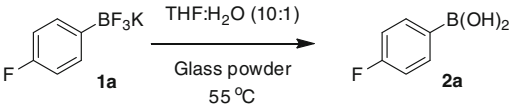

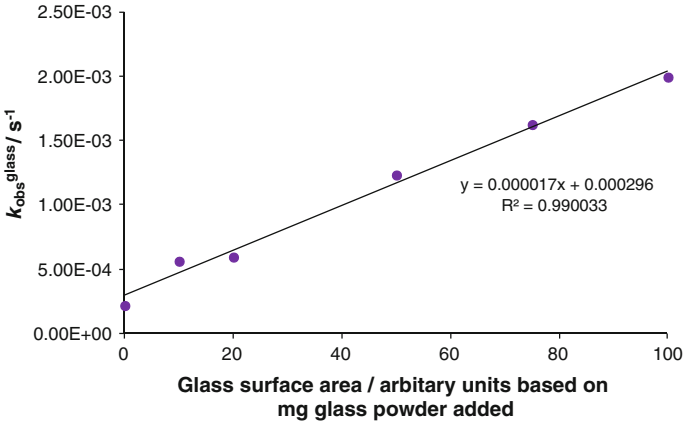

Fig. 4.7 Increasing fluorophilic capacity on the hydrolysis of **1a** to **2a** in a glass Schlenk tube, leading to an increase in the rate $\left(k_{\text{glass}}^{\text{obs}}\right)$. Note background hydrolysis from Schlenk tube mediated fluoride sequestration, when 0 mg added glass powder

Hydrolysis (**1a** → **2a**) rate profiles proceeded with simple pseudo first order decays and without an induction period. The rate ($k_{\text{obs}}^{\text{glass}}$) was directly proportional to both the mass of glass powder added (PC), Fig. 4.7, and the grade of glass added (NU), consistent with an increasing surface area providing a greater fluorophilic capacity to the system.

All attempts to recover fluoride from the glass surface *via* various organic solvent, aqueous, acidic and basic washes were unsuccessful. It was proposed that SiF_4 could be generated, which has a boiling point of −86 °C, however, attempts to trap this in C_6D_6 at low temperature, in a Young's tap NMR tube, were again unsuccessful. The head space above reactions conducted in PTFE vessels, in which solution phase KHF_2 is detected (^{19}F NMR), was neutral (pH paper), whereas those above reactions with glass present, where KHF_2 is *not* detected, were acidic. This may be evidence for hydrolysis of the extremely volatile SiF_4, which liberates HF.

4.2.3 Equilibrium Studies

The equilibrium, under fluorophile-free conditions, between **1a** and **2a** was studied in order to gain a fuller understanding of the observations made thus far. Experiments were conducted in a PTFE lined NMR tube or a PTFE tube with samples removed using a plastic syringe and analysed (^{19}F and ^{11}B NMR) in PTFE lined NMR tubes. The approach to equilibrium from **1a** was simulated using data obtained in two separate runs (see inset Fig. 4.6). The model was consistent with that of the simple balanced equation, Scheme 4.11, giving an equilibrium constant of $K = 5.5 \times 10^{-8}$ (dimensionless).

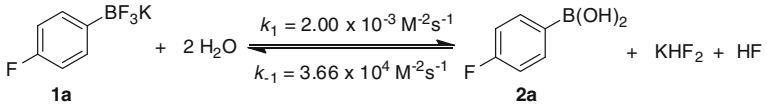

Scheme 4.11 Equilibrium model used for simulation of hydrolysis (**1a** → **2a**) data, see inset Fig. 4.8

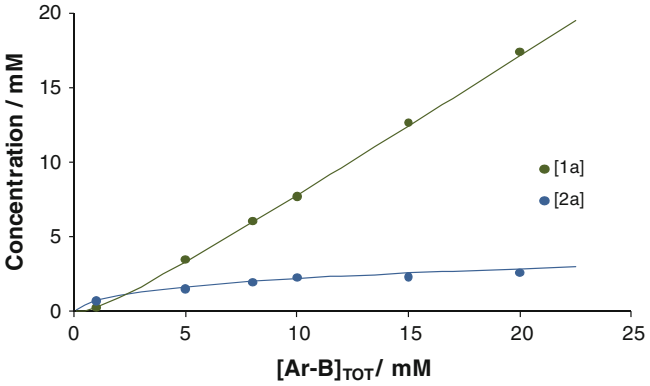

Fig. 4.8 Increasing initial **1a** concentration increases the proportion of **1a** at equilibrium. Lines through experimental data points are modelled data, Scheme 4.11

Consistent with the liberation of HF, when the pH was measured during the approach to equilibrium, a drop from neutrality to a pH of 4.5 was recorded, before rising to 5 upon the establishment of equilibrium Fig. 6.13 *vide infra*. The reasons behind this slight increase are currently not understood.

The effect of increasing concentrations of **1a** on the equilibrium proportions of **1a** and **2a** at 55 °C was tested. Interestingly, as the concentration of **1a** increased, smaller proportions of **2a** were liberated. For example, at 1 mM **1a** the proportion of **2a** at equilibrium was 73 %, whereas at 100 mM only 5 % of **2a** was liberated, Fig. 4.8. However, the absolute concentration of **2a** remained approximately constant whilst that of **1a** increased. This is due to the relative concentration of water being sufficiently high that it renders the forward term pseudo first order, whereas the reverse term is third order; thereby favouring the reverse process when the initial concentration of **1a** is high. The equilibrium constant ($K = 5.5 \times 10^{-8}$) derived from the simulations, Scheme 4.11, accurately reproduced the experimental data, Fig. 4.8.

The effect of increasing water concentration on the equilibrium proportions of **1a** and **2a** at both 25 and 55 °C was tested. Upon increasing the concentration of water in THF to 13 M, the expected 'Le Chatelier' shift in equilibrium towards **2a** (up to 38 %) occurred. However, above water concentrations of 13 M the proportion of **2a** did not continue to increase, rather it plateaued and slightly decreased as the concentration approached 55 M, Fig. 4.9. One rationale for these

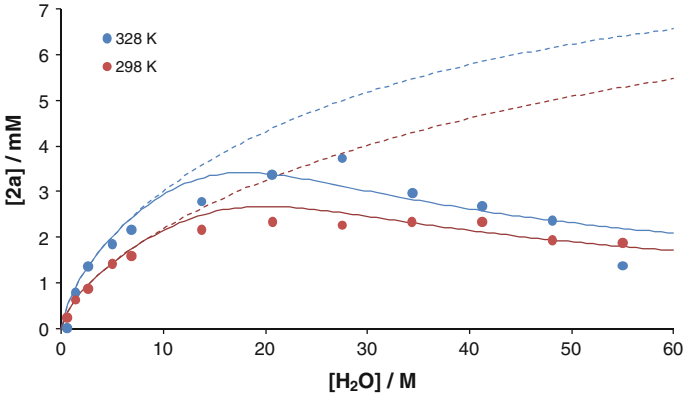

Fig. 4.9 Effect of increasing water concentration on equilibrium (**1a/2a**) proportions. *Solid lines* are modelled data including solvation model, *dashed lines* are predicted data without the solvation model

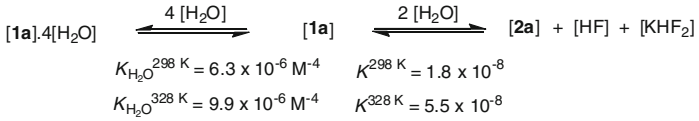

Scheme 4.12 Extended equilibrium model to include a solvation stabilisation of **1a** at high water concentration, with *K* for each step at the two temperatures tested

observations under neutral conditions is that water stabilises the ionic nature of **1a**, possibly through hydration of the potassium ion, thereby inhibiting formation of KHF_2. As a consequence of this effect the model required an additional stabilisation term to accurately simulate the data at high water concentrations. It was found that the addition of four water molecules to **1a** best represented the stabilisation, as three were insufficient, whilst five were too stabilising, Scheme 4.12.

The temperature dependency observed in these studies prompted a Van't Hoff analysis of the system. Due to the nature of the solvents and the analysis technique used (^{19}F NMR), a temperature range of only 30 °C was tested, which is generally not adequate to determine the thermodynamic parameters accurately. Nonetheless, increasing temperatures liberated increasing proportions of **2a**, confirming the endothermic nature of the forward reaction. The Van't Hoff plot ($K_{app} = [\mathbf{2a}][HF][KHF_2]/[\mathbf{1a}][H_2O]^2 = [\mathbf{2a}]^3/25*[\mathbf{1a}]$) revealed this endotherm to be marginal ($\Delta H = 0.4$ kJmol^{-1}); the entropic change was similarly small ($\Delta S = -0.5$ Jmol^{-1}K^{-1}), as would be expected from a *formal* third order (Scheme 4.11) reaction in both directions, Fig. 4.10.

The observations made herein, on the equilibration between **1a** and **2a**, may be useful in the optimisation of reactions of RBF_3K salts under hydrolytic conditions.

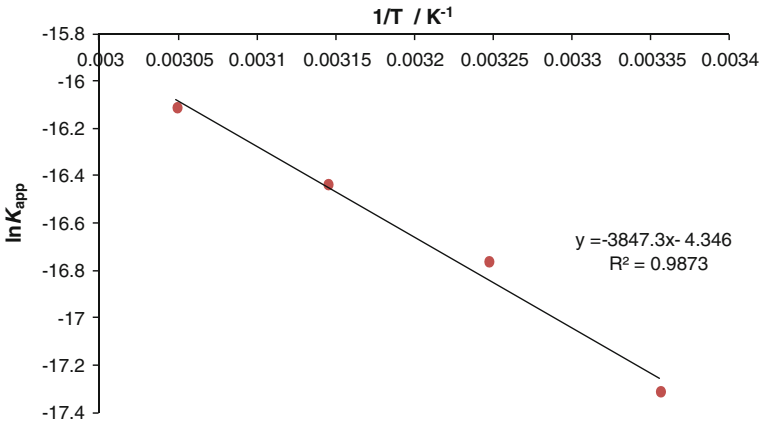

Fig. 4.10 Van't Hoff plot of the equilibrium between **1a** (initial concentration = 8 mM) and **2a** at 25, 35, 45 and 55 °C in THF:water (10:1)

4.2.4 B–F Versus B–C Bond Cleavage

It has been established, through the observed exchange between [$^2H_0$]-**1a** and [$^2H_4$]-**2a** to give [$^2H_4$]-**1a** and [$^2H_0$]-**2a**, Sect. 3.4.3 *vide supra*, that mixed intermediates **7a** (Ar–B(OH)F_2^-) and **8a** (Ar–B(OH)$_2F^-$) are accessed during SM couplings, but remain in undetectably low concentrations. However, this fluoride/hydroxide exchange was also observed (^{19}F NMR) in an *anhydrous* THF solution, whereby the expected solvent mediated transport of the anions cannot occur. This suggests that the reaction proceeds *via* a four centred transition state, either involving the ligands (F/OH, ***A***) or aryl groups (4-F-C_6H_4, ***B***), Fig. 4.11. The latter proposal would imply C–B, rather than B–F, bond cleavage, and negate the necessity for the intermediacy of mixed species **7a** and **8a**.

To probe this issue [$^{10}B_{0.95}$]-**1a** was prepared in two steps from isotopically enriched ^{10}B(OH)$_3$, and mixed with [$^2H_4$]-**2a** under the aqueous SM conditions of Scheme 4.9. Any cross-over products, [$^2H_4$,^{10}B]-**2a** or [$^2H_0$,^{11}B]-**2a**, formed would give evidence for C–B cleavage (***B***), without involvement of mixed species **7a** and **8a**. If cross-over products were not detected then it could be confirmed that ligand exchange occurred either directly under anhydrous conditions (***A***), or indirectly, mediated *via* solvent under hydrous conditions. The boronic acid products were

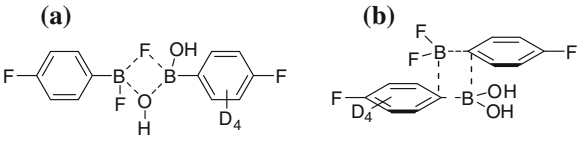

Fig. 4.11 Possible transition states for F^-/OH^- exchange under anhydrous THF conditions, as an implication when under SM coupling conditions (THF:water 10:1)

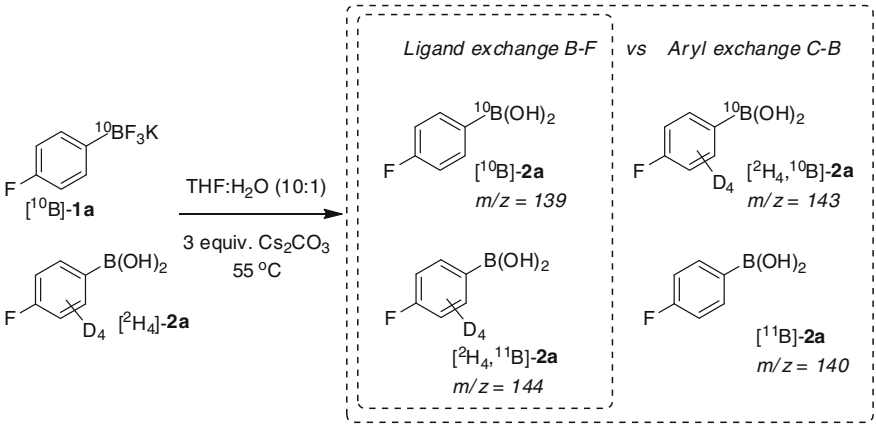

Scheme 4.13 Cross-over experiment indicating possible outcomes from observed (MS/EI) species

analysed (MS/EI), rather than the trifluoroborate, due to the gradual consumption of fluoride from the glass reaction vessel, Scheme 4.13.

Exchange, before complete consumption of fluoride by the glass, was confirmed by the observed (^{19}F NMR) formation of [$^2H_4$]-**1a**. However, upon completion of the reaction, no boronic acid cross over products were detected (MS/EI; $m/z = 140$ and 143), above that expected from the natural abundance (20 %) ^{10}B isotopologue of [$^2H_4$]-**2a** ($m/z = 143$). Therefore, although species such as **7a** and **8a** are not detected under these SM coupling conditions, this experiment again confirms their short-lived existence in the equilibrium between **1a** and **2a**. Interestingly, even when a range of anhydrous conditions (toluene, 100 °C, high concentration, 24 h; THF, 60 °C, high concentration, 24 h), thought to be primed for C–B cleavage through a dimeric transition state, were tested, the greatest level of cross-over products generated was only 7.5 %. With hindsight, dehydration of [$^2H_4$]-**2a** to the corresponding boroxine **61a**, may have stabilised it towards C–B cleavage.

4.2.5 Phase Splitting and the Effect of pH

4.2.5.1 Phase Splitting

It was recently noted by Hartwig [44] that the addition of an inorganic base to a homogenous solution of THF/water caused a phase splitting. This was confirmed under the general conditions of Scheme 4.9 as an extremely small, clear and colourless bilayer. Often very difficult to observe, the aqueous phase would appear at the bottom of the flask or as 'droplets' which adhered to the sides. In wide bottomed flasks, such as round bottomed flasks or large Schlenk tubes, the minor

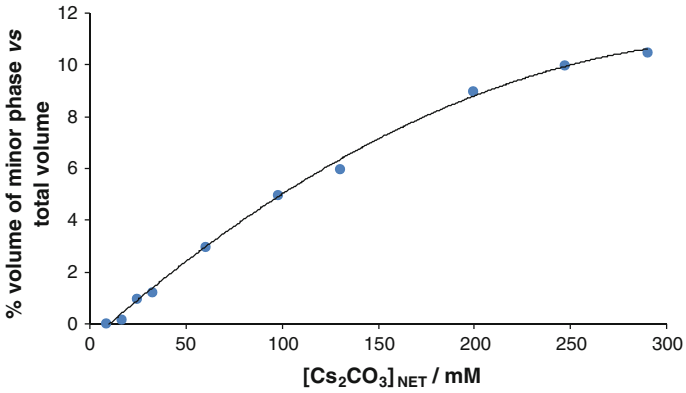

Fig. 4.12 Cs_2CO_3 titration into THF:water (10:1), causing a phase separation

phase was almost impossible to visually distinguish from the bulk phase. To study how the extent of phase separation correlated to the total concentration of Cs_2CO_3 added, the base was titrated into THF:water (10:1) and the phase boundary level noted in a burette specially adapted for the experiment, Fig. 4.12.

Under the general conditions of Scheme 4.9, the Cs_2CO_3 concentration (24 mM) generates a bilayer of only 1–2 % of the total volume. However, even upon complete dissolution of 3 equivalents of the base, the pH in the bulk phase is only marginally basic (pH = 7–8, pH paper) but the minor bilayer is strongly basic (pH = > 12, pH paper). The origin of the phase splitting can now be explained: the Cs_2CO_3 is not soluble in the THF/water mixture, rather it 'pulls' out the water to form a saturated basic aqueous biphase, leaving the bulk phase slightly drier. At high concentrations of total Cs_2CO_3 the proportion of biphase grew above that of the amount of water added (9 %), indicating a volume increase due to the aqueous saturation of Cs_2CO_3. Further increases in added Cs_2CO_3 resulted in the solid base not dissolving.

As the pH does not significantly increase in the bulk phase upon increasing Cs_2CO_3 concentration these observations now explain why successive additions of Cs_2CO_3 to a solution of **2a** in THF:water (10:1) had no effect on the equilibrium position between **2a** and **60a** (Fig. 3.15 *vide supra*).

4.2.5.2 Phase Splitting in SM Couplings

Molander has reported, for example in the SM coupling of alkenyltrifluoroborates [45], that silyl protecting groups remain intact in the fluoride rich environment of a SM coupling employing R-BF_3K salts. This unusual stability of silyl functionality towards fluoride can be explained in terms of the phase splitting. Analysis (^{19}F NMR) of the bulk phase, in the hydrolysis of **1a**, indeed indicated no "free" fluoride in solution, unlike the minor phase where fluoride was detected. Metastable

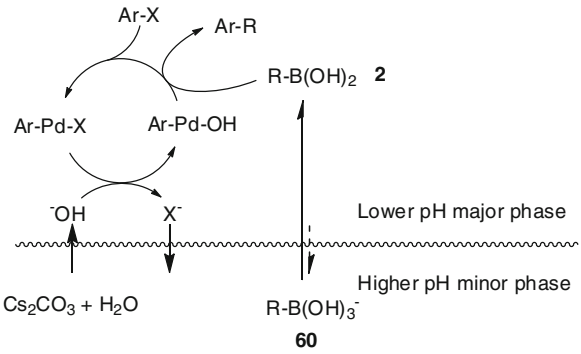

Scheme 4.14 Biphase controlled pH; facilitation of transmetalation through R-$B(OH)_2$ formation

dispersions of fluoride may be liberated in the bulk phase but then rapidly dissolve in the minor phase, thereby causing the silyl protecting groups no harm.

Hartwig [44], Amatore and Jutand [46], and Schmidt [47] have all independently demonstrated that it is the boronic acid ($Ar–B(OH)_2$) **2** and not the trihydroxyboronate ($Ar–B(OH)_3^-$) **60** that is the active transmetalating species in SM couplings, (Sect. 3.1.1 *vide supra*). Formation of the boronate species **60** attenuates turnover by suppressing the availability of the active boronic acid **2**. The equilibrium position between these species is highly base concentration/pH dependent (Sect. 3.4.2 *vide supra*), with a high pH promoting formation of the inactive species **60**. Therefore, the observations made herein regarding the connection between pH and the biphase may be integral to successful SM couplings: the boron reagent can exist as the boronic acid in the bulk phase due to the lower pH, and OH^- undergoes phase-transfer from the minor phase to form the key transmetalating Pd complex (Ar-Pd-OH), Scheme 4.14. Indeed in a 10:1 ratio of THF:water, >90 % of the boron reagent exists as the boronic acid (Sect. 3.3.1, *vide supra*). In this way SM coupling attenuation *via* boronate **60** generation is minimal.

The observations detailed herein may explain the extensive use of biphasic SM couplings: a survey (SciFinder, Chemical Abstracts Service, Columbus, OH) of 36976 biaryl couplings between 1981–2011 showed that >53 % contained water as a cosolvent of which at least 73 % were predicted to be biphasic. For example, the use of toluene:water or benzene:water were popular combinations where parallel conclusions can be drawn. Where water was not added as a cosolvent, the use of alcoholic solvents (IPA, EtOH, MeOH) was common. In these cases, formation of the less Lewis acidic boronic ester may occur, which may attenuate formation of the inactive trihydroxyboronate **60** from residual water, and/or transmetalate directly with the Ar-Pd-OH species.

4.2.5.3 pH Measurements

Monitoring the pH (pH probe, uncalibrated) during the hydrolysis of **1a** to **2a** proved very informative. Solvent (THF:water, 10:1) was added to a solid mixture

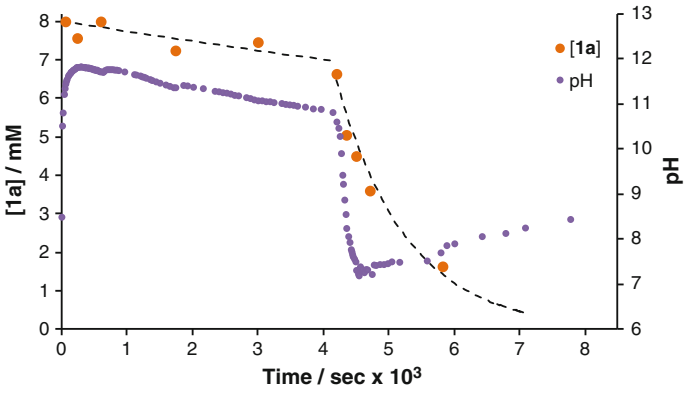

Fig. 4.13 pH (right-hand y-axis) and **1a** concentration (left-hand y-axis) versus time (x-axis), where a long induction period and high pH was observed. *Dashed lines* are first order decays ($t_{1/2}$ (0–4.5 s x 10^3) = 5.5 h; $t_{1/2}$ (4.5–7 s x 10^3) = 12 min)

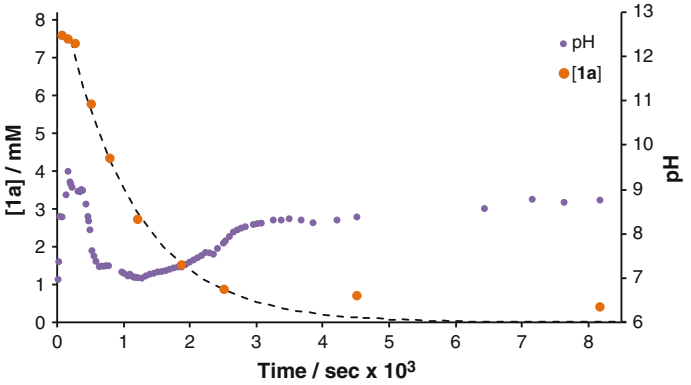

Fig. 4.14 pH (right-hand y-axis) and **1a** concentration (left-hand y-axis) versus time (x-axis), where a short induction period and lower pH was observed. *Dashed lines* are first order decays ($t_{1/2}$ (0–0.3 s x 10^3) = 5.5 h; $t_{1/2}$ (0.3–6 s x 10^3) = 12 min)

of 3 equiv. Cs_2CO_3 and **1a**, during which time the pH rose as the base dissolved, bringing small proportions of hydroxide into the bulk phase. On some occasions the pH reached as high as 12, which corresponded to a very long induction period during which only a minor proportion of **1a** underwent hydrolysis, Fig. 4.13. After the induction period, hydrolysis proceeded by a pseudo first order decay accompanied by a drop in approximately 4 pH units. As the rate of reaction slowed down, with less HF being liberated, the pH gradually increased.

On other occasions the pH did not reach 12 and the induction period was much shorter; however, when fast hydrolysis ensued, an accompanying decrease in pH was observed, Fig. 4.14.

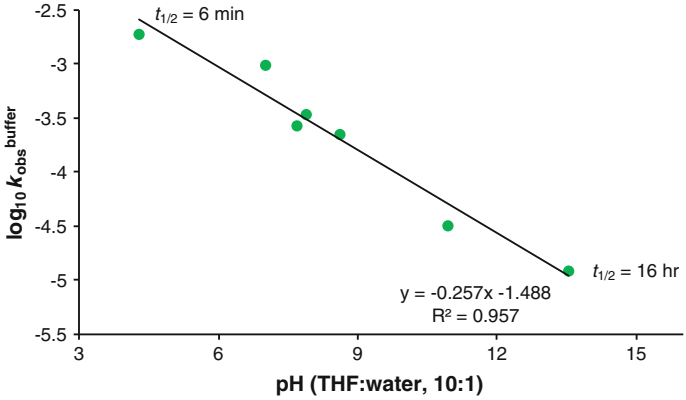

Fig. 4.15 Rate of hydrolysis (log scale) versus pH, indicating a specific acid-catalysed mechanism

The observed relationship between rate and pH prompted an investigation into the rates of hydrolysis in homogeneous solutions; to remove any issues associated with the unusual pH gradient of the biphasic system. Therefore, by employing 3 equivalents of an organic base (Hünig's base, NEt_3 or DBU), it was found that the rate was proportional to the pKa of the base (NEt_3 ($pK_a = 10.8$): $t_{1/2} = 33$ min; Hünig's base ($pK_a = 11.3$): $t_{1/2} = 43$ min; DBU ($pK_a = 12$): $t_{1/2} = 2.9$ h). However, a slightly more informative approach was to consider the effect of pH on the hydrolysis rate; by employing a range of homogeneous buffers. Typical aqueous buffers, e.g. phosphates, were not suitable due to the phase splitting engendered in a THF:water solution. Amine bases (NEt_3, Hünig's base, DBU, P_4-*t*Bu) were used in a large excess (100 mM) along with more traditional organic buffers such as TRIS and MOPS buffer. The pH of these buffers in THF:water (10:1) solutions were recorded (pH probe, uncalibrated) and the kinetics of the hydrolysis (**1a** → **2a**) were measured (*in situ* ^{19}F NMR), Fig. 4.15.

As the pH dropped, the rate (k_{obs}^{buffer}) increased substantially: a pH range of 10 units switched the $t_{1/2}$ from 6 min to 16 h, which suggests, that although the process had previously [39] been proposed to be effected by base, it actually proceeds *via* an acid-catalysed mechanism. The linearity of the plot and buffer concentration independence confirmed the *specific* rather than *general* nature of the acid catalysis. The acid catalysed pathway may originate from a decrease in the activation barrier upon HF-abstraction of KF from R-BF_3K to form KHF_2.

Rather paradoxically, although base is required to sequester the HF/KHF_2, thereby driving the reaction to completion, acid is required to catalyse the equilibrium, leading to the fast first order decays, Figs. 4.13 and 4.14. The reaction is potentially autocatalytic as HF is formed, which reduces the pH, but is only slowly mopped up by a mass transfer mechanism from either the glass surface or the strongly basic minor biphase.

The base mediated suppression of solvolysis during the induction period originates from the buffering of the bulk phase by the strongly basic minor phase. The buffering capacity is dependent on at least three processes: ***i***) the rate of equilibration to liberate HF/KHF_2, ***ii***) the rate of sequestration of HF/KHF_2 by the base or glass and ***iii***) the rate of hydroxide or carbonate transfer from the minor phase to the bulk phase. Since process ***ii*** depends on the surface area of the vessel and process ***iii*** depends on the interfacial surface area and mixing efficiency of the biphase, the reaction environment becomes a vital component to the rates of hydrolysis. The strong rate dependence on pH, and buffering capacity of the system, now explains the variability exhibited in different reaction vessels by the biphasic system (Cs_2CO_3), in the induction periods and ensuing first order decay, Fig. 4.5.

When the concentration of **1a** decreases, its rate slowly deviated from a first order decay (after 2.5 s x 10^3, Fig. 4.14) which is coupled to an increase in the pH. The rate of hydroxide diffusion into the bulk phase is now evidently greater than the rate of HF production, thereby switching off the acid catalysed pathway. The implications of this observation in SM coupling may be that it takes a disproportionately long time to reach completion due to the considerably slower release rate of the active species.

4.2.5.4 Hydrolysis Attenuation with Ultrasound

To demonstrate the importance of process ***iii***, hydrolysis of **1a** under the general conditions of Scheme 4.9, conducted in an NMR tube, was subjected to 20 s of ultrasound at the start of reaction prior to *in situ* analysis (^{19}F NMR), Fig. 4.16.

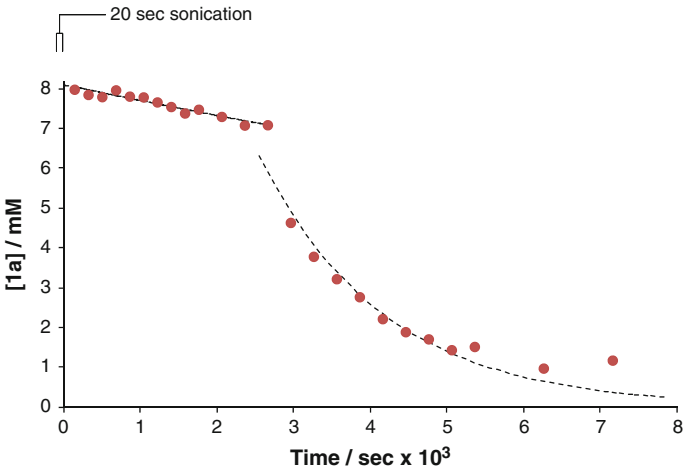

Fig. 4.16 20 seconds prior sonication of the hydrolysis of **1a** (THF:water 10:1, 3 equiv. Cs_2CO_3, 55 °C) in a 5 mm OD NMR tube. *Dashed lines* are first order decays ($t_{1/2}$ (0–2.5 s x 10^3) = 4 h; $t_{1/2}$ (2.5–6 s x 10^3) = 16 min)

Remarkably, 20 s of ultrasound engendered a 45 min induction period, the time taken for the phases to fully separate and the pH to drop enough for acid catalysis to proceed. When a biphasic mixture (3 equiv. Cs_2CO_3, THF:water 10:1) of boronic acid **2a** was sonicated, ^{19}F NMR indicated no increase in the concentration of trihydroxyboronate **60a** species. This inferred that sonication did not increase the pH in the bulk phase above that which is normally accessed, but created a greater interfacial surface area, rendering the transfer of hydroxide to the bulk phase very efficient. The sequestration of liberated HF/KHF_2 is therefore rapid, suppressing the acid catalysis, rather than creating a large increase in the pH in the bulk phase.

It was recognised that the attenuation of R-BF_3K salt hydrolysis, upon sonication of the biphasic reaction mixture, could potentially be exploited for chemoselective SM coupling of a boronic acid in the presence of a R-BF_3K salt. Initial studies were influenced by Molander [48, 49] who hydroborated an olefin with 9-BBN. In the presence of a potassium organotrifluoroborate, one can selectively cross-couple the 9-BBN moiety under anhydrous conditions; a subsequent switch to aqueous conditions prompts the trifluoroborate moiety to hydrolyse then cross-couple, all in "one-pot". This concept was demonstrated in two forms: firstly (***1.***) the trifluoroborate was attached to the aryl halide component of the first cross-coupling,[49] and secondly (***2.***), it was appended to the initial olefin, e.g. potassium vinyltrifluoroborate (**1 k**),[50] Scheme 4.15.

Using ultrasound to attenuate the hydrolysis, rather than anhydrous conditions, would be a simple improvement from switching the whole solvent system. Upon cessation of sonication the trifluoroborate could hydrolyse and undergo a subsequent cross-coupling with a different electrophilic Ar-Br.

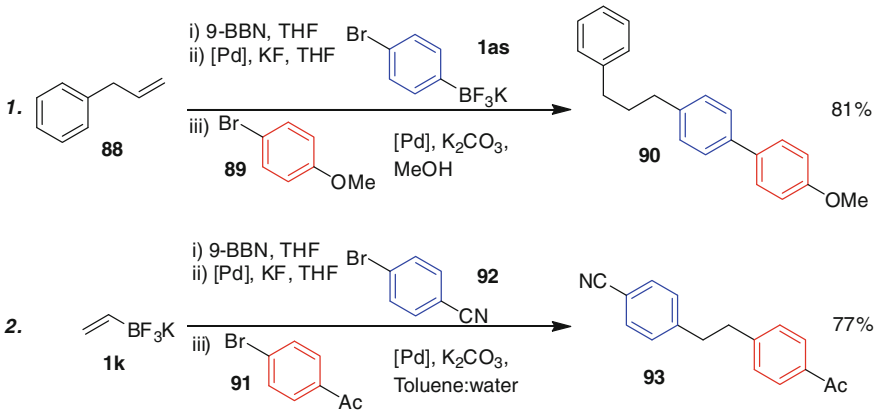

Scheme 4.15 Solvent mediated chemoselective couplings, whereby trifluoroborates **1as** and **1 k** remain intact during the SM coupling of the 9-BBN moiety under anhydrous conditions, followed by a transfer to solvolytic conditions where it undergoes hydrolysis and cross-coupling with organohalides **89** and **91** respectively, to give **90** and **93**

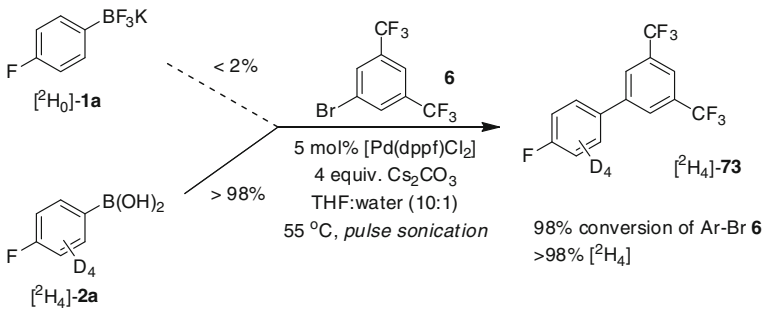

Scheme 4.16 Ultrasound mediated chemoselective SM coupling of **2a** with **6**, in the presence of **1a** under solvolytic conditions

Initial attempts at the sequential SM coupling of the ethyl 1,2-dianion equivalent, 1,2-diboraethane (***2.***) Scheme 4.15, under the general conditions of Scheme 4.9 with sonication, were unsuccessful. Attention was subsequently focussed on providing a proof of principle, so the system was simplified by separating the boron moieties into separate molecules. With [^{2}H$_4$]-**2a**, **1a** and two different electrophiles in the same vessel it was hoped that during sonication [^{2}H$_4$]-**2a** would cross-couple with the most reactive electrophile, then, upon ceasing sonication, **1a** would hydrolyse and cross-couple with the other electrophile. Unsurprisingly this ambitious task did not work as planned. Various alterations were made including the addition of the second electrophile after the first coupling, as well as using large excesses of the second electrophile, neither of which yielded the desired products. The catalyst system was identified as the cause of the problem, through the observation of palladium black formation. Therefore, the catalyst loadings were varied and the ultrasound reduced to pulses with rapid stirring to ensure efficient buffering between the phases. 4 x 10 s pulses of ultrasound every 10 min proved most successful, as [^{2}H$_4$]-**2a** was completed converted to [^{2}H$_4$]-**73** in the presence of **1a**, Scheme 4.16. Unfortunately, the active palladium catalyst did not survive long enough to effect the post-hydrolysis coupling of **1a**.

4.2.6 Vessel Dependency in SM Coupling

The slow-release of boronic acids from R-BF$_3$K salts, which can be replicated *via* slow addition the boronic acid, reduces side reactions such as protodeboronation and oxidative homocoupling, Sect. 3.5.3 *vide supra*. Furthermore, this release rate of active species from R-BF$_3$K has been found to be very dependent on the vessel shape, and on the magnetic stirring speed. The connection between side-product generation and vessel shape was investigated by studying two SM couplings in Schlenk tubes differing only in the shape of their base. The difference in base

shape causes a difference in the buffering ability of the bulk phase from the minor phase due to different mixing efficiencies. The reactions were run under air to keep the level of O_2 constant, thus deliberately providing a competitive side reaction (oxidative homocoupling; alternatively a R-BF_3K salt whose corresponding boronic acid is sensitive to protodeboronation could have been employed) for the boronic acid. The vessel material, stirring rates and volumes were identical and mixing vortices were negligible.

The tube with a cone shaped base effected poor phase contact between the biphase, thus HF was inefficiently consumed and the pH was allowed to drop, inducing fast hydrolysis ($t_{1/2} = 10$ min). The ratio of cross-coupled product to homo-coupled + phenol (**73/9** + **10**) was 1.5; similar to that detected when starting from **2a** directly, Sect. 3.5.3 *vide supra*. In contrast, the tube with a hemispherical base ensured good mixing and a higher pH in the bulk phase, suppressing acid-catalysis, leading to slow hydrolysis ($t_{1/2} = 4.4$ h). The ratio of cross-coupled to homo-coupled + phenol (**73**/9 + **10**) in this case was 2.4, Fig. 4.17.

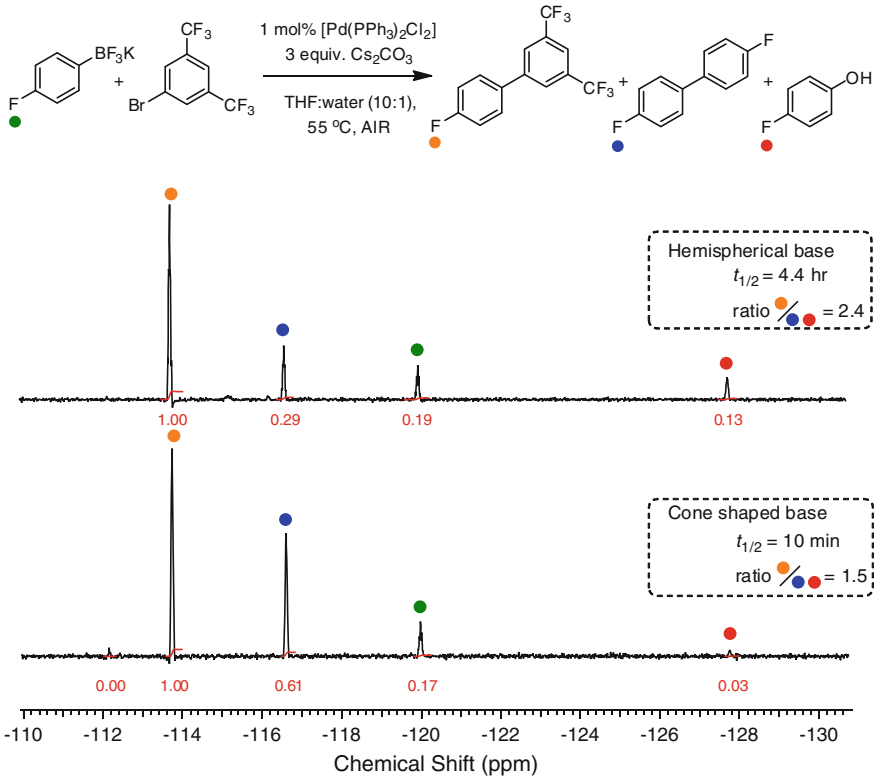

Fig. 4.17 ^{19}F NMR of two SM couplings in (upper spectrum) a hemispherical shaped base Schlenk tube and (lower spectrum) a cone shaped base Schlenk tube, indicating the dependency of side-product formation on the release rate of boronic acid **2a**

It was observed that the ratio between the homo-coupled product **9** and phenol **10** varied between the two experiments. The reported mechanism [50] infers the ratio should be 2:1, which was mirrored in the tube with the hemispherical base. In contrast, less phenol was generated in the tube with the cone shaped base, where a 1:1 (**9**:**10**) ratio was observed. The higher level of fluoride present, from the rapid hydrolysis, may interfere with the proposed oxidant ($HOOB(OH)_2$). Alternatively, **1a** has been shown to quench a THF based oxidant, Sect. 3.5.2 *vide supra*, which may be related to this observation, but a precise mechanistic rationale is currently not known.

Although these experiments are slightly artificial as the concentration of O_2 present would, under regular laboratory inert procedures, be lower than that provided by a head space gas of air, they clearly demonstrate the significant impact changes in the reaction environment can have upon the reaction efficiency. Additionally, if the boronic acid is unstable towards protodeboronation, then the release rate, which is dependent on the mixing efficiency of the system, will be paramount to the success of the reaction.

4.2.7 Uncatalysed Hydrolysis

Low levels of conversion from **1a** to **2a** were detected during the induction period, even when the pH was high, Figs. 4.13 and 4.16. This is contradictory to the proposed acid catalysed hydrolysis, which must, therefore, imply the existence of another, much slower route that is uncatalysed. The mechanism proposed by Perrin [37], suggests the first step of the reaction to be the dissociation of KF, which forms the extremely Lewis acidic difluoroborane **11**. This undergoes the fluoride/hydroxide exchanges to give the boronic acid **2**. This direct uncatalysed loss of KF would be responsible for the slow hydrolysis that is observed. When the HF, generated by uncatalysed hydrolysis, reduces the pH of the bulk phase to a critical level, the faster acid catalysed pathway predominates, Fig. 4.13.

In summary, two pathways have been identified for the hydrolysis of **1a** to **2a** depending on the pH of the solution, Scheme 4.17. At high pH the uncatalysed

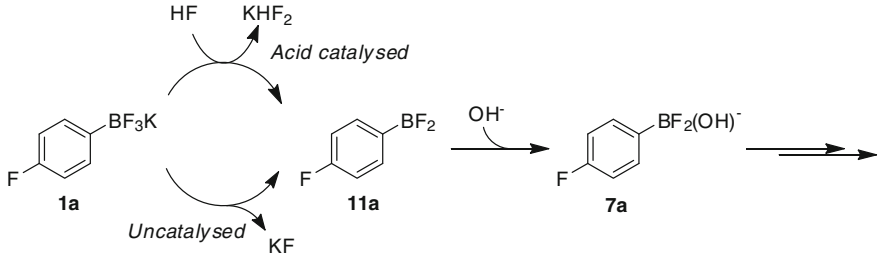

Scheme 4.17 Two routes identified for the generation of difluoroborane species **11a** from **1a**

pathway operates and the base sequesters the HF; whereas at lower pH, a specific acid catalysed process occurs in which the glass surface acts as the primary HF sink, leading to the etching of glassware.

4.3 Hydrolysis of R-BF_3K Salts

To test the generality of the observations made using test substrate **1a**, it was decided that a range of different R-BF_3K salts should be investigated. It was considered unlikely that they would all behave similarly to **1a**, therefore expanding the study to include as diverse substrates as possible would be highly informative. In addition, it was hoped that a general predictive model could be generated, thereby facilitating future optimisation of R-BF_3K salts under solvolytic conditions.

The hydrolytic equilibria (K_{app}) and the rates of glass (k_{obs}^{glass}) and base (k_{obs}^{base}, homogeneous (DBU) and biphasic (Cs_2CO_3)) mediated hydrolysis were measured for eight substrates. This was followed by glass and biphasic (Cs_2CO_3) base mediated hydrolysis rate measurements on a further ten substrates.

4.3.1 Hydrolytic Equilibria and Glass-Mediated Hydrolysis

As with substrate **1a**, the first eight R-BF_3K salts tested exhibited clean pseudo first order decays (k_{obs}^{glass}), under the base-free conditions in the presence of glass, Scheme 4.18, (typical first order plot shown in Fig. 4.18). There was no evidence of any induction periods and, in most cases, no rapid pre-equilibria, as had been observed in the absence of any glass and base, Fig. 4.6.

Hydrolytic half lives ranged from 7 min–12 h, where the cyclopropyltrifluoroborate salt (**1x**) was found to be the most reactive, and the phenylethynyltrifluoroborate salt (**1c**) the least, Fig. 4.19.

The equilibrium concentrations of **1**(**a**, **c**, **k**, **x**, **y**, **ar**, **at**, **au**, **av**) and **2** (**a**, **c**, **k**, **x**, **y**, **ar**, **at**, **au**, **av**) were analysed (^{11}B NMR) in the absence of any fluorophile (base or glass) at 55 °C. In order to calculate the equilibrium constant (K) the concentrations of KF and KHF_2 have to be known. However, due to signal broadening (^{19}F NMR) it was not possible to accurately integrate the relevant signals; therefore, their concentrations were assumed from the stoichiometry of the reaction to be that of the boronic acid **2**, Scheme 4.19. A calibration curve, of water

Scheme 4.18 General conditions used for the glass-mediated rate measurements

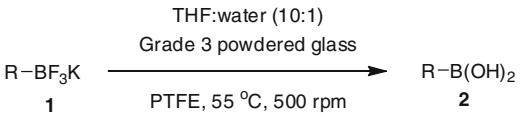

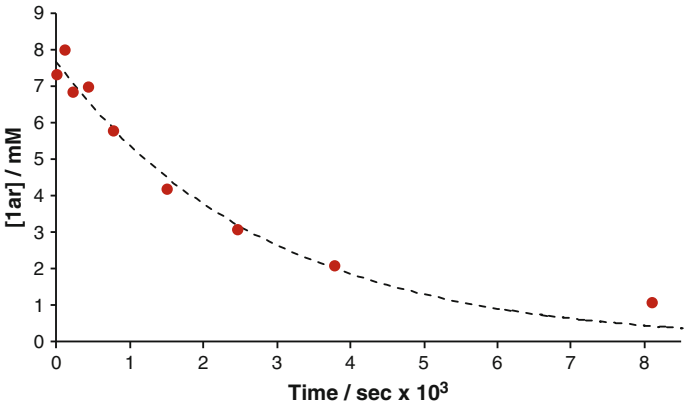

Fig. 4.18 The first order decay (THF:water 10:1, 55 °C) of potassium 2-furyltrifluoroborate salt (**1ar**) mediated by glass (20 mg, grade 3)

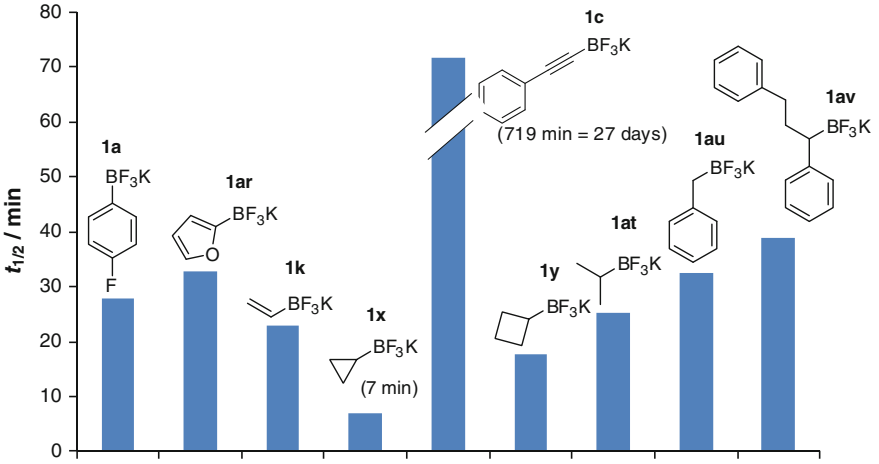

Fig. 4.19 Hydrolytic (THF:water 10:1, glass powder, 55 °C) half lives of R-BF_3K species mediated by glass powder (20 mg, grade 3)

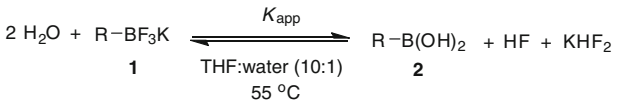

$$K_{app} = [\mathbf{2}]^3 / 25^*[\mathbf{1}]$$

Scheme 4.19 Hydrolytic equilibrium for R-BF_3K salts and K_{app} calculation

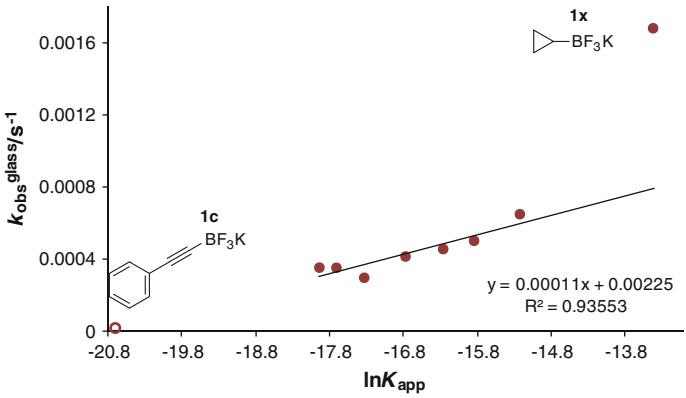

Fig. 4.20 Rates of glass-mediated hydrolysis (k_{obs}^{glass}) of **1** correlate well with the experimentally determined equilibrium constant ($\ln K_{app}$)

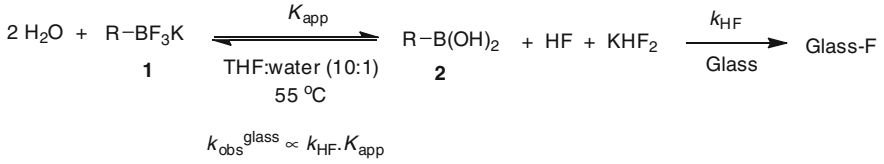

Scheme 4.20 Processes leading to the observed rate constant for hydrolysis mediated by glass

concentration in THF versus volume, confirmed the concentration of water in the system (10:1) to be 5 M, therefore, the apparent equilibrium constant (K_{app}) was calculated for each substrate.

LnK_{app} correlated well with rates of glass mediated hydrolysis for all substrates, except **1x**, confirming the constant fluorophilic capacity of the glass, Fig. 4.20 and Scheme 4.20. A hydrolytic equilibrium was not detected in substrate **1c** due to the stability of the alkynyl moiety under the conditions of Scheme 4.19. Furthermore, the instability of the alkynylboronic acid **2c** towards protodeboronation (Sect. 4.5.3 *vide infra*) infers this substrate may decompose faster than it can equilibrate. However, extrapolation of the trend predicts the theoretical K_{app} would be 1.02×10^{-9} (dimensionless), Fig. 4.20.

The exceptionally reactive **1x** clearly does not fit the correlation, Fig. 4.20. As the equilibrium proportion of boronic acid (61 %) is so high, in comparison to those that fit the trend, it may be that the glass powder is unable to sufficiently buffer the acid catalysis arising from the increased levels of HF in solution. Therefore, the measured rate is a combination of the rapid acid-catalysed route to equilibrium, and the glass mediated consumption of fluoride. Interestingly this analysis would imply that upon the addition of more glass, the observed rate would decrease as the system is better able to buffer the rapid establishment of equilibrium, in contrast to **1a**, Sect. 4.2 *vide supra*. Nevertheless, if the rate of hydrolysis

had been measured from equilibrium, by the addition of glass at that point, then k_{obs}^{glass} for **1x** is predicted to fit the correlation. In all other cases the glass powder is successfully able to control the acid catalysis so no significant pre-equilibria are included into the observed rate measurement (k_{obs}^{glass}). As boronic acid equilibrium proportions decrease below that of **1x** (61 %), the combination of forward reaction processes will slowly move towards being that dependent on the consumption of fluoride (k_{HF}), i.e. the rate becomes sensitive to the glass surface area, Scheme 4.20. However the absolute rate of sequestration (k_{obs}^{glass}) increases with increasing HF concentration, generated from increasing $\ln K_{app}$.

A structural basis was sought to rationalise the range of hydrolysis rates, which span 2–3 orders of magnitude. Qualitatively these observations can be correlated to the ability of the organic moiety to stabilise the trifluoroborate (**1**), or the intermediate difluoroborane (**11**, R-BF_2). Unsaturated, electron rich, moieties destabilise **1** and stabilise **11** through π-donation, therefore, leading to greater values of K_{app}, and more rapid rates of hydrolysis, Fig. 4.21. Stabilisation through hyperconjugation of **11**, and destabilisation of **1** through steric decompression from alkyl groups are similar rate enhancing effects. On the contrary, increasing s character at the carbon bound to boron and electron withdrawing arenes will stabilise the negativity of **1**, e.g. alkynyl substrate **1c**, Fig. 4.21, and retard the rate.

A more quantitative approach was sought, which would lead to better understanding and hence a finer predictive model. It was hypothesised that the B–F (r(B–F)) or C–B (r(C–B)) bond lengths would signal changes in the structural characteristics that govern the rates of hydrolysis. Organotrifluoroborate salts are renowned for being crystalline; therefore it was proposed that relevant bond-lengths could be extracted from single-crystal diffraction data. Unfortunately, of the nine R-BF_3K salts currently being studied, only three afforded crystals suitable for diffractometry, despite numerous attempts at various crystallisation techniques, including: layering, vapour diffusion, cooling of solvent/anti-solvent mixtures and solvent evaporation. Encouragingly, of the successful examples, the alkynyl substrate **1c** (140.8 pm) displayed a much shorter r(B–F) than the vinyl **1 k** (142.6 pm), whose rate of hydrolysis is two orders of magnitude slower. A further survey of all literature potassium organotrifluoroborate crystal structures (20 examples) added further strength to the connection between r(B–F) and structure. However, due to asymmetric crystal packing effects, occasionally the three r(B–F) from the R-BF_3K salt were very different from each other, causing analytical ambiguities. Moreover, far greater accessibility of r(B–F) data was required.

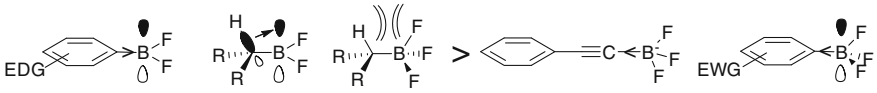

Fig. 4.21 Qualitative structural rationale for the stabilisation of difluoroboranes and the destabilisation and stabilisation of trifluoroborate species, leading to the range of observed rates (k_{obs}^{glass})

Efforts then focussed on computationally optimised structures of the R-BF_3K salts being studied (**1a**, **1c**, **1 k**, **1x**, **1y**, **1ar**, **1at**, **1au**, **1av**), with DFT providing the greatest accuracy to computational time ratio. The 6−31 + G(d) basis set was found to be sufficient at the B3LYP level of theory: the calculations were simple to execute and had times ranging from 10 min–15 h, depending on the number of atoms present. All calculated r(B–F) were normalised to the value calculated for BF_3 ($r(B–F)_{BF3}$ = 132.213 pm, $\Delta r(B–F) = r(B–F) - r(B–F)_{BF3}$), to account for any disparities in future parameterisations used in the replication or application of this study.

The optimised R-BF_3K structures gave Δr(B–F), which loosely correlated ($R^2 = 0.646$; without **1c** and **1x**) with K_{app}. The intermediate difluoroborane (**11**) structures were subsequently optimised, where it was found a vast improvement in the correlation ($R^2 = 0.848$; all substrates except **1c**) could be made between $\ln K_{app}$ and the calculated energy difference between R-BF_3^- and R-BF_2 (ΔG^{θ}); consistent with the proportionality between the two parameters expressed by the Van't Hoff equation ($\Delta G^{\theta} = -RT\ln K$). However, it was found that average $\Delta r(B–F)_{av.}$ in the intermediate difluoroborane **11** (R-BF_2) gave the best correlation ($R^2 = 0.935$; all substrates except **1c**) with the experimentally determined $\ln K_{app}$, Fig. 4.22. Whilst the equilibrium proportion (x_2) of boronic acid gave an even better correlation ($R^2 = 0.974$) with the Δr(B–F), it is better rationalised *via* the use of K_{app}. The use of the neutral **11** additionally satisfies parameterisation issues associated with the anionic nature, or counter-cation bearing, organotrifluoroborate salt **1**. In general, the mean average ($\Delta r(B–F)_{av.}$) of the two Δr(B–F) was used for analysis.

Assuming the establishment of equilibrium is very much more rapid than the sequestration of fluoride by the glass, and that glass successfully buffers the acid catalysis, Scheme 4.20; the correlation of glass mediated hydrolysis rates (k_{obs}^{glass}) with $\ln K_{app}$, Fig. 4.22, and $\ln K_{app}$ with $\Delta r(B–F)_{av}$, Fig. 4.20, implies that k_{obs}^{glass}

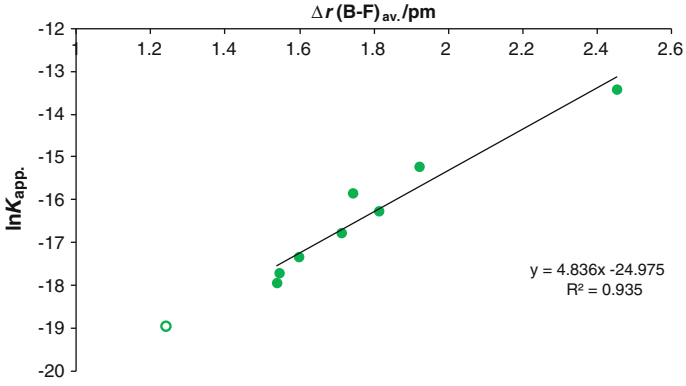

Fig. 4.22 The correlation between experimentally determined equilibrium constant ($\ln K_{app}$) and $\Delta r(B–F)_{av.}$of the difluoroborane (**11**). Open circle is the predicted position of substrate **11c**

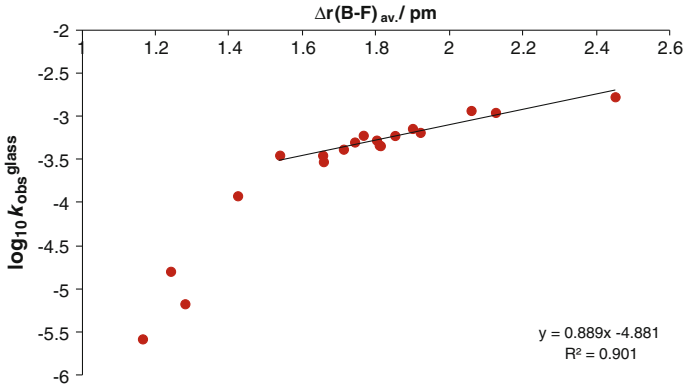

Fig. 4.23 Rates of hydrolysis mediated by glass correlate to $\Delta r(\text{B–F})_{\text{av}}$. of the difluoroborane **11** over 1.5 pm

should also correlate with $\Delta r(\text{B–F})_{\text{av}}$. Pleasingly, a satisfactory correlation ($R^2 = 0.901$) was observed between the experimentally determined $\log_{10} k_{\text{obs}}{}^{\text{glass}}$ and $\Delta r(\text{B–F})_{\text{av}}$., for substrates that have normalised bond lengths greater than 1.5 pm, Fig. 4.23. Below this value the rate of equilibrium establishment is slower than the rate of fluoride sequestration, due to the increased stability of the trifluoroborate induced by the organic moiety. In these cases the glass powder consumes the HF before any significant acid catalysis can ensue.

Although contextually artificial, due to the lack of base, these experiments confirm the connection to $\Delta r(\text{B–F})_{\text{av}}$. and provide a useful reference point when comparing to the addition of base. It should be noted that these rates are relative to the conditions employed herein, Scheme 4.18, as the addition of more glass powder would increase the rates, Fig. 4.7, and hence move all of the points upwards.

4.3.2 Base-Mediated Hydrolysis

Attention returned to the conditions pertinent to SM coupling where base is present to facilitate the transmetalation. The kinetics of hydrolysis mediated by base, were measured for both homogeneous and heterogeneous systems, with the homogenous (DBU) reactions serving as a comparative platform to the heterogeneous reactions (Cs_2CO_3).

4.3.2.1 DBU

The kinetics were assumed to be more reliable than those measured under the Cs_2CO_3 conditions, due to the lack of any biphase induced sampling or stirring

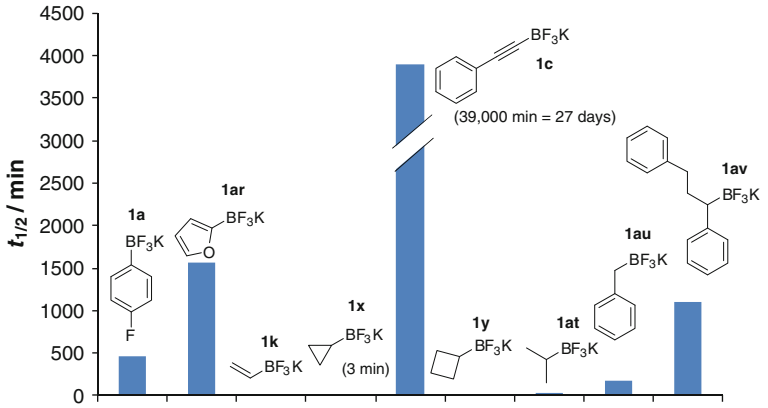

Fig. 4.24 Hydrolytic (THF:water 10:1, 3 equiv. DBU, glass powder, 55 °C) half-lives of R-BF_3K species under homogeneous basic conditions

issues. The pattern of homogeneous half-lives, Fig. 4.24, roughly mirrored those mediated by glass, Fig. 4.19, albeit substantially amplified. Substrate **1x** hydrolysed most rapidly with a half life of 3 min, and **1c** was the slowest at roughly 27 days. Unfortunately, this half-life is only approximate due to the low conversions achieved. Nonetheless, these experiments provide contextual support for the more relevant biphasic conditions.

4.3.2.2 Cs_2CO_3

Due to the sensitivity of hydrolytic rate profiles under biphasic (Cs_2CO_3) SM coupling conditions to the reaction environment, reactions were conducted under identical conditions: as well as the same PTFE reaction vessel being employed throughout, reactions were carried out at the same concentration (8 mM), volume (6.6 mL), mass of added glass powder (20 mg), magnetic stirrer bar shape and size, stirring speed (500 rpm) and positioning in the oil bath. Under these constraints the rates were found to be reproducible, Fig. 4.25.

Due to the lower pH, the rates of hydrolysis mediated by Cs_2CO_3 were, in general, greater than those mediated by DBU. The exception to the trend was benzyltrifluoroborate salt **1au** and alkynyl **1c** where the rate did not decrease on switching to Cs_2CO_3, of which, the reasons are currently not understood. The range of half-lives expanded from 2 min to roughly 40 days for substrates **1x** and **1c**, respectively.

By comparing rates mediated by base, to those mediated by glass, the substrates fall broadly into two classes; with base either causing rate enhancement or rate retardation. Analogous to **1a**, hydrolysis of the 2-furanyl (**1ar**), benzyl (**1au**), 1,3-diphenylpropyl (**1av**) and phenylethynyl (**1c**) trifluoroborates, was strongly retarded by base. The latter was almost inert to hydrolysis; whilst the boronic acid derived from **1c** was not detected (^{11}B NMR), boric acid, the product consistent

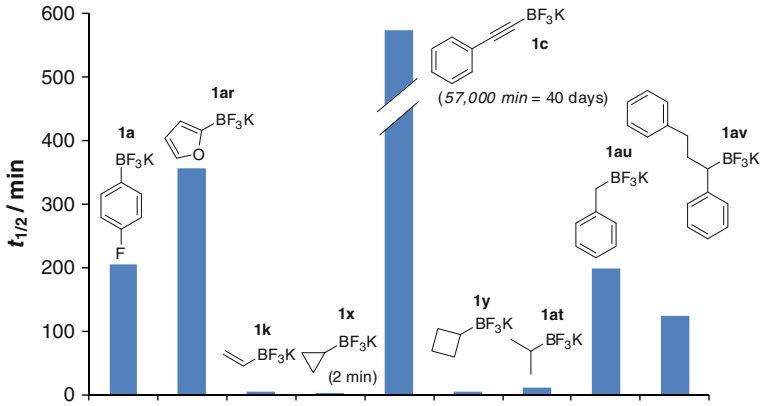

Fig. 4.25 Hydrolytic (THF:water 10:1, 3 equiv. Cs_2CO_3, glass powder, 55 °C) half-lives of R-BF3 K species under biphasic basic conditions

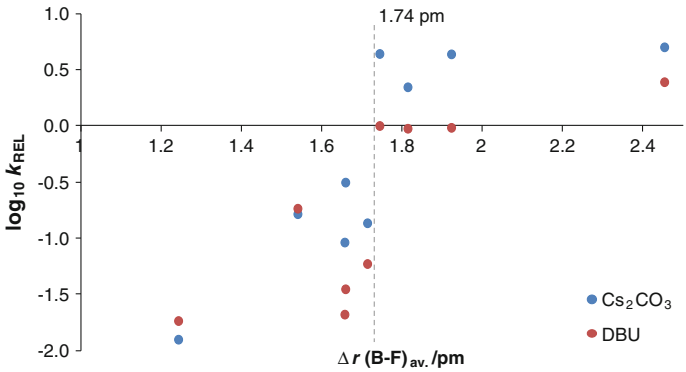

Fig. 4.26 Relative rate ($\log_{10}(k_{obs}{}^{base}/k_{obs}{}^{glass})$) versus $\Delta r(B–F)_{av}$

with rapid protodeboronation of it, was detected. In contrast, Cs_2CO_3 induced substantial rate acceleration in trifluoroborates based on vinyl (**1 k**), cyclopropyl (**1x**), cyclobutyl (**1y**) and isopropyl (**1at**) moieties. When the relative rate of glass and base mediated hydrolysis ($\log_{10}(k_{obs}{}^{base}/k_{obs}{}^{glass})$) was plotted against $\Delta r(B–F)_{av}$ it became clearer how the substrates were affected by base: those above the x-axis were accelerated and those below were decelerated, Fig. 4.26.

Although the relationship between the rates and $\Delta r(B–F)_{av}$. appeared slightly ambiguous, the substrates could be divided about 1.74 pm into two classes; those whose hydrolysis was accelerated or decelerated by Cs_2CO_3. The reasons behind this significant value were not fully understood but it was proposed that a possible change in mechanism occurred at this point. Clearly, more data was required; therefore, rates of hydrolysis under the biphasic Cs_2CO_3 conditions were measured for an expanded set of substrates based on phenyl (**1d**), *β*-styryl (**1 l**),

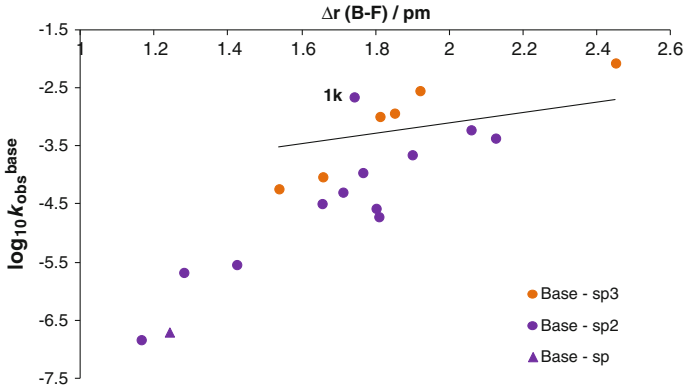

Fig. 4.27 Bond elongation (Δr(B–F)$_{av.}$) of difluoroborane **11** versus rates ($\log_{10}k_{obs}^{base}$) of hydrolysis under basic (Cs_2CO_3) conditions. *Solid line* represents rates of hydrolysis mediated by glass (Δr(B–F) = 1.5–2.4 pm)

4-methoxyphenyl (**1o**), 1-naphthyl (**1p**), 3,5-bis(trifluoromethyl)phenyl (**1p**), cyclohexyl (**1q**), 4-methylphenyl (**1z**), 3-nitrophenyl (**1aa**), 2-naphthyl (**1aw**) and 4-trifluoromethylphenyl (**1ax**) moieties.

It quickly became apparent that the critical bond length of 1.74 pm was, in fact, not significant and the rates of biphasic base mediated hydrolysis (k_{obs}^{base}) for the nineteen substrates tested spanned more than five orders of magnitude. It was found that absolute $\log_{10}k_{obs}^{glass}$ correlated well with Δr(B–F) of **11** after the separation of sp^2 and sp^3 substrates, Fig. 4.27, with the only major outlier as the vinyltrifluoroborate salt **1 k**, *vide infra*. Electron poor aromatic systems, with $\Delta r(B–F)_{av.} < 1.5$ pm, exhibited half lives ranging from days to months. Above 1.5 pm, for alkyl and electron rich aryl systems, rates increased exponentially where half lives ranged from hours to minutes. By including the line derived from the data for glass-mediated hydrolysis, Fig. 4.23, as a reference point, the effect of added base is better represented, Fig. 4.27, than the relative plot, Fig. 4.26.

4.3.3 Hydrophilic Hydrolysis

The rate of hydrolysis of vinyltrifluoroborate salt **1 k** was initially misleading and gave rise to the idea that a "critical bond length ($\Delta r(B–F)_{av.} = 1.74$ pm)" was significant. However, with the introduction of the expanded set of hydrolysis data, it was eventually recognised as an outlier. The kinetics and computational calculations were repeated a number of times to validate the reproducibility of the data, and the identity of the product was confirmed (^{11}B and ^{1}H NMR) as the vinylboronic acid (**2 k**). Despite it behaving "normally" under the conditions without base (k_{obs}^{glass}), discussions thus far of the hydrolytic mechanisms do not explain the magnitude (10^2 × faster) of the observed rate differences.

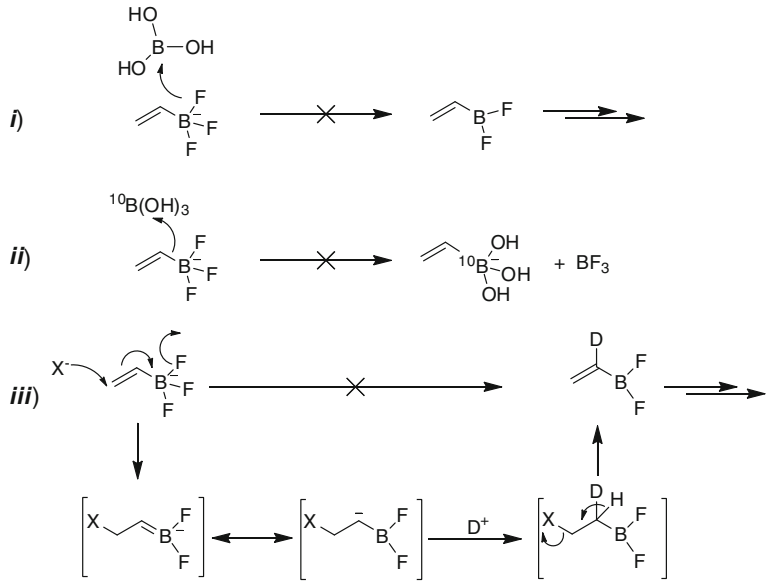

Scheme 4.21 Mechanistic proposals (***i***, ***ii*** and ***iii***) for the rapid base mediated hydrolysis of **1 k**

It was therefore proposed that hydrolysis of **1 k** occurred *via* a distinct mechanism, for which several hypotheses were advanced. Firstly it was found that the commercial sample of **1 k** contained 2.5 % contamination of KBF_4, which may hydrolyse *in situ* to $B(OH)_3$. The $B(OH)_3$ has the potential to act as a catalytic fluoride carrier, the presence of which may result in an extremely rapid overall rate, ***i*** Scheme 4.21. However, the addition of a catalytic quantity of KBF_4 to the hydrolysis of **1 k** had no effect on the rate of hydrolysis. Secondly, with the potential of C–B bond cleavage already disproven in **1a**, Sect. 4.2.3 *vide supra*, the unlikely possibility of vinyl migration from **1 k** to $B(OH)_3$ was considered, ***ii*** Scheme 4.21. As expected, this unlikely scenario proved incorrect as the addition of $^{10}B(OH)_3$ in the reaction mixture showed no incorporation of ^{10}B into the product, Scheme 4.21. Finally, the possibility of a reversible nucleophilic attack onto the *β*-position of the vinyl moiety could aid the departure of F^-, ***iii*** Scheme 4.21. To investigate this possibility, attempts were made to synthesise [*E*-*β*-^{2}H]-**1 k**, whose label would get scrambled if this mechanism were operating. However the synthesis was halted after the realisation that the α-carbanion intermediate would get trapped in a protic solvent, Scheme 4.21. Analysis (^{1}H NMR) of the α-position of the hydrolysis product in d_8-THF:D_2O (10:1) (3 equiv. Cs_2CO_3) was complicated by the quadrupolar broadening induced by the adjacent boron. Therefore, the SM coupling product of **1 k** with 3,5-bis(trifluoromethyl)bromobenzene (**6**) was used to analyse the α-position of the resulting styrene (**94**). However, ^{1}H NMR indicated no [^{2}H] incorporation, thus disproving this mechanism.

Separating the phases of a reaction mixture containing **1 k** and Cs_2CO_3 in THF:water (10:1) and subsequent analysis (^{11}B NMR), indicated that a significant proportion of the vinyl moiety resided in the basic aqueous layer. Evidently, the small organic group renders the overall reagent sufficiently hydrophilic to partition into the aqueous layer. Under these very basic conditions (pH = 12–13), hydrolysis and sequestration of HF is extremely rapid and the generation of the vinyltrihydroxyboronate (**60 k**) results, Sect. 3.4.2 *vide supra*, which then diffuses back to the bulk phase as boronic acid **2 k**, as confirmed by ^{11}B NMR. Comparison of this hydrophilicity to a number of other substrates (**1y**, **1p**, **1at**) demonstrated that a smaller proportion of the isopropyl moiety also resided in the aqueous biphase, although given its inherent reactivity, this partitioning was considered less significant. As expected, the partitioning of naphthyl (**1p**) and cyclobutyl (**1y**) moieties were insignificant in the aqueous layer.

Extension of this analysis suggested that the potassium ethynyltrifluoroborate (**1ay**) had the potential to undergo rapid hydrolysis because of its assumed hydrophilic similarity to **1 k**. However, as with its sp-hybridised cousin **1c**, hydrolysis under basic conditions gave 0 % conversion after 2 h, whereas **1 k** went to complete conversion after 1.5 h. The extreme stability of these sp surrogates was later confirmed by the lack of significant reaction when Cs_2CO_3 was titrated into a solution of **1ay** in water, conditions which rapidly consume all other classes of trifluoroborate salts, Sect. 3.4.2 *vide supra*. Only traces of $CsB(OH)_4$ were detected from protodeboronation of the hydrolysis product **2ay**.

4.4 Mechanistic Summary

The rates of hydrolysis of a wide range of organotrifluoroborate salts have been measured under SM coupling conditions, for which the mechanisms can be summarised by three pathways: Acid-catalysed, Uncatalysed and Hydrophilic, Scheme 4.22. The rate limiting loss of KF can occur directly (k_{dir}, k_{dir}') at high pH, or aided by HF (k_{cat}) at low pH.

For substrates whose $\Delta r(B–F)_{av.} < 1.75$ pm, e.g. electron poor/neutral aromatics or benzylic moieties, the organic group is sufficiently stabilising in **1** or destabilising in the difluoroborane (**11**) to give very slow rates of direct (k_{dir}) KF loss. These substrates require acid catalysis (k_{cat}) to efficiently hydrolyse, leading to strong rate suppression upon the addition of base. Therefore, under the basic conditions of SM coupling, hydrolysis rates are very slow.

However, substrates whose $\Delta r(B–F)_{av.} > 1.75$ pm, e.g. very electron rich aromatics or alkyl moieties, the organic group is sufficiently stabilising in **11**, or destabilising in **1**, to give rapid rates of direct KF loss. In these cases even at the high pH environment of SM couplings, rapid hydrolysis ensues. Rates for electron rich aryl moieties were found to be the least reproducible. This is due to the inefficient suppression of acid catalysis due to the accelerated liberation of HF by

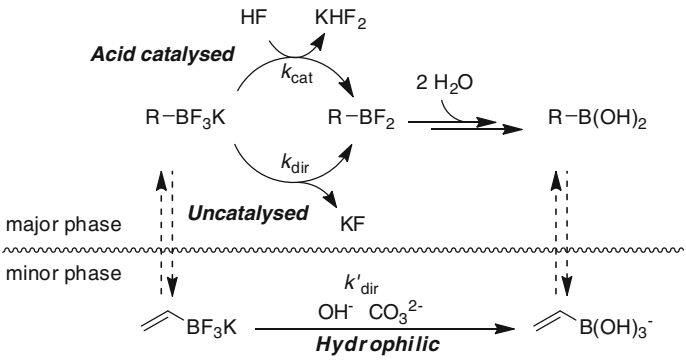

Scheme 4.22 Summary of the hydrolytic mechanisms of R-BF_3K salts

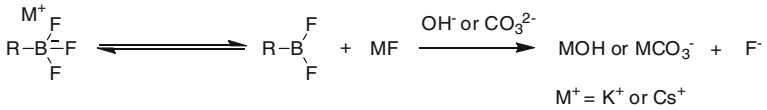

Scheme 4.23 A possible Cs_2CO_3 induced rate enhancing mechanism

the direct pathway, causing the balance between the pathways to be extremely sensitive to stirring and sampling.

It was found that with alkyl moieties (**1w**, **1x**, **1y**, **1at**) k_{dir} was so rapid that the rate limiting step became the sequestration of fluoride. Therefore, upon the addition of base (k_{obs}^{base}), an increase in rate (compared to k_{obs}^{glass}) was observed, due to the efficiency of base to neutralise the HF. However, k_{obs}^{base} can only be accelerated by base to the point where k_{dir} becomes rate limiting. Upon increasing the concentration of DBU, no effect was observed on the rate of hydrolysis of **1x** and **1y**, but in both cases k_{obs}^{Cs2CO3} was higher than k_{obs}^{DBU}. This suggested that either the kinetic basicity of biphasic Cs_2CO_3 solutions is higher than that of the homogeneous DBU reactions, and therefore the rate limiting k_{dir} has not been reached, or, alternatively, that Cs_2CO_3 is able to assist in the dissociation of MF by interaction of OH^- or CO_3^- with M^+, Scheme 4.23, similar to that proposed by Hutton [39].

4.5 Classifications

Having measured their rates of hydrolysis, the nineteen R-BF_3K salts (**1a**, **1c**, **1d**, **1 k**, **1 l**, **1o**, **1p**, **1q**, **1w**, **1x**, **1y**, **1z**, **1aa**, **1ar**, **1at**, **1au**, **1av**, **1aw** and **1ax**) were subdivided into three classes (**I**, **II** and **III**) depending on their half life under the basic (Cs_2CO_3) conditions employed herein, Scheme 4.9.

4.5.1 Class I

Class **I** reagents, e.g. vinyl (**1 k**), 4-methoxyphenyl (**1o**), *β*-styryl (**1 l**), cyclohexyl (**1w**), cyclopropyl (**1x**), cyclobutyl (**1y**), 4-methylphenyl (**1z**) and isopropyl (**1at**) were very reactive, exhibiting half lives of less than 1 h. The direct dissociation pathway (k_{dir}) is so efficient that their hydrolysis is very difficult to control. The boronic acid is liberated very quickly, rendering it susceptible to the degradation pathways appropriate to the particular substrate. In addition, HF is released rapidly, which leads to possible problems with glassware etching, especially if the reaction is poorly stirred.

Whilst it is often proposed [3, 51] that alkylboronic acids readily undergo protodeboronation, the SM coupling conditions optimised for cyclopropyltrifluoroborate salt **1x** [51], are very forcing: 110 °C, 16 h. As the liberation of the boronic acid takes just 2 % of the time taken for coupling, this demonstrates the great stability of cyclopropylboronic acid (**2x**) towards protodeboronation under the reaction conditions. Transmetalation is evidently slow, but high yields are also reported by Wallace [52], and by Deng [53], who directly use **2x**.

To gauge the advantages of using R-BF_3K salts in Class **I**, potassium cyclobutyltrifluoroborate (**1y**) was further studied. The SM coupling of boronic acid **2y** and trifluoroborate **1y** with 3,5-bis(trifluoromethyl)bromobenzene (**6**) were compared, and shown to be identical (^{11}B NMR) after 1 h under the optimised SM coupling conditions [51], Fig. 4.28. The harsh conditions (100 °C, 24 h) used, again confirmed both the stability of **2y** in the solution phase and the slow transmetalation affinity.

The use of **1y** instead of **2y** is further questioned, as it is not commercially available, but is prepared with KHF_2 from **2y** itself. The workup from the

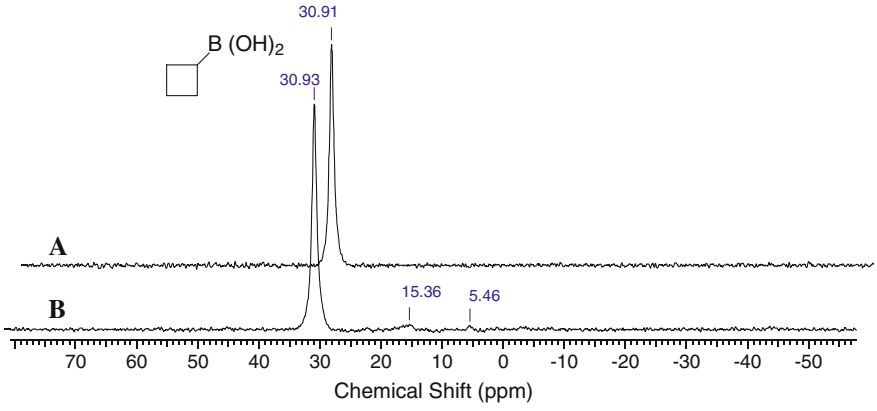

Fig. 4.28 ^{11}B NMR spectra (**A** is offset from **B**) of the SM coupling (2 mol % $Pd(PPh_3)_2Cl_2$, 3 equiv. Cs_2CO_3, toluene:water (10:1), 100 °C) of (**A**- potassium cyclobutyltrifluoroborate (**1y**) and (**B**-cyclobutylboronic acid (**2y**) with **6**, after 1 h of reaction

preparation of **1y** is lengthy, and the isolation procedure involves multiple extractions, giving the product in only a 63 % yield [51]. Nonetheless, the trifluoroborate salt is an air stable, monomeric and crystalline solid, unlike **2y**. Exposure of **2y** to air caused it to fume and exothermically decompose, which necessitated the use of a glove box during manipulations. Analysis (^{11}B NMR) of the tarred solid remaining, after exposure of **2y** to air, indicated boric acid was primarily produced. Attempts were made to trap the gaseous co-product at low pressure, directly in the Young's tap NMR tube; however, analysis (^{1}H NMR) was ambiguous with no evidence of a cyclobutanyl ring present.

The solution/air stability contradiction of **2y** can be explained in terms of the increased propensity of autoxidation in dry samples of alkylboronic acids [54]. The solid boronic acid contains varying quantities of cyclic or linear boroxines, which may act as radical initiators for the atmospheric oxidation. Whereas under SM coupling conditions (toluene:water 10:1 and THF:water 10:1) the degree of water present means that it primarily exists as the monomeric boronic acid, therefore avoiding oxidation, even when the solution is oxygenated.

4.5.2 Class II

Class **II** reagents, e.g. 4-fluorophenyl (**1a**), phenyl (**1d**), 1-, or 2-, naphthyl (**1p**, **1aw**), 2-furanyl (**1ar**), benzyl (**1au**) and 1,3 diphenylpropyl (**1av**), underwent hydrolysis with half lives in the range of 1 h–1 day. The balance between the two pathways was not as close as Class **I** reagents, therefore, their kinetic profiles were less sensitive to their reaction environment. The acid catalysed pathway can be controlled and therefore HF is efficiently mopped up by the base, leading to minimal etching of the glassware. The effect of additional glass powder on the rate of hydrolysis (Cs_2CO_3, THF:water 10:1, 55 C) of **1a** was shown to have no effect, thus confirming the efficient fluorophilic role of the base, for this type of substrate, under these conditions.

Through careful consideration of all the factors (stirring rate, vessel shape, biphase volume, substrate concentration, water concentration, temperature, glass surface area) governing hydrolysis rates, it is possible to successfully manipulate the rate to match that of catalytic turnover, thereby keeping the boronic acid in very low concentration. Under these conditions the boronic acid does not accumulate/degrade and therefore the cross-coupling reaction gives very clean reactions and high yields of product. The use of R-BF_3K salts is therefore considered to be worthy and has great potential for use in couplings of unstable boronic acids, or even couplings conducted in air when in combination with a suitable catalyst system.

4.5.3 Class III

Class **III** reagents, e.g. phenylethynyl (**1c**), 3,5-bis(trifluoromethyl)phenyl (**1q**), 3-nitrophenyl (**1aa**) and 4-trifluoromethylphenyl (**1ax**), are exceptionally stable and undergo very slow hydrolysis with half lives of greater than 1 day. In some cases (**1c**, **1q**), boric acid rather than boronic acid was detected (^{11}B NMR), which may be unsurprising considering the time for reaction, $t_{1/2} < 65$ days at 55 °C.

The conditions used to cross couple such species are typically harsh (reflux, 12–36 h) which could either be necessitated by the very slow hydrolysis, or the very slow transmetalation, of the resulting boronic acid. Comparison of the time taken for SM coupling between **1q** and 4-bromobenzonitrile (**92**), with boronic acid **2q** and **92**, indicated that hydrolysis of **1q** is the rate limiting step of the process. Therefore, by considering the difference in the time taken for hydrolysis ($t_{1/2} = 65$ days) and cross-coupling (100 % conversion = 1 day) it has to be assumed that the trifluoroborate directly transmetalates with [Pd^{II}], which is in stark contrast to that previously proposed, Sect. 3.4.3, *vide supra*. Although the activation barrier for transmetalation of R-BF_3K salts is much higher than that of boronic acids, Sect. 3.4.3, *vide supra*, it is still plausibly lower than that of the direct loss of KF leading to hydrolysis.

Consequently, Class **III** substrates use unnecessarily harsh conditions for their coupling, which may lead to other problems such as catalyst degradation. Therefore, unless the boronic acid derivative is very unstable, the use of R-BF_3K salts does not improve the reaction outcome by significantly increasing reaction times, so direct use of the boronic acid maybe favoured. However, like Class **I** reagents, the benefits of using R-BF_3K salts may still arise in their physical and monomeric properties, although in general sp^2 Class **III** boronic acids are more stable than the Class **I** alkylboronic acids.

4.5.3.1 Hydrolysis then Cross-Coupling

Due to the exceptional stability of the phenylethynyltrifluoroborate salt (**1c**) towards hydrolysis, it was proposed that 1 equiv. of tartaric acid (**3**) could destabilise **1c** into revealing boronic acid **2c**, followed by an SM coupling, which would give a methodology with milder conditions and shorter reaction times than employing **1c** directly [55]. However, when this hypothesis was tested (i) 1 equiv. **3**, THF:water 10:1; (ii) cannula filtration; (iii) 1 mol % [Pd(dppf)Cl_2], 3 equiv. Cs_2CO_3, 1 equiv. **6**) it gave the cross-coupled product **95** less efficiently (44 % conversion in 5.5 h) than when the trifluoroborate **1c** was employed directly (77 % conversion in 5.5 h). This superior coupling efficiency was unexpected considering the extraordinary stability towards hydrolysis of **1c** ($t_{1/2} = 40$ days). Further investigations revealed that complete consumption of **1c** to **2c** occurred upon the addition of **3**, but rapid protodeboronation to phenylacetylene (**41**) followed,

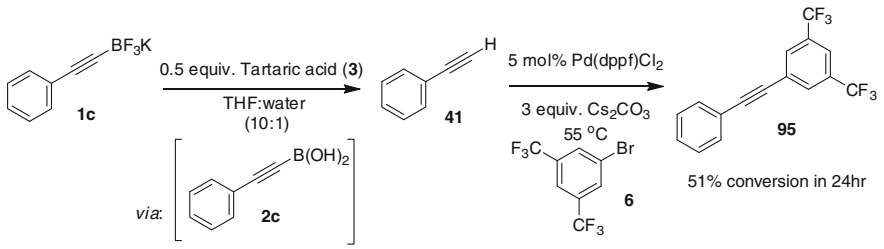

Scheme 4.24 Sequential hydrolysis, protodeboronation and cross-coupling of **1c**, to give diaryl acetylene **95**

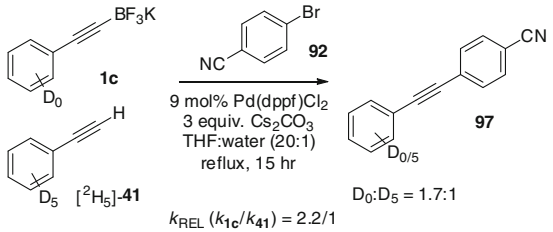

Scheme 4.25 Competition between the SM coupling of **1c** and Sonogashira coupling of **41** to generate **97**, under formally SM coupling conditions

Scheme 4.24. The observed formation of the diaryl acetylene **95** must, therefore, arise from a copper-free Sonogashira reaction [56, 57].

A competition reaction was used to investigate whether this copper-free Sonogashira reaction was occurring, rather than direct transmetalation of **1c**, under the SM conditions optimised by Molander [55]. In order for the product forming pathways to be differentiated in the product, deuterated phenylacetylene [$^2H_4$]-**41** was competed with **1c** for limiting arylbromide **92**. [$^2H_4$]-**41** was synthesised *via* a Sonogashira coupling between [$^2H_5$]-bromobenzene ([$^2H_5$]-**39**) and TMS-acetylene (**96**), followed a by deprotection with K_2CO_3 in CH_3OH. The SM coupling competition with 4-bromobenzonitrile (**92**) gave a mixture of labelled and unlabelled cross-coupled products arising from both starting materials in a 1.7:1 ratio, favouring direct **1c** transmetalation, Scheme 4.25. By modelling the partitioning in the system the relative rate constants (k_{rel}) were calculated as being 2.2:1 in favour of the SM pathway.

Therefore, although the copper-free Sonogashira does proceed under SM conditions, this result confirms the direct transmetalation of **1c**. This is fully consistent with the observation that alkynyl SM couplings proceed just as successfully under non-solvolytic anhydrous conditions [55]. Similar non-solvolytic, or ethanolic NEt_3, conditions were observed to work with the exceptionally stable potassium pentafluorophenyltrifluoroborate salt (**1an**) [58]. Although not tested, it is

envisaged that all Class **III** substrates would cross-couple equally well under anhydrous conditions, as compared to standard solvolytic conditions.

4.6 Prediction of Hydrolysis Rates

4.6.1 DFT

In order to build up a strong predictive model, the geometries of a further thirty two difluoroboranes (**11**) of varying structure and hybridisation at the carbon bound to boron were optimised (DFT; 6−31 + G(d), B3LYP). In order to avoid any parameterisation issues in the future use of this study, all B–F bond lengths were again normalised to BF_3 (r(B–F)$_{BF3}$ = 132.213 pm, Δr(B–F) = r(B–F)−r(B–F)$_{BF3}$), and C–B bond lengths to HC ≡ C-BF_2 (r(C–B)$_{CB}$ = 151.700 pm, Δr(C–B) = r(C–B) − r(C–B)$_{CB}$). Provided that BF_3 and HC ≡ C-BF_2 are calculated in conjunction with the substrate in question, this approach should ensure that slightly different basis sets can be used to accurately compare to the rate data reported herein.

For the nineteen substrates whose rates have been tested, it was found that to generate the best correlation between Δr(B–F) and k_{obs}^{base}, the substrates had to be classed into two categories—"normal" and "asymmetric". This categorisation originated from significant differences in the two Δr(B–F) of **11** in some substrates containing considerable asymmetry in the organic moiety, which led to difficulties in accurate predictions. If the difference between the two Δr(B–F) is <0.1 pm then the substrate is considered to be "normal". If, however, the difference is >0.1 pm then the substrate is considered to be "asymmetric", Fig. 4.29.

If the substrate is "normal" then Δr(B–F)$_{av.}$ (Δr(B–F)$_{av.}$ = (r(B–F)$_1$ + r(B–F)$_2$)/2) can be used to obtain the predicted rate from the Δr(B–F) versus

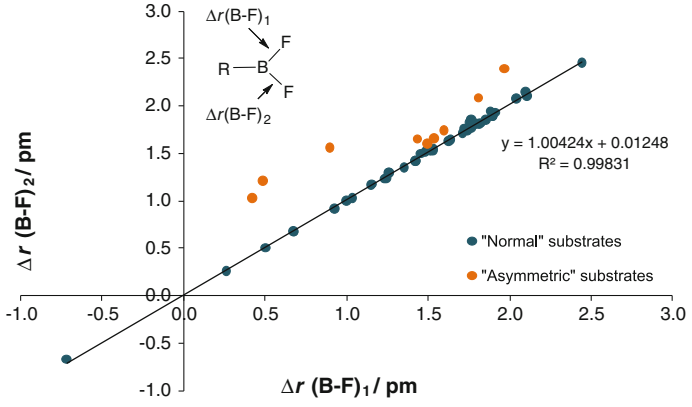

Fig. 4.29 Differentiation between "normal" and "asymmetric" substrates by the two Δr(B–F) values for the difluoroborane (**11**)

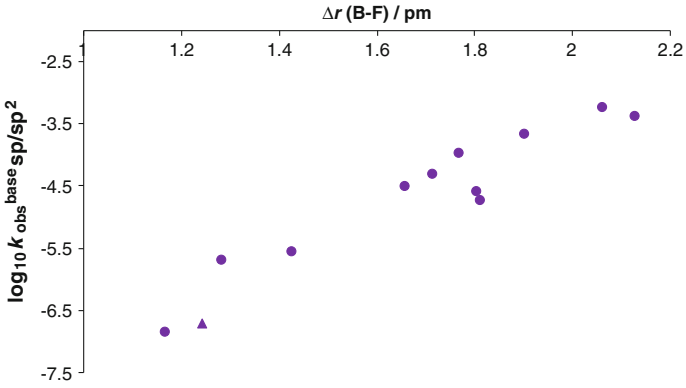

Fig. 4.30 Δr(B–F) versus $\log_{10}k_{obs}{}^{base}$ for sp and sp^2 substrates used for the prediction of untested substrates

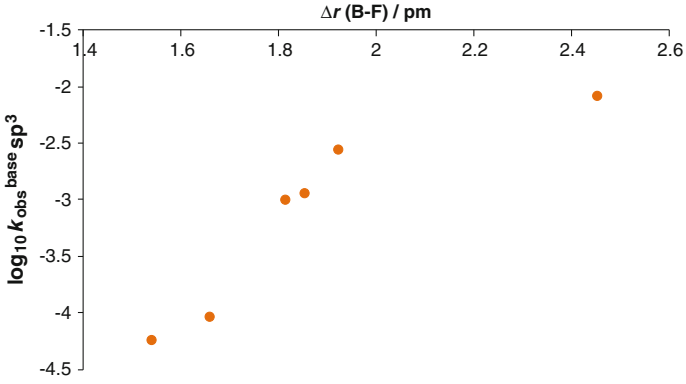

Fig. 4.31 Δr(B–F) versus $\log_{10}k_{obs}{}^{base}$ for sp^3 substrates used for the prediction

$\log_{10}k_{obs}{}^{base}$ plot, differentiating whether the carbon bound to boron is sp^2, Fig. 4.30, or sp^3, Fig. 4.31.

If, however, the difference between $\Delta r(B–F)_1$ and $\Delta r(B–F)_2$ is ≥ 0.1 pm, the average would probably sit off the trend, as a significant level of asymmetry exists in the molecule. In this case one $\Delta r(B–F)_{1/2}$ may better predict the rate of hydrolysis than the other. The method for determining which $\Delta r(B–F)_{1/2}$ to use comes from the comparison of Δr(B–F) to Δr(C–B), where $\Delta r(B–F)_{av}$. for all "normal" substrates correlates excellently ($R^2 = 0.967$ (sp^3), 0.964 (sp^2) and 0.998 (sp)) when differentiated by hybridisation, Fig. 4.32 and Table 4.1. As expected, an inversely proportional relationship is observed; reactive species exhibit short Δr(C–B) which simultaneously lengthens the Δr(B–F); stable species exhibit longer Δr(C–B) such that Δr(B–F) are reduced.

"Asymmetric" substrates display greater spread along the y-axis of Fig. 4.32 when co-plotted with "normal" substrates, Fig. 4.33. Then, whichever Δr(B–F)

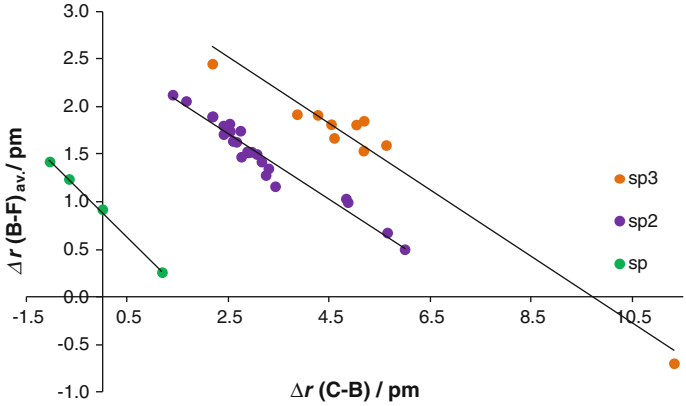

Fig. 4.32 $\Delta r(\text{B–F})_{\text{av.}}$ versus $\Delta r(\text{C–B})$ for all "normal" substrates calculated

Table 4.1 Correlation equations for each hybridisation class

	Correlation
sp^3	$\Delta r(\text{B–F}) = -0.3492\ \Delta r(\text{C–B}) + 3.3938$
sp^2	$\Delta r(\text{B–F}) = -0.3442\ \Delta r(\text{C–B}) + 2.5700$
sp	$\Delta r(\text{B–F}) = -0.5231\ \Delta r(\text{C–B}) + 0.8944$

(long, short or average) is closest to the "normal" line of best fit, should be used to predict rates from the Δr(B–F) versus $\log_{10}k_{\text{obs}}^{\text{base}}$ plot, Figs. 4.30 and 4.31.

It can be clearly seen from the square markers of Fig. 4.33, which Δr(B–F) should be used. The closer the Δr(B–F) lies to the line of best fit, Fig. 4.33, the more accurate rate prediction can be achieved. As such, rates predicted from Δr(B–F) values that deviate substantially from the Δr(B–F)/Δr(C–B) correlation inherently carry greater uncertainty.

Of the substrates whose rates of hydrolysis have been tested, 1-naphthyl (**1p**) and 2-furanyl (**1ar**) are classed as "asymmetric". It is in this way that their Δr(B–F) has been plotted against hydrolysis rate, Fig. 4.30.

There are a small number of substrates, e.g. mesityl and C_6F_5, which are categorised as "normal" substrates, as their two Δr(B–F) are within 0.1 pm, but lie away from the Δr(B–F)/Δr(C–B) correlation, Fig. 4.33. For these "unusual" examples it is estimated their rate of hydrolysis will not be easily predicted by this model, as they may not sit on the Δr(B–F)/$\log_{10}k_{\text{obs}}^{\text{base}}$ correlation, Fig. 4.30.

4.6.2 Swain-Lupton ℜ Values

It was proposed that the organic moiety of the difluoroborane (**11**) could be considered as a substituent on an aromatic ring, where π-donation to a sp^2 atom, R-BF_2 ≈ R-C_{Ar}, Scheme 4.26, can be measured using LFER analysis. The Swain-

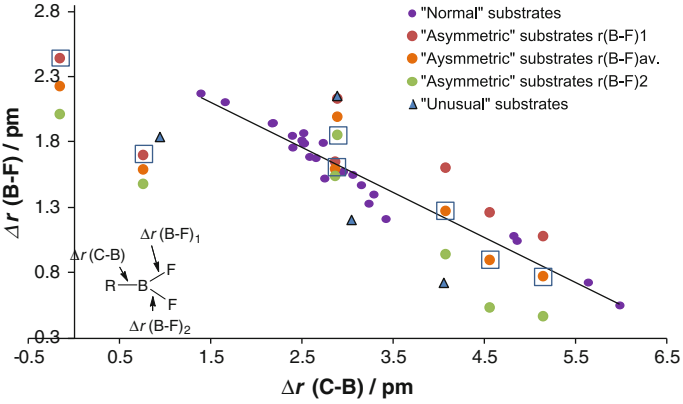

Fig. 4.33 Co-plot of "asymmetric" and "normal" sp^2 substrates of Δr(B–F) versus Δr(C–B). Whichever asymmetric point is closest to the "normal" line is used for prediction; as indicated by square markers. For identification of "asymmetric" and "unusual" substrates see Tables 6.14 and 6.19

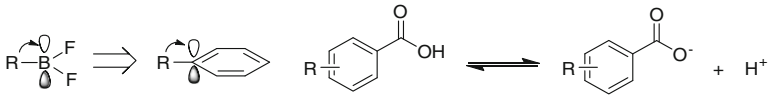

Scheme 4.26 Resonance of R in R-BF_2 analogous to a substituent on an aromatic ring

Lupton resonance ($\Re_{SL}$) parameter, which can be easily sourced from the literature [59], is a function of the Hammett (σ_p and σ_m) values, and measures the resonance stabilising ability of 'R' groups by comparison to the pK_a of *para*- and *meta*-substituted benzoic acids, Scheme 4.26.

Of the fifty one difluoroborane structures optimised (DFT, B3LYP 6−31 + G(d)) only 41 $\Re_{SL}$ values exist, but good correlations with $\Delta r(B–F)_{av}$. were found for each substrate class, confirming the connection between the parameters, Fig. 4.34 (Table 4.2). A few outliers exist, including sterically hindered *o*-aryl substituents and the 2-pyridyl moiety, as well as a whole class of XBF_2, where X = halogen, NH_2, SH, SiH_3, H, OH, or OMe.

This LFER type analysis was then applied to the base mediated hydrolysis (k_{obs}^{glass}) of the nineteen substrates tested, for which only fourteen $\Re$ values exist. The modified $\Re$ value ($\Re_{MOD} = 1.385\sigma_p - 1.297\sigma_m - 0.033$), which Hansch, Leo and Taft utilised [59], correlated reasonably well ($R^2 = 0.9418$) with rates of hydrolysis. However there were two exceptions to the correlation; firstly the vinyltrifluoroborate **1 k**, which is a mechanistic outlier undergoing hydrolysis *via* the hydrophilic pathway, and secondly the cyclobutyltrifluoroborate **1y**, in which the reported σ_p and σ_m values do not mirror those of similar structures, thereby inferring doubt upon the value of $\Re$.

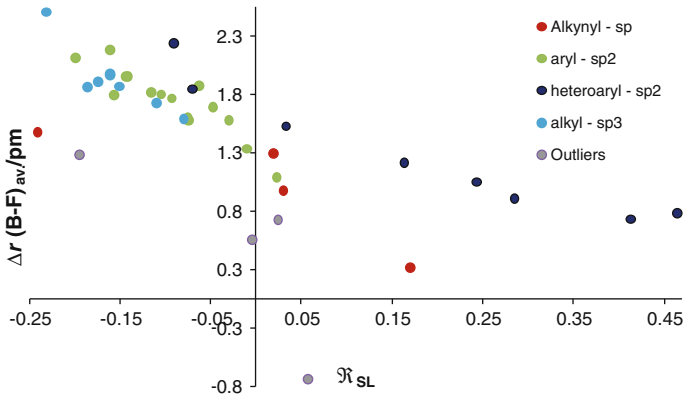

Fig. 4.34 $\Delta r(\text{B–F})_{\text{av}}$.*vs* $\Re_{\text{SL}}$, differentiated by substrate class

Table 4.2 Correlations between $\Re_{\text{SL}}$ and $\Delta r(\text{B–F})_{\text{av}}$

Substrate class	Correlation	R^2
Alkynyl—sp	$\Delta r(\text{B–F})_{\text{av.}} = -2.567\Re_{\text{SL}} + 0.9497$	0.7434
Heteroaryl—sp^2	$\Delta r(\text{B–F})_{\text{av.}} = -2.4651\Re_{\text{SL}} + 1.6771$	0.9165
Aryl—sp^2	$\Delta r(\text{B–F})_{\text{av.}} = -4.0287\Re_{\text{SL}} + 1.3179$	0.7886
Alkyl—sp^3	$\Delta r(\text{B–F})_{\text{av.}} = -5.1482\Re_{\text{SL}} + 1.0671$	0.7957

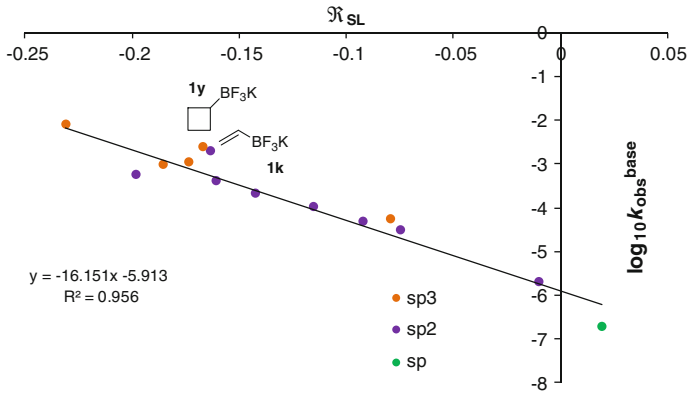

Fig. 4.35 $\Re_{\text{SL}}$ versus $\log_{10}k_{\text{obs}}{}^{\text{base}}$, line of best fit does not include substrates **1 k** and **1y**, see main text for details

It was found this correlation could be improved ($R^2 = 0.9558$, without **1 k** and **1y**) by applying the original Swain Lupton value ($\Re_{\text{SL}} = 1.355\sigma_{\text{p}} - 1.19\sigma_{\text{m}} - 0.03$), which essentially includes an α (0.921) term to adjust the proportions of σ_{p} and σ_{m}, Fig. 4.35. The use of this parameter is encouraged, as it gives a very good rate prediction and is simple to calculate from σ_{p} and σ_{m} values.

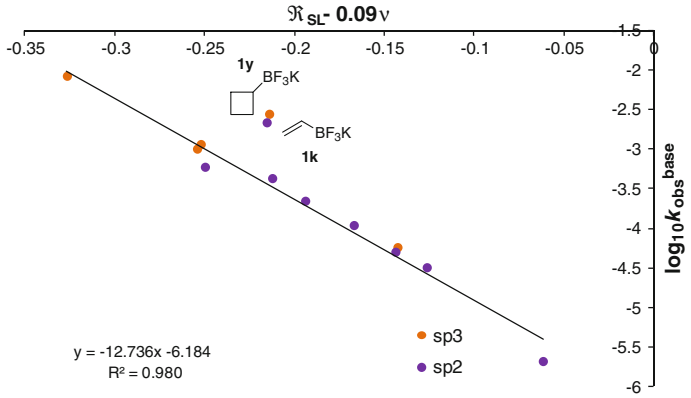

Fig. 4.36 The correlation between $\Re_{SL}-0.09\nu$ and $\log_{10}k_{obs}^{base}$, with the exceptions of **1y** and **1 k**, see main text for details

Table 4.3 Prediction of hydrolysis rates using $\Re_{SL}-0.09\nu$

	Equation	R^2
$\Re_{SL}$	$\log_{10}k_{obs}^{base} = -16.1507\Re_{SL}-5.9129$	0.9558
$\Re_{SL}-0.09\upsilon$	$\log_{10}k_{obs}^{base} = -12.7359(\Re_{SL}-0.09\upsilon)-6.1838$	0.9801

It was observed that sp^3 systems hydrolysed at a slightly greater rate than their $\Re_{SL}$ predicted. This is likely due to a steric decompression effect alleviating strain between the sp^3 carbon, and the tetrahedral "ate" species. This enhanced steric pressure around boron is not taken into account by the resonance parameter, $\Re_{SL}$. Therefore by incorporation of the Charton steric parameter (ν) the correlation could be significantly improved ($R^2 = 0.9801$, without **1 k**, **1y** and **1c** of which no ν was available) and as such gives, again, a more reliable predictive model, Fig. 4.36. The best correlation with the rate ($\log_{10}k_{obs}^{base}$) was found when 9 % ν is removed from $\Re_{SL}$ ($\Re_{SL} - 0.09\nu$). However, the main drawback of this approach comes from the scarcity of ν values, of which no sp examples exist, hence its exclusion from the plot. However for sp^3 and sp^2 examples, approximations can be made from substrates of a similar structure, which in this context had no detrimental effect on the fit. As such, ν for phenyl (0.57) was used for 2-furyl (**1ar**), phenylethenyl (**1 l**) and all other aryl (**1a**, **1d**, **1o**, **1z**, **1aa**) substrates.

Therefore, by utilisation of $\Re_{SL}$, with or without ν, it is possible to calculate an approximate hydrolysis rate under the general SM conditions of Scheme 4.9, from the equations given in Table 4.3. The advantage of using this method is that it is not necessary to consider the hybridisation of the carbon bound to boron, as it is when using Δr(B–F).

4.7 Summary

The hydrolysis of **1a** to **2a** under typical SM coupling conditions (THF:water (10:1), 3 equiv. Cs_2CO_3, 55 °C) has been studied. Two distinct pathways have been identified for the rate limiting loss of KF which depend on the pH of the solution: at high pH a slow uncatalysed direct KF loss is dominant, whereas at low pH a faster acid-catalysed KF loss dominants.

The biphasic nature of the conditions used was found to create an uneven pH gradient very much dependent on the mixing efficiency of the system. These observations revealed the hydrolytic vessel dependency, and the sensitivity of the reaction to the glass surface area. Manipulation of the biphase to control the two pathways was explored through the use of ultrasound. The hydrolytic release rate was then directly correlated to the outcome of the SM coupling between **1a** and **6**; with fewer side-products forming in a vessel with better mixing, where the acid-catalysis could be suppressed and the active species kept in low concentration.

The rates of hydrolysis of a further eighteen R-BF_3K salts were measured, which spanned five orders of magnitude. Δr(B–F) of **11** was shown to be a reliable indicator of the structural characteristics which determine hydrolysis rate, and thus correlate well to rates mediated by glass (above 1.5 pm), as well as those mediated by Cs_2CO_3 (after differentiation by hybridisation). Furthermore, it was found that Swain-Lupton ($\Re_{SL}$) values in combination with a Charton steric parameter (-0.09υ) could also correlated well to rates of hydrolysis under the SM coupling conditions (Cs_2CO_3). Both parameters can be used for the prediction of hydrolysis rates of untested substrates in order to aid optimisations of R-BF_3K salts under solvolytic conditions.

References

1. Z.F. Dorwald, *Side Reactions in Organic Synthesis* (Wiley-VCH, Weinheim, 2004)
2. B. Abarca, R. Ballesteros, F. Blanco, A. Bouillon, V. Collot, J.-R. Dominguez, J.-C. Lancelot, S. Rault, Tetrahedron **60**, 4887–4893 (2004)
3. D.M. Knapp, E.P. Gillis, M.D. Burke, J. Am. Chem. Soc. **131**, 6961–6963 (2009)
4. T. Kinzel, Y. Zhang, S.L. Buchwald, J. Am. Chem. Soc. **132**, 14073–14075 (2010)
5. K.L. Billingsley, S.L. Buchwald, Angew. Chem. Int. Ed. **47**, 4695–4698 (2008)
6. G.R. Dick, E.M. Woerly, M.D. Burke, Angew. Chem. Int. Ed. **51**, 2667–2672 (2012)
7. P.B. Hodgson, F.H. Salingue, Tetrahedron Lett. **45**, 685–687 (2004)
8. W. Ren, J. Li, D. Zou, Y. Wu, Y. Wu, Tetrahedron **68**, 1351–1358 (2012)
9. H.G. Kuivila, J.F. Reuwer, J.A. Mangravite, J. Am. Chem. Soc. **86**, 2666–2670 (1964)
10. H.G. Kuivila, K.V. Nahabedian, J. Am. Chem. Soc. **83**, 2159–2163 (1961)
11. H.G. Kuivila, J.F. Reuwer Jr, J.A. Mangravite, Can. J. Chem. **41**, 3081–3090 (1963)
12. H.G. Kuivila, K.V. Nahabedian, J. Am. Chem. Soc. **83**, 2164–2166 (1961)
13. K.V. Nahabedian, H.G. Kuivila, J. Am. Chem. Soc. **83**, 2167–2174 (1961)
14. K.L. Billingsley, K.W. Anderson, S.L. Buchwald, Angew. Chem. Int. Ed. **45**, 3484–3488 (2006)
15. K. Billingsley, S.L. Buchwald, J. Am. Chem. Soc. **129**, 3358–3366 (2007)

16. N. Kudo, M. Perseghini, G.C. Fu, Angew. Chem. Int. Ed. **45**, 1282–1284 (2006)
17. D.X. Yang, S.L. Colletti, K. Wu, M. Song, G.Y. Li, H.C. Shen, Org. Lett. **11**, 381–384 (2009)
18. N.Y. Adonin, D.E. Babushkin, V.N. Parmon, V.V. Bardin, G.A. Kostin, V.I. Mashukov, H.-J. Frohn, Tetrahedron **64**, 5920–5924 (2008)
19. J. Chen, A. Cammers-Goodwin, Tetrahedron Lett. **44**, 1503–1506 (2003)
20. T. Korenaga, T. Kosaki, R. Fukumura, T. Ema, T. Sakai, Org. Lett. **7**, 4915–4917 (2005)
21. Y. Nishihara, H. Onodera, K. Osakada, Chem. Commun. 192–193 (2004)
22. G. Zou, Y.K. Reddy, J.R. Falck, Tetrahedron Lett. **42**, 7213–7215 (2001)
23. J.Z. Deng, D.V. Paone, A.T. Ginnetti, H. Kurihara, S.D. Dreher, S.A. Weissman, S.R. Stauffer, C.S. Burgey, Org. Lett. **11**, 345–347 (2009)
24. N. Leconte, A. Keromnes-Wuillaume, F. Suzenet, G. Guillaumet, Synlett **2007**, 204–210 (2007)
25. A.P. Lightfoot, S.J.R. Twiddle, A. Whiting, Synlett **2005**, 529–531 (2005)
26. Y. Yamamoto, M. Takizawa, X.-Q. Yu, N. Miyaura, Angew. Chem. Int. Ed. **47**, 928–931 (2008)
27. H. Noguchi, K. Hojo, M. Suginome, J. Am. Chem. Soc. **129**, 758–759 (2007)
28. M. Nakamura, K. Matsuo, S. Ito, E. Nakamura, J. Am. Chem. Soc. **126**, 3686–3687 (2004)
29. W.M. Czaplik, M. Mayer, A. Jacobi Von Wangelin, Angew. Chem. Int. Ed. **48**, 607–610 (2009)
30. E.P. Gillis, M.D. Burke, Aldrichim. Acta **42**, 17–27 (2009)
31. E.M. Woerly, A.H. Cherney, E.K. Davis, M.D. Burke, J. Am. Chem. Soc. **132**, 6941–6943 (2010)
32. C. Wang, F. Glorius, Angew. Chem. Int. Ed. **48**, 5240–5244 (2009)
33. E.P. Gillis, M.D. Burke, J. Am. Chem. Soc. **129**, 6716–6717 (2007)
34. S.J. Lee, K.C. Gray, J.S. Paek, M.D. Burke, J. Am. Chem. Soc. **130**, 466–468 (2008)
35. E.P. Gillis, M.D. Burke, J. Am. Chem. Soc. **130**, 14084–14085 (2008)
36. J.-K. Lee, M.C. Gwinner, R. Berger, C. Newby, R. Zentel, R.H. Friend, H. Sirringhaus, C.K. Ober, J. Am. Chem. Soc. **133**, 9949–9951 (2011)
37. D.M. Perrin, R. Ting, C.W. Harwig, J. Lo, Y. Li, M.J. Adam, T.J. Ruth, J. Org. Chem. **73**, 4662–4670 (2008)
38. M. Butters, J.N. Harvey, J. Jover, A.J.J. Lennox, G.C. Lloyd-Jones, P.M. Murray, Angew. Chem. Int. Ed. **49**, 5156–5160 (2010)
39. C.A. Hutton, A.K.L. Yuen, Tetrahedron Lett. **46**, 7899–7903 (2005)
40. G.A. Molander, B. Canturk, Angew. Chem. Int. Ed. **48**, 9240–9261 (2009)
41. G.A. Molander, L.N. Cavalcanti, B. Canturk, P.-S. Pan, L.E. Kennedy, J. Org. Chem. **74**, 7364–7369 (2009)
42. E. Vedejs, R.W. Chapman, S.C. Fields, S. Lin, M.R. Schrimpf, J. Org. Chem. **60**, 3020–3027 (1995)
43. G.W. Kabalka, V. Coltuclu, Tetrahedron Lett. **50**, 6271–6272 (2009)
44. B.P. Carrow, J.F. Hartwig, J. Am. Chem. Soc. **133**, 2116–2119 (2011)
45. G.A. Molander, L.A. Felix, J. Org. Chem. **70**, 3950–3956 (2005)
46. C. Amatore, A. Jutand, G. Le Duc, Chem. Eur. J. **17**, 2492–2503 (2011)
47. A.F. Schmidt, A.A. Kurokhtina, E.V. Larina, Russ. J. Gen. Chem. **81**, 1573–1574 (2011)
48. G.A. Molander, D.L. Sandrock, J. Am. Chem. Soc. **130**, 15792–15793 (2008)
49. G.A. Molander, D.L. Sandrock, Org. Lett. **11**, 2369–2372 (2009)
50. C. Adamo, C. Amatore, I. Ciofini, A. Jutand, H. Lakmini, J. Am. Chem. Soc. **128**, 6829–6836 (2006)
51. G.A. Molander, P.E. Gormisky, J. Org. Chem. **73**, 7481–7485 (2008)
52. D.J. Wallace, C. Chen, Tetrahedron Lett. **43**, 6987–6990 (2002)
53. S.-M. Zhou, M.-Z. Deng, L.-J. Xia, M.-H. Tang, Angew. Chem. Int. Ed. **37**, 2845–2847 (1998)
54. D.G. Hall, *Structure, Properties, and Preparation of Boronic Acid Derivatives. Overview of their Reactions and Applications* (Wiley-VCH, Weinheim, 2005)
55. G.A. Molander, B.W. Katona, F. Machrouhi, J. Org. Chem. **67**, 8416–8423 (2002)

56. N.E. Leadbeater, B.J. Tominack, Tetrahedron Lett. **44**, 8653–8656 (2003)
57. M. García-Melchor, M.C. Pacheco, C. Nájera, A. Lledós, G. Ujaque, ACS Catal. **2**, 135–144 (2012)
58. G.A. Molander, B. Biolatto, J. Org. Chem. **68**, 4302–4314 (2003)
59. C. Hansch, A. Leo, R.W. Taft, Chem. Rev. **91**, 165–195 (1991)

Chapter 5
Conclusions and Future work

5.1 Summarised Mechanistic Regimes

Scheme 5.1

5.2 Organotrifluoroborate Preparation

5.2.1 Conclusions

For the preparation of potassium organotrifluoroborates, KHF_2 has become the standard fluorinating reagent of boronic acids for the past 17 years [1], allowing the application of R-BF_3K salts to expand. However, the isolation procedure involves a lengthy evaporation and extraction process, which often requires Soxlet extraction. In addition, the use of KHF_2 liberates HF *in situ*, which can heavily etch common laboratory and industrial glassware thus necessitating the use of specialist plastic/PTFE derived labware.

It was envisaged that KHF_2 could be replaced by a combination of KF and a mild, non-etching acid (HA), thereby rendering the system HF-free. Conditions were optimised employing potassium 4-fluorophenyltrifluoroborate (**1a**) as a test substrate due the ease of *in situ* analysis offered by ^{19}F NMR, Scheme 5.2.

An aqueous solution of KF (4–4.5 equiv.) was added to a mixture of the boronic acid (**2**) in acetonitrile and stirred. To this was added a solution of tartaric acid (**3**) (2.05–2.5 equiv.) in THF, dropwise. The conjugate base, potassium bitartrate (**52**), formed upon consumption of liberated KOH and rapidly precipitated out of solution, thereby driving the equilibrium towards formation of the R-BF_3K salt, Scheme 5.3

The very low solubility of **52** caused it to precipitate out as a fine suspension, leading to difficulties in filtration. However it was found that the use of 7 % (v/v) water, which could be conveniently added as a KF solution, effected a coagulation of the by-product, thus facilitating filtration. Due to the co-precipitation of any

A. J. J. Lennox, *Organotrifluoroborate Preparation, Coupling and Hydrolysis*, Springer Theses, DOI: 10.1007/978-3-319-01134-9_5,

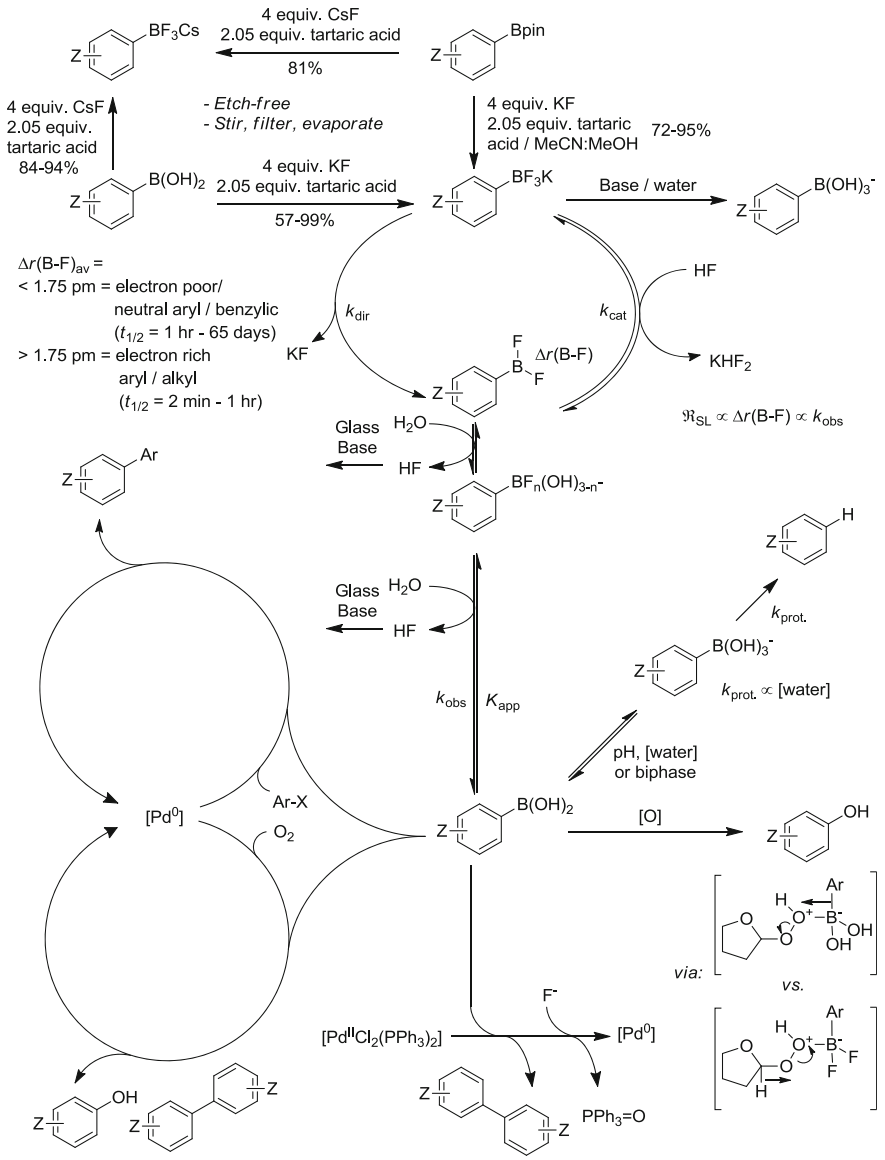

Scheme 5.1 Schematic representation of the major mechanistic regimes presented in this thesis

excess KF or *in situ* generated KHF_2 (<5 %), isolation of pure R-BF_3K salt was achieved by a simple evaporation of the filtrate, bypassing the requirement for extraction.

A range of boronic acids (1 mmol scale, 21 examples) containing electron rich and poor aryl/heteroaryl, alkyl and alkenyl moieties were smoothly converted to the corresponding R-BF_3K salts in good to excellent yields, Sect. 2.2.2, Table 2.5.

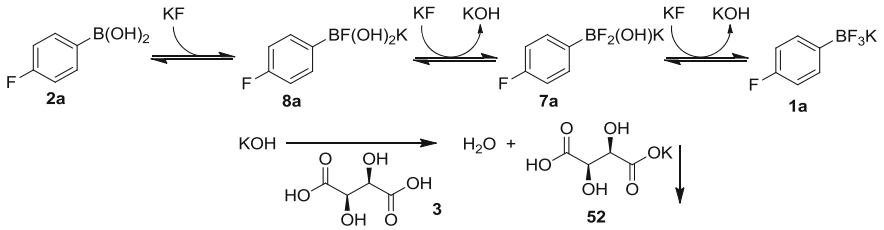

Scheme 5.2 Precipitation-driven equilibrium of **2a**–**1a** under non-etching conditions

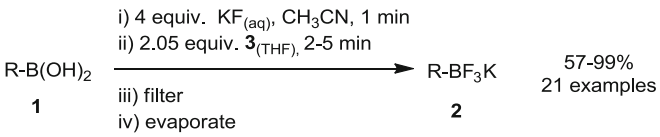

Scheme 5.3 General conditions for the preparation of R-BF_3K salts from boronic acids

Pleasingly, their purities were found to be equal to or better than commercial material or those prepared *via* the use of KHF_2. Upon 18 fold scale-up, the procedure gave improved yields for the generation of **1u** (3.9 g, 95 %) and **1p** (4.2 g, >99 %), thereby confirming the potential of the methodology for industrial application, Sect. 2.2.3.

The extent to which the process caused glassware etching was tested by repeating the procedure in the same reaction flask. The flask used for the generation of **1a** from **2a** *via* the KHF_2 route became extremely clouded after 20 batch runs. By comparison, the flask used in the KF/tartaric acid route was crystal clear, even after 30 batch runs, Sect. 2.2.4.

The methodology was extended to include the use of boronic acid pinacol esters (**4**) as starting materials, Sect. 2.3.1. The pre-complexation of fluoride to the boron species was found to be integral to the overall conversion of **4**, which in the case of the pinacol ester, under the conditions (CH_3CN) optimised for boronic acids, was low. A solvent switch to CH_3OH:CH_3CN (1:1) ensured excellent conversions, followed by dilution with CH_3CN to aid in the flocculation of **52** and co-precipitation of all potassium salts. These alternative reaction conditions gave reliably good to excellent isolated yields and purities for a range of electron rich and poor aryl, alkyl and allyl R-BF_3K salts, Scheme 5.4.

Finally, cesium organotrifluoroborate salts (**5**) were similarly prepared in excellent yields (84–94 %) and purities from boronic acids (**2**), by simply exchanging KF for CsF, Sect. 2.4.1. This provides the safest and simplest route to these salts, as other procedures employ toxic HF. In the conversion of pinacol esters to cesium organotrifluoroborate salts (**5**), the increased solubility of CsF in methanol and subsequent contamination of the product, necessitated a smaller proportion of CH_3OH (CH_3CN:CH_3OH, 9:1).

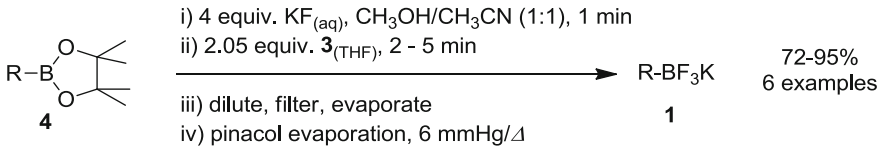

Scheme 5.4 Optimised conditions for preparation of R-BF_3K salts from pinacol esters

5.2.2 Future work

5.2.2.1 Isolation of Mixed Intermediate

When the very electron-poor boronic acids, 3-nitrophenyl **2aa** and 3,5-bis(trifluoromethyl)phenyl **2q**, were subjected to the standard loadings of KF (4 equiv.) and tartaric acid (2.05 equiv.), incomplete conversion (95 %) to the corresponding R-BF_3K salts **1aa** and **1q** resulted; even after recrystallisation of the starting material from water. ^{19}F and ^{11}B NMR confirmed that trifluoroborates **1aa** and **1q** were contaminated by a mixed species of the type R-$BF_n(OH)_{3-n}K$ (**7**/**8**), in the isolated solid material.

The attempted preparation of mixed species **7a** derived from the slightly more electron rich **1a** led to decomposition upon isolation. It was therefore assumed that this type of species were particularly unstable, especially due to the very limited *in situ* spectroscopic evidence for them, Sect. 3.4.3.

However, if conditions could be found (e.g. 1 equiv. **3**, Scheme 5.5) to prepare and characterise (NMR, X-ray crystallography) this stabilised electron-poor mixed species, it would be the first of such to be reported. The subsequent reactivity and solubility studies could reveal interesting differences to R-BF_3K salts or organoboronic acids.

5.2.2.2 Preparation of R-BF_3K Salts from Intermediate Boronic Esters

The borylation/fluorination of Grignard reagents or organolithium reagents provides an extremely important route to the preparation of R-BF_3K salts, which can presently only be achieved by the use of KHF_2.

The potential for the KF/tartaric acid methodology to be adapted for the use in these contexts was demonstrated by the generation of **1c** and **1d**, from their

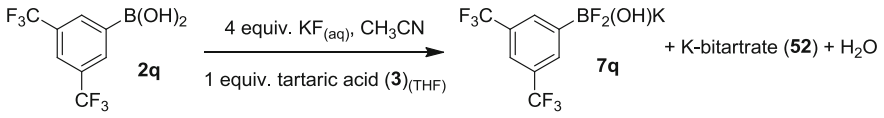

Scheme 5.5 Possible conditions for the preparation of mixed fluoro/hydroxy electron poor aryl boronate **7q**

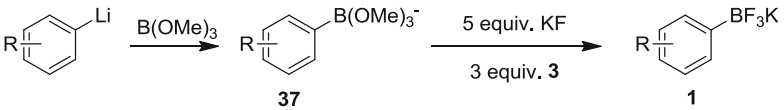

Scheme 5.6 Preparation of R-BF_3K salts from intermediate methylboronate esters

organolithiated precursors. The precise loadings of KF and tartaric acid were only briefly optimised, and therefore gave only moderate yields and purities. Through the *in situ* analysis (^{11}B NMR) of each stage in the reaction (lithiation, borylation, fluorination), it should be possible to further optimise the procedure to generate excellent yields of the desired R-BF_3K salts, Scheme 5.6. In addition to the etch-free conditions, a highly useful improvement on current methodologies would be created if the procedure involved the simple regular work-up sequence: filter/evaporate.

Unfortunately, when Grignard reagents were employed, little success in the preparation of vinyl trifluoroborate **1 k** was observed, thereby illustrating the potential difficulties in future optimisation. Nevertheless, many solvents, addition sequences and reagent loadings are yet to be tested, which may lead to the rapid formation and simple isolation of the pure R-BF_3K salts.

5.2.2.3 Sodium Organotrifluoroborate Salt

Sodium organotrifluoroborates (**48**) are not commonly used in organic synthesis, as their preparation has not been facile prior to the recent commercial introduction of sodium bifluoride. Their application may expand if their physical and chemical characteristics are explored, and are found to be advantageous to the potassium salts.

The potential for the MF/tartaric acid methodology to be adapted to accommodate NaF is very high. Initial investigations confirmed (^{19}F and ^{11}B NMR) the *in situ* stability of the sodium salts, however upon isolation, decomposition to the protodeboronated product dominated, although the identity of the counter-cation was not fully established. Due to the low solubility of NaF in CH_3CN, it is proposed that a decreased complexation of fluoride to boron is responsible for the observed problems. The introduction of a proportion of CH_3OH has previously been shown to successfully avert these issues, Scheme 5.7

5.2.2.4 *In Situ* Generation of HF

Through the precipitation of bitartrate **52**, tartaric acid (**3**) has been shown to be an efficient ‘alkali-metal sponge’, and thus provides a new route to HF production when in combination with alkali-metal fluorides, which may be very useful in a number of different contexts.

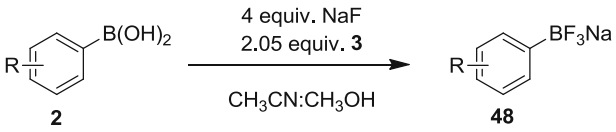

Scheme 5.7 Proposed preparation of sodium organotrifluoroborate salts

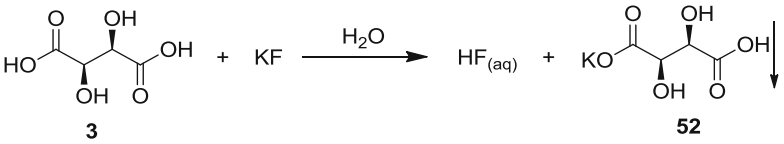

Scheme 5.8 Mild preparation of HF after precipitation of potassium bitartrate (**52**)

Current protocols for the preparation of $HF_{(aq)}$, involve the particularly harsh combination of CaF_2 and H_2SO_4 at 265 °C. Initial studies demonstrated that **52** precipitated out of water at room temperature, thereby formally giving aqueous hydrofluoric acid, Scheme 5.8. However, the concentration limits of the procedure were not tested, and as such it may be found that the usefully high concentrations cannot be generated. In addition, the purity of the $HF_{(aq)}$ filtrate was not tested and thus may contain small quantities of unreacted tartaric acid (**3**).

By employing two equivalents of MF, MHF_2 is formally generated, which could possibly be isolated upon filtration and evaporation. This methodology could be used for the controlled release of HF or MHF_2 for a number of applications, e.g. silyl deprotection.

5.3 Organotrifluoroborate Coupling

5.3.1 Conclusions

The use of organotrifluoroborate salts in SM coupling, has grown to the point where conditions have been optimised for the coupling of multiple functionalities [2]. Reports of higher yields and cleaner reactions, compared to the traditional use of organoboronic acids, are widespread [2]. It was commonly proposed that the origin of these advantages lay in the generation of a transmetalating species that was superior to that of the boronic acid, and was generally considered to be a mixed fluoro/hydroxy boron-ligated 'ate' species **7/8**. The aim of this study was to establish whether there was a significant difference between the use of boronic acids (**2**) and organotrifluoroborates (**1**), followed by the elucidation of where any differences originated.

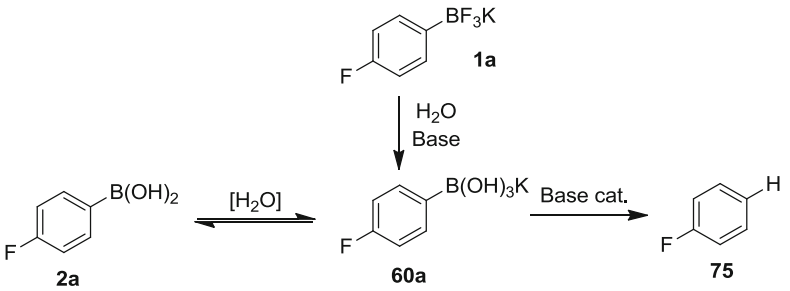

Scheme 5.9 Equilibrium between **2a** and **60a**, dependent on the concentration of water when under basic THF:water conditions, and subsequent protodeboronation of **60a**

Potassium 4-fluorophenyltrifluoroborate **1a** was used as a test substrate under two typical SM conditions: toluene:water (3:1) and THF:water (10:1).

In toluene:water (3:1), SM couplings with **1a** (3 equiv. K_2CO_3, 0.5 mol % $[PdCl_2(PPh_3)_2]$, 80 °C) only reached low (30 %) conversions. It was found **1a** underwent instantaneous hydrolysis in the highly basic aqueous phase leading to the production of trihydroxyboronate **60a**, which rapidly underwent base-catalysed protodeboronation (**60a** → **75**), Sect. 3.3.1. Studies in a more homogenous system (THF:water), illustrated that a reduction in the concentration of water favoured the boronic acid **2a** formation over boronate formation **60a**, thus substantially reducing the rate of base-catalysed protodeboronation, Sect. 3.3.1, Scheme 5.9.

In THF:water (10:1), the observation of $[^2H_4]$-**1a**, through the exchange of $[^2H_4]$-**2a** and $[^2H_0]$-**1a**, established that hydrolytic equilibrium between **1a** and **2a** was rapid. However, fluoride sequestration by the base or glassware effected complete conversion to **2a**, without ever detecting (^{19}F NMR) any mixed intermediates **7a** or **8a**, Sect. 3.5.3.

DFT calculations (B3LYP/6-31G*, lacv3p) performed on the transmetalation between Ph-BX_3^-(X = OH or F) and $[Pd(Ph)PPh_3]$ indicated that the lowest energy barrier for reaction, came when all three ligands around boron were OH; consistent with the decreasing nucleophilic ability to transfer the phenyl moiety to palladium with increasing fluoride ligation, Sect. 3.4.5. Experimentally, these observations were confirmed through the SM coupling (3 equiv. Cs_2CO_3, 1 mol % $[PdCl_2(PPh_3)_2]$, THF:water (10:1)) competition between $[^2H_4]$-**2a** and $[^2H_0]$-**1a**, whereby the majority of cross-coupled product **73** contained the $[^2H_4]$ label during the early stages of reaction, thus establishing **2a** as the most reactive species, Sect. 3.4.5. This evidence suggested that the undetected mixed intermediates **7a** and **8a** did not contribute to catalytic turnover as it was predominated by **2a**.

The difference in side-product formation between reagents **1a** and **2a**, was not therefore due to a superior transmetalating species, but in how **1a** was able to attenuate the side reactions which consumed **2a**. These were found to be in the

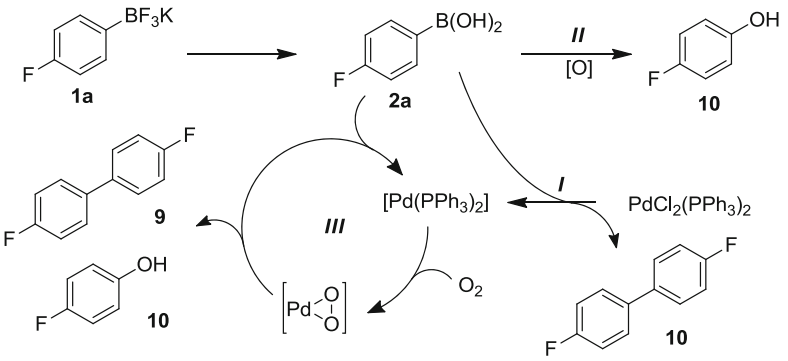

Scheme 5.10 Summary of the organoboron reagent side reactions occurring in SM coupling. In all three examples starting from trifluoroborate **1a** led to lower levels in side-products than starting from boronic acid **2a**

precatalyst activation (***I***), oxidation by a THF derived oxidant (***II***) and in the palladium-catalysed oxidative homocoupling (***III***), Scheme 5.10:

(1) The use of **1a** was able to effect a fluoride-catalysed hydrolytic reduction of the precatalyst ($[PdCl_2(PPh_3)_2]$) [3], thereby avoiding the generation of a homocoupled product **9**. This was confirmed by the transfer of ^{18}O from $H_2^{18}O$ to triphenylphosphine oxide (**77**)—the oxidised by-product [3], Sect. 3.5.1.
(2) In non-ultra pure THF, containing low levels of highly oxidising peroxides, **1a** was found to exhibit a quenching effect, while 2a was efficiently oxidised to phenol **10**. It is proposed this occurs *via* a Lewis acid induced bifurcation of intermediate **79**, Sect. 3.5.2.
(3) Finally, the *in situ* slow hydrolysis from the inert **1a** to the more reactive **2a**, ensures it stays in low concentration, thereby effecting a shift in the catalytic resting state. Transmetalation with $[Pd^{II}(Ar)(OH)]$ becomes turnover limiting, which attenuates the competitive palladium-catalysed oxidative homocoupling. A reduction in the level of these side-products was also observed when the slow-release was imitated *via* slow, syringe pump addition of **2a** to a SM coupling reaction performed in air, Sect. 3.5.2.

5.3.2 Future Work

5.3.2.1 Methanol

The investigations thus far have been conducted in two of the three commonly used solvent systems for the SM coupling of R-BF_3K salts (toluene:water, THF:water), with studies in methanol still remaining. Preliminary investigations showed kinetics of SM coupling in "anhydrous" methanol to be unusual: initially, catalytic turnover

was very rapid, but after ca. 70 % conversion substantial rate deceleration was observed, Sect. 3.2.2. In contrast, bench-grade methanol facilitated a very rapid reaction which proceeded to complete conversion in less than 30 min.

Further study should include confirmation and kinetic analysis of the fate of R-BF_3K salts under SM conditions in methanol. Following this, analogous competition experiments to those employing [$^2H_4$]-**2a**, Sect. 3.4.5, may be very helpful in elucidating the active species under these conditions.

5.3.2.2 THF Hydroperoxide

The current proposal of the quenching of the THF-derived oxidant is based on evidence which has disproved the roles of particular variables, e.g. endogenous fluoride. However, the product, butyrolactone, of the Lewis acidic bifurcation of **79** was only confirmed (^{1}H NMR) when **1a** was replaced by $BF_3.OEt_2$. More spectroscopic evidence is required of this by-product to strengthen the proposal for when **1a** is employed.

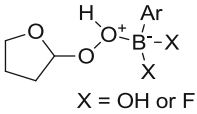

79

Alternatively, computationally simulating the bifurcation of intermediate **79**, when boron is ligated with hydroxide and fluoride, may be integral to revealing how sensitive the system is to changes in the Lewis acidity of the boron centre. Indeed, switching the organic moiety (4-F-C_6H_4) of **2a** for hydroxide ($B(OH)_3$) was enough to engender a quenching effect.

5.3.2.3 Attenuated Oxidation in the Presence of Fluoride or 1a

Palladium-catalysed oxidative homocoupling, the mechanism of which was elucidated by Amatore and Jutand [4], consumes three molecules of boronic acid per turnover: two to form the homocoupled product **9**, while a further one is oxidised by the liberated $B(OOH)OH_2$ to phenol **9**. During the studies of SM couplings under aerobic conditions, Sect. 3.5.3, this 1:1 ratio of side-products was confirmed when **2a** was employed as the coupling partner. However, when **1a** was employed, it was observed (^{19}F NMR) that this ratio of side-products was not maintained: a lower than expected level of phenol **10** was generated.

1a has been shown to successfully quench a THF-derived oxidant, Sect. 3.5.2, but mechanistic elucidations into this additional peroxide quenching ability would be highly useful, with the potential for SM coupling optimisations under aerobic conditions.

Mechanistic studies would be conducted in an analogous manner to those of the THF-derived oxidant. By carrying out the SM coupling of **2a** under aerobic conditions, it would be possible to test the effect of various additives and establish whether it is a fluoride or **1a** specific quenching effect. Amatore and Jutand [4] proposed that the liberated $B(OOH)OH_2$ forms H_2O_2 *in situ* which acts as the primary oxidant. However, it may directly oxidise THF to form the same THF oxidising agent **78**, whose quenching mechanisms from **1a** have been previously proposed, Sect. 3.5.2.

5.4 Organotrifluoroborate Hydrolysis

5.4.1 Conclusions

In establishing the 'slow-release' of **2a** from **1a** as an integral feature of the reactivity of organotrifluoroborate salts in general, the hydrolytic mechanisms of this release were considered. **1a** was used as the test substrate and studied under typical SM coupling conditions (THF:water (10:1), 3 equiv. Cs_2CO_3, 55 °C).

It was immediately apparent that rate profiles were reaction vessel dependent, which initially appeared variable and unpredictable, Sect. 2.4.1. In some cases rapid pseudo first order decays of **1a** ensued after a variable induction period, and in other cases a much slower decay occurred without an induction period. Confirmation of the hydrolytic equilibrium between **1a** and **2a** was established in a fluorophile-free (no base or glass) environment, and the subsequent addition of glass powder to the equilibrated system, ensured complete consumption of **1a**. Increasing the surface area of glass in the system sequestered the fluoride more efficiently, which led to faster rates of hydrolysis, thus confirming the constant fluorophilic properties of glass in the reaction, Sect. 4.2.2, Scheme 5.11.

Through monitoring the rates of hydrolysis of **1a** in homogenous solutions at different pH, it became apparent that a specific acid-catalysed mechanism was dominant. Indeed, at the end of the induction period a precipitous drop in pH accompanied the rapid pseudo first order decay in **1a**, Sect. 4.2.4. Thus, under the basic, biphasic conditions of THF:water (10:1) with 3 equiv. Cs_2CO_3, the pH gradient between the major phase and the minor phase was highly dependent on the mixing efficiency of the system, which in turn was dependent on the vessel shape and stirring speed. Therefore systems with efficient mixing, e.g. round

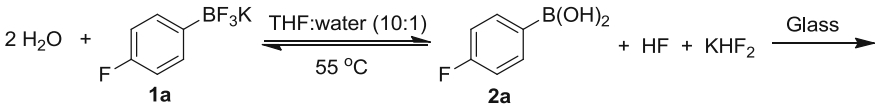

Scheme 5.11 Hydrolytic equilibrium between **1a** and **2a**, with sequestration of fluoride driving the equilibrium towards **2a**

bottomed flasks, could attenuate the acid catalysis, leading to slow rates of hydrolysis. Ultrasound was used to demonstrate the high sensitivity of the reaction to mixing: after a reaction was subjected to only 20 s of sonication, a 45 min induction period resulted, Sect. 4.2.5.

In parallel to the acid-catalysed pathway, it was shown that a much slower, uncatalysed pathway gave **2a** from **1a**, even at high pH. Systems with poor mixing of the biphase meant the balance between the acid-catalysed and uncatalysed routes could not be properly controlled.

Hydrolysis rates were measured for a further 18 substrates, whose rate constants spanned 2.5 orders of magnitude when mediated by glass $\left(k_{\text{obs}}{}^{\text{glass}}\right)$, and 5 orders of magnitude when mediated by base $\left(k_{\text{obs}}{}^{\text{base}}\right.$; $Cs_2CO_3$and DBU$\left.\right)$, Sect. 4.3. Electron poor aryl systems, e.g. 3-nitrophenyl **1aa**, were almost inert to hydrolysis under the basic conditions of SM coupling. These substrates require acid catalysis to efficiently hydrolyse and thus transmetalate directly under the basic SM coupling conditions. Hydrolysis rates of very electron rich aryl and alkyl systems, e.g. cyclobutyl **1y**, were very rapid, whereby the uncatalysed hydrolysis dominants, making the boronic acid release rate very difficult to control. Substrates in between these extremes, e.g. 2-naphthyl **1aw**, were found to hydrolyse at similar rates to catalytic turnover, thereby implying very clean, high yielding SM couplings.

Bond elongation in the DFT derived difluoroborane **11** was found to successfully signal changes in the structural characteristics which determined hydrolytic equilibria (K_{app}) and hydrolysis rates $\left(k_{\text{obs}}{}^{\text{glass}}\right.$ and $\left.k_{\text{obs}}{}^{\text{base}}\right)$. The correlations found formed the basis of a model that can be used to predict hydrolysis rates from the DFT optimised geometries of untested substrates, Sect. 4.6.

Finally, it was found that the Swain-Lupton resonance value ($\Re$) could similarly be employed to correlate with hydrolysis rates, and thus be utilised as an easily sourced predictive parameter, Sect. 4.6.2. To account for the additional steric decompression effects pertinent to alkyltrifluoroborate hydrolysis an improved correlation was observed when the Charton steric parameter was included.

These findings aid in the optimisations of SM coupling reactions of organotrifluoroborate salts. For example, by switching from a pointed reaction vessel to a round bottomed flask, medicinal chemists at GSK [5] were able to significantly improve yields. The slower hydrolysis of the aminomethyltrifluoroborate salts attenuated protodeboronation of the corresponding boronic acids.

5.4.2 Future Work

5.4.2.1 Improving the Predictive Model

A model has been established to predict hydrolysis rates from B–F bond lengths (Δr(B–F)) in the corresponding difluoroborane (**11**), where the data was differentiated by hybridisation of the carbon bound to boron. The rates of hydrolysis for

nineteen substrates were tested, but representation from a large number of structural motifs is still missing. For example, the cross-coupling of aminomethyltrifluoroborate salts forms an important transformation in medicinal chemistry, however the calculated Δr(B–F) is very different to those tested in this study, thus rendering its prediction difficult. Therefore, to incorporate greater structural variation in the model, it is necessary to select and measure hydrolysis rates of substrates with a wider range of Δr(B–F).

It would also be very useful to probe how the rates of hydrolysis of "unusual" substrates, e.g. 2-nitrophenyltrifluoroborate salt **1az**, compared to those already tested. The DFT derived optimised geometry of the difluoroborane **11az**, indicated N donation to B to form an intramolecular Lewis acid/Lewis base adduct. Due to the substantial bond elongation from this complexation, a reliable prediction of hydrolysis rate $\left(k_{\text{obs}}{}^{\text{base}}\right)$ is very unlikely.

5.4.2.2 Preparative Hydrolysis/Cross-Coupling

It was proposed that the addition of a Bronsted acid and a fluorophile to a Class **III** reagent would rapidly reveal the corresponding boronic acid *via* the acid-catalysed pathway and provide a new methodology for the preparative hydrolysis of stable R-BF_3K salts. If this were to directly precede SM coupling, lower reaction times and temperatures could be obtained, yet maintaining the physical attributes R-BF_3K salts contribute to the process.

Previous reports on the preparative hydrolysis of electron-poor aryltrifluoroborates make use of long reaction times (24 h) [6] and high temperatures (70 °C) [7], thus rendering their use, in combination with coupling, pointless. However these reports only focused on the use of an efficient fluorophile, e.g. silica gel [6], alumina [7] or iron$^{(III)}$ chloride [8]. It was envisaged that fast and efficient hydrolysis could be effected by employing tartaric acid (**3**) (1 equiv.), as a "potassium sponge" to destabilise the trifluoroborate, followed by a basic fluorophile to sequester the residual HF. Due to its extreme hydrolytic stability, potassium 3,5-bis(trifluoromethyl)phenyltrifluoroborate (**1q**) was used as a test substrate to study the hydrolysis step. Due to the very insoluble CaF_2, $Ca(OH)_2$ was found to be well suited to the role of fluorophile, Scheme 5.12.

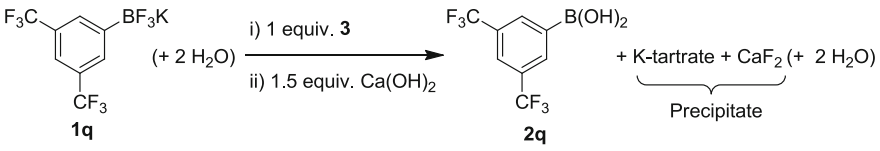

Scheme 5.12 Proposed facile preparative hydrolysis of stable R-BF_3K salts, employing tartaric acid (**3**) and $Ca(OH)_2$, whose bi-products readily precipitate out of solution

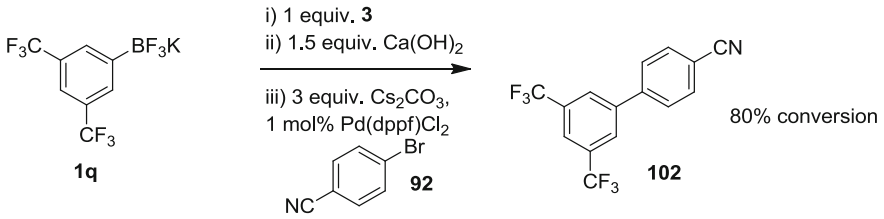

Scheme 5.13 Sequential hydrolysis and cross-coupling of Class III reagent **1q**

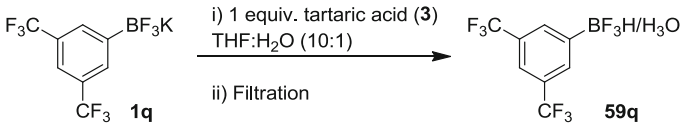

Scheme 5.14 Preparation of proton/hydronium 3,5-bis(trifluoromethyl)trifluoroborate salt (**59q**)

Initial investigations in THF:water (10:1) were promising, with reactions proceeding at room temperature in 10 min. However, the level of conversion was inconsistent due to the addition of $Ca(OH)_2$ causing the pH to rise, switching off the acid catalysis. In addition, formation of the stabilised (trihydroxy)boronate **60q** led to problems with purification. Therefore, various solvent mixtures, concentrations and addition rates were screened. Highest conversions (92 %) were achieved by the addition of a tartaric acid solution in THF to **1q** in THF:water (25:1), followed by the addition of solid $Ca(OH)_2$, and finally the addition of water, dropwise, to prevent the pH rising too high.

When the semi-optimised hydrolysis procedure preceded the addition of Cs_2CO_3 (3 equiv.), [Pd(dppf)Cl_2] (1 mol %) and Ar-Br (**92**), the resulting boronic acid smoothly cross-coupled to **102**, Scheme 5.13. However, incomplete initial hydrolysis resulted in only partial conversion to cross-coupled product **102**. This highlighted the capriciousness of the procedure, thus warranting further study into the first hydrolysis step.

In addition, the trifluoroborate functionality was preserved (as observed by ^{19}F, ^{11}B NMR) in the isolated product generated after treatment of **1q** with tartaric acid (**3**) and subsequent filtration of bitartrate **52** (no fluorophile). It is thus assumed that a proton or hydronium cation is balancing the charge in this very electron poor substrate, Scheme 5.14. These species have been reported to be very unstable when the organic moiety is a simple phenyl group [9]. Isolation, characterisation and a study into its chemical and physical properties may be highly informative.

References

1. E. Vedejs, R.W. Chapman, S.C. Fields, S. Lin, M.R. Schrimpf, J. Org. Chem. **60**, 3020–3027 (1995)
2. G.A. Molander, B. Canturk, Angew. Chem. Int. Ed. **48**, 9240–9261 (2009)
3. J.G. Verkade, M.R. Mason, Organometallics **9**, 864–865 (1990)
4. C. Adamo, C. Amatore, I. Ciofini, A. Jutand, H. Lakmini, J. Am. Chem. Soc. **128**, 6829–6836 (2006)
5. A. Nadin, GSK, Personal communication to GCL–J (2012)
6. G.A. Molander, L.N. Cavalcanti, B. Canturk, P.-S. Pan, L.E. Kennedy, J. Org. Chem. **74**, 7364–7369 (2009)
7. G.W. Kabalka, V. Coltuclu, Tetrahedron Lett. **50**, 6271–6272 (2009)
8. D.W. Blevins, M.-L. Yao, L. Yong, G.W. Kabalka, Tetrahedron Lett. **52**, 6534–6536 (2011)
9. R.A. Batey, T.D. Quach, Tetrahedron Lett. **42**, 9099–9103 (2001)

Chapter 6
Experimental

6.1 Experimental: General Experimental Details

6.1.1 Techniques

Manipulations involving air and moisture sensitive materials were conducted employing standard Schlenk-line techniques, using vacuum lines attached to a double manifold with greaseless J. Youngs valves equipped with an oil pump (0.1 mmHg) under an atmosphere of dry nitrogen. Where air/moisture sensitive reactions were conducted, glassware and needles were placed in an oven (200 °C) prior to use and allowed to cool under an atmosphere of dry nitrogen or under vacuum at 0.1 mmHg (oil pump). Liquid reagents, solutions or solvents were added via cannula or gas-tight syringe through rubber septa (balanced by a nitrogen outlet); solid reagents were added via Schlenk type adapters. The removal of solvents *in vacuo* was achieved using a Büchi rotary evaporator (bath temperatures up to 40 °C) at a pressure of 15 mmHg (diaphragm pump), or at 0.1 mmHg (oil pump) on a vacuum line at room temperature.

6.1.2 Solvents

Dry solvents were obtained by passing solvent through a column of anhydrous alumina using equipment from *Anhydrous Engineering* situated in the University of Bristol chemistry department. Strauss flasks, fitted with a greaseless J. Youngs valve, were used to collect anhydrous solvents, and were dispensed using gas-tight syringes balanced by a nitrogen inlet. Solvents that required degassing were subjected to three cycles of freeze–pump–thaw with the exception of THF and water. THF was distilled under N_2, over sodium/benzophenone ketyl, and water was sparged with N_2 via bubbling for at least 30 min. Commercial grade solvents

A. J. J. Lennox, *Organotrifluoroborate Preparation, Coupling and Hydrolysis*, Springer Theses, DOI: 10.1007/978-3-319-01134-9_6,

were used for chromatography and extraction; petrol refers to the fraction of petroleum-ether boiling in the range of 40–60 °C. Deuterated solvents for NMR analysis were purchased from *Cambridge Isotopes Limited.*

6.1.3 Chromatography

TLC analysis was conducted employing commercially available Merck Kieselgel $60F_{254}$ glass backed plates. Visualisation was achieved by either UV fluorescence (254 nm) or basic $KMnO_4$ solution and heat; relative front values (R_F) are quoted as the ratio between the distances from the baseline to the spot and the solvent front. Column chromatography on silica-gel was performed using Fluorochem 60 silica: 230–400 mesh (40–63 μm). The crude material was applied to the column as a solution in the appropriate eluent or by pre-adsorption onto the silica, as appropriate.

6.1.4 Analysis

6.1.4.1 NMR

NMR spectra were acquired on *Varian 400, Varian 500, JEOL GX 300, ECP400* or *Eclipse 300* spectrometers. All chemical shifts were quoted in parts per million (ppm); ^{1}H and ^{13}C NMR spectra were referenced to TMS as an internal standard, or residual protons of the deuterated solvent, ^{19}F to $CFCl_3$ and ^{11}B to $BF_3.OEt_2$ with a deuterated solvent unless otherwise stated. The following abbreviations (and their combinations) were used to label the multiplicities: s (singlet), d (doublet), t (triplet), q (quartet), m (multiplet), br (broad), app (apparent), Wfn (window function). Coupling constants, *J*, in the ^{1}H and ^{13}C NMR spectra were calculated using *ACDLabs* to the nearest 0.1 Hz. In the ^{11}B NMR spectra they were calculated to the nearest 1 Hz. Assignment of signals in ^{1}H and ^{13}C NMR were performed using ^{1}H–^{1}H COSY, HMQC, HSQC, HMBC and TOCSY experiments where appropriate.

6.1.4.2 IR

IR spectra were recorded in the range 4,000–600 cm^{-1} on a *Perkin-Elmer Spectrum One FT-IR* spectrometer, either as neat films or solids compressed onto a diamond window. Abbreviations used are: w (weak, 0–40 %), m (medium, 40–70 %), s (strong, 70–100 %) and br (broad).

6.1.4.3 Mass Spectrometry

Mass spectra were determined by the University of Bristol mass spectrometry service by either electron impact (EI) or chemical ionisation (CI) using a *Fisons VG Analytical Autospec* spectrometer, or by electrospray ionisation (ESI±) using a *Brüker Daltonics Apex IV* spectrometer.

6.1.4.4 Elemental Analysis

Elemental analysis was performed on a *Euro EA 3000* instrument.

6.1.5 Kinetic Simulations

Kinetic simulations were performed employing *MacKinetics v0.9.1b,* Leipold Associates, USA, 1997.

6.2 Experimental: Organotrifluoroborate Preparation

6.2.1 Specific Experimental Details

6.2.1.1 NMR Analysis

Coupling constants, J, in the ^{1}H and ^{13}C NMR spectra were calculated using *ACDLabs* to the nearest 0.1 Hz. In the ^{11}B NMR spectra they were calculated to the nearest 1 Hz. We note that there are discrepancies between $^{1}J_{B-F}$ in the ^{19}F and ^{11}B NMR spectra; possibly arising from asymmetry in the ^{19}F multiplets. On this basis the ^{11}B value is probably the most reliable, and therefore only this value is reported. In addition, ^{19}F and ^{11}B chemical shifts were often observed to be 2–5 ppm different from those reported in the literature; although the same external references have been used. The ^{11}B and ^{19}F chemical shifts we report are consistent between our samples and commercial materials. NMR tubes constructed from borosilicate glass were used, which caused, depending on the concentration of the sample, a significant background signal in the ^{11}B NMR spectra (very broad peaks centred at $\delta = 32$, -5 and -37 ppm). Assignment of signals in ^{1}H and ^{13}C NMR were performed using ^{1}H–^{1}H COSY, HMQC, HSQC, HMBC and TOCSY experiments where appropriate.

6.2.1.2 Reagents

Reagents and materials purchased from commercial suppliers were used without further purification unless stated. *β*-styryl (**2l**), 1-naphthyl (**2p**), 3,5-bis(trifluoromethyl)phenyl (**2q**), 4-nitrophenyl (**2r**), chlorophenyl (**2s**), 4-cyanophenyl (**2t**), 3-acetylphenyl (**2u**), cyclopropyl (**2x**) cyclobutyl (**2y**) and 4-methylphenyl (**2z**) boronic acids, *o*-iodobenzoic acid (**53**) and cesium fluoride were purchased from *Sigma Aldrich.* Phenyl (**2d**) and 3-aminophenyl (**2ad**) boronic acids were purchased from *Alfa Aesar.* 4-*t*-butylphenyl (**2ab**), 2-fluoro-3-pyridyl (**2ah**), *N*-Boc-5-bromo-2-indolyl (**2ag**), 3-quinonyl (**2af**) boronic acids and allyl boronic acid pinacol ester (**4aj**) were purchased from *Frontier Scientific.* 4-Fluorophenylboronic acid (**1a**) was purchased from *Maybridge.* 3-nitrophenyl (**2aa**) and 4-acetylphenyl (**2ae**) boronic acids were purchased from *Lancaster.* Potassium fluoride was purchased from *Fluka*. L-(+)-Tartaric acid (**3**) was purchased from *Acros Organics.* Cyclohexylboronic acid pinacol ester (**4w**) and 4-biphenylboronic acid pinacol ester (**4ai**) were kindly donated by Prof. V. K. Aggarwal, Dr. T. G. Elford and M. Burns (University of Bristol).

6.2.2 Preparation of R–BF_3K Salts from Boronic Acids

6.2.2.1 Optimisation

Effect of KF on 2a in methanol

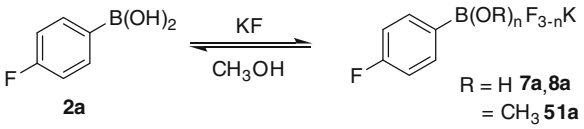

2a

Potassium fluoride (4 equiv., 1×10^{-3} mol, 58 mg) was added to a solution of 4-fluorophenylboronic acid (**2a**) (1 equiv., 0.25×10^{-3} mol, 35 mg) in methanol (1 mL) and stirred for 10 min before being analysed by $^{19}F/^{11}B$ NMR, Fig. 2.1.

6.2.2.2 The Optimised Procedure

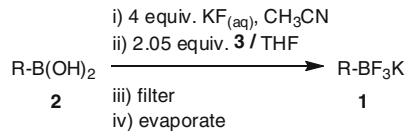

2 **1**

To a suspension of the organoboronic acid (**2**, 1 mmol) in acetonitrile (4 mL) was added potassium fluoride (4 equiv., 4 mmol, 232 mg) in H_2O (0.4 mL) at room temperature. The mixture was stirred until complete dissolution of **2** (usually

0.5–5 min). L-(+)-tartaric acid (**3**, 2.05 equiv., 2.05 mmol, 308 mg) was dissolved into THF (1.5 mL, gentle heat and agitation is required for rapid dissolution) and added drop-wise to the rapidly stirring biphasic mixture over a period of one minute. A white precipitate formed instantly which flocculated over a period of 1–5 min. (If the precipitate did not settle upon cessation of stirring in this time, additional acetonitrile was added (3–4 mL). If it still did not settle, extra water (0.1–0.2 mL) was added and the mixture stirred for a further 10–20 min). The reaction mixture was then diluted with acetonitrile (1 mL) and filtered. The flask and filter cake were rinsed with further portions of acetonitrile (3 × 5 mL) and then the combined filtrates were concentrated *in vacuo* to give the corresponding potassium organotrifluoroborate (**1**) as a solid, which was further dried under high vacuum if required.

Potassium 4-fluorophenyltrifluoroborate [1]

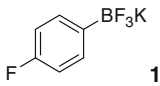

1a

Prepared from 4-fluorophenylboronic acid (**2a**) according to the general procedure and isolated as a white solid (202 mg, >99 % yield). **^{1}H NMR** (300 MHz, DMSO-d_6): $\delta = 7.31$ (app. t; Wfn (sine bell): dd, $^{3}J_{H-H} = 8.5$ Hz, $^{4}J_{H-F} = 6.9$ Hz, 2H), 6.87 (app. t, Wfn (sine bell): ddq, $^{3}J_{H-F} = 10.0$ Hz, $^{3}J_{H-H} = 8.5$ Hz, $^{5}J_{H-F} = 0.7$ Hz, 2H); **^{11}B NMR** (96 MHz, DMSO-d_6): $\delta = 2.1$ (br.); **^{19}F NMR** (283 MHz, DMSO-d_6): $\delta = -118.4$ (s, 1F), -138.7 (br., 3F); **^{13}C{^{1}H} NMR** (100 MHz, DMSO-d_6): $\delta = 160.93$ (d, $^{1}J_{C-F} = 237.5$ Hz), 132.80 (d, $^{3}J_{C-F} = 6.0$ Hz), 112.67 (d, $^{2}J_{C-F} = 18.5$ Hz), *C*–B signal not observed due to quadrupolar relaxation.

^{1}H and ^{13}C{^{1}H} NMR data are in accordance with that previously reported [1].

Potassium phenyltrifluoroborate [1]

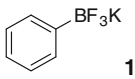

1d

Prepared from phenylboronic acid (**2d**), which had been recrystallised from water, according to the general procedure and isolated as a white solid (165 mg, 90 % yield). **^{1}H NMR** (300 MHz, CD_3CN): $\delta = 7.44$ (d, $^{3}J_{H-H} = 6.6$ Hz, 2H), 7.19–7.08 (m, 3H); **^{11}B NMR** (96 MHz, CD_3CN): $\delta = 2.5$ (q, $^{1}J_{B-F} = 54$ Hz); **^{19}F NMR** (283 MHz, CD_3CN): $\delta = -142.2$ (m); **^{1}H NMR** (400 MHz, DMSO-d_6): $\delta = 7.32$ (d, $^{3}J_{H-H} = 6.4$ Hz, 2H), 7.10−6.99 (m, 3H); **^{13}C{^{1}H} NMR** (100 MHz, DMSO-d_6): $\delta = 131.86$ (s), 126.76 (s), 125.45 (s), *C*–B signal not observed due to quadrupolar relaxation.

^{1}H and ^{13}C{^{1}H} NMR data are in accordance with that previously reported [1].

Potassium β-styryltrifluoroborate [2]

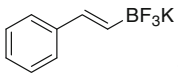

1l

Prepared from β-styrylboronic acid (**2l**), which had been recrystallised from water, according to the general procedure and isolated as a white solid (189 mg, 90 % yield). **^{1}H NMR** (300 MHz, acetone-d_6): = 7.34 (app d, $^{3}J_{H–H}$ = 7.4 Hz, 2H), 7.22 (app dd, $^{3}J_{H–H}$ = 7.4 Hz, $^{3}J_{H–H}$ = 7.4 Hz, 2H), 7.08 (app tt, $^{3}J_{H–H}$ = 7.4 Hz, $^{4}J_{H–H}$ = 3.2 Hz, 1H), 6.65 (d, $^{3}J_{H–H}$ = 18.2 Hz, 1H), 6.32 (dq, $^{3}J_{H–H}$ = 18.2 Hz, $^{3}J_{H–F}$ = 3.7 Hz, 1H); **^{11}B NMR** (96 MHz, acetone-d_6): δ = 2.1 (q, $^{1}J_{B–F}$ = 47 Hz); **^{19}F NMR** (283 MHz, acetone-d_6): δ = −141.6 (m); **^{13}C{^{1}H} NMR** (75 MHz, acetone-d_6): δ = 141.04 (s), 133.94 (s), 128.14 (s), 125.76 (s), 125.67 (s), *C*–B signal not observed due to quadrupolar relaxation.

Data are in accordance with that previously reported [2].

Potassium 4-methoxyphenyltrifluoroborate [3]

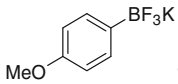

1o

Prepared from 4-methoxyphenylboronic acid (**2o**) according to the general procedure and isolated as a white solid (180 mg, 84 % yield). **^{1}H NMR** (300 MHz, acetone-d_6): δ = 7.38 (d, $^{3}J_{H–H}$ = 8.3 Hz, 2H), 6.68 (d, $^{3}J_{H–H}$ = 8.3 Hz, 2H), 3.69 (s, 3H); **^{11}B NMR** (96 MHz, acetone-d_6): δ = 2.7 (q, $^{1}J_{B–F}$ = 50 Hz); **^{19}F NMR** (283 MHz, acetone-d_6): δ = −142.8 (m).

Data are in accordance with that previously reported [3].

Potassium 1-naphthyltrifluoroborate [4]

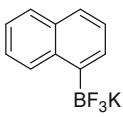

1p

Prepared from 1-naphthylboronic acid (**2p**) according to the general procedure and isolated as a white solid (225 mg, 96 % yield). **^{1}H NMR** (300 MHz, acetone-d_6): δ = 8.59–8.56 (m, 1H), 7.70–7.67 (m, 2H), 7.56 (d, $^{3}J_{H–H}$ = 8.0 Hz, 1H), 7.30–7.23 (m, 3H); **^{11}B NMR** (96 MHz, acetone-d_6): δ = 2.9 (q, $^{1}J_{B–F}$ = 54 Hz); **^{19}F NMR** (283 MHz, acetone-d_6): δ = −138.3 (m); **^{1}H NMR** (400 MHz, DMSO-d_6): δ = 8.41–8.39 (m, 1H), 7.74–7.70 (m, 1H), 7.60–7.54 (m, 2H), 7.35–7.26 (m, 3H); **^{13}C{^{1}H} NMR** (100 MHz, DMSO-d_6): δ = 137.20 (s), 133.55 (s), 130.87 (s), 129.14 (q, $J_{C–F}$ = 3.4 Hz), 127.97 (s), 125.80 (s), 125.52 (s), 124.49 (s), 123.98 (s), *C*–B signal not observed due to quadrupolar relaxation.

The general procedure was repeated on an 18 mmol scale to afford the title compound **1p** as a white solid (4.21 g, >99 %).

Data are in accordance with that previously reported [4].

Potassium 3,5-bis(trifluoromethyl)phenyltrifluoroborate [1]

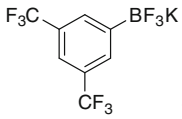

1q

Prepared from 3,5-bis(trifluoromethyl)phenylboronic acid (**2q**) according to the general procedure but employing a greater loading of KF (4.5 equiv., 261 mg) and L-(+)-tartaric acid (2.5 equiv., 375 mg), and isolated as an off-white solid (0.307 g, 96 % yield). **^{1}H NMR** (300 MHz, CD_3CN): $\delta = 7.96$ (s, 2H), 7.73 (s, 1H); **^{11}B NMR** (96 MHz, CD_3CN): $\delta = 1.7$ (q, $^{1}J_{B-F} = 47$ Hz); **^{19}F NMR** (283 MHz, CD_3CN): $\delta = -63.0$ (s, 6F), -143.7 (m). **^{1}H NMR** (400 MHz, DMSO-d_6): $\delta = 7.76$ (s, 2H), 7.73 (s, 1H); **^{13}C{^{1}H} NMR** (100 MHz, DMSO-d_6):131.79 (s), 128.73 (q, $^{2}J_{C-F} = 31.5$ Hz), 124.79 (q, $^{1}J_{C-F} = 272.9$ Hz), 119.35–119.21 (m), *C*–B signal not observed due to quadrupolar relaxation.

Data are in accordance with that previously reported [1], other than the $^{13}C\{^{1}H\}$ NMR data where we note some discrepancies.

Potassium 4-nitrophenyltrifluoroborate [5]

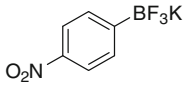

1r

Prepared from 4-nitrophenylboronic acid (**2r**) according to the general procedure and isolated as a pale yellow solid (180 mg, 79 % yield). A greater volume of acetonitrile (25 mL) was used to wash the filter cake due the slightly lower solubility of **1r**. **^{1}H NMR** (300 MHz, acetone-d_6): $\delta = 7.98$ (d, $^{3}J_{H-H} = 8.3$ Hz, 2H), 7.68 (d, $^{3}J_{H-H} = 8.3$ Hz, 2H); **^{11}B NMR** (96 MHz, acetone-d_6): $\delta = 1.9$ (q, $^{1}J_{B-F} = 50$ Hz); **^{19}F NMR** (283 MHz, acetone-d_6): $\delta = -142.8$ (m); **^{1}H NMR** (400 MHz, DMSO-d_6): $\delta = 7.99$ (d, $^{3}J_{H-H} = 8.3$ Hz, 2H), 7.57 (d, $^{3}J_{H-H} = 8.3$ Hz, 2H); **^{13}C{^{1}H} NMR** (100 MHz, DMSO-d_6): $\delta = 146.38$ (s), 132.75 (s), 121.78 (s), *C*–B signal not observed due to quadrupolar relaxation.

Data are in accordance with that previously reported [5].

Potassium 3-chlorophenyltrifluoroborate [6]

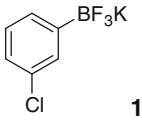

1s

Prepared from 3-chlorophenylboronic acid (**2s**), which had been recrystallised from water, according to the general procedure and isolated as a white solid (203 mg, 93 % yield). **^{1}H NMR** (300 MHz, acetone-d_6): $\delta = 7.43$ (s, 1H), 7.38 (d, $^{3}J_{H-H} = 6.9$ Hz, 1H), 7.13–7.01 (m, 2H); **^{11}B NMR** (96 MHz, acetone-d_6): $\delta = 2.1$ (q, $^{1}J_{B-F} = 52$ Hz); **^{19}F NMR** (283 MHz, acetone-d_6): $\delta = -143.3$ (m);

$^{13}C\{^1H\}$ NMR (76 MHz, acetone-d_6) $\delta = 133.09$ (s), 132.34 (s), 130.79 (s), 128.93 (s), 125.74 (s), *C*–B signal not observed due to quadrupolar relaxation.

^1H NMR and $^{13}C\{^1H\}$ NMR data are in accordance with that previously reported [6].

Potassium 4-cyanophenyltrifluoroborate [5]

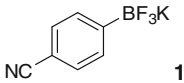

1t

Prepared from 4-cyanophenylboronic acid (**2t**), which had been recrystallised from water, according to the general procedure and isolated as an off-white solid (167 mg, 88 % yield). **^1H NMR** (300 MHz, acetone-d_6): $\delta = 7.62$ (d, $^3J_{H–H} = 7.9$ Hz, 2H), 7.45 (d, $^3J_{H–H} = 7.9$ Hz, 2H); **^{11}B NMR** (96 MHz, acetone-d_6): $\delta = 1.9$ (q, $^1J_{B–F} = 50$ Hz); **^{19}F NMR** (283 MHz, acetone-d_6): $\delta = -144.0$ (m); **^1H NMR** (400 MHz, DMSO-d_6): $\delta = 7.52$ (d, $^3J_{H–H} = 8.0$ Hz, 2H), 7.49 (d, $^3J_{H–H} = 8.0$ Hz, 2H); **$^{13}C\{^1H\}$ NMR** (100 MHz, DMSO-d_6): $\delta = 132.59$ (s), 130.53 (s), 120.62 (s), 108.22 (s), *C*–B signal not observed due to quadrupolar relaxation.

Data are in accordance with that previously reported [5].

Potassium 3-acetylphenyltrifluoroborate [7]

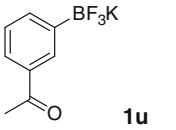

1u

Prepared from 3-acetylphenylboronic acid (**2u**) according to the general procedure and isolated as a white solid (186 mg, 82 % yield). **^1H NMR** (300 MHz, acetone-d_6): $\delta = 8.11$ (s, 1H), 7.71–7.66 (m, 2H), 7.21 (dd, $^3J_{H–H} = 7.3$ Hz, $^3J_{H–H} = 7.3$ Hz, 1H) 2.50 (s, 3H); **^{11}B NMR** (96 MHz, DMSO-d_6): $\delta = 2.2$ (br.); **^{19}F NMR** (283 MHz, DMSO-d_6): $\delta = -139.3$ (br); **$^{13}C\{^1H\}$ NMR** (76 MHz, acetone-d_6) $\delta = 198.32$ (s), 136.64 (s), 135.70 (s), 131.84 (s), 126.39 (s), 125.03 (s), 25.90 (s), *C*–B signal not observed due to quadrupolar relaxation.

The general procedure was repeated on an 18 mmol scale to afford the title compound **1u** as a white solid (3.86 g, 95 %).

Data are in accordance with that previously reported [7].

Potassium cyclopropyltrifluoroborate [1]

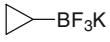

1x

Prepared from cyclopropylboronic acid (**2x**) according to the general procedure but employing a greater loading of KF (4.5 equiv., 261 mg) and L-(+)-tartaric acid

(**3**) (2.5 equiv., 375 mg) and isolated as a white solid (104 mg, 70 % yield). **^{1}H NMR** (300 MHz, DMSO-d_6): $\delta = -0.05$ to -0.23 (m, 4H), -0.80 to -0.89 (m, 1H); **^{11}B NMR** (96 MHz, DMSO-d_6): $\delta = 3.0$ (q, $^{1}J_{B-F} = 57$ Hz); **^{19}F NMR** (283 MHz, DMSO-d_6): $\delta = -140.7$ (m); **^{13}C{^{1}H} NMR** (75 MHz, DMSO-d_6): $\delta = 0.80$ (q, $^{3}J_{C-F} = 2.5$ Hz), *C*–B signal not observed due to quadrupolar relaxation.

^{1}H NMR and ^{13}C{^{1}H} NMR data are in accordance with that previously reported [1].

Potassium cyclobutyltrifluoroborate [8]

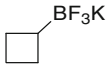

1y

Prepared from cyclobutylboronic acid (**2y**) according to the general procedure but employing a greater loading of KF (4.5 equiv., 261 mg) and L-(+)-tartaric acid (**3**) (2.5 equiv., 375 mg), and isolated as a white solid (93 mg, 57 % yield). **^{1}H NMR** (300 MHz, DMSO-d_6): $\delta = 1.80-1.62$ (m, 6H), 1.16 (br. 1H); **^{11}B NMR** (96 MHz, DMSO-d_6): $\delta = 3.7$ (q, $^{1}J_{B-F} = 61$ Hz); **^{19}F NMR** (283 MHz, DMSO-d_6): $\delta = -143.9$ (m); **^{13}C{^{1}H} NMR** (75 MHz, DMSO-d_6): $\delta = 23.80$ (q, $^{3}J_{C-F} = 2.9$ Hz), 21.5 (s), *C*–B signal not observed due to quadrupolar relaxation.

Data are in accordance with that previously reported [8].

Potassium 4-methylphenyltrifluoroborate [1]

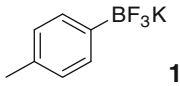

1z

Prepared from 4-methylphenylboronic acid (**2z**) according to the general procedure and isolated as a white solid (177 mg, 89 % yield). **^{1}H NMR** (300 MHz, acetone-d_6): $\delta = 7.35$ (d, $^{3}J_{H-H} = 7.5$ Hz, 2H), 6.90 (d, $^{3}J_{H-H} = 7.5$ Hz 2H), 2.21 (s, 3H); **^{11}B NMR** (96 MHz, acetone-d_6): $\delta = 2.8$ (q, $^{1}J_{B-F} = 52$ Hz); **^{19}F NMR** (283 MHz, acetone-d_6): $\delta = -142.2$ (m);**^{1}H NMR** (400 MHz, DMSO-d_6): $\delta = 7.19$ (d, $^{3}J_{H-H} = 7.3$ Hz, 2H), 6.89 (d, $^{3}J_{H-H} = 7.3$ Hz, 2H), 2.20 (s, 3H); **^{13}C{^{1}H} NMR** (100 MHz, DMSO-d_6): $\delta = 133.61$ (s), 131.90 (s), 127.45 (s), 21.57 (s), *C*–B signal not observed due to quadrupolar relaxation.

^{1}H and ^{13}C{^{1}H} NMR data are in accordance with that previously reported [1].

Potassium 3-nitrophenyltrifluoroborate [1]

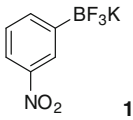

1aa

Prepared from 3-nitrophenylboronic acid (**2aa**) according to the general procedure but employing a greater loading of KF (4.5 equiv., 261 mg) and L-(+)-tartaric acid (**3**) (2.5 equiv., 375 mg), and isolated as a cream solid (199 mg, 87 % yield). **^{1}H NMR** (300 MHz, CD_3CN): $\delta = 8.24$ (s, 1H), 7.97 (ddd, $^{3}J_{H-H} = 8.1$ Hz, $^{4}J_{H-H} = 2.5$ Hz, $^{4}J_{H-H} = 1.1$ Hz, 1H), 7.83 (d, $^{3}J_{H-H} = 7.2$ Hz, 1H), 7.40 (app t, Wfn (sine bell):dd, $^{3}J_{H-H} = 8.1$ Hz, $^{3}J_{H-H} = 7.2$ Hz, 1H); **^{11}B NMR** (96 MHz, CD_3CN): $\delta = 1.9$ (q, $^{1}J_{B-F} = 50$ Hz); **^{19}F NMR** (283 MHz, CD_3CN): $\delta = -142.6$ (m); **^{1}H NMR** (400 MHz, DMSO-d_6): $\delta = 8.12$ (s, 1H), 7.94 (ddd, $^{3}J_{H-H} = 8.1$ Hz, $^{4}J_{H-H} = 2.5$ Hz, $^{4}J_{H-H} = 1.1$ Hz, 1H), 7.75 (d, $^{3}J_{H-H} = 7.3$ Hz, 1H), 7.41 (app t, Wfn (sine bell): dd, $^{3}J_{H-H} = 7.3$ Hz, $^{3}J_{H-H} = 8.1$ Hz, 1H); **^{13}C{^{1}H} NMR** (100 MHz, DMSO-d_6): $\delta = 147.44$ (s), 138.77 (s), 128.36 (s), 125.81 (s), 120.78 (s), *C*–B signal not observed due to quadrupolar relaxation; **^{11}B NMR** (96 MHz, DMSO-d_6): $\delta = 1.6$ (q, $^{1}J_{B-F} = 45$ Hz)

Data are in accordance with that previously reported [1].

Potassium 4-t-butylphenyltrifluoroborate [9]

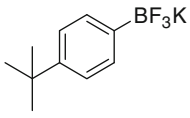

1ab

Prfepared from 4-*t*-butylphenylboronic acid (**2ab**), which had been recrystallised from water, according to the general procedure and isolated as a white solid (235 mg, 98 % yield). **^{1}H NMR** (300 MHz, DMSO-d_6): $\delta = 7.24$ (d, $^{3}J_{H-H} = 7.7$ Hz, 2H), 7.11 (d, $^{3}J_{H-H} = 7.7$ Hz, 2H), 1.24 (s, 9H); **^{11}B NMR** (96 MHz, DMSO-d_6): $\delta = 2.3$ (br.); **^{19}F NMR** (283 MHz, DMSO-d_6): $\delta = -138.5$ (br.); **^{13}C{^{1}H} NMR** (75 MHz, DMSO-d_6): $\delta = 146.73$ (s), 131.10 (br. m), 122.84 (s), 33.89 (s), 31.34 (s), *C*–B signal not observed due to quadrupolar relaxation.

Data are in accordance with that previously reported [9].

Potassium 2,6-difluorophenyltrifluoroborate [1]

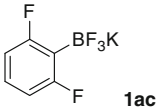

1ac

Prepared from 2,6-difluorophenylboronic acid (**2ac**) according to the general procedure and isolated as a white solid (172 mg, 78 % yield). **^{1}H NMR** (300 MHz, acetone-d_6): $\delta = 7.05$ (tt, $^{3}J_{H-H} = 8.1$ Hz, $^{4}J_{H-F} = 6.6$ Hz, 1H), 6.62 (second order m, 2H); **^{11}B NMR** (96 MHz, acetone-d_6): $\delta = 1.3$ (q, $^{1}J_{B-F} = 47$ Hz); **^{19}F NMR** (283 MHz, acetone-d_6): $\delta = -105.0$ (s, 1F), -135.3 (m); **^{1}H NMR** (400 MHz, DMSO-d_6): $\delta = 7.08$ (tt, $^{3}J_{H-H} = 8.1$ Hz, $^{4}J_{H-F} = 6.8$ Hz, 1H), 6.66 (second order m, 2H); **^{13}C{^{1}H} NMR** (100 MHz,

DMSO-d_6): 166.6 (dd, $^1J_{F–C} = 242.1$ Hz, $^3J_{F–C} = 17.7$ Hz), 128.11 (t, $^3J_{F–C} = 10.0$ Hz), 110.68 (second order m), *C*–B signal not observed due to quadrupolar relaxation.

Data are in accordance with that previously reported [1]

Potassium 3-aminophenyltrifluoroborate

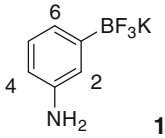

1ad

Prepared from 3-aminophenylboronic acid monohydrate (**2ad**) according to the general procedure and isolated as a pale brown solid (151 mg, 76 % yield). **^{1}H NMR** (300 MHz, CD_3CN): $\delta = 6.94$ (dd, $^3J_{H–H} = 7.5$ Hz, $^3J_{H–H} = 7.5$ Hz, 1H, C(5)H), 6.80–6.79 (m, 2H, C(2)H, C(6)H), 6.46 (ddd, $^3J_{H–H} = 7.5$ Hz, $^4J_{H–H} = 2.4$ Hz, $^4J_{H–H} = 0.9$ Hz, 1H, C(4)H), 3.52 (br, NH_2); **^{11}B NMR** (96 MHz, CD_3CN): $\delta = 2.4$ (q, $^1J_{B–F} = 54$ Hz); **^{19}F NMR** (283 MHz, CD_3CN): $\delta = -142.1$ (m); **^{13}C{^{1}H} NMR** (126 MHz, CD_3CN): 145.86 (s, C(3)), 127.25 (s, C(5)), 121.32 (q, $^3J_{C–F} = 1.9$ Hz, C(6)), 118.33 (q, $^3J_{C–F} = 1.91$ Hz, C(2)), 112.19 (s, C(4)), *C*–B signal not observed due to quadrupolar relaxation; **IR** (solid): $\upsilon/cm^{-1} = 3{,}420$, 3,342, 3,215, 3,037, 1,700, 1,632, 1,613, 1,579, 1,436, 1,295, 1,275, 1,183, 1,165, 1,006, 964, 929. **Elemental Anal.**: Calc'd for $C_6H_6BF_3KN$: C 36.21, H 3.04, N 7.04, found C 36.02, H 3.15, N 6.91; **HRMS** (ESI^-): calc'd for $C_{12}H_{12}B_2F_6N_2K$ [2 M − K^+] 359.0733- found 359.0738, calc'd for $C_6H_6BF_3N$ [M − K^+] 160.0551—found 160.0558.

Potassium 4-acetylphenyltrifluoroborate [7]

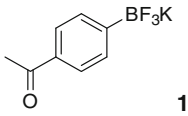

1ae

Prepared from 4-acetylphenylboronic acid (**2ae**) according to the general procedure and isolated as a white solid (129 mg, 57 % yield). **^{1}H NMR** (300 MHz, DMSO-d_6): $\delta = 7.71$ (d, $^3J_{H–H} = 7.9$ Hz, 2H), 7.45 (d, $^3J_{H–H} = 7.9$ Hz, 2H), 2.50 (s, 3H); **^{11}B NMR** (96 MHz, DMSO-d_6): $\delta = 1.9$ (br); **^{19}F NMR** (283 MHz, DMSO-d_6): $\delta = -140.0$ (br); **^{13}C{^{1}H} NMR** (76 MHz, DMSO-d_6): 198.76 (s), 134.80 (s), 131.94 (s), 126.86 (s), 27.08 (s); *C*–B signal not observed due to quadrupolar relaxation.

Data are in accordance with that previously reported [7].

Potassium 3-quinolinyltrifluoroborate [10]

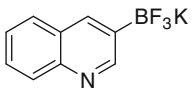

1af

Prepared from 3-quinolinylboronic acid (**2af**) according to the 'pinacol ester general procedure' (CH_3OH:CH_3CN (1:1), dilute with CH_3CN; vide infra) but employing a greater loading of KF (4.5 equiv., 261 mg in H_2O (0.44 mL)) and L-(+)-tartaric acid (**3**) (2.5 equiv., 375 mg in THF (1.8 mL)). The crude product was isolated as a colourless gelatinous solid, which, if left overnight, further solidified to a pale brown crystalline solid (172 mg). **^{1}H NMR** (300 MHz, DMSO-d_6): $\delta = 8.96$ (s, 1H), 8.68 (s, 1H), 8.14 (d, $^3J_{H–H} = 8.1$ Hz, 1H), 8.08 (d, $^3J_{H–H} = 8.4$ Hz, 1H), 7.86 (m, 1H), 7.71 (m, 1H); **^{11}B NMR** (96 MHz, DMSO-d_6): $\delta = 1.7$ (br.); **^{19}F NMR** (283 MHz, DMSO-d_6): $\delta = -139.1$ (br.); **^{13}C{^{1}H} NMR** (125 MHz, DMSO-d_6): $\delta = 150.32$ (app. s), 144.18 (app. s), 140.46 (s), 130.81 (s), 128.36 (s), 128.34 (s), 127.34 (s), 123.46 (s), *C*–B signal not observed due to quadrupolar relaxation. The crude product was dissolved in acetone (5 mL) and stirred over K_2CO_3 (3 equiv., 3 mmol, 414 mg) for 20 min, with two short intermittent (30 s) periods of sonication, before being filtered. The filtrate was concentrated under reduced pressure to give the title compound **1af** as an off-white solid (161.4 mg, 69 %). **^{1}H NMR** (300 MHz, DMSO-d_6): $\delta = 8.85$ (s, 1H), 8.10 (s, 1H), 7.90 (d, $^3J_{H–H} = 8.4$ Hz, 1H), 7.84 (d, $^3J_{H–H} = 8.1$ Hz, 1H), 7.59 (m, 1H), 7.46 (m, 1H); **^{11}B NMR** (96 MHz, DMSO-d_6): $\delta = 2.2$ (br.); **^{19}F NMR** (283 MHz, DMSO-d_6): $\delta = -138.6$ (br.); **^{13}C{^{1}H} NMR** (75 MHz, DMSO-d_6): $\delta = 155.18$ (s), 146.72 (s), 137.36 (s), 128.45 (s), 128.14 (s), 127.62 (s), 127.32 (s), 125.08 (s), *C*–B signal not observed due to quadrupolar relaxation.

Data are in accordance with that previously reported [10].

Potassium N-Boc-5-bromo-2-indolyltrifluoroborate

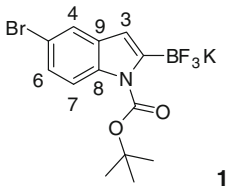

1ag

Prepared from *N*-Boc-5-bromo-2-indolylboronic acid (**2ag**) according to the general procedure and isolated as an off white-solid (363.2 mg, 90 % yield). **^{1}H NMR** (300 MHz, DMSO-d_6): $\delta = 7.95$ (d, $^3J_{H–H} = 8.8$ Hz, 1H, C(7)H), 7.59 (d, $^4J_{H–H} = 2.0$ Hz, 1H, C(4)H), 7.21 (dd, $^3J_{H–H} = 8.8$ Hz, $^4J_{H–H} = 2.0$ Hz, 1H, C(6)H), 6.41 (s, 1H, C(3)H), 1.56 (s, 9H, *N*-Boc); **^{11}B NMR** (96 MHz, DMSO-d_6: $\delta = 0.4$ (br.); **^{19}F NMR** (283 MHz, DMSO-d_6): $\delta = -136.41$ (br.); **^{13}C{^{1}H} NMR** (126 MHz, DMSO-d_6): 151.13 (s, C(C = O)), 136.32 (s, C(8)), 132.78 (s, C(9)), 123.96 (s, C(6)), 121.54 (s, C(4)), 116.19 (s, C(7)), 113.79 (s, C(5)), 110.72 (br. C(3)),

81.86 (s, C(C–O)), 27.58 (s, C(*t*-Bu)), *C*–B signal not observed due to quadrupolar relaxation; **IR** (solid): υ/cm^{-1} = 1,705, 1,541, 1,444, 1,359, 1,310, 1,278, 1,241, 1,207, 1,162, 1,136, 1,091, 980, 948; **Elemental Anal.**: calc'd for $C_{13}H_{13}BBrF_3KNO_2$: C 38.84, H 3.26, N 3.48, found C 39.10, H 3.23, N 3.63; **HRMS** (ESI^+): calc'd for $C_{13}H_{13}BBrF_3K_2NO_2$ [M + K^+] 439.9443, found 439.9433.

Potassium 2-fluoro-3-pyridyltrifluoroborate [10]

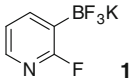

1ah

Prepared from 2-fluoro-3-pyridylboronic acid (**2ah**) according to the pinacol ester general procedure (CH_3OH:CH_3CN (1:1), dilute with CH_3CN; vide infra) but employing a greater loading of KF (4.5 equiv., 261 mg in H_2O (0.44 mL)) and L-(+)-tartaric acid (**3**) (2.5 equiv., 375 mg in THF (1.8 mL)), and isolated as a white solid (172 mg, 85 % yield). **^{1}H NMR** (300 MHz, DMSO-d_6): δ = 7.92 (m, 1H), 7.76 (m. 1H), 7.05 (m. 1H); **^{11}B NMR** (96 MHz, DMSO-d_6): δ = 1.1 (q, $^1J_{B–F}$ = 47 Hz); **^{19}F NMR** (283 MHz, DMSO-d_6): δ = -62.50 (s, 1F), −138.40 (m, 3F); **^{13}C{^{1}H} NMR** (125 MHz, DMSO-d_6): δ = 166.30 (d, $^1J_{C–F}$ = 235 Hz), 144.75, (dq, $^3J_{C–F}$ = 12.4 Hz, $^3J_{C–F}$ = 2.4 Hz), 144.48 (d, $^3J_{C–F}$ = 14.3 Hz), 120.48 (d, $^4J_{C–F}$ = 3.8 Hz), *C*–B signal not observed due to quadrupolar relaxation; **Elemental Anal.**: Calc'd for $C_5H_3BF_4KN$: C 29.58, H 1.49, N 6.90, found C 29.63, H 1.65, N 7.08;

Data are in accordance with that previously reported [10].

6.2.2.3 Purity Comparison

Potassium 3-nitrophenyltrifluoroborate (**1aa**) was prepared from 3-nitrophenylboronic acid (**2aa**) via the KHF_2 method in 86 % yield. In parallel to this, **1aa** was synthesised from **2aa** via the general procedure for the KF/tartaric acid method in 87 % yield, but employing a slightly greater loading of KF (4.5 equiv.) and L-(+)-tartaric acid (**3**, 2.5 equiv.), which was previously found to be necessary for this particular substrate. The purity of **1aa** generated by both methods was assessed by elemental analysis and compared to commercially purchased material and reported data [11] for the same compound, Table 2.7.

6.2.2.4 Glassware Etching

Repeated preparation of 1a in brand new glassware

KHF_2 method

A degree of variability exists between the various methods employing KHF_2, for example in the amount of KHF_2 used (2.5–8 equiv.) and in the work-up procedure,

therefore the most typical one was chosen [1]. The following procedure was performed in *20* batch runs in a brand new 25 mL round bottomed flask.

Potassium bifluoride (4 equiv., 3×10^{-3} mol, 234 mg) in water (1.2 mL) was added dropwise to a stirring solution of 4-fluorophenylboronic acid (**2a**) (1 equiv., 0.75×10^{-3} mol, 105 mg,) in methanol (1.5 mL). The reaction mixture was stirred for a further 30 min before the solvents were removed *in vacuo*. The residue was extracted with acetone (3×5 mL) and filtered, before the filtrate was concentrated to give potassium 4-fluorophenyltrifluoroborate (**1a**), Figs. 2.2 and 2.3.

KF/Tartaric acid method

The general procedure (0.75 mmol scale) for the synthesis of **1a** from **2a** was performed *30* times, in a brand new 25 mL round bottomed flask, Figs. 2.2 and 2.3.

Solution phase KHF_2 comparison

KHF_2 method

Potassium bifluoride (4 equiv., 3.0×10^{-3} mol, 234 mg) in water (1.2 mL) was added dropwise to a stirring solution of 4-fluorophenylboronic acid (**2a**) (1 equiv., 7.5×10^{-4} mol, 105 mg) in methanol (1.5 mL) in a PTFE lined test tube. Trifluoroacetamide (0.1 mmol, 11.3 mg) was added as an internal standard. The solution was stirred for 10 min before a sample was removed and placed in a PTFE lined NMR tube and analysed by ^{19}F NMR, Fig. 2.4.

KF/tartaric acid method

Potassium fluoride (4 equiv., 3.0×10^{-3} mol, 174 mg) in water (0.3 mL) was added to a stirring solution of 4-fluorophenylboronic acid (**2a**) (1 equiv., 7.5×10^{-4} mol, 105 mg) in acetonitrile (3.0 mL) in a PTFE lined test tube. To this was added L-(+)-tartaric acid (**3**) (2.05 equiv., 1.5×10^{-3} mol, 230 mg) in THF (1.13 mL) and stirred for 1 min. A sample was removed, placed into a PTFE lined NMR tube and analysed by ^{19}F NMR, Fig. 2.4.

6.2.3 Preparation of R–BF_3K Salts from Boronic Esters

6.2.3.1 Pinacol Esters

Preparation of organoboronic acid pinacol esters

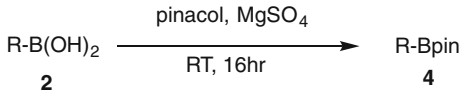

To the organoboronic acid (**2**) (1 equiv., 4×10^{-3} mol) and pinacol (1.5 equiv., 6×10^{-3} mol, 708 mg) was added THF (7.5 mL) and stirred until complete dissolution of the solids. Flame dried $MgSO_4$ (5 equiv., 2.0×10^{-2} mol, 2.40 g) was added and the reaction was stirred for 16 h at room temperature before the volatiles were removed *in vacuo*. The residue was extracted into hexanes (3×5 mL), taken through a 4 cm plug of silica-gel and eluted with hexane: ethylacetate (4:1, 30 mL). The eluate was concentrated to give the corresponding organoboronic acid pinacol ester (**4**), and used without further purification.

4-Fluorophenylboronic acid pinacol ester [12]

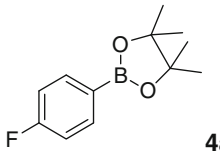

4a

Prepared from 4-fluorophenylboronic acid (**2a**) according to the general procedure and was isolated as a clear colourless oil (598 mg, 66 % yield). **^{1}H NMR** (300 MHz, $CDCl_3$): $\delta = 7.81$ (dd, $^3J_{H-H} = 8.4$ Hz, $^4J_{H-F} = 6.2$ Hz, 2H), 7.06 (dd, $^3J_{H-F} = 9.5$ Hz, $^3J_{H-H} = 8.4$ Hz, 2H), 1.35 (s, 12H); **^{11}B NMR** (96 MHz, $CDCl_3$): $\delta = 29.7$ (br.); **^{19}F NMR** (283 MHz, $CDCl_3$): $\delta = -108.3$ (m); **^{13}C{^{1}H} NMR** (75 MHz, $CDCl_3$): $\delta = 165.09$ (d, $^1J_{C-F} = 250.6$ Hz), 136.96 (d, $^3J_{C-F} = 7.7$ Hz), 114.82 (d, $^2J_{C-F} = 20.8$ Hz), 83.88 (s), 24.84 (s), *C*–B signal not observed due to quadrupolar relaxation.

Data are in accordance with that previously reported [12].

3-Nitrophenylboronic acid pinacol ester [13]

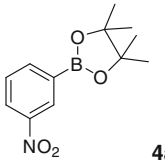

4aa

Prepared from 3-nitrophenylboronic acid (**2aa**) according to the general procedure (2 mmol scale) and was isolated as a pale yellow solid (0.349 g, 70 % yield). **^{1}H NMR** (300 MHz, $CDCl_3$): $\delta = 8.65$ (s, 1H), 8.31 (ddd, $^3J_{H-H} = 8.3$ Hz, $^4J_{H-H} = 2.4$ Hz, $^4J_{H-H} = 1.1$ Hz, 1H), 8.11 (d, $^3J_{H-H} = 7.2$ Hz, 1H), 7.55 (app t, Wfn (sine bell): dd, $^3J_{H-H} = 8.3$ Hz, $^3J_{H-H} = 7.2$ Hz, 1H), 1.37 (s, 12H); **^{11}B NMR** (96 MHz, $CDCl_3$): $\delta = 29.4$ (br.); **^{13}C{^{1}H} NMR** (75 MHz, $CDCl_3$): $\delta = 147.92$ (s), 140.73 (s), 129.52 (s), 128.83 (s), 125.95 (s), 84.67 (s), 24.93 (s), *C*–B signal not observed due to quadrupolar relaxation.

Data are in accordance with that previously reported [13].

4-*t*-Butylphenylboronic acid pinacol ester [14]

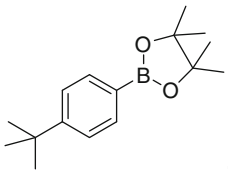

4ab

Prepared from 4-*t*-butylphenylboronic acid (**2ab**) according to the general procedure (2 mmol scale) and was isolated as a white solid (404 mg, 77 % yield). **^{1}H NMR** (300 MHz, $CDCl_3$): $\delta = 7.78$ (d, $^{3}J_{H-H} = 8.1$ Hz, 2H), 7.43 (d, $^{3}J_{H-H} = 8.1$ Hz, 2H), 1.35 (s, 12H) 1.34 (s, 9H); **^{11}B NMR** (96 MHz, $CDCl_3$): $\delta = 30.2$ (br.); **^{13}C{^{1}H} NMR** (75 MHz, $CDCl_3$): $\delta = 154.47$ (s), 134.67 (s), 124.67 (s), 83.58 (s), 34.87 (s), 31.16 (s), 24.80 (s), *C*–B signal not observed due to quadrupolar relaxation.

Data are in accordance with that previously reported [14].

Fluoride complexation studies

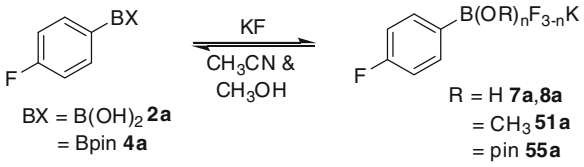

Effect of KF on **4a** in acetonitrile

Potassium fluoride (4 equiv., 1.0×10^{-3} mol, 58.0 mg) in water (0.1 mL) was added to a solution of 4-fluorophenylboronic acid pinacol ester (**4a**) (1 equiv., 2.5×10^{-4} mol, 55.5 mg) in acetonitrile (1 mL) and stirred for 2 min before being analysed by ^{11}B NMR, Fig. 2.5.

Effect of KF on **2a** in acetonitrile

Potassium fluoride (4 equiv., 1×10^{-3} mol, 58 mg) in water (0.1 mL) was added to a solution of 4-fluorophenylboronic acid (**2a**) (1 equiv., 2.5×10^{-4} mol, 35 mg) in acetonitrile (1 mL) and stirred for 2 min before being analysed by ^{19}F/^{11}B NMR, Fig. 2.7.

Effect of KF on **4a** in acetonitrile:methanol (1:1)

Potassium fluoride (4 equiv., 1.0×10^{-3} mol, 58.0 mg) in water (0.1 mL) was added to a solution of 4-fluorophenylboronic acid pinacol ester (**4a**) (1 equiv., 2.5×10^{-4} mol, 55.5 mg) in acetonitrile (0.5 mL)/methanol (0.5 mL) and stirred for 2 min before being analysed by ^{19}F/^{11}B NMR, Fig. 2.7.

Preparation of organotrifluoroborate salts from pinacol esters

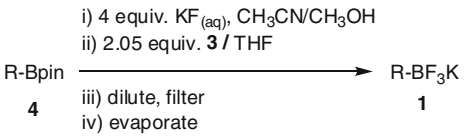

To the organoboronic acid pinacol ester (**4**) (1 mmol) was added methanol (2 mL) then acetonitrile (2 mL), followed by potassium fluoride (4 equiv., 4×10^{-3} mol, 232 mg) in H_2O (0.4 mL) at room temperature. The mixture was stirred until complete dissolution of **4** (0.5–1 min). L-(+)-tartaric acid (**3**) (2.05 equiv., 2.05×10^{-3} mol, 308 mg) was dissolved into THF (1.5 mL, gentle heat and agitation is required for rapid dissolution) and added drop-wise to the rapidly ($\approx$1,000 rpm) stirring biphasic mixture over a period of 5 min, as a white precipitate formed. The reaction was stirred for 2 min, diluted with acetonitrile (3 mL) and stirred for a further 2 min before being diluted again with acetonitrile (1 mL) and filtered. The flask and filter cake were rinsed with further portions of acetonitrile (3 × 5 mL) and then the combined filtrates were concentrated *in vacuo* to give a mixture of the corresponding potassium organotrifluoroborate (**1**) and pinacol. Pinacol was removed by evaporation at 6 mmHg with gentle heating using a heat gun, until there were no visible signs of the condensed pinacol around the flask (5–10 min) [15]. The solid was scraped off the sides of the flask and subjected to further heating (10–15 min) at this reduced pressure. In most cases this amount was sufficient, however in some cases further heating was required.

Potassium 4-fluorophenyltrifluoroborate [1]

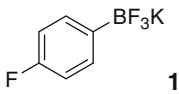

1a

Prepared from 4-fluorophenylboronic acid pinacol ester (**4a**) according to the general procedure and was isolated as a white solid (189 mg, 94 % yield). Analytical data identical with that reported above.

Potassium cyclohexyltrifluoroborate [16]

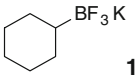

1w

Prepared from cyclohexylboronic acid pinacol ester (**4w**) according to the general procedure and was isolated as a white solid (159 mg, 84 % yield). **^{1}H NMR** (300 MHz, DMSO-d_6): $\delta = 1.57$–1.46 (m, 5H), 1.10–0.81 (m, 5H), −0.05 (br, 1H); **^{19}F NMR** (283 MHz, DMSO-d_6): $\delta = -144.2$ (br); **^{11}B NMR** (96 MHz,

DMSO-d_6): $\delta = 3.6$ (q, $^1J_{B-F} = 61$ Hz); **^{13}C{^{1}H} NMR** (75 MHz, DMSO-d_6): $\delta = 29.46$ (s), 28.81 (s), 28.06 (s), *C*–B signal not observed due to quadrupolar relaxation.

Data are in accordance with that previously reported [16].

Potassium 3-nitrophenyltrifluoroborate [1]

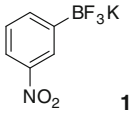

1aa

Prepared from 3-nitrophenylboronic acid pinacol ester (**4aa**) according to the general procedure and was isolated as a pale yellow solid (204 mg, 84 % yield). Analytical data identical with that reported above.

Potassium 4-*t*-butylphenyltrifluoroborate [9]

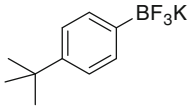

1ab

Prepared from 4-*t*-butylphenylboronic acid pinacol ester (**4ab**) according to the general procedure and was isolated as a white solid (247 mg, 95 % yield). Analytical data identical with that reported above.

Potassium 4-biphenyltrifluoroborate [17]

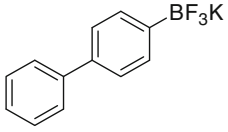

1ai

Prepared from 4-biphenylboronic acid pinacol ester (**4ai**) according to the general procedure and was isolated as a white solid (186 mg, 72 % yield). **^{1}H NMR** (300 MHz, DMSO-d_6): $\delta = 7.61$–7.58 (m, 2H), 7.44–7.37 (m, 6H), 7.29 (m, 1H); **^{19}F NMR** (283 MHz, DMSO-d_6): $\delta = -138.9$ (br); **^{13}C{^{1}H} NMR** (76 MHz, DMSO-d_6): $\delta = 141.48$ (s), 136.78 (s), 131.96 (s), 128.76 (s), 126.51 (s), 126.33(s) 124.67 (s), *C*–B signal not observed due to quadrupolar relaxation.

Data are in accordance with that previously reported [17].

Potassium allyltrifluoroborate [18]

1aj

Prepared from allylboronic acid pinacol ester (**4aj**) according to the general procedure and was isolated as a white solid (0.111 mg, 75 % yield). **^{1}H NMR**

(300 MHz, acetone-d_6): $\delta = 5.94$ (ddt, $^3J_{H–H} = 17.0$ Hz, $^3J_{H–H} = 9.9$ Hz, $^3J_{H–H} = 7.7$ Hz, 1H), 4.63 (d, $^3J_{H–H} = 17.0$ Hz, 1H), 4.53 (d, $^3J_{H–H} = 9.9$ Hz, 1H), 1.09 (br., 2H); **^{19}F NMR** (283 MHz, acetone-d_6): $\delta = -140.6$ (m); **^{11}B NMR** (96 MHz, acetone-d_6): $\delta = 3.4$ (q, $^1J_{B–F} = 61$ Hz); **^{13}C{^{1}H} NMR** (125 MHz, acetone-d_6): $\delta = 143.68$ (br.), 109.52 (s), *C*–B signal not observed due to quadrupolar relaxation.

Data are in accordance with that previously reported [18].

6.2.3.2 Methyl/Isopropyl Esters Prepared *In Situ*

Potassium phenyltrifluoroborate

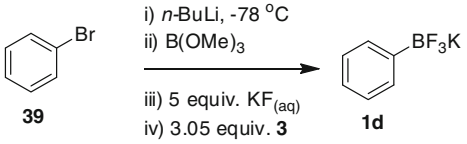

To a two necked round bottomed flask was added bromobenzene (**39**) (1 equiv., 1×10^{-3} mol, 157 mg) and THF (1 mL) and cooled to −78 °C. *n*-Butyllithium (1 equiv., 1×10^{-3} mol, 0.402 mL of 2.49 M soln in hexanes) was added dropwise to the solution and stirred for a further 30 min. The reaction mixture was then cannulated into a solution of trimethylborate (1.01 equiv., 1.01×10^{-3} mol, 105 mg) in THF (1.5 mL) at −78 °C and stirred for a further 30 min at this temperature. The reaction was warmed to 5 °C whereupon KF (5 equiv., 5×10^{-3} mol, 290 mg) in water (0.5 mL) was added. The solution was vigorously stirred as L-(+)-tartaric acid (**3**) (3.05 equiv., 3.05×10^{-3} mol, 457 mg) in THF (2.2 mL) was added dropwise over a period of 2 min. The solution was then filtered, and the filtrate was concentrated *in vacuo*. The solid was recrystallised from boiling acetonitrile to give potassium phenyltrifluoroborate (**1d**) as a white solid (33.3 mg, 18 %). **^{1}H NMR** (300 MHz, CD_3CN): $\delta = 7.44$ (d, $^3J_{H–H} = 6.6$ Hz, 2H), 7.19–7.08 (m, 3H); **^{11}B NMR** (96 MHz, CD_3CN): $\delta = 2.5$ (q, $^1J_{B–F} = 54$ Hz); **^{19}F NMR** (283 MHz, CD_3CN): $\delta = -142.2$ (m).

^{1}H NMR data are in accordance with that previously reported [1]. ^{19}F and ^{11}B NMR data is identical to that of commercial material.

Potassium phenylethynyltrifluoroborate

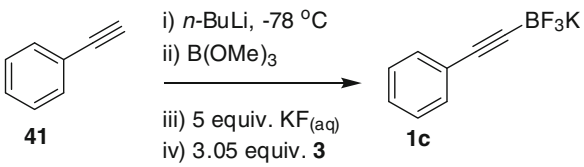

The following procedure has not been optimised, but for comparison the same reaction was conducted using the KHF_2 method [19], giving potassium phenylethynyltrifluoroborate (**1c**) in 32 % yield.

Phenylacetylene (**41**) was distilled over 4 Å molecular sieves and used immediately.

To a two necked round bottomed flask was added phenylacetylene (**41**) (1 equiv., 1×10^{-3} mol, 102 mg) and THF (1 mL) and cooled to −60 °C. *n*-Butyllithium (1 equiv., 1×10^{-3} mol, 0.402 mL of 2.49 M soln in hexanes) was added dropwise to the solution and stirred for a further 10 min. The reaction mixture was then cannulated into a solution of trimethylborate (1.01 equiv., 1.01×10^{-3} mol, 105 mg) in THF (1.5 mL) at −78 °C and stirred for a further hour at this temperature. The reaction was warmed to −20 °C and stirred for 30 min before being warmed to 5 °C whereupon KF (5 equiv., 5×10^{-3} mol, 290 mg) in water (0.5 mL) was added. The solution was vigorously stirred as L-(+)-tartaric acid (**3**) (3.05 equiv., 3.05×10^{-3} mol, 457 mg) in THF (2.2 mL) was added dropwise over a period of 2 min. The solution was then filtered and the filtrate was concentrated *in vacuo* to give potassium phenylethynyltrifluoroborate (**1c**) as a white solid (99.9 mg, 48 %). **^{1}H NMR** (300 MHz, DMSO-d_6): $\delta = 7.29-7.23$ (m, 5H); **^{19}F NMR** (283 MHz, CD_3CN): −134.7 (m); **^{11}B NMR** (96 MHz, DMSO-d_6): $\delta = -2.5$ (br).

^{1}H NMR data is in accordance with that previously reported [1]. ^{19}F and ^{11}B NMR data is identical to that of commercial material.

6.2.4 *Preparation of R–BF_3^- Salts with Different Counter Cations*

6.2.4.1 Cesium Salts

Prepared from boronic acids

The general procedure outlined for the preparation of potassium organotrifluoroborates from boronic acids was followed, but replacing potassium fluoride with cesium fluoride.

Cesium 1-naphthyltrifluoroborate

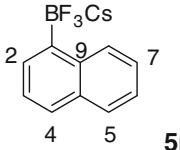

5p

Prepared from 1-naphthylboronic acid (**2p**) according to the general procedure (0.5 mmol scale) and was isolated as a white solid (143 mg, 87 % yield). **^{1}H NMR**

(500 MHz, acetone-d_6): $\delta = 8.60$–8.58 (m, C(8)H, 1H), 7.71–7.68 (m, C(2)H, C(5)H, 2H), 7.57 (d, $^3J_{H–H} = 8.0$ Hz, C(4)H, 1H), 7.30–7.26 (m, C(3)H, C(6)H, C(7)H, 3H); **^{11}B NMR** (96 MHz, acetone-d_6): $\delta = 2.9$ (q, $^1J_{B–F} = 56$ Hz); **^{19}F NMR** (283 MHz, acetone-d_6): $\delta = -135.0$ (m); **^{13}C{^{1}H} NMR** (126 MHz, acetone-d_6): $\delta = 138.74$ (s, C(9)), 135.00 (s, C(10)), 132.22 (s, C(8)), 130.20 (q, $^3J_{C–F} = 1.9$ Hz, C(2)), 128.76 (s, C(5)), 126.68 (s, C(4)), 126.33 (s, C(3)), 125.11 (s, C(6)), 124.59 (s, C(7)), *C*–B signal not observed due to quadrupolar relaxation; **Elemental Anal.**: Calc'd for $C_{10}H_7BCsF_3$: C 36.63, H 2.15, found C 36.50, H 2.22; **IR** (solid): $\upsilon/cm^{-1} = 3{,}057$, 1,770, 1,506, 1,328, 1,270, 1,228, 1,167, 1,081, 1,051, 965, 941; **HRMS** (ESI$^-$): calc'd for $C_{20}H_{14}B_2F_6Cs$ [2M − Cs$^+$] 523.0246—found 523.0241, calc'd for $C_{10}H_7BF_3$ [M − Cs$^+$] 195.0598—found 195.0603.

Cesium 4-nitrophenyltrifluoroborate

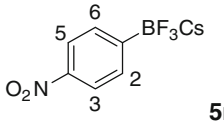

5r

Prepared from 4-nitrophenylboronic acid (**2r**) according to the general procedure (0.5 mmol scale) and was isolated as a pale yellow solid (136 mg, 84 % yield). **^{1}H NMR** (500 MHz, DMSO-d_6): $\delta = 7.98$ (d, $^3J_{H–H} = 8.3$ Hz, C(3)H, C(5)H, 2H), 7.57 (d, $^3J_{H–H} = 8.3$ Hz, C(2)H, C(6)H, 2H); **^{11}B NMR** (96 MHz, DMSO-d_6): $\delta = 1.9$ (br.); **^{19}F NMR** (283 MHz, DMSO-d_6): $\delta = -139.9$ (br.); **^{13}C{^{1}H} NMR** (126 MHz, DMSO-d_6): $\delta = 145.80$ (s, C(4)), 132.16 (q, $^3J_{C–F} = 1.9$ Hz, C(2), C(6)), 121.18 (s, C(3), C(5)), *C*–B signal not observed due to quadrupolar relaxation; **Elemental Anal.**: Calc'd for $C_6H_4BCsF_3NO_2$: C 22.32, H 1.25, N 4.34, found C 22.69, H 1.36, N 4.39; **IR** (solid): $\upsilon/cm^{-1} = 3{,}058$, 1,700, 1,506, 1,344, 1,271, 1,228, 1,167, 1,081, 1,051, 982, 942; **HRMS** (ESI$^-$): calc'd for $C_{12}H_8B_2F_6N_2O_4Cs$ [2M − Cs$^+$] 512.9634—found 512.9632, calc'd for $C_6H_4BF_3NO_2$ [M − Cs$^+$] 190.0293—found 190.0299.

Cesium 4-methylphenyltrifluoroborate

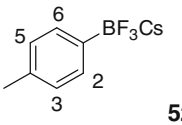

5z

Prepared from 4-methylphenylboronic acid (**2z**) according to the general procedure (0.5 mmol scale) and was isolated as a white solid (137 mg, 94 % yield). **^{1}H NMR** (500 MHz, CD_3CN): $\delta = 7.31$ (d, $^3J_{H–H} = 7.6$ Hz, C(2)H, C(6)H, 2H), 6.98 (d, $^3J_{H–H} = 7.6$ Hz, C(3)H, C(5)H, 2H), 2.26 (s, CH_3, 3H); **^{11}B NMR** (96 MHz, CD_3CN): $\delta = 2.5$ (q, $^1J_{B–F} = 54$ Hz); **^{19}F NMR** (283 MHz, CD_3CN):

$\delta = -139.4$ (m); **^{13}C{^{1}H} NMR** (126 MHz, CD_3CN): $\delta = 135.54$ (s, C(4)), 132.79 (q, $^{3}J_{C-F} = 1.9$ Hz, C(2), C(6)), 128.62 (s, C(3), C(5)), 21.73 (s, *C*H$_3$), *C*–B signal not observed due to quadrupolar relaxation; **Elemental Anal.**: Calc'd for $C_7H_7BCsF_3$: C 28.81, H 2.42, found C 29.18, H 2.46; **IR** (solid): $\upsilon/cm^{-1} = 3{,}044$, 1,700, 1,612, 1,506, 1,227, 1,191, 1,081, 1,051, 964, 929; **HRMS** (ESI$^-$): calc'd for $C_{14}H_{14}B_2F_6Cs$ [2M − Cs$^+$] 451.0246—found 451.0244, calc'd for $C_7H_7BF_3$ [M − Cs$^+$] 159.0598—found 159.0605.

Prepared from boronic esters

Cesium 4-fluorophenyltrifluoroborate

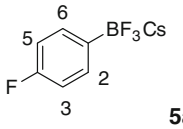

5a

Prepared from 4-fluorophenylboronic acid pinacol ester (**4a**) according to the general procedure (0.5 mmol scale) with a slight modification of solvent (CH_3CN:CH_3OH, 9:1), and cesium fluoride replacing potassium fluoride. It was isolated as a white solid (120 mg, 81 % yield). **^{1}H NMR** (300 MHz, DMSO-d_6): $\delta = 7.30$ (m, C(2)H, C(6)H, 2H), 6.86 (m, C(3)H, C(5)H, 2H); **^{19}F NMR** (283 MHz, DMSO-d_6): −118.5 (s, 1F), −138.4 (br, 3F);**^{11}B NMR** (96 MHz, DMSO-d_6): $\delta = 2.0$ (br); **^{13}C{^{1}H} NMR** (75 MHz, DMSO-d_6): $\delta = 160.90$ (d, $^{1}J_{C-F} = 237.7$ Hz, C(4)), 132.78 (d, $^{3}J_{C-F} = 4.7$ Hz, C(2), C(6)), 112.65 (d, $^{2}J_{C-F} = 18.5$ Hz, C(3), C(5)), *C*–B signal not observed due to quadrupolar relaxation; **IR** (solid): $\upsilon/cm^{-1} = 3{,}024$, 1,590, 1,511, 1,393, 1,211, 1,193, 955, 932, 813; **HRMS** (ESI$^-$): calc'd for $C_6H_4BF_4$ [M − Cs$^+$] 163.0348—found 163.0353.

6.2.4.2 Sodium Salts

Sodium naphthyltrifluoroborate

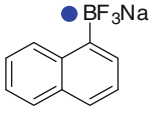

48p

The general procedure for the preparation of potassium organotrifluoroborate salts from boronic acids was followed, but with NaF replacing KF. Sodium naphthyltrifluoroborate (**48p**) was not isolated, but was detected (ca. 45 %, ^{19}F and ^{11}B NMR) *in situ*, Fig. 6.1.

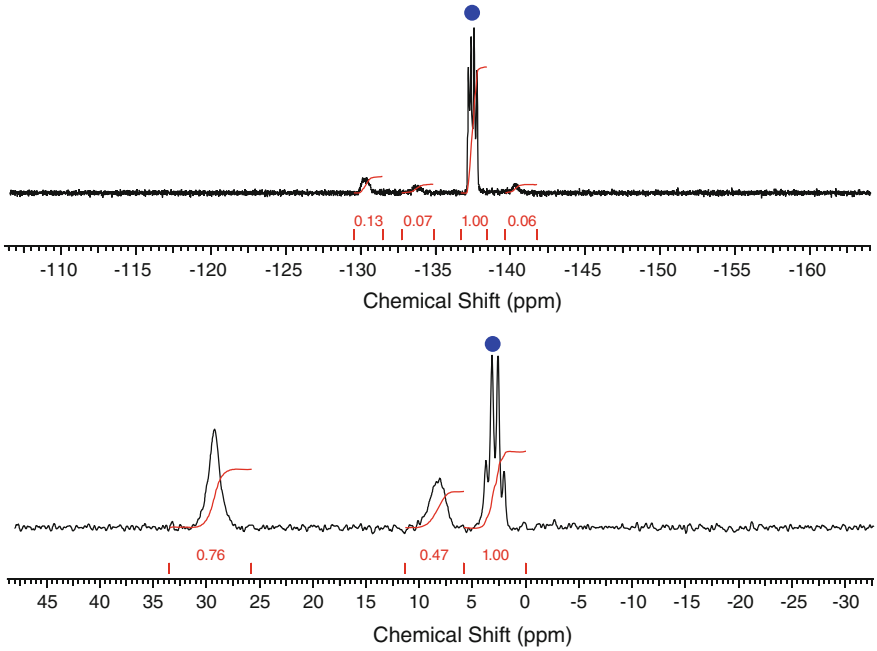

Fig. 6.1 ^{19}F NMR (*upper spectrum*) and ^{11}B NMR (*lower spectrum*) of the naphthyltrifluoroborate salt *in situ*

6.3 Experimental: Organotrifluoroborate Coupling

6.3.1 Specific Experimental Details

6.3.1.1 Reagents

Reagents and materials purchased from commercial suppliers were used without further purification unless stated. 1,3-Bis(trifluoromethyl)-5-bromobenzene (**6**), 4-fluorophenylboronic acid (**2a**), 1 M tetrabutylammonium fluoride (TBAF) in tetrahydrofuran (THF), bromine, potassium bromide, and triphenylphosphine were purchased from *Sigma Aldrich*. Potassium 4-fluorophenyltrifluoroborate (**1a**), benzotrifluoride, anhydrous iron(III) chloride (stored under argon), cesium carbonate and triisoproylborate were purchased from *Alfa Aesar*. Sodium thiosulphate, sodium sulphate and potassium carbonate were purchased from *Fisher Scientific*. [$^2H_5$]-Fluorobenzene ([$^2H_5$]-**75**) was purchased from *Cambridge Isotopes Limited.* *n*-Butyllithium (2.46 N in hexane) was purchased from *Acros Organics* and titrated into a known concentration of diphenylacetic acid in THF. Tri(o-tolyl)phosphine were purchased from *Fluka*. Bis(triphenylphosphine)palladium(II) chloride was prepared by a known method [20].

6.3.2 Initial Investigations

6.3.2.1 Substrates and Conditions

General conditions for the kinetics of SM coupling in a Schlenk tube

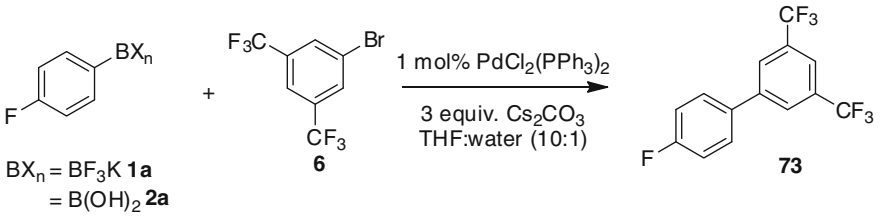

Bis(triphenylphosphine)palladium(II) chloride (1 mol %, 6.6×10^{-7} mol, 0.45 mg) in dry degassed THF (1 mL) was added to a Schlenk tube containing a solution of **6** (1 equiv., 6.6×10^{-5} mol, 19.1 mg), cesium carbonate (1.32×10^{-4} mol, 43×10^{-3} g) and either **1a** (1 equiv., 6.6×10^{-5} mol, 13.3 mg) or **2a** (1 equiv., 6.6×10^{-5} mol, 9.2 mg) in degassed THF (6.5 mL) and D_2O (0.75 mL) under an inert atmosphere of dry N_2. The reaction was stirred at 55 °C whilst samples (0.6 mL) were removed at regular time intervals with a gas-tight syringe, and kept at 0 °C before analysis by ^{19}F NMR. Each sample was run unlocked and spectra were acquired by accumulating 128 scans at 25 °C and 470.3 MHz. For a typical spectrum from the SM coupling of **1a** and **2a** with **6** see Fig. 3.3.

6.3.2.2 Solvent Study

General conditions for analysis by GC (FID)

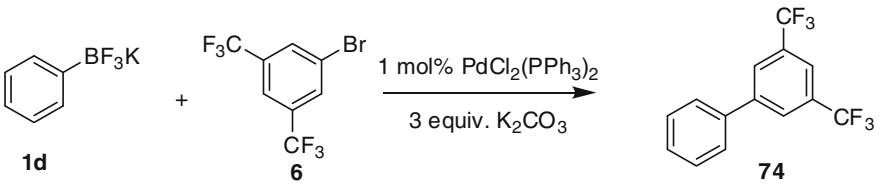

The following procedure was performed in bench-grade methanol, anhydrous methanol, THF:water (10:1), toluene:water (3:1) and anhydrous toluene.

3,5-Bis(trifluoromethyl)bromobenzene (**6**) (1 equiv., 5.8×10^{-4} mol, 170 mg) and a drop of benzotrifluoride were added to a stirring solution of potassium phenyltrifluoroborate (**1d**) (1 equiv., 5.8×10^{-4} mol, 107 mg), cesium carbonate (1.96×10^{-3} mol, 0.064 g) and bis(triphenylphosphine)palladium(II) chloride (1 mol %, 5.8×10^{-6} mol, 4.1 mg) in degassed solvent (4 mL) at 60 °C. Samples

(0.1 mL) were removed, at regular time intervals, into vials containing $NH_4Cl_{(aq)}$ and hexane. After briefly agitating the mixture, the organic phase was taken through a small silica-gel plug and washed through with hexane, before being analysed by GC (FID), Fig. 3.4.

6.3.3 Incomplete Conversions Study

6.3.3.1 Toluene:water (3:1)

Addition of more 1d

The "General conditions for analysis by GC (FID)", outlined above (Sect. 6.3.2.2 *vide supra*), were employed in toluene:water (3:1), with the addition of **1d** (1 equiv., 5.8×10^{-4} mol, 107 mg) after 42 min, Fig. 3.5.

Addition of more catalyst precursor

The "General conditions for analysis by GC (FID)", outlined above (Sect. 6.3.2.2 *vide supra*), were employed in toluene:water (3:1), with the addition of $[Pd(PPh_3)_2Cl_2]$ (1 mol %, 5.8×10^{-6} mol, 4.1 mg) after 42 min, Fig. 3.5.

^{19}F NMR in situ monitoring

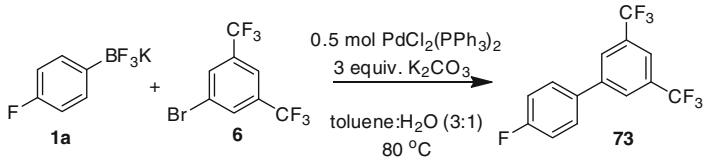

1,3-Bis(trifluoromethyl)-5-bromobenzene (**6**) (1 equiv., 7.53×10^{-4} mol, 224 mg) and a drop of benzotrifluoride were added to a stirring solution of potassium 4-fluorophenyltrifluoroborate (**1a**) (1 equiv., 7.5×10^{-4} mol, 152 mg), potassium carbonate (3 equiv., 2.26×10^{-3} mol, 311 mg) and bis(triphenylphosphine)palladium(II) chloride (0.5 mol %, 3.8×10^{-6} mol, 2.6 mg) in degassed toluene (12 mL) and degassed water (4 mL) at 80 °C. Samples (0.6 mL toluene, 0.2 mL water) for ^{19}F NMR analysis were removed from each layer and placed immediately into ice cooled tubes at regular time intervals. The water samples were topped up with additional water (0.4 ml) and both were stored at 0 °C until ^{19}F NMR analysis. Each sample spent no longer than 5 min on the spectrometer sample rack at room temperature, (conditions which were shown to generate <1 % conversion), and were analysed with 128 scans at 25 °C and 470.3 MHz, Figs. 3.6 and 3.7.

Preparation of ^{19}F NMR reference compounds

4′-Fluoro- 3,5-bis(trifluoromethyl)biphenyl

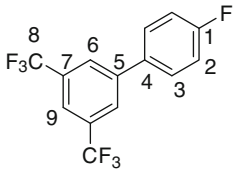

73

1,3-Bis(trifluoromethyl)-5-bromobenzene (**6**) (1 equiv., 1×10^{-3} mol, 293 mg) and bis(triphenylphosphine)palladium(II) chloride (1 mol %, 1×10^{-5} mol, 7.0 mg) were added, with stirring, to a mixture of potassium 4-fluorophenyltrifluoroborate (**1a**) (1 equiv., 1×10^{-3} mol, 202 mg) and potassium carbonate (3 equiv., 3×10^{-3} mol, 414 mg) in methanol (10 mL). The reaction was performed under a N_2 atmosphere at 80 °C for 16 h, and was followed by TLC (100 % hexanes) analysis. The clear brown solution was quenched with saturated $NH_4Cl_{(aq)}$ (10 mL) and the resultant organics were extracted with hexanes (2 × 10 mL), dried over anhydrous $MgSO_4$, filtered and concentrated *in vacuo*. The resultant material was purified by column chromatography (100 % hexanes) to give the title compound as a white crystalline solid (6.79×10^{-4} mol, 2.09×10^{-1} g, 68 %). $\mathbf{R_f}$ (hexanes) = 0.83; **Mp:** 51–52 °C; **^{1}H NMR** (300 MHz, $CDCl_3$): δ = 7.89 (s, C(6)H, C(6′)H), 7.78 (s, C(9)H), 7.51 (m, C(3)H, C(3′)H), 7.13 (m, C(2)H, C(2′)H); **^{13}C NMR** (76 MHz, $CDCl_3$): δ = 163.40 (d, $^1J_{C-F}$ = 249.6 Hz, C(1)), 142.39 (s, C(5)), 134.47 (s, C(4)), 132.30 (q, $^2J_{C-F}$ = 33 Hz, C(7)), 129.11 (d, $^3J_{C-F}$ = 8.3 Hz, C(3)), 127.15 (s, C(6)), 123.40 (q, $^1J_{C-F}$ = 273.0 Hz, C(8)), 121.03 (s, C(9)), 116.41 (d, $^2J_{C-F}$ = 21.8 Hz, C(2)); **^{19}F NMR** (283 MHz, d_8-toluene): δ = −62.50 (s, 6F), −112.78 (m, 1F); **Elemental Anal.:** calc'd. for $C_{14}H_7F_7$: C 54.56, H 2.29, found C 54.77, H 2.48; **IR** (solid): ν/cm^{-1} = 3,099 (br, w), 2,921 (br, w), 1,382 (s), 1,276 (s), 1,117 (s), 1,097.29 (s), 900.9 (m), 836 (s), 680.7 (m); **MS(CI)** *m/z* (%): 337.2 (20), 309.1 (65) [$M + H^+$], 308.1 (60) [M^+], 290.1 (27) [$M + H–F^+$], 289.1 (100) [$M–F^+$]; **HRMS (CI):** calc'd for $C_{14}H_8F_7$: 309.0514, found 309.0504.

4,4′-Difluorobiphenyl [21]

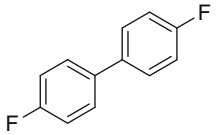

9

4-Fluorophenylboronic acid (**2a**) (1 equiv., 4.5×10^{-4} mol, 63 mg) was dissolved into a solution of palladium(II) acetate (5 mol %, 2.25×10^{-5} mol, 5 mg) and triphenylphosphine (10 mol %, 4.5×10^{-5} mol, 12 mg) in toluene (5 mL). Potassium carbonate (2.5 equiv., 1.125×10^{-3} mol, 155 mg) was added and the mixture was stirred at 60 °C for 300 min. Upon completion, as followed by TLC

(100 % hexanes), the reaction was quenched with water (20 mL), extracted with DCM (3 × 10 mL) and washed with brine (10 mL). The organics were dried over anhydrous $MgSO_4$, filtered and concentrated *in vacuo,* before purification by column chromatography (100 % hexanes) to give the title compound as a white crystalline solid (1×10^{-4} mol, 10 mg, 44 %). **^{1}H NMR** (300 MHz, $CDCl_3$): $\delta = 7.49$ (dd, $^3J_{H-H} = 8.6$ Hz, $^4J_{H-F} = 5.4$ Hz, 4H), 7.12 (app t, Wfn (sine bell): dd $^3J_{H-H} = 8.6$ Hz, $^3J_{H-F} = 8.6$ Hz, 4H). **^{19}F NMR** (283 MHz, $CDCl_3$): $\delta = 115.61$ (s, 2F). **^{13}C NMR** (100 MHz, $CDCl_3$): 162.5 (d, $^1J_{C-F} = 246$ Hz, 2C), 136.5 (s, 2C), 128.68 (d, $^3J_{C-F} = 8.1$ Hz, 2C), 115.75 (d, $^2J_{C-F} = 20.1$ Hz, 2C). **MS (CI)** *m/z* (%): 190 (100).

Data are in accordance with that previously reported [21].

3,3′,5,5′-tetrakis(trifluoromethyl)biphenyl [22]

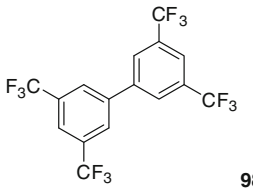

98

Zinc dust (2.4 equiv., 6.12×10^{-4} mol, 4 mg), potassium bromide (16 mol %, 4.28×10^{-5} mol, 5.1 mg), triphenylphosphine (57 mol % 1.46×10^{-4} mol, 38 mg) and nickel (II) chloride (57 mol %, 1.46×10^{-4} mol, 19 mg) were dissolved in dry DMF (4 mL) under N_2 and heated to 60 °C with stirring. 1,3-bis(trifluoromethyl)-5-bromobenzene (**6**) (1 equiv., 2.6×10^{-4} mol, 76 mg) was added and the reaction was monitored by TLC (95:5 hexanes:ethyl acetate). After 300 min the reaction was quenched with water (100 mL), filtered through Celite, and extracted with hexanes (3 × 20 mL). The organics were dried over $MgSO_4$, filtered, concentrated *in vacuo* and the resultant crude material purified by column chromatography (95:5 hexanes:ethyl acetate) to give the title compound as light brown crystals (6.34×10^{-5} mol, 27 mg, 24 %). **^{1}H NMR** (400 MHz, d_8-toluene): $\delta = 7.11$ (s, 4H), 7.48 (s, 2H); **^{19}F NMR** (376 MHz, d_8-toluene): $\delta = 62.61$ (s, 12F); **MS (CI)** *m/z* (%): 426 (100)

Data are in accordance with that previously reported [23].

THF/water ratio on the 2a and 60a equilibrium

Potassium 4-fluorophenylboronate (**60a**) was generated *in situ* from a stock solution of **1a** (1 equiv., 2.43×10^{-4} mol, 49 mg) and potassium carbonate (3 equiv., 9.71×10^{-4} mol, 136 mg) in D_2O (3.5 mL), and was subsequently added (0.5 mL) to various ratios of THF/water without inertion. The following THF:water ratios and final volumes (mL) were used: 10:1 (5.5), 5:1 (9), 2:1 (4.5), 1:1 (2), 1:2 (1.5), 1:5 (1.2), 1:10 (0.55). The resulting homogeneous solutions were

stirred for 15 min at room temperature before a sample (0.5 mL) was removed and analysed by ^{19}F NMR, Fig. 3.8.

A sample from each of 10:1 THF:water, and 1:5 THF:water were left sealed, at room temperature, for 12 days and then analysed by ^{19}F NMR, Fig. 3.9.

6.3.4 Organotrifluoroborate Activation

6.3.4.1 Toluene:water (3:1)

KF addition to SM coupling

The "General conditions for analysis by GC (FID)", outlined above (Sect. 6.3.2.2 *vide supra*), were employed, with the addition of KF (3.5 equiv., 2.0×10^{-3} mol, 118 mg) from the start, Fig. 3.11.

KF titration of 1a

KF was titrated into a solution of phenylboronic acid (**2d**) (1 equiv., 4.1×10^{-4} mol, 50 mg) in water (4 mL), in one equivalent amounts up to a total of 4, followed by further additions of 9 and 16 equivalents. After each addition, the solution was stirred for two min and a sample was removed and analysed by ^{11}B NMR, Fig. 3.12.

6.3.4.2 Water

Base titrations

Base titrations were conducted at room temperature and without inertion.

1a (1 equiv., 4.95×10^{-4} mol, 100 mg) was dissolved in D_2O (7 mL) and K_2CO_3 was added in half equivalent amounts, with stirring, from 0 to 4 equivalents, then a further 2 and 4 equivalents were added, bringing the total to 10. Samples (0.5 mL) were removed 5 min after each addition of base and analysed by ^{19}F and ^{11}B NMR, Figs. 3.13 and 3.14.

The above procedure was repeated with **2a** (1 equiv., 4.95×10^{-4} mol, 69 mg), instead of **1a**, Fig. 3.15.

The above procedure was repeated in THF:water (10:1, 7 mL), instead of water, Fig. 3.15.

The above procedure was repeated three times with the addition of a different quantity of KF (4 equiv., 106 mg; 8 equiv., 213 mg; 12 equiv., 319 mg) from the start, Fig. 3.16.

The above procedure was repeated with Cs_2CO_3 and KOH, instead of K_2CO_3, Fig. 6.2.

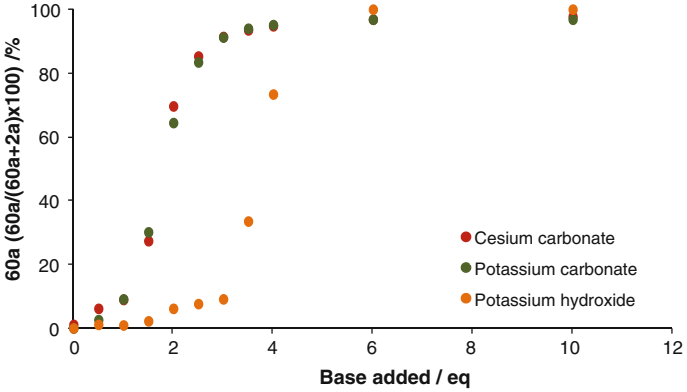

Fig. 6.2 Base titration of **2a** with Cs_2CO_3, K_2CO_3 and KOH. A higher concentration of KOH is required to effect the same change as Cs_2CO_3 and K_2CO_3, as it is monobasic

$BF_3(OH)K$ study

Conditions were used that had previously been found to produce detectable levels of $B(OH)F_3K$, with a substrate stable to protodeboronation on the relevant time scales. For the preparation of [^{10}B]-potassium 4-fluorophenyltrifluoroborate ([^{10}B]-**1a**) see Sect. 6.4.2.4 *vide infra*.

[^{10}B]-**1a** (1 equiv., 6.00×10^{-5} mol, 12.1 mg) was added as a solid to a PTFE lined NMR tube. To this was added D_2O (0.3 mL) followed by Cs_2CO_3 (0.5 equiv., 3.00×10^{-5} mol, 9.78 mg) in D_2O (0.06 mL). The tube was shaken for approximately 10 min before being analysed by ^{19}F NMR (128 scans, 25 °C), Fig. 6.3.

This procedure was repeated (2 × scale) but stirred in a glass test tube for 10 min before a sample was removed and placed in an NMR tube *without* a PTFE liner, Fig. 6.3.

^{19}F EXSY NMR

Conditions were found which exhibited the largest proportion of the mixed fluoro/hydroxy species **7a/8a**, by screening a range of THF/water ratios and concentrations of base. Potassium carbonate (0.5 equiv., 2.64×10^{-6} mol, 0.36 mg) and **1a** (1 equiv., 5.28×10^{-6} mol, 1.1 mg) were dissolved in THF/water (1:10, 0.66 mL) in an NMR tube at room temperature. Exchange spectroscopy was performed by employing a standard Chempack 2D NOESY experiment, modified for multinuclear analysis on the *Varian 500 MHz* spectrometer, Fig. 3.17.

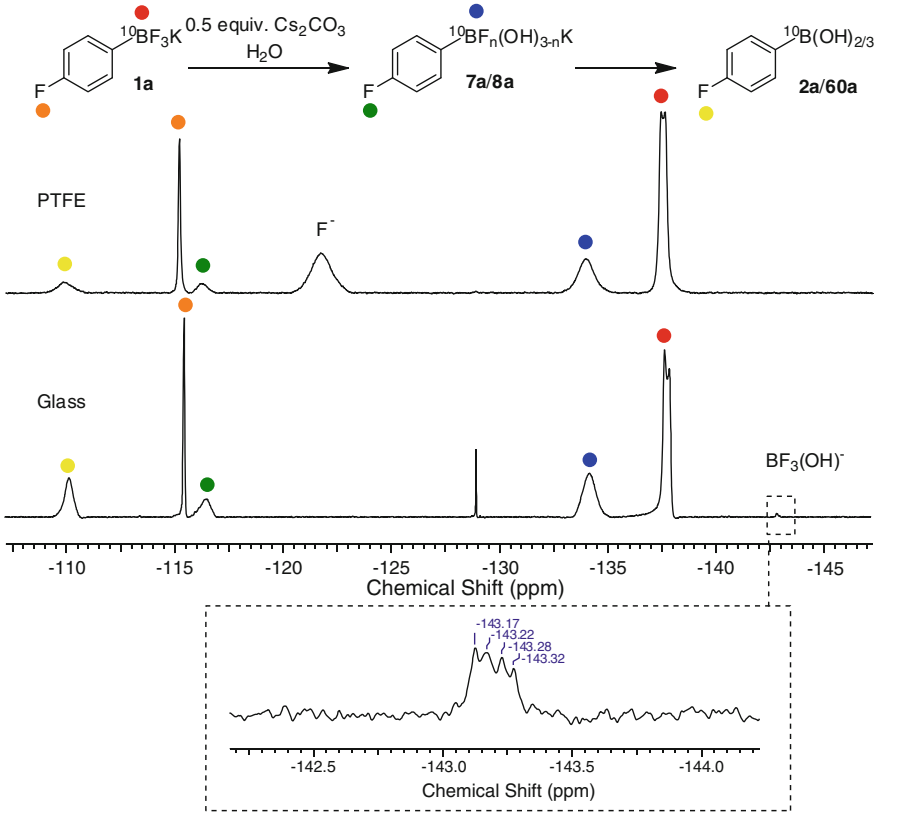

Fig. 6.3 ^{19}F NMR of **1a** with 0.5 equiv. Cs_2CO_3 in THF:water (1:10) conducted in PTFE (*upper spectrum*) and glass (*lower spectrum*). $BF_3(OH)K$ is only observed when conducted in glass, and shows characteristic splitting from natural abundance boron (^{11}B 80 %, spin = 3/2, and ^{10}B 20 %, spin = 3)

6.3.4.3 THF: Water (10:1)

Kinetics of SM coupling in an NMR tube

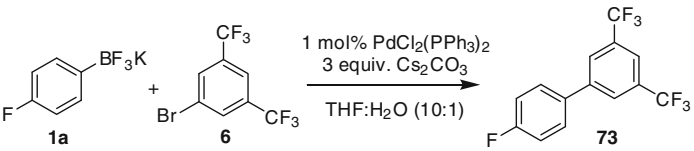

1,3-Bis(trifluoromethyl)-5-bromobenzene (**6**) (1 equiv., 4.4×10^{-5} mol, 12.7 mg) and benzotrifluoride (internal ^{19}F NMR standard, 1 drop) were added to a solution of 4-fluorophenyltrifluoroborate (**1a**) (1 equiv., 4.4×10^{-5} mol, 8.9 mg) and cesium carbonate (3 equiv., 1.32×10^{-4} mol, 43 mg) in degassed THF (4.5 mL)/D_2O (0.5 mL) at 0 °C, under an inert atmosphere of dry N_2. To this was added bis(triphenylphosphine)palladium(II) chloride (1 mol %, 4.4×10^{-7} mol, 0.3 mg) in dry, degassed THF (0.5 mL). A sample (0.6 mL) was removed and placed, under inertion, in a 5 mm OD NMR tube at 0 °C, and was sealed with a J. Young valve. The reaction was initiated in the tube by agitating it in a Dewar of water at 55 °C before inserting the NMR tube into the *Varian 500 MHz* NMR probe (preheated to 55 °C). A time delayed array was then used to analyse the reaction by ^{19}F NMR (470 MHz, D_2O), recording spectra every 100 s for the first 1,000 s of reaction, every 200 s for 1,000–2,000 s of reaction and every 600 s for the remainder of the reaction. Each spectrum comprised of 64 pulses taking a total of 93 s; time points were assumed to be that of the median time during the acquisition, Fig. 3.18.

Hydrolysis of 1a to 2a

NMR tube

4-Fluorophenyltrifluoroborate (**1a**) (1 equiv., 4.4×10^{-5} mol, 8.9 mg) was dissolved in degassed THF:D_2O (10:1, 5.5 mL) at 0 °C. A sample (0.6 mL) was removed and placed in an NMR tube. The reaction was initiated in the tube by agitating it in a Dewar of water at 55 °C, before inserting the NMR tube into the *Varian 500 MHz* NMR probe (preheated to 55 °C). A time delayed array was then used to analyse the reaction by ^{19}F NMR (470 MHz, D_2O), recording spectra every 100 s for the first 2,000 s of reaction and every 600 s remaining 4,000 s. Each spectrum comprised of 64 pulses taking a total of 93 s; time points were assumed to be that of the median time during the acquisition, Fig. 3.19.

The above procedure was repeated with the addition of 1,3-Bis(trifluoromethyl)-5-bromobenzene (**6**) (1 equiv., 4.4×10^{-5} mol, 12.7 mg) and Cs_2CO_3 (3 equiv., 1.32×10^{-4} mol, 43 mg) from the start, Table 6.1.

The above procedure was repeated with just the addition of Cs_2CO_3 (3 equiv., 1.32×10^{-4} mol, 43 mg) from the start, Table 6.1.

Table 6.1 First order rate constants for the hydrolysis of **1a** to **2a** in an NMR tube, indicating no significant effects of **6** or [Pd] on hydrolysis rate

Additive	k_{obs}/s^{-1}
None	9.8×10^{-4}
6 + Cs_2CO_3[a]	7.2×10^{-4}
Cs_2CO_3[a]	7.6×10^{-4}
$[Pd(PPh_3)_2Cl_2]$	9.4×10^{-4}

[a] First order decay proceeded after an induction period (200–300 s)

The above procedure was repeated with the addition of bis(triphenylphosphine)palladium(II) chloride (1 mol %, 4.4×10^{-7} mol, 0.3 mg) from the start, Table 6.1.

Schlenk tube

4-Fluorophenyltrifluoroborate (**1a**) (1 equiv., 4.4×10^{-5} mol, 8.9 mg) was added to a stirring solution of degassed THF:D_2O (10:1, 5.5 mL) at 55 °C in a 15 mm wide Schlenk tube. Samples were removed at regular time intervals and placed into pre-cooled (0 °C) NMR tubes before being analysed by ^{19}F NMR, where they were subjected to 128 scans at 25 °C, Fig. 3.19.

PTFE tube

4-Fluorophenyltrifluoroborate (**1a**) (1 equiv., 4.4×10^{-5} mol, 8.9 mg) was added to a stirring solution of degassed THF:D_2O (10:1, 5.5 mL) at 55 °C in a PTFE beaker. The reaction mixture was transferred to a Pyrex beaker after 4,200 s of reaction. Samples were removed at regular time intervals and placed into pre-cooled (0 °C) NMR tubes before being analysed by ^{19}F NMR, where they were subjected to 128 scans at 25 °C, Fig. 6.4.

Preparation of [$^2H_4$]-2a

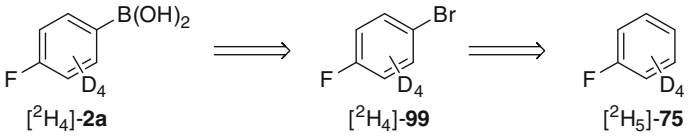

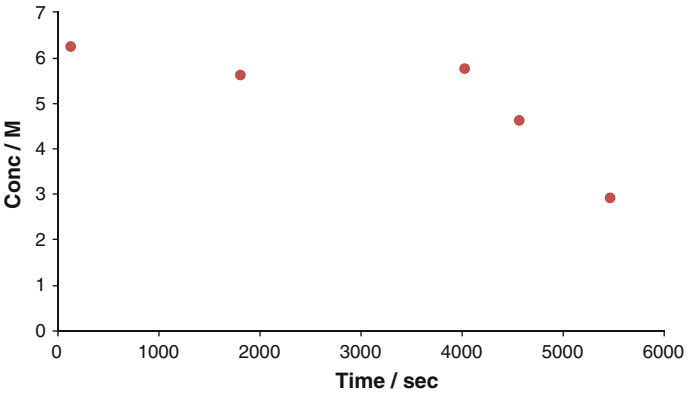

Fig. 6.4 Concentration of **1a** vs. time. No hydrolysis of **1a** to **2a** occurred in a PTFE beaker (0–4,200 s), followed by transfer to a Pyrex beaker (4,200–5,500 s) which effected the transformation

[$^2H_4$]-4-bromofluorobenzene [24]

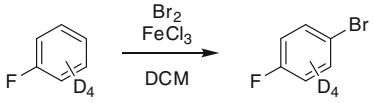

[$^2H_5$]-**75** [$^2H_4$]-**99**

To a condenser fitted round bottomed flask, a solution of bromine (1.07 equiv., 4.8×10^{-2} mol, 7.76 g) in dry DCM (8 mL) was added drop-wise, over a period of 20 min, to a mixture of anhydrous iron(III) chloride (18.5 mol %, 8.23×10^{-4} mol, 134 mg) and [$^2H_5$]-fluorobenzene ([$^2H_5$]-**75**) (1 equiv., 4.45×10^{-2} mol, 4.5 g) in dry DCM (8 mL) at 18 °C. The resultant mixture was stirred for a further 90 min at room temperature. It was then washed with water (3 × 12 mL), sodium thiosulphate$_{(aq)}$ (7 mL of 0.72 M) and again with water (1 × 12 mL). The organics were dried over Na_2SO_4, filtered and evaporated before purification by atmospheric distillation (165 °C), giving the title compound as a clear colourless oil (3.4×10^{-2} mol, 6.04 g, 75 %). **^{19}F NMR** (283 MHz, $CDCl_3$): $\delta = 115.72$ (s, 1F); **^{13}C NMR** (100 MHz, $CDCl_3$): 161.89 (d, $^1J_{C–F} = 246.9$ Hz), 132.58 (td, $^1J_{C–D} = 25.9$ Hz, $^3J_{C–F} = 8.02$ Hz), 117.14 (td, $^1J_{C–D} = 25.9$ Hz, $^2J_{C–F} = 23.08$ Hz), 116.38 (s); **^{2}D NMR** (76.7 MHz, CH_2Cl_2): $\delta = 7.52$ (s, 2D), 7.04 (s, 2D); **MS(CI)** *m/z* (%): 178.0 (50), 179.1 (100), 180.0 (52), 181.1 (95), 182.1 (5).

^{19}F and ^{13}C NMR shifts are consistent with those based on the unlabelled compound [25].

[$^2H_4$]-4-fluorophenylboronic acid [26]

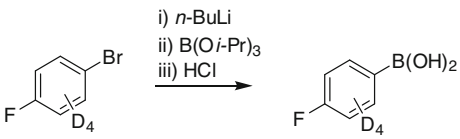

[$^2H_4$]-**99** [$^2H_4$]-**2a**

[$^2H_5$]-4-bromofluorobenzene ([$^2H_4$]-**99**) (1 equiv., 1.0×10^{-2} mol, 1.79 g) was dissolved in a mixture of dry toluene (16 mL) and dry THF (4 mL) under a N_2 atmosphere and cooled to −78 °C. *n*-Butyllithium (1.2 equiv., 1.2×10^{-2} mol, 4.87 mL of 2.46 M solution) was added drop-wise to the stirring solution over a period of 30 min. The reaction mixture was stirred at −78 °C for a further 60 min, triisopropylborate (1.2 equiv., 1.2×10^{-2} mol, 2.28 g) was then added, before being allowed to warm to −20 °C, at which point HCl (12 mL of 2 M solution) was added. The reaction was allowed to reach room temperature and the layers were separated. The organics were washed with water (2 × 15 mL) and the

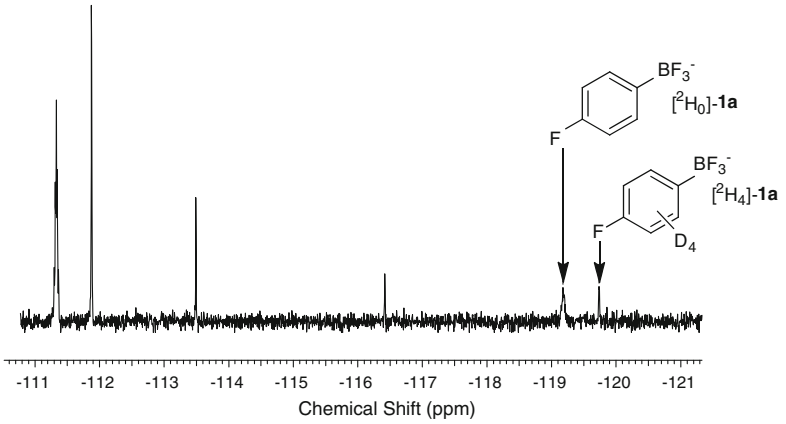

Fig. 6.5 ^{19}F NMR of the SM coupling of [^{2}H$_4$]-**2a** and [^{2}H$_0$]-**1a** with **6**, showing the generation of [^{2}H$_4$]-**1a** from [^{2}H$_4$]-**2a**

aqueous layer extracted with ethyl acetate (2 × 15 mL). The organics were combined, dried over Na_2SO_4, filtered and evaporated leaving the title compound as a white solid (9.7×10^{-2} mol, 1.4 g, 97 %). **^{19}F NMR** (283 MHz, $CDCl_3$): $\delta = 111.72$ (s, 1F); **^{2}D NMR** (77 MHz, CH_2Cl_2): $\delta = 8.3$ (s, 2D), 7.62 (s, 2D); **^{11}B NMR** (96 Hz, d_6-DMSO): 28.03 (s, 1B).

^{19}F and ^{11}B NMR shifts are consistent with those based on the unlabelled compound [27].

Exchange between 1a and 2a

PTFE vessel

To a solid mixture of [^{2}H$_4$]-**2a** (1 equiv., 4.4×10^{-5} mol, 6.3 mg) and [^{2}H$_0$]-**1a** (1 equiv., 4.4×10^{-5} mol, 8.9 mg) was added THF:water (10:1, 5.5 mL) and stirred at 55 °C for 10 min. A sample was removed from the reaction, both at the start, and at the end of heating, and placed in a PTFE lined NMR tube at 0 °C before being analysed by ^{19}F NMR, Fig. 3.20.

SM coupling between [^{2}H$_4$]-**2a** and [^{2}H$_0$]-**1a** with **6**

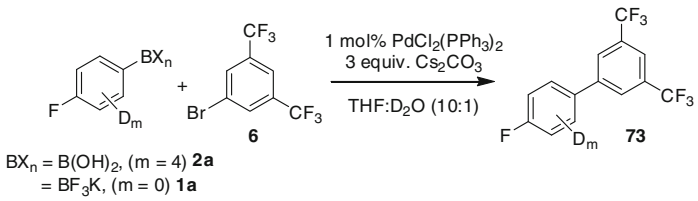

Bis(triphenylphosphine)palladium(II) chloride (1 mol %, 4.4×10^{-7} mol, 0.3 mg) and **6** (1 equiv., 4.4×10^{-5} mol, 12.7 mg) were added to a Schlenk tube containing a solution of [$^2H_0$]-**2a** (1 equiv., 4.4×10^{-5} mol, 8.9 mg), [$^2H_0$]-**1a** (1 equiv., 4.4×10^{-5} mol, 6.2 mg) and cesium carbonate (1.32×10^{-4} mol, 43 mg) in degassed THF:D_2O (10:1, 5.5 mL) under an inert atmosphere of dry N_2, and was stirred at 55 °C. A sample was removed after 30 min and analysed by ^{19}F NMR, Fig. 6.5.

Boronic acid/trifluoroborate competition

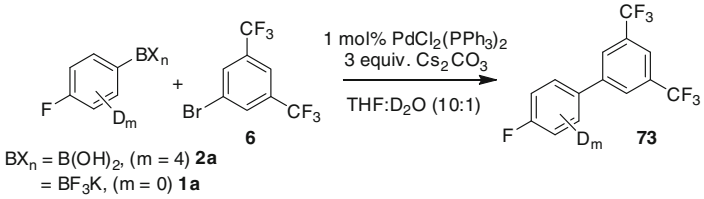

Five reactions were conducted employing five different ratios of [$^2H_0$]-**1a**:[$^2H_4$]-**2a** (90:10, 70:30, 50:50, 30:70, 10:90; 6.6×10^{-5} mol overall) in separate Schlenk tubes.

Bis(triphenylphosphine)palladium(II) chloride (1 mol %, 6.6×10^{-7} mol, 0.45 mg) in dry degassed THF (0.5 mL) was added to a Schlenk tube containing a solution of **6** (1 equiv., 6.6×10^{-5} mol, 19.1 mg), cesium carbonate (3 equiv., 1.32×10^{-4} mol, 43 mg) and a mixture of [$^2H_0$]-**1a**:[$^2H_4$]-**2a** (1 equiv. overall, 6.6×10^{-5} mol) in degassed THF (7.5 mL) and D_2O (0.75 mL) under an inert atmosphere of dry N_2. The reaction was stirred at 55 °C whilst samples (0.6 mL) were removed at regular time intervals with a gas tight syringe and kept at 0 °C before analysis by ^{19}F NMR at 25 °C, Fig. 3.22.

The same set of experiments were undertaken in an NMR tube with *in situ* ^{19}F NMR analysis directly in the *Varian 500 MHz* probe (55 °C), Fig. 3.23. Reactions were conducted employing the procedure outlined in "Kinetics of SM coupling in an NMR tube", *vide supra*.

6.3.5 Side Product Study

6.3.5.1 Precatalyst Activation (*I*)

4,4′-difluorobiphenyl (9) generation

The "General conditions for the kinetics of SM coupling in a Schlenk tube", Sect. 6.3.2.1, *vide supra*, were followed; separately employing **1a** and **2a**, Fig. 3.24.

The "Kinetics of SM coupling in an NMR tube" Sect. 6.3.4.3 *vide supra*, were followed, separately employing **1a** and **2a**, Fig. 3.25. In attempts to detect **9**, the procedure was repeated with increasing catalyst loadings in the SM coupling of **1a**, however **9** was not detected in any cases.

Partitioning of mechanisms

To test the point at which the fluoride catalysed hydrolytic reduction of palladium (II) was out-competed by the double transmetalation/reductive elimination, the first sample from each of the [$^2H_0$]-**1a**/[$^2H_4$]-**2a** ratios (90:10, 70:30, 50:50, 30:70, 10:90) from the "Boronic acid/trifluoroborate competition" Sect. 6.3.4.3, *vide supra*, was kept under inertion at 0 °C before ^{19}F NMR analysis. Homocoupled product **9** was only observed in ratios of 50:50, 30:70, 10:90 ([$^2H_0$]-**1a**:[$^2H_4$]-**2a**).

[^{18}O]-H_2O experiments

Isolated triphenylphosphine oxide

Parallel reactions of the SM coupling of **1a** and **2a** with **6** were assembled under the "General conditions for the kinetics of SM coupling in a Schlenk tube", Sect. 6.3.2.1 *vide supra*, except that water was replaced with $H_2^{18}O$ (70 % ^{18}O). Without removing samples the reaction stirred at 55 °C for 60 min, before isolation of triphenylphosphine oxide. The THF was evaporated under a stream of N_2 and the residue dissolved in ethyl acetate (4 mL), washed with water (4 mL) and evaporated under a stream of N_2. The residue was triturated with hexanes (4 mL) and then taken up in ethyl acetate (1 mL) and analysed by MS (CI) and ^{31}P {^{1}H} NMR, Fig. 3.26.

In situ ^{31}P NMR analysis

The coupling between **1a** and **6** was conducted under the "Kinetics of SM coupling in an NMR tube" Sect. 6.3.4.3 *vide supra*, but replacing water with $H_2^{18}O$ (70 % ^{18}O). Tri(*p*-tolyl)phosphine oxide (1 mol %, 4.4×10^{-7} mol, 1.4×10^{-4} g) was added as an internal integration and chemical shift standard. ^{31}P {^{1}H} NMR (202 MHz) analysis was conducted immediately, at 55 °C, acquiring a total of 30,000 scans, Fig. 3.27.

Heterogeneous mercury droplet test

Parallel reactions of the SM coupling of **1a** and **2a** with **6** were assembled under the "General conditions for the kinetics of SM coupling in a Schlenk tube", Sect. 6.3.2.1 *vide supra*. After 600 s at 55 °C, one drop of mercury was added to the reaction whilst sampling into NMR tubes continued, Fig. 6.6 (**1a** + **6**) and Fig. 6.7 (**2a** + **6**).

Uncatalysed hydrolytic reduction of palladium (II)

See "Slow syringe pump addition", Sect. 6.3.5.3 *vide infra*, for the observation of no **9** generation during the initial stages of reaction, whilst cross-coupling proceeds.

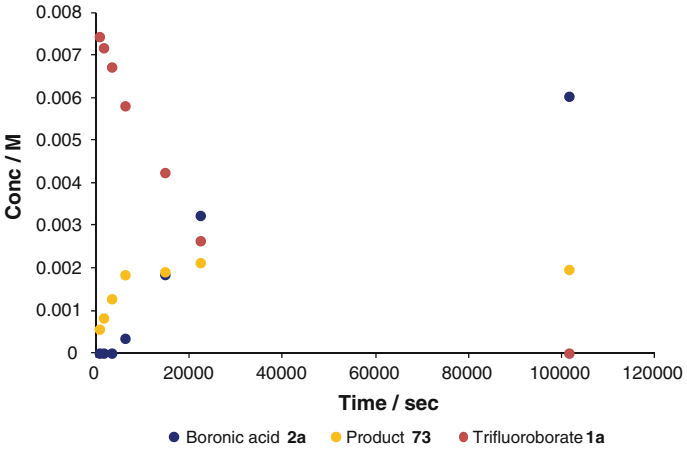

Fig. 6.6 SM coupling of **1a** with **6**, where one drop of mercury has been added after 6,000 s. Hydrolysis proceeds, even though catalytic turnover has been attenuated

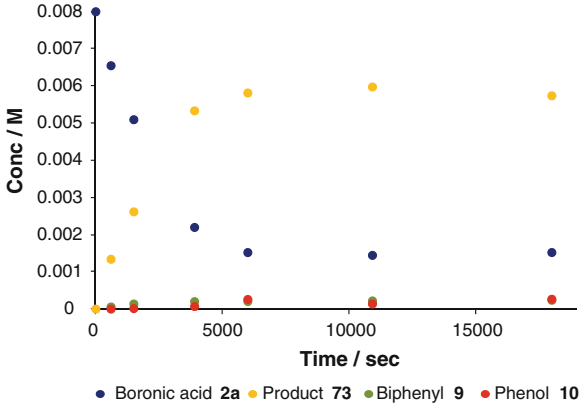

Fig. 6.7 SM coupling of **2a** with **6**, where one drop of mercury has been added after 6,000 s

6.3.5.2 THF Hydroperoxide (*II*)

Generation of "Oxidising THF"

"Oxidising THF" (THF solutions of 2-hydroperoxytetrahydrofuran (**78**), ca. 1–14 mM) was generated by bubbling air into a Strauss flask of pre-distilled (sodium/benzophenone ketyl) THF (30 mL) for 2 h, then left over night open to the atmosphere under light.

Table 6.2 Series of additives tested to elucidate the quenching observed of a THF derived oxidant from **1a**.[a]

Entry	1st period additive	1st period	2nd period additive	2nd period	Oxidation of 2[a]/% [b] (%)
1	Nothing	55 °C (75 min)	[$^2H_4$]-**2a**	55 °C (60 min)	85
2	Cs_2CO_3	25 °C (75 min)	[$^2H_4$]-**2a**	55 °C (60 min)	69
3	Cs_2CO_3	55 °C (75 min)	[$^2H_4$]-**2a**	55 °C (60 min)	77
4	Nothing	55 °C (75 min)	[$^2H_4$]-**2a**, Cs_2CO_3	55 °C (60 min)	87
5	TBAF + Cs_2CO_3	55 °C (60 min)	[$^2H_4$]-**2a**	55 °C (60 min)	97
6	KF + Cs_2CO_3	55 °C (60 min)	[$^2H_4$]-**2a**	55 °C (60 min)	88
7	**1a** + Cs_2CO_3	55 °C (25 min)	[$^2H_4$]-**2a**	55 °C (60 min)	21
8	**1a** + Cs_2CO_3	55 °C (50 min)	[$^2H_4$]-**2a**	55 °C (60 min)	30
9	**1a** + Cs_2CO_3	55 °C (75 min)	[$^2H_4$]-**2a**	55 °C (60 min)	36
10	BF_3.OEt	55 °C (75 min)	[$^2H_4$]-**2a**	55 °C (60 min)	15
11	$B(OH)_3$	55 °C (75 min)	[$^2H_4$]-**2a**	55 °C (60 min)	20

[a] Precise level of **2a** oxidation should not be interpreted too literally due to the large errors associated with the uncertainties of oxidant concentration. Instead, the general trends should be noted

[b] normalised mol % of 4-fluorophenol (**10**) by ^{19}F NMR

Oxidation of 2a and the quenching effect of various additives

Reactions were conducted in two periods:

1st Period: to a solution of "oxidising THF" (0.7 mL) and degassed water (0.07 mL) was added an additive (cesium carbonate (3 equiv., 1.85×10^{-6} mol, 6.0 mg); TBAF (3 equiv., 1.85×10^{-6} mol, 0.018 mL 1 M solution in THF); KF (3 equiv., 1.85×10^{-6} mol, 1.0 mg); BF_3.OEt (1 equiv., 6.16×10^{-6} mol, 0.9 mg); $B(OH)_3$ (1 equiv., 6.16×10^{-6} mol, 0.1 mg) or **1a** (1 equiv., 6.16×10^{-6} mol, 1.2 mg)), and was stirred at 55 °C or room temperature.

2nd Period: [$^2H_4$]-**2a** (1 equiv., 6.16×10^{-6} mol, 0.88 mg) was added and then heated for 60 min. A sample was removed from the reaction and analysed by ^{19}F NMR, Table 6.2.

6.3.5.3 Oxidative Homocoupling (*3.*)

SM couplings in air

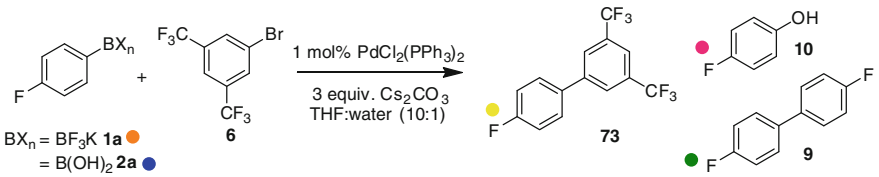

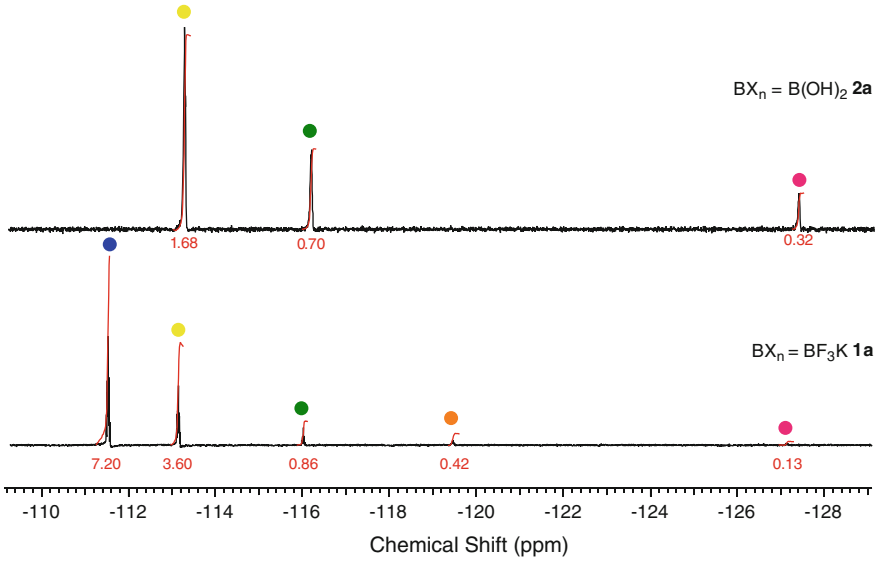

Fig. 6.8 ^{19}F NMR of the SM coupling of **2a** (*upper spectrum*) with **6** and **1a** (*lower spectrum*) with **6** after 6 h at 55 °C. **73/9 + 10** = 1.65 when starting from **2a** and 3.64 when starting from **1a**. Note the slower SM coupling employing **1a** has not reached completion, due to aerobic catalyst degradation. Build up of the hydrolysis product **2a** therefore occurs

Parallel reactions of the SM coupling of **1a** and **2a** with **6** were assembled under the "General conditions for the kinetics of SM coupling in a Schlenk tube", Sect. 6.3.2.1 *vide supra*, with the head space gas left open to air, Fig. 6.8.

Tested differences between 1a and 2a

Base concentration

Eight parallel SM couplings between **2a** with **6** were assembled under the "General conditions for the kinetics of SM coupling in a Schlenk tube", Sect. 6.3.2.1 *vide supra*, each containing a different concentration of Cs_2CO_3 (0.1 equiv., 0.5 equiv., 1 equiv., 1.5 equiv., 2 equiv., 2.5 equiv., 3 equiv., 4 equiv., of 8 mM **2a**) and the head space gas was left open to air. The reaction was not sampled throughout, but left stirring until complete conversion of **6** (6 h) at 55 °C, before a sample (0.6 mL) was removed and analysed by ^{19}F NMR, Fig. 6.9.

Glass surface

An SM coupling between **2a** and **6** was assembled under the "General conditions for the kinetics of SM coupling in a Schlenk tube", Sect. 6.3.2.1 *vide supra*, in a Schlenk tube which had previously been used, and not cleaned, for a SM coupling of **1a** with **6**. The head space gas was left open to air and the reaction was not sampled throughout, but left stirring for 6 h at 55 °C before a sample (0.6 mL) was removed and analysed by ^{19}F NMR, Fig. 6.10.

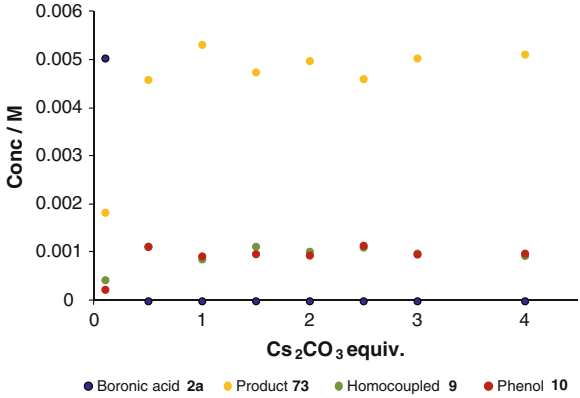

Fig. 6.9 Concentration of each species at reaction completion (0.1 equiv. Cs_2CO_3 did not reach completion), demonstrating the level of side product generation (**9** + **10**) to be not dependent on the Cs_2CO_3 concentration

Hydrolysis salts

1a (1 equiv., 6.6×10^{-5} mol, 13.3 mg) was added to a solution of Cs_2CO_3 (3 equiv., 1.32×10^{-4} mol, 43 mg) in degassed THF:water (10:1, 8.25 mL) and stirred at 55 °C for 6 h during which time **1a** hydrolysed to **2a**. Bis(triphenylphosphine)palladium(II) chloride (1 mol %, 6.6×10^{-7} mol, 0.45 mg), and **6** (1 equiv., 6.6×10^{-5} mol, 19.1 mg) were added, and the reaction stirred at 55 °C for a further 4 h with the head space gas left open to the air. A sample was removed upon reaction completion and analysed by ^{19}F NMR, Fig. 6.11.

Effect of phenol

An SM coupling between **2a** and **6** was assembled under the "General conditions for the kinetics of SM coupling in a Schlenk tube", Sect. 6.3.2.1 *vide supra*, with the addition of 4-fluorophenol (**10**) (1 equiv., 4.4×10^{-5} mol, 1.0 mg), and with the head space gas left open to the air. The reaction was not sampled throughout, but left stirring until complete conversion of **6** (6 h) at 55 °C before a sample (0.6 mL) was removed and analysed by ^{19}F NMR.

Ratio of **73/9** + **10** without phenol = 1.82
Ratio of **73/9** + **10** with phenol = 1.79

The dependence of the level of oxidative side products on the concentration of ArBr 6

Eleven reactions were assembled in open carrousel vessels.

2a (4.4×10^{-5} mol, 6.16×10^{-3} g) and cesium carbonate (1.32×10^{-4} mol, 4.3×10^{-2} g) were dissolved in degassed THF (4.5 mL)/H_2O (0.5 mL). To this was added 1,3-Bis(trifluoromethyl)-5-bromobenzene (**6**) (0, 0.002, 0.004, 0.006,

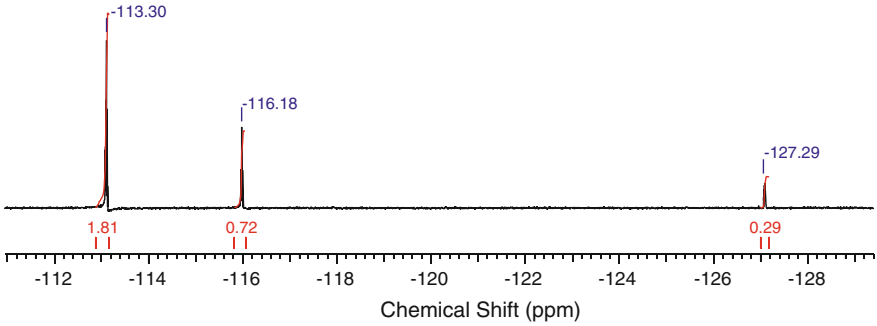

Fig. 6.10 ^{19}F NMR spectrum of the SM coupling of **2a** with **6** in a Schlenk tube that had previously been used and not cleaned from a SM coupling of **1a** with **6**, generating a ratio of **73/9 + 10** = 1.8. ($\delta_{73} = -113.30$ ppm, $\delta_{9} = -116.18$ ppm, $\delta_{10} = -127.29$ ppm)

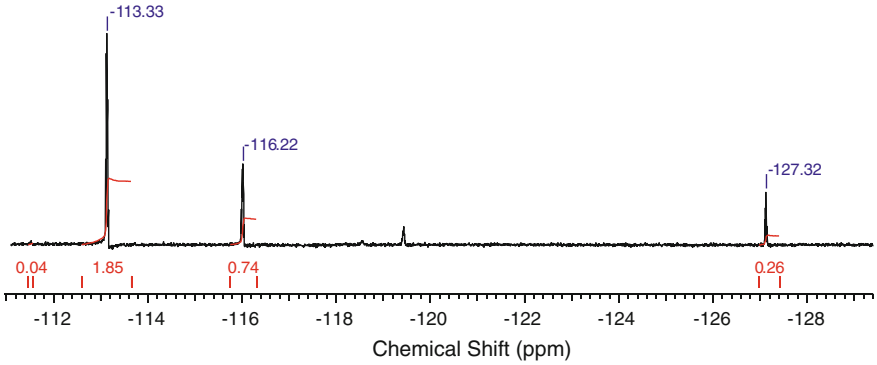

Fig. 6.11 ^{19}F NMR of the SM coupling of **1a** in air, having been allowed to completely hydrolyse to **2a** prior to the addition of **6** and the catalyst precursor, generating a ratio of **73/9 + 10** = 1.85 ($\delta_{73} = -113.33$ ppm, $\delta_{9} = -116.22$ ppm, $\delta_{10} = -127.32$ ppm)

0.008, 0.016, 0.024, 0.032, 0.04, 0.06, 0.08 M), benzotrifluoride (2 drops) and bis(triphenylphosphine)palladium(II) chloride (1 mol %, 0.5 mL of 0.86 M sol^{n} in dry THF) with stirring at 55 °C. The reactions were left to go to complete conversion (6 h) before ^{19}F NMR was used to analyse the samples, Fig. 3.28.

The dependence of the level of oxidative side-products on the concentration of 2a

Nine reactions were assembled in open carrousel vessels.

2a and cesium carbonate (3 equiv., 1.32×10^{-4} mol, 43 mg) were dissolved in degassed THF (4.5 mL)/H_2O (0.5 mL). Two concentrations of 1,3-bis(trifluoromethyl)-5-bromobenzene (**6**) (1 equiv., 0.008 M and 2 equiv., 0.016 M) were used for the concentration assay of **2a** (0.008, 0.006, 0.004 and 0.002 M for 0.008 M of **6**; and 0.008, 0.0064, 0.0048, 0.0032 M and 0.0016 M for 0.016 M of **6**), which was added with benzotrifluoride (2 drops) and bis(triphenylphosphine)palladium

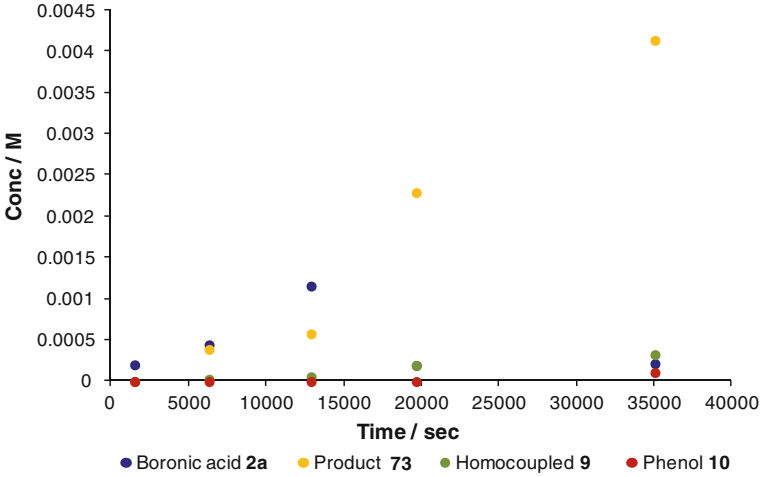

Fig. 6.12 Syringe pump addition of **2a** to an SM coupling with **6** conducted in air, leading to a ratio of **73/9** + **10** of >9.5

(II) chloride (1 mol %, 0.5 mL of 0.86 M sol^{n} in dry THF) to the stirring solution at 55 °C. The reactions were left to go to complete conversion (6 h) before ^{19}F NMR was used to analyse a sample from each reaction, Fig. 3.29.

Slow syringe pump addition

A solution (400 μL) of **2a** (57.8 mM) and cesium carbonate (180 mM) was added via a syringe pump, over a period of 400 min, to a solution of 1,3-bis(trifluoromethyl)-5-bromobenzene (**6**) (6.51×10^{-5} mol, 19 mg), and bis(triphenylphosphine)palladium(II) chloride (1 mol %, 6.4×10^{-7} mol, 0.5 mg) in (initially) degassed THF (7 mL)/water (0.7 mL) (10:1), with stirring, under air. Samples (0.6 mL) were removed and placed immediately into pre-cooled NMR tubes and kept at 0 °C until ^{19}F NMR analysis, Fig. 6.12.

6.4 Experimental: Organotrifluoroborate Hydrolysis

6.4.1 Specific Experimental Details

6.4.1.1 Reagents

Reagents and materials purchased from commercial suppliers were used without further purification unless stated. 1,3-Bis(trifluoromethyl)-5-bromobenzene (**6**), potassium phenylethynyl (**1c**), phenyl (**1d**), vinyl (**1 k**), 3,5-bis(trifluoromethyl)phenyl (**1q**), cyclopropyl (**1x**), 4-methylphenyl (**1z**), 2-furyl (**1ar**), benzyl

(**1au**), 2-naphthyl (**1aw**) and 4-trifluoromethylphenyl (**1ax**) trifluoroborates, [$^2H_5$]-bromobenzene ([$^2H_5$]-**39**), diisopropylethylamine, triethylamine, 3-(*N*-morpholino)propanesulfonic acid (MOPS) and boric acid (99 % ^{10}B) were purchased from *Sigma Aldrich.* Potassium 4-fluorophenyltrifluoroborate (**1a**), benzotrifluoride, 1,8-diazabicycloundec-7-ene (DBU), di-*n*-butylamine, 4-bromobenzonitrile (**92**), potassium 3-nitrophenyltrifluoroborate (**1aa**), copper(I)iodide were purchased from *Alfa Aesar.* Trimethylsilylacetylene (**96**), cesium carbonate, sodium sulphate and potassium carbonate were purchased from *Fisher Scientific.* 4-Fluorophenylboronic acid (**2a**) was purchased from *Maybridge.* Tris(hydroxymethyl)aminomethane (TRIS) was purchased from *Melford.* Bis(triphenylphosphine)palladium(II) chloride [$PdCl_2(PPh_3)_2$] [20], dichloro-[1,1′-bis(diphenylphosphino)ferrocene]palladium(II) [$PdCl_2$(dppf)] [28], potassium cyclobutyltrifluoroborate (**1y**)[8] and [$^2H_4$]-4-fluorophenylboronic acid ([$^2H_4$]-**2a**) (Sect. 6.3.4.3 *vide supra*), were prepared by known methods. Potassium phenylethenyl (**1 l**), 4-methoxyphenyl (**1o**), 1-naphthyl (**1p**) and cyclohexyl (**1w**) trifluoroborates were prepared via the *KF/tartaric acid* route detailed in Chap. 2. Potassium isopropyltrifluoroborate (**1at**) and 1,3-diphenylpropyl (**1av**) were kindly donated by Prof. V. K. Aggarwal and Dr. T. G. Elford (University of Bristol).

6.4.2 Hydrolysis of Potassium 4-Fluorophenyltrifluoroborate

6.4.2.1 Reaction Vessel Dependency

Kinetics

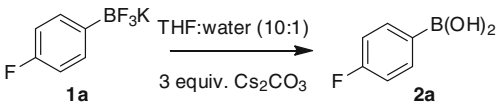

The reaction vessel, (**B**) 50 mL rbf, (**C**) 15 mm wide conical-shaped base Schlenk tube, (**D**, **E**) 15 mL wide hemi-spherical base Schlenk tube, (**F**) 15 mm wide PTFE test tube and (**G**) 15 mm wide PTFE test tube with added glass powder (20 mg grade 3), was charged with potassium 4-fluorophenyltrifluoroborate (**1a**) (1 equiv., 4.36×10^{-5} mol, 8.8 mg), cesium carbonate (3 equiv., 1.3×10^{-4} mol, 43 mg) and an appropriate magnetic stirring bar for the vessel. A preheated (55 °C) solution of THF:water (10:1, 5.5 mL) was added and stirred at 500 rpm (unless otherwise indicated). Samples (ca. 10 over a 2/3 h period) were removed with a plastic syringe and placed immediately in PTFE lined NMR tubes, pre-cooled to 0 °C. The samples were kept at that temperature until they were placed directly into the *Eclipse 300* NMR probe. Each sample was analysed by ^{19}F NMR and subject to 128 pulses (4 min 17 s) at 25 °C, Fig. 4.4 and 4.5.

This procedure was repeated in a standard (**A**) 5 mm OD NMR tube on 0.1 times the scale. Rather than removing samples, the reaction mixture was briefly

Table 6.3 Induction periods and half-lives for the hydrolysis of **1a** to **2a** in various reaction vessels

Entry	Vessel type	Induction period/min	$t_{1/2}$/min
A	5 mm NMR tube	5	15
B	50 mL round bottomed flask	15	269
C	15 mm Schlenk tube with conical base	0	10
D	15 mm Schlenk tube with hemispherical base[a]	25	104
E	15 mm Schlenk tube with hemispherical base	105	263
F	15 mm PTFE tube	15	200
G	15 mm PTFE tube with added glass powder	0	209

[a] Stirred at 100 rpm

shaken, then immediately placed into the *Varian 500* probe which was preheated to 55 °C. The reaction was monitored by ^{19}F NMR using a time delayed array to separate the acquisitions. These acquisitions were every 300 s for the first 1.5 h of reaction then every 900 s for the remaining hour, Table 6.3, Figs. 4.4 and 4.5.

6.4.2.2 The Effect of Glass

Addition of glass powder to pre-equilibrated system

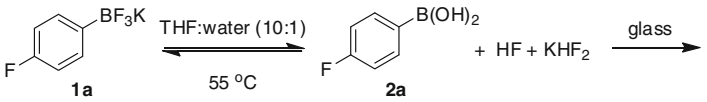

Potassium 4-fluorophenyltrifluoroborate (**1a**) (4.4×10^{-5} mol, 8.8 mg) was heated at 55 °C in a stirring solution of THF:water (10:1, 5.5 mL) in a PTFE lined test tube. After 280 min, glass powder (20 mg grade 3) was added. Samples (0.5 mL) were removed throughout the reaction with a plastic syringe and placed immediately in pre-cooled (0 °C) PTFE lined NMR tubes. The samples were kept at that temperature until they were placed directly into the *Eclipse 300* NMR probe. Each sample was analysed by ^{19}F NMR and subject to 128 pulses (4 min 17 s) at 25 °C, Fig. 4.6.

Effect of glass surface area on hydrolysis rate

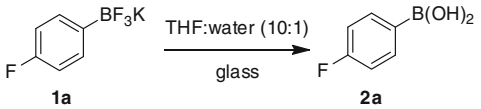

Two sets of experiments were performed (by Paul Cogswell (PC) and Nina Ursinyova (NU), University of Bristol) where either the mass of glass powder was

Table 6.4 Pseudo first-order rate constants and half-lives for the hydrolysis of **1a** to **2a** with different amounts of glass powder added

Mass of glass/mg[a]	k_{obs}^{glass}/s^{-1}	$t_{1/2}$/min
0	2.17×10^{-4}	53
10	5.62×10^{-4}	21
20	5.94×10^{-4}	19
50	1.23×10^{-3}	9
75	1.62×10^{-3}	7
100	1.99×10^{-3}	6

[a] Reactions performed in a glass Schlenk tube

Table 6.5 Pseudo first-order rate constants and half-lives for the hydrolysis of **1a** to **2a** with different grades of glass powder added

Grade of glass[a]	k_{obs}^{glass}/s^{-1}	$t_{1/2}$/min
1	9.00×10^{-5}	128
2	2.80×10^{-4}	41
3	4.20×10^{-4}	28
3[b]	8.00×10^{-4}	14

[a] Reactions performed in a 15 mm PTFE tube
[b] Reaction performed in a 15 mm Schlenk tube

varied in a Schlenk tube (PC) or the grade of glass powder was varied in a PTFE vessel (NU).

Glass powder (0.0 g, 1.0×10^{-2} g, 2.0×10^{-2} g, 5.0×10^{-2} g, 7.5×10^{-2} g, 1.0×10^{-1} g/Grades 1, 2 and 3 – 2.00×10^{-2} g) was added to a Schlenk tube (PC) or a PTFE test tube (NU) loaded with a stirrer bar and sealed with a rubber septum under a N_2 atmosphere. Degassed THF:H_2O (10:1, 8.25 mL) was then added and the test tube was placed into a preheated oil bath at 55 °C. After 10 min of stirring, potassium 4-fluorophenyltrifluoroborate (**1a**) (6.6×10^{-5} mol, 1.33×10^{-2} g) was added and samples (0.3 mL) were removed into pre-cooled (0 °C) PTFE lined NMR tubes at regular time intervals using a plastic syringe. These were stored at 0 °C prior to ^{19}F NMR analysis where they were subject to a maximum of 5 min at room temperature. Spectra were acquired by accumulating 128 scans at 25 °C, Fig. 4.7, Tables 6.4 and 6.5.

6.4.2.3 Equilibrium Studies

Rate measurement of approach to equilibration from 1a

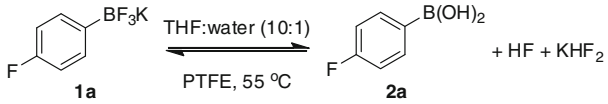

Potassium 4-fluorophenyltrifluoroborate (**1a**) (1 equiv., 4.36×10^{-6} mol, 0.88 mg) was added as a solid to a PTFE lined NMR tube. To this was added

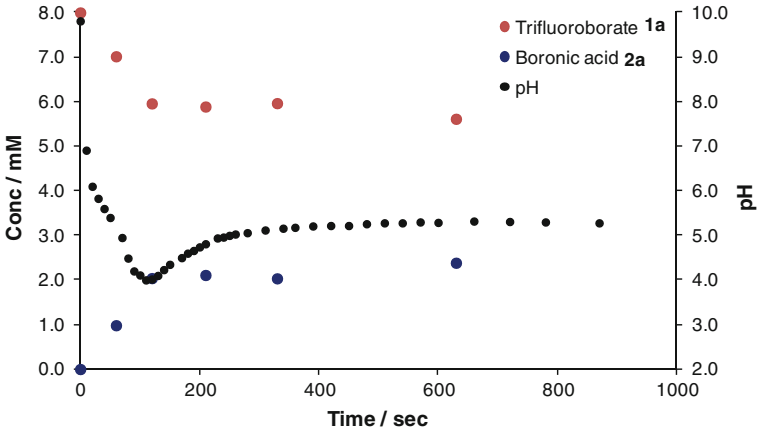

Fig. 6.13 Concentration and pH vs. time for the approach to equilibrium between **1a** and **2a**

firstly dry THF (0.5 mL) and lastly D_2O (0.05 mL) before being briefly shaken and placed immediately into the preheated (55 °C) *Varian 500* NMR probe. The reaction was monitored by ^{19}F NMR using a time delayed array to separate the acquisitions. Each acquisition was 64 scans (93 s) long with a time delay between separate acquisitions of 0 s. To ensure high accuracy, this experiment was repeated a further two times, inset Fig. 4.6 and Scheme 4.11.

pH monitoring

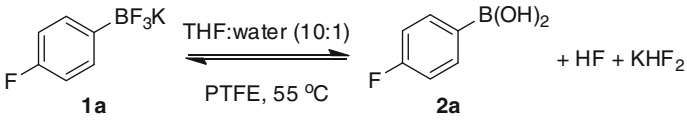

A pre-heated (55 °C) solution of THF:water (10:1, 6.6 mL) was added to a solid mixture of potassium 4-fluorophenyltrifluoroborate (**1a**) (1 equiv., 5.28×10^{-5} mol, 10.6 mg) and Cs_2CO_3 (3 equiv., 1.58×10^{-4} mol, 51.6 mg) in a 15 mm diameter PTFE lined test tube. This stirring (100 rpm) solution was heated at 55 °C and the pH was read from an uncalibrated Hanna HI 98103 pH probe every 10 s for the first 10 min and every 30 s for the following 2 h. Samples (0.3 mL) were removed throughout the reaction using a plastic syringe and placed in pre-cooled (0 °C) PTFE lined NMR tubes. The samples were kept at that temperature until they were placed directly into the *Eclipse 300* NMR probe. Each sample was analysed by ^{19}F NMR and subject to 128 pulses (4 min 17 s) at 25 °C, Fig. 6.13.

Effect of initial 1a concentration on 1a/2a equilibrium position

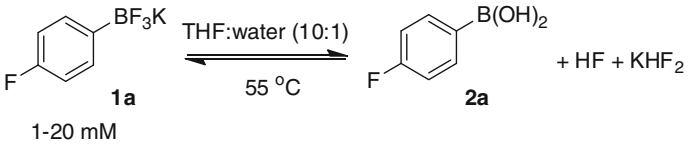

Potassium 4-fluorophenyltrifluoroborate (**1a**) (5.5×10^{-7}, 2.75×10^{-6}, 4.4×10^{-6}, 8.25×10^{-6} and 1.1×10^{-5} mol) was added as a stock solution in dry THF (0.5 mL) to a PTFE lined NMR tube. To this was added D_2O (0.05 mL), bringing the total THF:water ratio to 10:1, the volume to 0.55 mL and the concentration of **1a** to 1, 5, 8, 10, 15 and 20 mM respectively. The tube was briefly shaken and placed immediately into the preheated (55 °C) *Varian 500* NMR probe. Each sample was given 15 min of heating before being analysed by ^{19}F NMR (2,000–200 scans depending on the concentration, 55 °C), Fig. 4.8 and Table 6.6.

Table 6.6 Concentration of **2a** and **1a** at equilibrium (55 °C) at various initial **1a** concentrations

$[Ar–B]_{TOT}$/mM	[2a]/mM[a]	[1a]/mM[a]	[2a]/[1a]
1	0.73	0.27	0.37
5	1.51	3.49	2.31
8	1.97	6.07	3.08
10	2.30	7.70	3.36
15	2.34	12.66	5.41
20	2.60	17.40	6.68

[a] Peak integrations from ^{19}F NMR

Effect of water concentration on 1a/2a equilibrium position

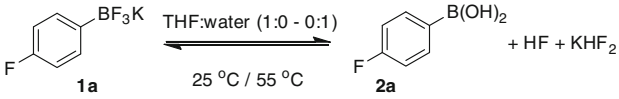

Potassium 4-fluorophenyltrifluoroborate (**1a**) (3.9×10^{-6} mol, 0.8 mg) was added to a PTFE lined NMR tube in THF:water (20:1, 10:1, 7:1, 3:1, 1.66:1, 1:1, 1:1.66, 1:3, 1:7, 0:1) (0.5 mL). The tube was heated at 55 °C in a water bath for 20 min before being placed into a preheated (55 °C) *Eclipse 300* NMR probe where it was analysed by ^{19}F NMR (200 scans, 55 °C).

This procedure was repeated at 25 °C. The samples were allowed to equilibrate for one hour at 25 °C before being analysed by ^{19}F NMR (200 scans, 25 °C), Fig. 4.9 and Table 6.7.

Table 6.7 Concentration of **2a** at equilibrium at various water concentrations, tested at 25 and 55 °C

$[H_2O]$	$[2a]^{25\ °C}$/mM[a]	$[2a]^{55\ °C}$/mM[a]
0.55	0.24	0.00
1.38	0.62	0.78
2.61	0.86	1.36
4.99	1.41	1.85
6.88	1.58	2.16
13.75	2.16	2.78
20.63	2.34	3.37
27.50	2.26	3.73
34.38	2.33	2.96
41.25	2.33	2.68
48.13	1.92	2.36
55.00	1.87	1.37

[a] Peak integrations from ^{19}F NMR

Van't Hoff analysis

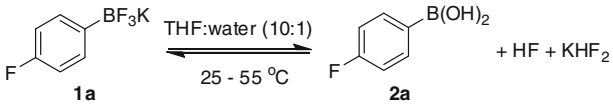

Potassium 4-fluorophenyltrifluoroborate (**1a**) (1 equiv., 3.20×10^{-6} mol, 0.64 mg) in dry THF (0.4 mL) was added to a PTFE lined NMR tube containing D_2O (0.04 mL), bringing the total ratio to 10:1, the volume to 0.44 mL and the concentration of **1a** to 8 mM. The tube was immediately placed into the *Varian 500* probe at 25 °C. It was analysed (^{19}F NMR) at four different temperatures (25, 35, 45 and 55 °C). The reaction was subjected to 15 min equilibration time at each temperature before the acquisition (120 scans) began. Measurements were performed twice at each temperature and equilibrium analysed as follows $K_{app} = [\mathbf{2a}][HF][KHF_2]/[\mathbf{1a}][H_2O]^2 = [\mathbf{2a}]^3/25*[\mathbf{1a}]$, Fig. 4.10. *However, it must be emphasised that this analysis is highly dependent on the accuracy of the initial concentrations (**1a** and H_2O) and should be interpreted accordingly.*

6.4.2.4 B–F Versus B–C Bond Cleavage

Degenerate exchange between 1a and 2a

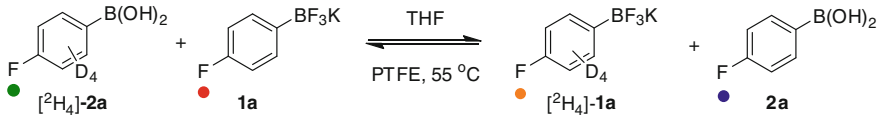

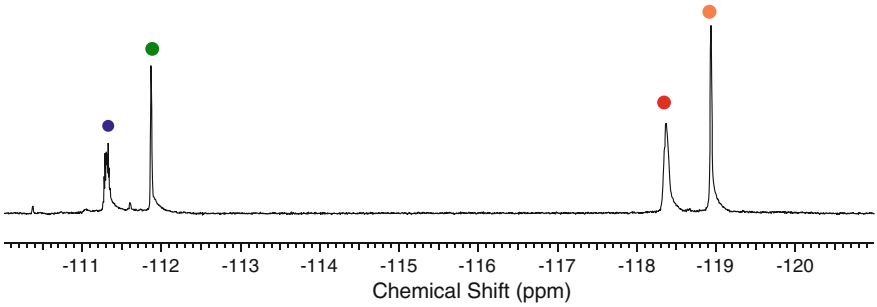

Fig. 6.14 ^{19}F NMR of the degenerate exchange between [$^{2}H_4$]-**2a** and [$^{2}H_0$]-**1a** in anhydrous THF

1a (1 equiv., 2.2 × 10^{-5} mol, 4.4 mg) and [$^{2}H_4$]-**2a** (1 equiv., 2.2 × 10^{-5} mol, 3.16 mg) were added as solids to dry THF (5 mL) in a PTFE lined test tube. The solution was heated at 55 °C for two hours under an atmosphere of dry N_2. A sample was removed with a plastic syringe and placed immediately into a PTFE lined NMR tube, which was analysed by ^{19}F NMR (128 scans, 25 °C), Fig. 6.14.

Synthesis of [^{10}B]-potassium 4-fluorophenyltrifluoroborate ([^{10}B]-1a)

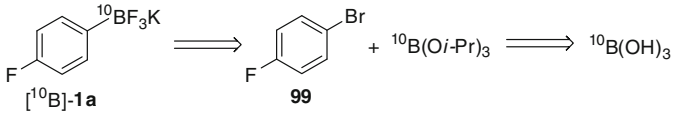

[^{10}B]-B(O*i*-Pr)3

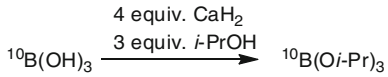

To an oven dried round-bottomed flask was charged [^{10}B]—boric acid (1 equiv., 0.03 mol, 1.83 g) and calcium hydride (4 equiv., 0.12 mol, 5.04 g) and then purged with nitrogen. Anhydrous isopropanol (3 equiv., 0.09 mol, 5.4 g) was added dropwise with stirring down a condenser and over a stream of N_2. After bubbling had ceased, the reaction mixture was heated to 90 °C for 12 h, after which the volatile compounds were pumped off *in vacuo* and trapped at −78 °C. The contents of the trap were then purified by reduced pressure distillation (47–50 °C at 30 mmHg) to give the title compound as a clear colourless oil (3.62 g, 64.5 %). **^{1}H NMR** (300 MHz, $CDCl_3$) δ = 4.34 (sept., $^{3}J_{H-H}$ = 6.0 Hz, 3H), 1.13 (d, $^{3}J_{H-H}$ = 6.0 Hz, 18H). ^{10}B incorporation was not determined for this material, but analysis of the **2a** derived from it, vide infra, confirmed high abundance.

Data are consistent with that expected based on published data for the same compound with natural abundance $^{10}B/^{11}B$ (20/80) [29].

[^{10}B]-Potassium 4-fluorophenyltrifluoroborate ([^{10}B]-**1a**)

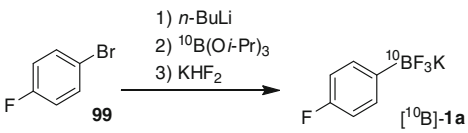

To a two necked round bottomed-flask, purged with nitrogen and a magnetic stirrer bar, was added 4-fluorobromobenzene (**99**) (1.2 equiv., 0.023 mol, 4.067 g) and dry diethylether (23 mL). A solution of *n*-butyllithium (1.2 equiv., 10.4 mL of a 2.22 M solution in THF) was added dropwise at −78 °C and stirred for 30 min before being allowed to warm to room temperature, and stirred for a further 15 min. This solution was then cannulated into a flask charged with [^{10}B]-B(O*i*-Pr)$_3$ (1 equiv., 0.019 mol, 3.623 g) in dry diethylether (76 mL) under an N_2 atmosphere at −78 °C, and was stirred for a further hour. The reaction mixture was again allowed to warm to room temperature before a saturated aqueous solution of KHF_2 (4.6 equiv., 0.087 mol, 6.8 g) was added dropwise. The solvent was removed *in vacuo* before the remaining solids were extracted with acetone (2 × room temperature, 2 × boiling), combined and filtered. The filtrate was concentrated *in vacuo* before the solids were taken up in the minimal volume of hot acetone, filtered and cooled to allow precipitation. Diethylether was added to complete precipitation before the solids could be collected by filtration, washed with diethylether and dried *in vacuo,* to give the title compound (3.45 g, 88 %) as a white solid. **^{1}H NMR** (300 MHz, d_6-acetone): $\delta = 7.45$ (app. t, 2H), 6.81 (app. t, 2H); **^{19}F NMR** (282 MHz, d_6-acetone): $\delta = -120.45$ (s, 1F), 142.3 (m, 3F); **MS (EI)**: analysis of the boronic acid [^{10}B]-**2a** derived by hydrolysis indicated 94.8 % ^{10}B incorporation: isotope cluster *m/z* (%) calc.: (for 94.5 % ^{10}B) 139.1 (100); 140.1 (12.4); 141.1 (0.96), observed: 139.1 (100); 140.1 (12.5); 141.1 (8).

Data are consistent with that expected based on published data for the same compound with natural abundance [$^{10}B/^{11}B$ (20/80) [1].

Exchange under SM coupling-like conditions

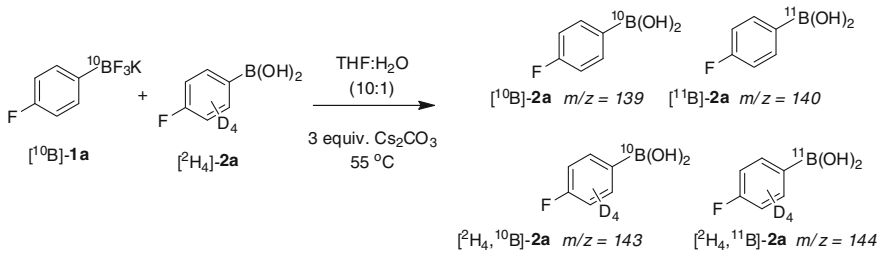

[^{10}B] Potassium 4-fluorophenyltrifluoroborate ([^{10}B]-**1a**) (1 equiv., 1.76×10^{-5} mol, 3.5 mg) and [$^{2}H_4$] 4-fluorophenylboronic acid ([$^{2}H_4$]-**2a**) (1 equiv., 1.76×10^{-5} mol, 2.5 mg) were added as solids to a Schlenk tube. To this was added THF (2 mL) and cesium carbonate (3 equiv., 1.06×10^{-4} mol, 34 mg) in water (0.2 mL). This stirring solution was then heated at 55 °C for five hours after ^{19}F NMR confirmed complete conversion to the 4-fluorophenylboronic acid (**2a**) had occurred. A sample was removed and immediately analysed by MS (EI). **MS** (EI) *m/z* (%): 139 (93.7), 140 (8.9), 141 (4.8), 142 (2.2), 143 (30.1), 144 (100), 145 (18.8).

6.4.2.5 Phase Splitting and the Effect of pH

Cs_2CO_3 titration

A 2 mL graduated pipette was filled with THF:water (10:1, 2 mL) until the solvent was above the top graduation mark. The outlet was then occluded with a small piece of molten plastic and the solvent removed until the meniscus was level with the top graduation mark. Cs_2CO_3 was then added in aliquots (1.59×10^{-5}–1.38×10^{-4} mol), and the apparatus gently agitated to ensure dissolution of the base and mixing of the phases before allowing it to settle for about a minute. The

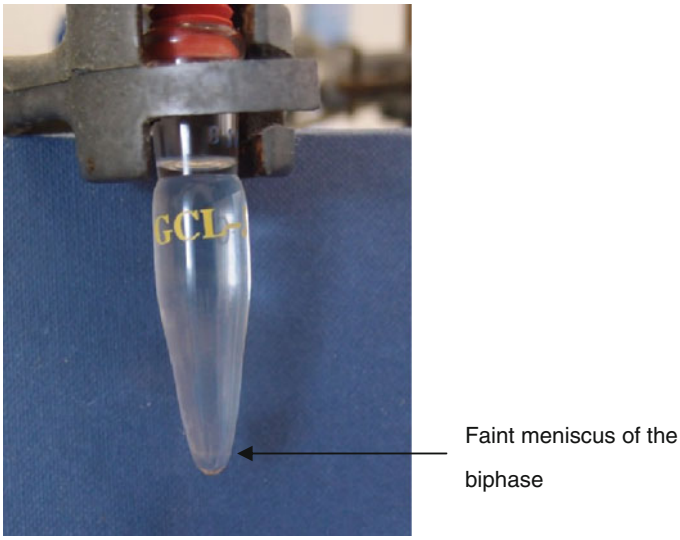

Fig. 6.15 Cs_2CO_3 (24 mM net) dissolved into THF:water (10:1), indicating the biphase which has formed

Table 6.8 Observed phase separation at increasing Cs_2CO_3 concentrations

$[Cs_2CO_3]_{NET}$/mM	Volume of minor phase versus total volume/%
8	0.05
16	0.2
24	1
32	1.25
60	3
97	5
130	6
199	9

level of the phase boundary was then noted after each addition, Fig. 4.12 (Table 6.8) (Fig. 6.15).

pH monitoring

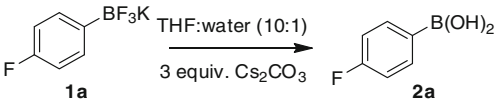

A pre-heated (55 °C) solution of THF:water (10:1, 6.6 mL) was added to a solid mixture of **1a** (1 equiv., 5.28×10^{-5} mol, 10.6 mg) and Cs_2CO_3 (3 equiv., 1.58×10^{-4} mol, 51.6 mg) in a 15 mm diameter Schlenk tube. The stirring (100 rpm) solution was heated at 55 °C and the pH was read from a Hanna HI 98103 pH probe (calibrated only to aqueous pH 7 (phosphate buffer) and aqueous pH 4 (phthalate buffer)) every 10 s for the first 10 min and every 30 s for the following 2 h. Samples (0.3 mL) were removed throughout the reaction using a plastic syringe and placed in pre-cooled PTFE lined NMR tubes at 0 °C. The samples were kept at that temperature until they were placed directly into the *Eclipse 300* NMR probe. Each sample was analysed by ^{19}F NMR and subjected to 128 pulses (4 min 17 s) at 25 °C, Figs. 4.13 and 4.14.

Organic bases

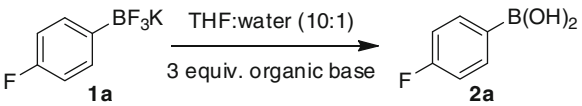

The following experiments were undertaken in a Norell S502 NMR tube in a *Varian 500* spectrometer probe. The bases tested were 1,8-Diazabicycloundec-7-ene (DBU), triethylamine and diisopropylethylamine (Hünigs base).

The organic base (3 equiv., 1.584×10^{-5} mol) in dry THF (0.3 mL) was added to the Norell S502 NMR tube containing D_2O (0.06 mL). This was followed by the addition of **1a** (1 equiv., 5.28×10^{-6} mol, 1.06 mg) in dry THF (0.3 mL); bringing the total THF:water ratio to 10:1 and volume to 0.66 mL, the base

concentration to 24 mM and the **1a** concentration to 8 mM. The tube was briefly shaken then immediately placed into the *Varian 500* probe which was preheated to 55 °C. The reaction was monitored by ^{19}F NMR using a time delayed array to separate the acquisitions. These acquisitions were every 300 s for the first 1.5 h of reaction then every 900 s for the remaining hour.

Buffered conditions

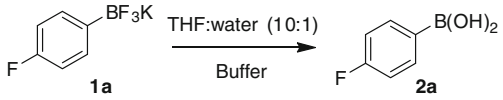

Solid buffer

The buffers employed in the hydrolysis of **1a** to **2a** were 3-(*N*-morpholino)propanesulfonic acid (MOPS) and tris(hydroxymethyl)aminomethane (TRIS).

The buffer (12.5 equiv., 6.6×10^{-5} mol) was added, as a solid, to a Norell 502 NMR tube containing THF:water (0.5 mL:0.06 mL). **1a** (1 equiv., 5.28×10^{-6} mol, 1.07 mg) in dry THF (0.1 mL) was then added; bringing the total THF:water ratio to 10:1 and volume to 0.66 mL, the buffer concentration to 100 mM and the **1a** concentration to 8 mM. The tube was briefly shaken then immediately placed into the *Varian 500* probe which was preheated to 55 °C. The reaction was monitored by ^{19}F NMR using a time delayed array to separate the acquisitions.

Table 6.9 pH of buffers (24 mM) used in the hydrolysis of **1a** to **2a**

Buffer (24 mM)	pH[a]	$k_{obs}{}^{buffer}/s^{-1}$	$t_{1/2}$/min
Et_3N	7.90	3.44E−04	34
Hünigs base	7.65	2.71E−04	43

[a] Uncalibrated

Table 6.10 pH of each buffer (100 mM) used in the homogeneous hydrolysis of **1a** to **2a**

Buffer (100 mM)	pH_1 [a]	pH_2 [a]	$pH_{av.}^{a}$	$k_{obs}{}^{buffer}/s^{-1}$	$t_{1/2}$/min
MOPS[b]	4.50	4.05	4.28	1.90×10^{-3}	6
None	7.00	7.00	7.00	9.84×10^{-4}	12
TRIS	8.90	8.30	8.60	2.25×10^{-4}	51
Et_3N[c]	8.00	7.75	7.86		
Hünigs base[c]	7.70	7.65	7.68		
DBU	11.05	10.80	10.93	3.22×10^{-5}	359
P_4 *t*–Bu	13.70	13.35	13.53	1.23×10^{-5}	942

[a] Uncalibrated
[b] MOPS solution was not completely homogeneous
[c] Kinetics were not undertaken due to the similarity of the pH to that at 24 mM, Table 6.10

These acquisitions were every 300 s for the first 1.5 h of reaction then every 900 s for the remaining hour, Fig. 4.15.

Liquid buffer

The buffers employed in the hydrolysis of **1a** to **2a** were *t*-butyl phosphazene base (P_4 *t*-Bu), 1,8-diazabicycloundec-7-ene (DBU),), triethylamine and diisopropylethylamine (Hünigs base).

The buffer (12.5 equiv., 6.6×10^{-5} mol) in dry THF (0.3 mL) was added to a Norell 502 NMR tube. To this was added **1a** (1 equiv., 5.28×10^{-6} mol, 1.07 mg) in dry THF (0.3 mL), followed by the addition of D_2O (0.06 mL); bringing the total THF:water ratio to 10:1, the base concentration to 100 mM and the **1a** concentration to 8 mM. The tube was briefly shaken then immediately placed into the *Varian 500* probe which was preheated to 55 °C. The reaction was monitored by ^{19}F NMR using a time delayed array to separate the acquisitions. These acquisitions were every 600 s for the first 2.5 h of reaction then every 1,800 s for the remaining 4 h, Fig. 4.15.

pH measurement

The pH of each buffer (MOPS (100 mM) and TRIS (100 mM)), no buffer and base (Et_3N (24 and 100 mM), Hunigs base (24 and 100 mM), DBU (100 mM) and P_4-*t*-Bu (100 mM)) were measured in THF:water (10:1) using a Hanna HI 98103 pH probe (calibrated only to aqueous pH 7 (phosphate buffer) and aqueous pH 4 (phthalate buffer)). The probe was given five aqueous washes in between measurements followed by a single wash of THF:water (10:1). The pH of each solution was measured twice and normalised to "no buffer" at pH 7, Fig. 4.15, Tables 6.9 and 6.10.

Hydrolysis attenuation with ultrasound

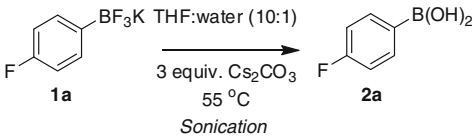

Cesium carbonate (3 equiv., 1.58×10^{-5} mol, 5.2 mg) in D_2O (0.06 mL) was added to the Norell 502 NMR tube containing THF (0.54 mL) and then sonicated for 20 s. **1a** (1 equiv., 5.28×10^{-6} mol, 1.1 mg) in dry THF (0.06 mL) was added to the pre-sonicated solution in the NMR tube; bringing the total THF:water ratio to 10:1 and volume to 0.66 mL, the cesium carbonate concentration to 24 mM and the **1a** concentration to 8 mM. The solution was then sonicated for a further 20 s before being placed directly into the preheated (55 °C) *Varian 500* probe. The reaction was monitored by ^{19}F NMR using a time delayed array to separate the

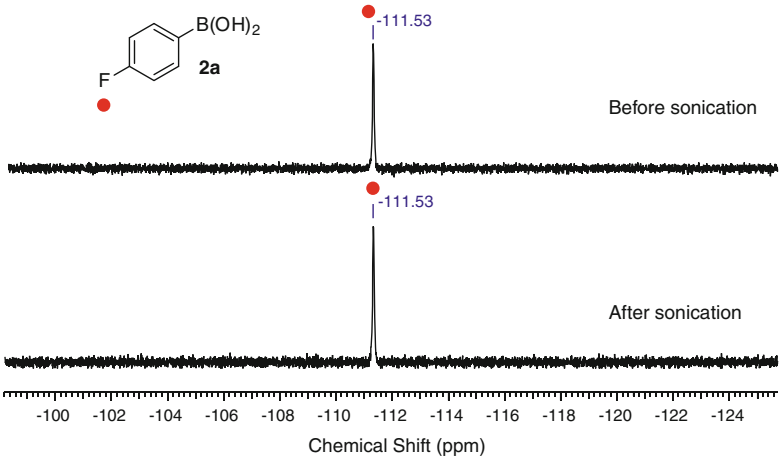

Fig. 6.16 ^{19}F NMR of **2a** in THF:water (10:1) with 3 equiv. Cs_2CO_3 before (*upper spectrum*) and after (*lower spectrum*) 1 min sonication

acquisitions. These acquisitions were every 180 s for the first 30 min then every 300 s for the following 50 min then every 900 s for the remaining two hours, Fig. 4.16.

Effect of ultrasound on boronic acid/boronate equilibrium

A NMR tube containing THF (0.8 mL) was charged with Cs_2CO_3 (3 equiv., 2.64×10^{-5} mol, 8.6 mg) in H_2O (0.1 mL). To this was added **2a** (1 equiv., 8.8×10^{-6} mol, 1.23 mg) in THF (0.2 mL). This sample was analysed by ^{19}F NMR at 55 °C before and immediately after one minute sonication. A time averaged ^{19}F NMR signal is indicative of Ar–$B(OH)_2$ (**2a**) ↔ Ar–$B(OH)_3^-$ (**60a**) equilibrium position, where $\delta = -111.5$ ppm: ≥95 % **2a** and $\delta = -118$ ppm: ≥95 % **60a**, Sect. 3.3, Fig. 3.7 *vide supra* and Fig. 6.16.

Chemoselective coupling

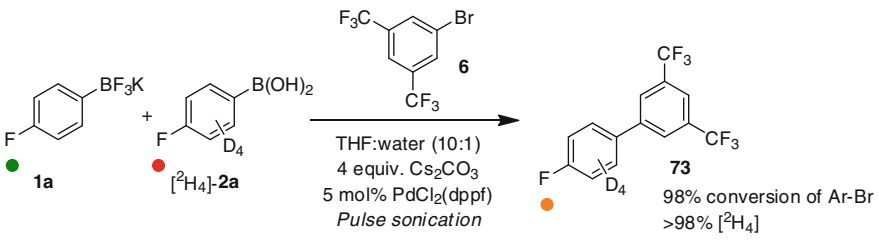

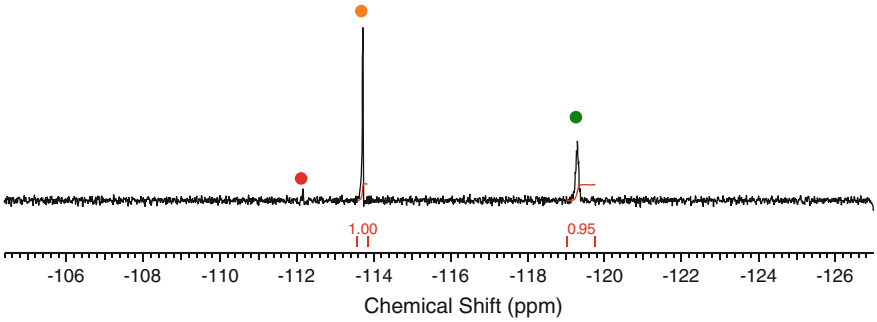

Fig. 6.17 ^{19}F NMR spectrum of the chemoselective SM coupling of [$^{2}H_4$]-**2a** with **6**, in the presence of **1a**, after 38 min at 55 °C

To a pre-sonicated mixture of Cs_2CO_3 (4 equiv., 1.23×10^{-4} mol, 40.1 mg), 1,3-bis(trifluoromethyl)-5-bromobenzene (**6**) (1 equiv., 3.08×10^{-5} mol, 9.0 mg), [$^{2}H_4$]-**2a** (1 equiv., 3.08×10^{-5} mol, 4.4 mg) and degassed THF (6.3 mL) and water (0.7 mL) was added **1a** (1 equiv., 3.08×10^{-5} mol, 6.2 mg) in THF (0.5 mL) dropwise and sonicated for a further 20 s. Dichloro-[1,l′-bis(diphenylphosphino)ferrocene]palladium(II) [$PdCl_2$(dppf)] (5 mol %, 1.54×10^{-6} mol, 1.1 mg) in THF (0.2 mL) was added dropwise to this vigorously stirring solution at 55 °C. The solution was subjected to 10 s sonication pulses every 10 min. A sample was removed after 40 min and placed into a pre-cooled (0 °C) PTFE lined NMR tube and analysed by ^{19}F NMR (128 scans at 25 °C), Fig. 6.17.

6.4.2.6 Vessel Dependency in SM Coupling

SM coupling under aerobic conditions

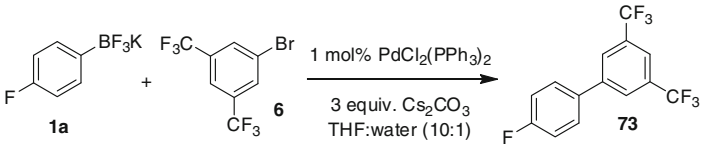

To a 15 mm wide Schlenk tube with a hemispherical base, under a N_2 atmosphere, was charged Cs_2CO_3 (3 equiv., 1.32×10^{-4} mol, 43 mg), degassed water (0.5 mL) and degassed THF (3 mL). To this was added 1,3-bis(trifluoromethyl)-5-bromobenzene (**6**) (1 equiv., 4.4×10^{-5} mol, 12.9 mg) in dry degassed THF (0.5 mL), **1a** (1 equiv., 4.4×10^{-5} mol, 8.9 mg) in dry degassed THF (0.5 mL) and finally bis(triphenylphosphine)palladium(II) chloride (1 mol %, 4.4×10^{-7}

mol, 0.3 mg) in dry degassed THF (1 mL), bringing the total THF:water ratio to 10:1 and volume to 5.5 mL and **1a** concentration to 8 mM.

The same procedure was repeated in parallel but in a 15 mm wide Schlenk tube with a conical shaped base.

In both cases ≥85 % of the reaction volume was within the cylindrical section of the tube. The top of the Schlenk tube was left open to the air, to keep the concentration of O_2 constant. The solution was stirred at a rate in which no vortex was produced and heated at 55 °C for 6 h, before being analysed by ^{19}F NMR (200 scans, 25 °C), Fig. 4.17.

6.4.2.7 Uncatalysed Hydrolysis

No specific experiments. Observations made from, for example, Fig. 4.13 or Fig. 4.16 .

6.4.3 Hydrolysis of R–BF_3K Salts

6.4.3.1 Hydrolytic Equilibria and Glass Mediated Hydrolysis

Hydrolytic equilibrium (K_{app}) of 1 and 2.

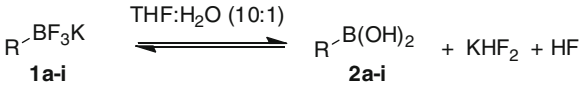

The potassium organotrifluoroborate (**1a**, **1ar**, **1 k**, **1x**, **1c**, **1y**, **1at**, **1au** and **1av**) (4.4×10^{-6} mol) was added as a solid to a PTFE lined Quartz NMR tube.

Table 6.11 Equilibrium populations of substrates **1a**, **1ar**, **1k**, **1x**, **1c**, **1y**, **1at**, **1au** and **1av** in THF:H_2O (10:1) at 55 °C at 8 mM

Substrate (8 mM)		x_1^a	x_2^b	K_{app}^c
4-Fluorophenyl	**1a**	0.75	0.25	5.3×10^{-8}
2-Furanyl	**1ar**	0.81	0.19	2.2×10^{-8}
Vinyl	**1 k**	0.67	0.33	1.4×10^{-7}
Cyclopropyl	**1x**	0.39	0.61	1.5×10^{-6}
Phenylethynyl	**1c**	–	–	–
Cyclobutyl	**1y**	0.61	0.39	2.5×10^{-7}
Isopropyl	**1at**	0.71	0.29	8.8×10^{-8}
Benzyl	**1au**	0.83	0.17	1.5×10^{-8}
1,3-Diphenylpropyl	**1av**	0.79	0.21	3.0×10^{-8}

[a] Where $x_1 = [\mathbf{1}]_{eq.}/([\mathbf{1} + \mathbf{2}]_{eq.})$—rounded up to 2 d.p
[b] Where $x_2 = [\mathbf{2}]_{eq.}/([\mathbf{1} + \mathbf{2}]_{eq.})$—rounded up to 2 d.p
[c] Where $K_{app} = [\mathbf{2}]^3 /(25*[\mathbf{1}])$

Table 6.12 Equilibrium populations of substrates **1a**, **1ar**, **1k**, **1x**, **1c**, **1y**, **1at**, **1au** and **1av** in THF:H_2O (10:1) at 55 °C at 100 mM

Substrate (100 mM)		x_1[a]	x_2[b]	K_{app}[c]
4-Fluorophenyl	**1a**	0.97	0.03	7.1×10^{-11}
2-Furanyl	**1ar**	0.97	0.03	7.1×10^{-11}
Vinyl	**1 k**	0.96	0.04	1.7×10^{-10}
Cyclopropyl	**1x**	0.89	0.11	3.8×10^{-9}
Phenylethynyl	**1c**	–	–	–
Cyclobutyl	**1y**	0.95	0.05	3.4×10^{-10}
Isopropyl	**1at**	0.97	0.03	7.1×10^{-11}
Benzyl	**1au**	0.93	0.07	9.4×10^{-10}
1,3-Diphenylpropyl	**1av**	0.92	0.08	1.4×10^{-9}

[a] Where $x_1 = [\mathbf{1}]_{eq.}/([\mathbf{1} + \mathbf{2}]_{eq.})$—rounded up to 2 d.p
[b] Where $x_2 = [\mathbf{2}]_{eq.}/([\mathbf{1} + \mathbf{2}]_{eq.})$—rounded up to 2 d.p
[c] Where $K_{app} = [\mathbf{2}]^3 /(25*[\mathbf{1}])$

THF:water (10:1, 0.55 mL) was added after which the tube was shaken and placed immediately into the preheated (55 °C) *Eclipse 300* probe. The sample was heated at 55 °C for 15 min before being analysed by ^{11}B NMR (2,500 scans) and ^{19}F NMR (200 scans) at 55 °C, Table 6.11 (8 mM) and Table 6.12 (100 mM).

Hydrolysis mediated by glass

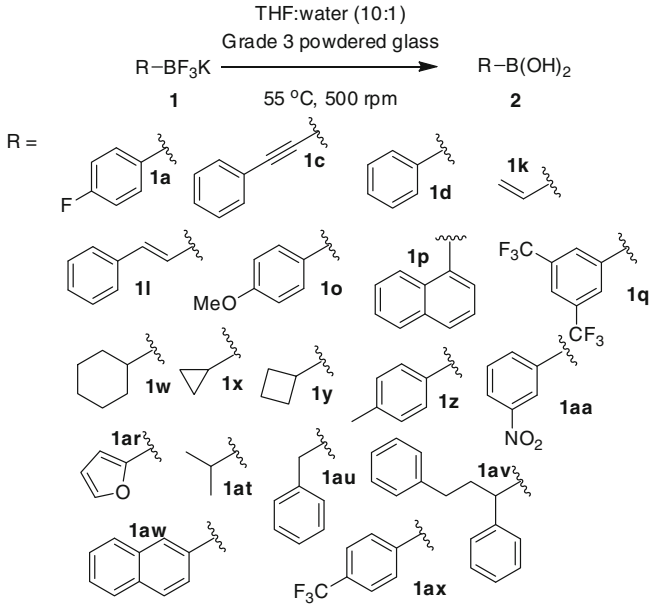

A preheated (55 °C) solution of THF:water (10:1, 6.6 mL) plus benzotrifluoride (10 μL) was added to the potassium organotrifluoroborate (**1**) (1 equiv., 5.28×10^{-5} mol) and glass powder (Grade 3, 20 mg) in a 15 mm diameter PTFE

flat-bottomed test tube. A sample (0.3 mL) was immediately removed with a plastic syringe and placed in a pre-cooled (0 °C) PTFE lined NMR tube. The solution was then stirred at 500 rpm and heated at 55 °C for 2 h to 5 days, depending on the substrate. Samples were removed at regular time intervals into pre-cooled (0 °C) PTFE lined NMR tubes. Each sample was analysed by ^{19}F NMR spectroscopy and was subjected to 128 scans at 25 °C. The integration of R–BF_3K peak was normalised against benzotrifluoride and concentrations calculated by comparison to the "0 s" time point assumed to be the known initial concentration, Fig. 4.19.

^{11}B NMR was used to confirm conversion to the appropriate boronic acid had occurred. The protodeboronated product (**75**) was observed from substrate **1c**.

Survey of B–F bond lengths from single crystal X-ray diffraction

The following structures were sourced from a substructure search of C–BF_3 on ConQuest [30] from The Cambridge Crystallographic Data Centre. Data from structures with a counter cation other than potassium were predominantly not included (with three exceptions—see entry 3, 8 and 11 Table 6.13).

Density Functional Theory (DFT)

Geometry optimisation in Gaussian 09 was carried out for species **1a**, **1c**, **1d**, **1k**, **1l**, **1o**, **1p**, **1q**, **1x**, **1y**, **1w**, **1z**, **1aa**, **1ar**, **1at**, **1au**, **1av**, **1aw** and **1ax** at the B3LYP level of theory, using the standard 6 − 31 + G(d) basis set for all atoms. The calculations were carried out using a continuum solvent model, the IEF-PCM model in Gaussian, with parameters for tetrahydrofuran as solvent, Tables 6.14 and 6.15.

Normalisation

Normalisation of the B–F bond lengths was conducted by taking the difference between the $r(\text{B–F})_{\text{av.}}$ in the difluoroborane (**11**) and $r(\text{B–F})_{\text{BF3}}$ in BF_3 (132.213 pm) to give Δr(B–F). Normalisation of the C–B bond was conducted by taking the difference between r(C–B) in the difluoroborane (**11**) and $r(\text{C–B})_{\text{CB}}$ in HC≡C–BF_2 (151.700 pm) to give Δr(C–B).

Table 6.13 Average B–F bond length from the available crystal structures of various potassium organotrifluoroborates

Entry	Structure	$r(\mathrm{B–F})_{av.}$/pm	CCDC number
1	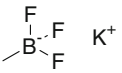	142.4	–
2	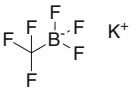	139.1	–
3	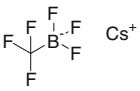	139.1	–
4	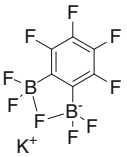	143.9	278389
5	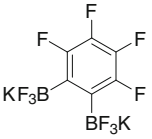	141.5	278193
6	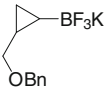	142.4	717834
7	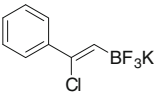	141.9	715783
8	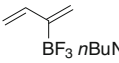	142.2	655091
9	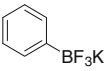	141.7	IUCr NA1133
10	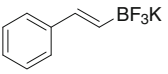	142.5	170861
11	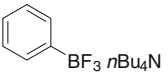	141.8	170890
12	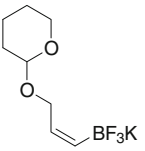	141.9	717377

(continued)

Table 6.13 (continued)

Entry	Structure	$r(B–F)_{av.}$/pm	CCDC number
13	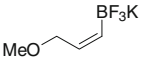	142.5	712290
14	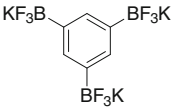	142.7	782522
15	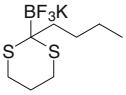	140.1	686771
16		140.5	670905
17	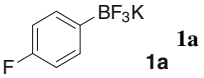 **1a** **1a**	142.4	859285
18	 **1c** **1c**	142.6	859286
19	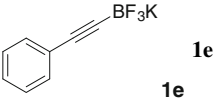 **1e** **1e**	140.8	859288
20	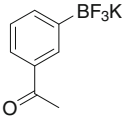	141.9	859287

Table 6.14 DFT derived geometry optimisations of R–BF_2 (**11**)

Substrate		r(B–F)$_1$/pm	r(B–F)$_2$/pm	r(B–F)$_{av}$/pm[a]	Δr(B–F)/pm
4-Fluorophenyl	**11a**	133.926	133.923	133.925	1.712
2-Furanyl[b]	**11ar**	133.868	133.647	133.758	1.655
Vinyl	**11 k**	133.978	133.932	133.955	1.742
Cyclopropyl	**11x**	134.657	134.671	134.664	2.451
Phenylethynyl	**11c**	133.454	133.454	133.454	1.241
Cyclobutyl	**11y**	134.146	134.121	134.134	1.920
Isopropyl	**11at**	134.074	133.976	134.025	1.812
Benzyl	**11au**	133.745	133.757	133.751	1.672
1,3-Diphenylpropyl	**11av**	133.750	133.870	133.810	1.597
Cyclohexyl	**11w**	134.065	134.064	134.065	1.851
Phenylethenyl	**11 l**	134.313	134.364	134.339	2.126
4-Methoxyphenyl	**11o**	134.292	134.252	134.272	2.059
4-Methylphenyl	**11z**	134.115	134.110	134.113	1.899
Phenyl	**11d**	133.981	133.976	133.979	1.766
1-Naphthyl[b]	**11p**	134.300	*134.022*	134.161	1.809
2-Naphthyl	**11aw**	134.004	134.025	134.015	1.801
4-CF_3-phenyl	**11ax**	133.637	133.636	133.637	1.424
3-Nitrophenyl	**11aa**	133.474	133.516	133.495	1.282
3,5 bis(CF_3)phenyl	**11q**	133.366	133.389	133.378	1.165

[a] This value used for normalisation of all "normal" substrates
[b] "Asymmetric" substrate; value in italics used for normalisation

Table 6.15 DFT derived geometry optimisations of R–BF_2 (**11**)

Substrate		r(C–B)/pm	Δr(C–B)/pm	Energy/a.u.
4-Fluorophenyl	**11a**	154.099	2.399	−555.592564
2-Furanyl	**11ar**	152.456	0.756	−454.127964
Vinyl	**11 k**	154.216	2.516	−302.683084
Cyclopropyl	**11x**	153.877	2.177	−341.987314
Phenylethynyl	**11c**	151.039	−0.661	−532.509487
Cyclobutyl	**11y**	155.553	3.853	−381.299782
Isopropyl	**11at**	156.726	5.026	−343.225837
Benzyl	**11au**	156.869	5.169	−495.658800
1,3-Diphenylpropyl	**11av**	157.317	5.617	−805.345403
Cyclohexyl	**11w**	156.876	5.176	−533.756690
Phenylethenyl	**11 l**	153.091	1.391	−570.880765
4-Methoxyphenyl	**11o**	153.357	1.657	−495.669190
4-Methylphenyl	**11z**	153.884	2.184	−456.349602
Phenyl	**11d**	154.199	2.499	−609.995016
1-Naphthyl	**11p**	154.586	2.886	−609.998863
2-Naphthyl	**11aw**	154.094	2.394	−793.408595
4-CF_3-phenyl	**11ax**	154.851	3.151	−660.862105
3-Nitrophenyl	**11aa**	154.934	3.234	−1,130.46592
3,5-bis(CF_3)phenyl	**11q**	155.121	3.421	−533.756690

6.4.3.2 Base Mediated Hydrolysis

DBU

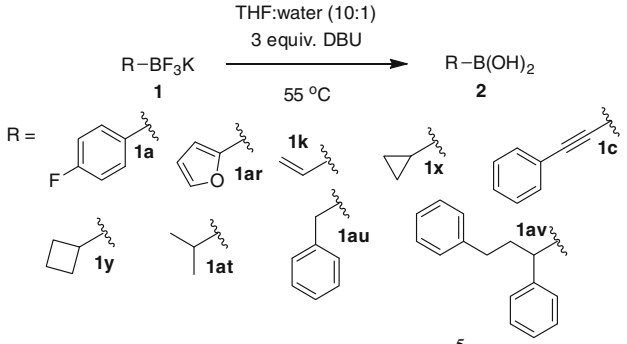

A solution of DBU (3 equiv., 1.32×10^{-5} mol, 2.0 mg) in THF (0.5 mL) containing benzotrifluoride (1/2 drop) was added to a PTFE lined NMR tube, charged with the potassium organotrifluoroborate (**1**) (1 equiv., 4.4×10^{-6} mol). After addition of D_2O (0.05 mL) the tube was briefly shaken then immediately placed into the preheated (55 °C) *Varian 500* probe. The reaction was monitored by ^{19}F NMR (128 scans, 55 °C) using a time delayed array to separate the acquisitions. The separation time ranged from 0 to 3,600 s depending on the substrate and extent of reaction.

The integration of R–BF_3K peak was normalised against the standard (benzotrifluoride) and concentrations were calculated by comparison to the first spectrum, assumed to be the known initial concentration, Fig. 4.24, Tables 6.16 and 6.17.

Cs_2CO_3

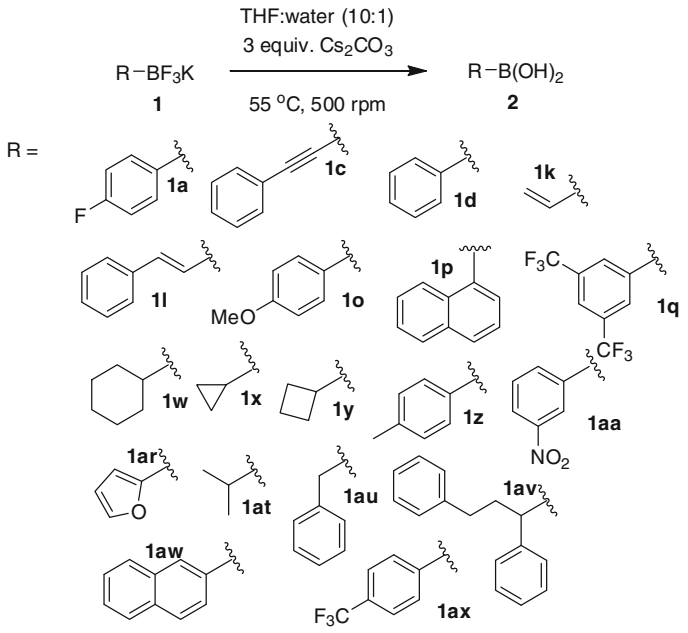

Table 6.16 Half life of hydrolysis for each substrate

Substrate		$t_{1/2}$ glass	$t_{1/2}$ Cs2CO3	$t_{1/2}$ DBU
4-Fluorophenyl	**1a**	28 min	3 h 20 min	7 h 50 min
2-Furanyl	**1ar**	33 min	6 h	26 h
Vinyl	**1 k**	23 min	5 min	23 min
Cyclopropyl	**1x**	7 min	1 min	3 min
Phenylethynyl	**1c**	12 h	40 days	27 days
Cyclobutyl	**1y**	18 min	4 min	18 min
Isopropyl	**1at**	25 min	11 min	27 min
Benzyl	**1au**	33 min	3 h 20 min	3 h
1,3-Diphenylpropyl	**1av**	39 min	2 h	18 h 20 min
Cyclohexyl	**1w**	19 min	9 min	
Phenylethenyl	**1 l**	10 min	27 min	
4-Methoxyphenyl	**1o**	10 min	19 min	
4-Methylphenyl	**1z**	16 min	51 min	
Phenyl	**1d**	19 min	1 h 40 min	
1-Naphthyl	**1p**	25 min	10 h	
2-Naphthyl	**1aw**	22 min	7 h 10 min	
4-CF_3-phenyl	**1ax**	1 h 30 min	2 days 18 h	
3-Nitrophenyl	**1aa**	2 days 13 h	5 days	
3,5-bis(CF_3)phenyl	**1q**	3 days	54 days	

A preheated (55 °C) solution of THF (6 mL) plus benzotrifluoride (10 μL) was added to the potassium organotrifluoroborate (**1**) (1 equiv., 5.28×10^{-5} mol) and glass powder (Grade 3, 20 mg) in a 15 mm diameter PTFE flat-bottomed test tube. A solution of Cs_2CO_3 (3 equiv., 1.58×10^{-4} mol, 51.6 mg) in water (0.6 mL) was added before immediately removing a sample (0.3 mL) into a pre-cooled (0 °C) PTFE lined NMR tube. The reaction was stirred at 500 rpm at 55 °C for 5 min—12 days depending on the substrate. Samples were removed at regular time intervals into pre-cooled (0 °C) PTFE lined NMR tubes. Each sample was analysed by ^{19}F NMR spectroscopy and was subjected to 128 scans at 25 °C. The integration of R–BF_3K peak was normalised against benzotrifluoride and concentrations calculated by comparison to the "0 s" time point assumed to be the known initial concentration, Fig. 4.25 and Tables 6.16 and 6.17.

^{11}B NMR was used to confirm conversion to the appropriate boronic acid had occurred. Conversion to the protodeboronated product **75** was observed from substrate **1c** and **1q**.

6.4.3.3 Hydrophilic Hydrolysis

1. ***Test for catalysis by KBF4***

The general conditions for the hydrolysis of **1 k** to **2 k**, as outlined in Sect. 6.4.3.2 (Cs_2CO_3), were followed with the addition of KBF_4 (0.15 equiv., 7.9×10^{-6} mol, 1.0 mg). A control reaction was conducted without the addition of KBF_4.

Table 6.17 Pseudo first order rate constant derived from the first order log plot for each substrate

Substrate		k_{obs}^{glass}/s^{-1}	k_{obs}^{Cs2CO3}/s^{-1}	k_{obs}^{DBU}/s^{-1}
4-Fluorophenyl	**1a**	4.2×10^{-4}	5.7×10^{-5}	2.5×10^{-5}
3-Furanyl	**1ar**	3.5×10^{-4}	3.2×10^{-5}	7.4×10^{-6}
Vinyl	**1 k**	5.0×10^{-4}	2.2×10^{-3}	5.0×10^{-4}
Cyclopropyl	**1x**	1.7×10^{-3}	8.4×10^{-3} [a]	4.1×10^{-3} [b]
Phenylethynyl	**1c**	1.6×10^{-5}	2.0×10^{-7}	3.0×10^{-7}
Cyclobutyl	**1y**	6.5×10^{-4}	2.8×10^{-3}	6.3×10^{-4} [c]
Isopropyl	**1at**	4.6×10^{-4}	1.0×10^{-3}	4.3×10^{-4}
Benzyl	**1au**	3.5×10^{-4}	5.8×10^{-5}	6.5×10^{-5}
1,3-Diphenylpropyl	**1av**	3.0×10^{-4}	9.3×10^{-5}	1.1×10^{-5}
Cyclohexyl	**1w**	6.0×10^{-4}	1.3×10^{-3}	
Phenylethenyl	**1 l**	1.1×10^{-3}	4.3×10^{-4}	
4-Methoxyphenyl	**1o**	1.2×10^{-3}	6.0×10^{-4}	
4-Methylphenyl	**1z**	7.2×10^{-4}	2.3×10^{-4}	
Phenyl	**1d**	6.0×10^{-4}	1.1×10^{-4}	
1-Naphthyl	**1p**	4.6×10^{-4}	1.9×10^{-5}	
2-Naphthyl	**1aw**	5.3×10^{-4}	2.7×10^{-5}	
4-CF_3-phenyl	**1ax**	1.2×10^{-4}	2.9×10^{-6}	
3-Nitrophenyl	**1aa**	5.2×10^{-6}	1.6×10^{-6}	
3,5-bis(CF_3)phenyl	**1q**	2.7×10^{-6}	1.5×10^{-7}	

[a] THF:water (20:1) $k_{obs}^{Cs2CO3} = 7.88 \times 10^{-3}\ s^{-1}$
[b] Double the concentration of DBU $k_{obs}^{DBU} = 4.0 \times 10^{-3}\ s^{-1}$
[c] Double the concentration of DBU $k_{obs}^{DBU} = 6.9 \times 10^{-4}\ s^{-1}$

$$k_{obs}^{KBF_4} = 2.9 \times 10^{-3}\ s^{-1}$$

$$k_{obs}^{control} = 3.0 \times 10^{-3}\ s^{-1}$$

2. ***Test for catalysis by B(OH)₃***

The general conditions for the hydrolysis of **1k** to **2k**, as outlined in Sect. 6.4.3.2 (Cs_2CO_3), were followed with the addition of [^{10}B]-$B(OH)_3$. (0.15 equiv., 7.9×10^{-6} mol, 0.5 mg). A control reaction was conducted without the addition of [^{10}B]-$B(OH)_3$.

$$k_{obs}^{B(OH)3} = 3.1 \times 10^{-3}\ s^{-1}$$

$$k_{obs}^{control} = 3.0 \times 10^{-3}\ s^{-1}$$

No growth of [^{11}B]-$B(OH)_3$ was observed (^{11}B NMR), which would be expected upon ^{10}B/^{11}B exchange, Fig. 6.18.

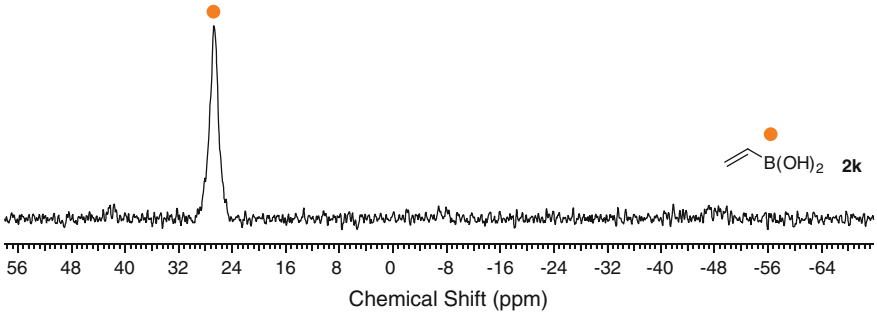

Fig. 6.18 ^{11}B NMR of the hydrolysis product of **1k** showing only vinylboronic acid (**2k**) ($\delta_B = 28$ ppm) present and no $^{11}B(OH)_3$ ($\delta_B = 18$ ppm)

3. ***Test for reversible nucleophilic attack***

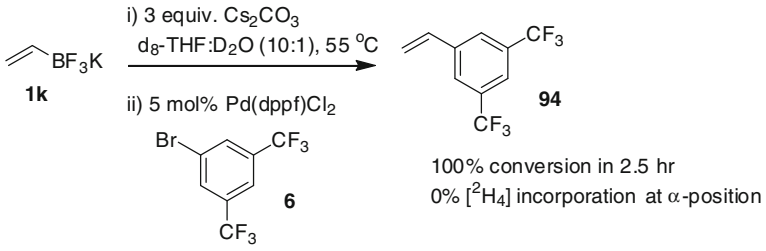

Potassium vinyltrifluoroborate **1k** (1 equiv., 5.28×10^{-5} mol, 7.1 mg) was added to a stirring mixture of Cs_2CO_3 (3 equiv., 1.58×10^{-4} mol, 51.6 mg) in d_8-THF:D_2O (10:1, 6.6 mL) and heated at 55 °C for 30 min. [Pd(dppf)Cl_2] (5 mol %, 7.92×10^{-7} mol, 1.93 mg) and 3,5-bis(trifluoromethyl)bromobenzene **6** were added and the reaction was stirred for a further 2.5 h at 55 °C. After TLC analysis (hexane: ethylacetate (95:1)) indicated complete conversion of **6**, a sample was removed and analysed by ^{1}H NMR. **^{1}H NMR**: (300 MHz, d_8-THF): 7.96 (s, 2H), 7.70 (s, 1H), 6.77 (dd, $^3J_{H-H} = 11.0$ Hz, $^3J_{H-H} = 17.6$ Hz, 1H), 5.90 (d, $^3J_{H-H} = 17.6$ Hz, 1H), 5.49 (d, $^3J_{H-H} = 11.0$ Hz, 1H).

Data are in accordance with that previously reported for the non-deuterated product [31].

Partitioning study

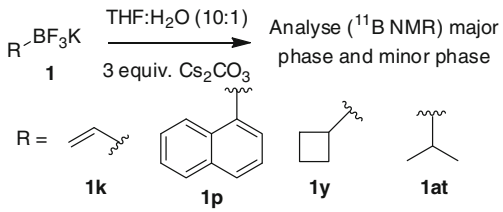

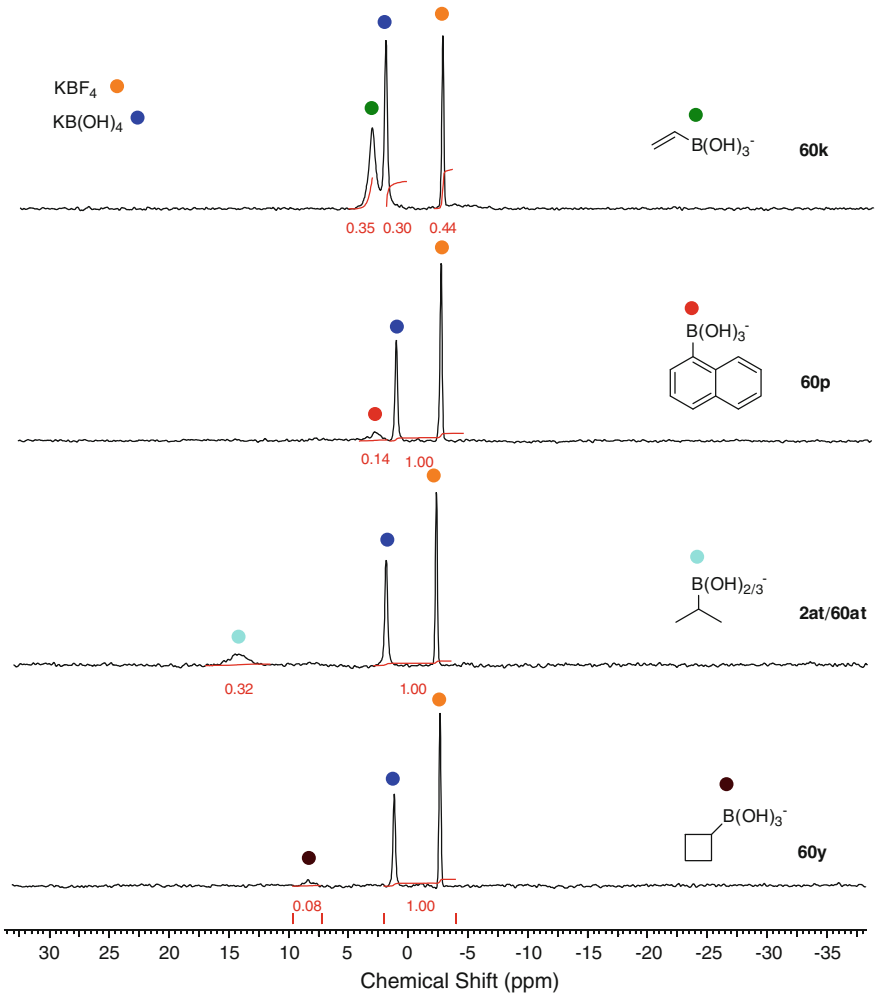

Fig. 6.19 ^{11}B NMR of the minor basic biphase, containing the product of the hydrolysis R–B(OH)$_3^-$ (note half integration due to peak overlap in **1k**). KBF_4 (internal standard) has partially hydrolysed to $KB(OH)_4$

THF (2 mL) was added to a test tube containing the potassium organotrifluoroborate (**1 k**, **1p**, **1y** and **1at**) (1 equiv., 1.1×10^{-4} mol). To this was added cesium carbonate (3 equiv., 3.3×10^{-4} mol, 107.6 mg) in water (0.2 mL) and stirred for one minute at room temperature. A sample (50 μL) was removed from the minor biphase and the major bulk phase and added directly to an NMR tube containing KBF_4 (10 mol %, 1.1×10^{-5} mol, 1.4 mg) and then diluted with water (0.5 mL). Each sample was analysed by ^{11}B NMR for 500 scans at 25 °C, Fig. 6.19.

A control experiment demonstrated that a proportion of KBF_4 hydrolysed to $KB(OH)_4$ under the strongly basic conditions of the minor biphase, giving rise to an extra peak (δ_B = 1.92–1.14 ppm) in the ^{11}B NMR spectrum.

Potassium ethynyltrifluoroborate

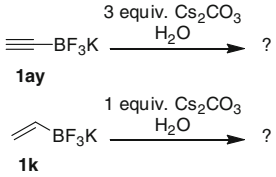

Cs_2CO_3 (3 equiv., 7.5×10^{-4} mol, 245 mg) was added to a solution of potassium ethynyltrifluoroborate (**1ay**) (1 equiv., 2.5×10^{-4} mol, 33.0 mg) in water (5 mL) and stirred at room temperature for 10 min. A sample was removed and analysed by ^{11}B NMR.

The procedure was repeated with potassium vinyltrifluoroborate (**1 k**) (1 equiv., 2.5×10^{-4} mol, 33.5 mg) but with one equivalent of Cs_2CO_3 (1 equiv., 2.5×10^{-4} mol, 81.5 mg), Fig. 6.20.

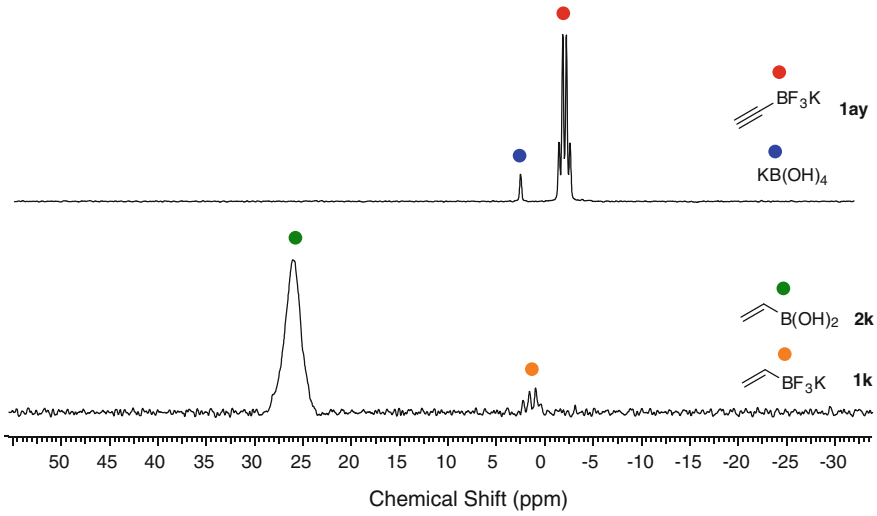

Fig. 6.20 ^{11}B NMR of (*upper spectrum*) potassium ethynyltrifluoroborate (**1ay**) treated with 3 equiv. Cs_2CO_3 in water, indicating only trace amounts of hydrolysis/protodeboronation ($B(OH)_4^-$) and (*lower spectrum*) potassium vinyltrifluoroborate (**1k**) treated with 1 equiv. Cs_2CO_3 in water, showing almost complete conversion to **2k**

6.4.4 Mechanistic Summary

For the kinetics of the hydrolysis of substrates **1x** and **1y** with double the concentration of DBU see Sect. 6.4.3.2.

6.4.5 Classifications

6.4.5.1 Class I

Cyclobutyl SM coupling [8]

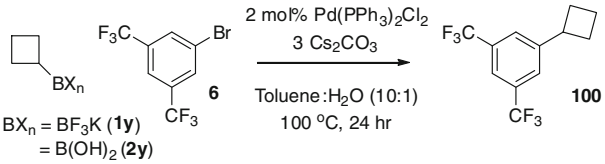

Dry and degassed toluene (3 mL) was added to a Schlenk tube, under an atmosphere of N_2, charged with a solid mixture of potassium cyclobutyltrifluoroborate (**1y**) (1 equiv., 1.65×10^{-4} mol, 26.7 mg), bis(triphenylphosphine)palladium(II) chloride (2 mol %, 3.3×10^{-6} mol, 2.3 mg) and Cs_2CO_3 (3 equiv., 4.95×10^{-4} mol, 161 mg). To this was added 1,3-bis(trifluoromethyl)-5-bromobenzene (**6**) (1 equiv., 1.65×10^{-4} mol, 48.3 mg) and water (0.03 mL). The stirring solution was heated at 100 °C for 24 h. A sample was removed after one hour and after 24 h and analysed by ^{19}F NMR (128 scans, 25 °C), Fig. 4.28.

A parallel reaction was run in which the above procedure was repeated where potassium cyclobutyltrifluoroborate (**1y**) was replaced with cyclobutylboronic acid (**2y**) (1 equiv., 1.65×10^{-4} mol, 16.5 mg) Fig. 4.28.

6.4.5.2 Class II

Effect of glass powder on hydrolysis rates under basic conditions

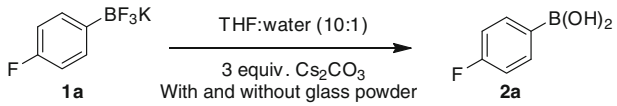

To one Schlenk tube containing potassium 4-fluorophenyltrifluoroborate (**1a**) (1 equiv., 5.28×10^{-5} mol, 10.6 mg) and cesium carbonate (3 equiv., 1.58×10^{-4} mol, 51.6 mg) was added THF (6 mL) and water (0.6 mL). To another identically shaped Schlenk tube was added glass powder (grade 3, 20 mg) along with the potassium 4-fluorophenyltrifluoroborate (**1a**) (1 equiv., 5.28×10^{-5} mol,

Table 6.18 Rates and half lives of the hydrolysis of **1a** with and without added glass powder

	k_{obs}/s^{-1}	$t_{1/2}$/min
With added glass powder	5.55×10^{-5}	208
Without added glass powder	5.61×10^{-5}	206

10.6 mg), cesium carbonate (3 equiv., 1.58×10^{-4} mol, 51.6 mg) and then THF (6 mL) and water (0.6 mL). The two solutions were heated at 55 °C and stirred at 500 rpm. Samples (0.3 mL) were removed at regular time intervals into pre-cooled (0 °C) PTFE lined NMR tubes. Each sample was analysed by ^{19}F NMR spectroscopy and was subjected to 128 scans at 25 °C, Table 6.18.

6.4.5.3 Class III

Hydrolysis then cross-coupling

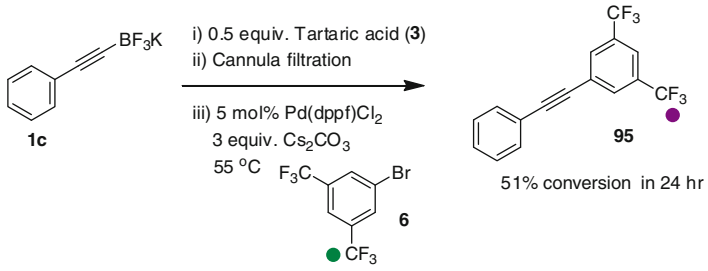

Tartaric acid (**3**) (0.5 equiv., 3.08×10^{-5} mol, 4.6 mg) was added to a solution of potassium phenylethynyltrifluoroborate (**1c**) (1 equiv., 6.16×10^{-5} mol, 12.8 mg) in degassed THF:water (10:1, 7.7 mL) and stirred under a N_2 atmosphere for 1 h at 55 °C. The solution was filtered through a cannular to a solid mixture of Cs_2CO_3 (3 equiv., 1.84×10^{-4} mol, 60.2 mg) and [Pd(dppf)Cl_2] (5 mol %, 3.08×10^{-6} mol, 2.3 mg) after which 3,5-bis(trifluoromethyl)bromobenzene (**6**) (1 equiv., 6.16×10^{-5} mol, 18.0 mg) was immediately added. The reaction was stirred at 55 °C and samples were removed periodically Samples were removed at regular time intervals into pre-cooled (0 °C) NMR tubes. Each sample was analysed by ^{19}F NMR spectroscopy and was subjected to 128 scans at 25 °C.

The reaction was repeated without the initial addition of tartaric and subsequent filtration, Fig. 6.21.

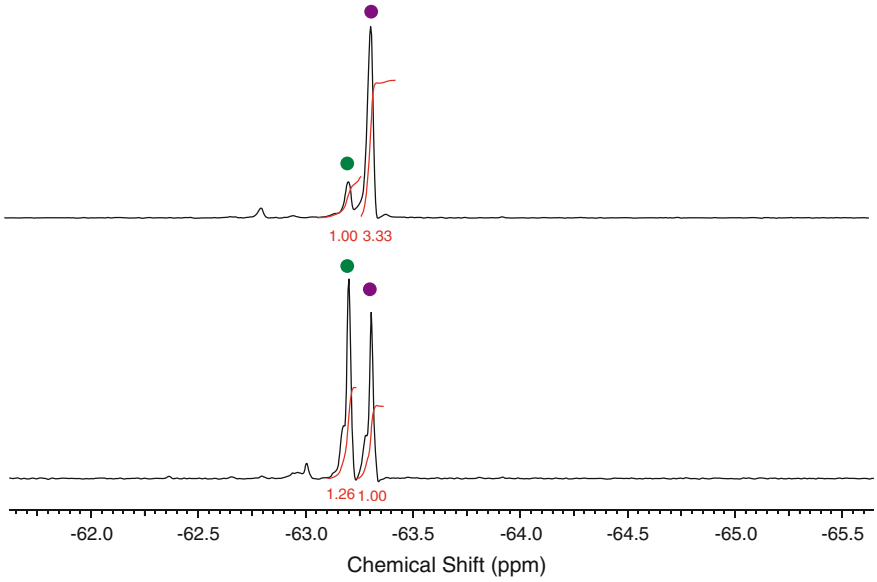

Fig. 6.21 ^{19}F NMR spectra of (*upper spectrum*) the SM coupling between **1c** and **6** after 5.5 h (no tartaric acid), and (*lower spectrum*) the SM coupling between **1c** and **6** (with tartaric acid/filtration treatment) after 5.5 h

Synthesis of [$^2H_5$]-phenylacetylene ([$^2H_5$]-41)

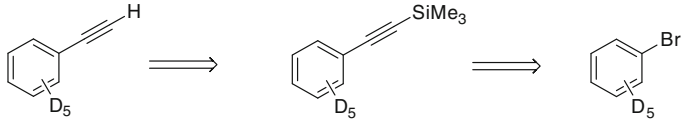

TMS-protected [$^2H_5$]-phenylacetylene ([$^2H_5$]-**101**)

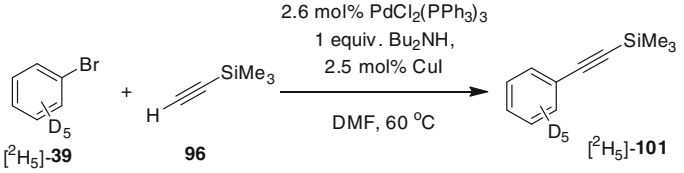

DMF was distilled from 4 Å molecular sieves and left to dry overnight before being degassed by three vacuum/N_2 cycles. Di-*n*-butylamine was distilled from calcium hydride under an atmosphere of dry N_2 prior to use.

To an oven-dried, N_2 purged Schlenk tube, was added firstly di-*n*-butylamine (1 equiv., 9.51×10^{-3} mol, 1.23 g) and DMF (11 mL), followed by [$^2H_5$]-bromobenzene ([$^2H_5$]-**39**) (1 equiv., 9.50×10^{-3} mol, 1.54 g) and TMS acetylene (**96**)

(1.01 equiv., 9.64×10^{-3} mol, 0.945 mg). Over a flow of nitrogen was then added copper iodide (2.5 mol %, 2.38×10^{-4} mol, 45 mg) and $PdCl_2(PPh_3)_2$ (2.6 mol %, 2.49×10^{-4} mol, 175 mg). The stirring solution was heated at 60 °C for 16 h before the mixture was poured onto $HCl_{(aq)}$ (0.1 N, 10 mL). The aqueous phase was extracted with diethylether (3 × 20 mL), the combined organics were washed with water (2 × 10 mL), sat. aqueous sodium bicarbonate (10 mL) and again with water (10 mL). The combined aqueous layers were extracted with diethylether (20 mL) which was added to the other organics, dried over $MgSO_4$, filtered and concentrated before being purified by column chromatography (100 % pentane, Rf = 0.4) to give a clear oil (48 %, >99 % ^2H, 4.6×10^{-3} mol, 824 mg) **^{1}H NMR** (300 MHz, $CDCl_3$): $\delta = 0.26$ (s, 9H); **^{13}C{^{1}H} NMR** (126 MHz, $CDCl_3$): $\delta = 131.54$ (t $^1J_{C-D} = 24.45$ Hz, 2C), 127.94 (t $^1J_{C-D} = 25.43$ Hz, 1C), 127.66 (t $^1J_{C-D} = 24.45$ Hz, 2C), 122.91 (s), 105.07 (s), 94.09 (s), 0.01 (s).

Data are in accordance with that previously reported [32].

[$^2H_5$]-Phenylacetylene ([$^2H_5$]-**41**)[33]

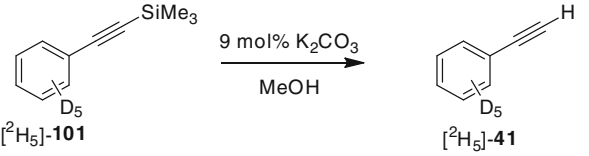

Anhydrous methanol was distilled from calcium hydride onto 4 Å molecular sieves prior to use.

[$^2H_5$]–TMS-phenylacetylene ([$^2H_4$]-**101**) (1 equiv., 3.9×10^{-3} mol, 700 mg) was added to a mixture of dry MeOH (11.7 mL) and potassium carbonate (9 mol %, 0.35×10^{-3} mol, 48 mg) and stirred at room temperature for three hours under an atmosphere of dry N_2. The volatiles were removed under reduced pressure before being immediately purified by Kügelrohr distillation to give a clear and colourless oil (15 %, 99 % [$^2H_5$], 5.7×10^{-4} mol, 61 mg). **^{1}H NMR** (300 MHz, $CDCl_3$): $\delta = 3.07$ (s); **^{13}C{^{1}H} NMR** (76 MHz, $CDCl_3$): $\delta = 131.70$ (t $^1J_{C-D} = 24.91$ Hz, 2C), 128.25 (t $^1J_{C-D} = 23.65$ Hz, 2C), 127.77 (t $^1J_{C-D} = 24.23$ Hz, 2C), 121.87 (s), 83.85 (s), 77.11 (s).

Data are in accordance with that previously reported [32].

Cross-coupling competition [34]

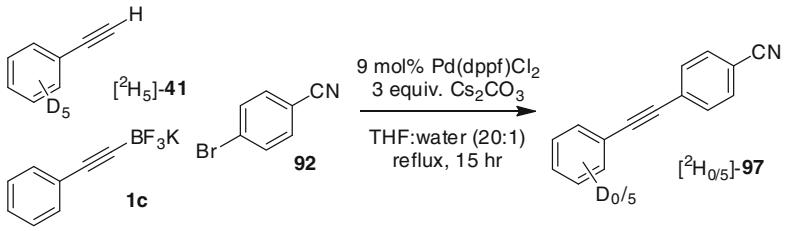

To an oven-dried Schlenk tube was added potassium phenylethynyltrifluoroborate (**1c**) (1 equiv., 2.5×10^{-4} mol, 52 mg), 4-bromobenzonitrile (**92**) (1 equiv., 2.5×10^{-4} mol, 45.5 mg), Pd(dppf)Cl_2 (9 mol %, 2.25×10^{-5} mol, 18.0 mg) and cesium carbonate (3 equiv., 7.5×10^{-4} mol, 244 mg). The vessel was purged with N_2 before a degassed solution of THF:water (20:1, 2.625 mL) and [$^2H_5$]-phenylacetylene ([$^2H_5$]-**41**) (1 equiv., 2.5×10^{-4} mol, 26.8 mg) were added simultaneously with stirring. The septum was replaced with a condenser over a flow of dry N_2 and the reaction mixture was refluxed at 75 °C for 15 h. The reaction mixture was then poured onto water (8 mL) and then extracted with diethylether (4 × 10 mL). The organics were combined, washed with $HCl_{(aq)}$ (1 N, 6 mL), water (2 × 10 mL) and lastly brine (10 mL) before being dried over Mg_2SO_4, filtered and concentrated. The crude material was purified by column chromatography (10 % EtOAc in Hexanes, Rf = 0.27) to give a white solid (55 %, 2.16×10^{-4} mol, 28 mg) **^{1}H NMR** (300 MHz, $CDCl_3$): $\delta = 7.64$ (m, 4H), 7.55 (m, 1.7H), 7.39 (m, 2.2H); **MS (EI)** *m/z* (%): 201.1 (18), 202.1 (18), 203.1 (100), 204.1 (32), 205.1 (8), 206.2 (4), 207.2 (7), 208.2 (58), 209.2 (22).

^{1}H NMR shifts are in accordance with that expected based on data published for the unlabelled compound [35].

6.4.6 Prediction of Hydrolysis Rates

6.4.6.1 DFT

The geometries of thirty-two difluoroborane (**11**) structures were optimised by DFT (6-31 + G(d), B3LYP), Tables 6.19 and 6.20.

Table 6.19 Geometry optimisation of the difluoroboranes (**11**)

Entry	Substrate	*r*(C–B)/pm	Δ*r*(C–B)/pm
1	3-pyridyl	154.449	2.749
2	4-pyridyl	156.559	4.859
3	2-pyrimidyl	157.340	5.640
4	4-pyrimidyl	156.843	5.143
5	5-pyrimidyl	154.743	3.043
6	3-pyridazyl	156.257	4.557
7	pyrrole	151.542	−0.158
8	2-pyridyl	155.773	4.073
9	2-thienyl	152.641	0.941
10	ethyl	156.229	4.529
11	$CH_2CH_2C_6H_4$	156.288	4.588
12	cyclopentyl	155.963	4.263
13	$C(CF_3)_3$	163.019	11.319
14	3-BrC_6H_4	154.653	2.953
15	4-BrC_6H_4	154.353	2.653
16	3-ClC_6H_4	154.596	2.896

(continued)

Table 6.19 (continued)

Entry	Substrate	r(C–B)/pm	Δr(C–B)/pm
17	4-ClC_6H_4	154.284	2.584
18	3-FC_6H_4	154.567	2.867
19	3-IC_6H_4[a]	154.432	2.732
20	4-$NO_2C_6H_4$	156.523	4.823
21	4-EtC_6H_4	153.873	2.173
22	4-IC_6H_4 [a]	154.218	2.518
23	C_6Cl_5	157.686	5.986
24	3-acetylC_6H_4	154.562	2.862
25	4-$CH_2OHC_6H_4$	154.226	2.526
26	4-CNC_6H_4	154.988	3.288
27	4-acetylC_6H_4	154.757	3.057
28	C_6F_5	155.755	4.055
29	mesityl	154.586	2.886
30	CC	151.700	0.000
31	$CCCF_3$	152.881	1.181
32	$CCCH_3$	150.656	−1.044

[a] DGDZVP basis set used

Table 6.20 Geometry optimisation of the difluoroboranes (**11**)

Entry	Substrate	r(B–F)$_1$/pm	r(B–F)$_2$/pm	r(B–F)$_{av}$/pm[a]	Δr(B–F)/pm
1	3-pyridyl	133.665	133.710	133.688	1.475
2	4-pyridyl	133.210	133.211	133.211	0.997
3	2-pyrimidyl	132.887	132.896	132.892	0.678
4	4-pyrimidyl[b]	133.247	132.634	*132.941*	0.727
5	5-pyrimidyl[c]	133.363	133.378	133.371	1.158
6	3-pyridazyl[b]	133.429	132.701	*133.065*	0.852
7	pyrrole[b]	*134.609*	134.181	134.395	2.396
8	2-pyridyl[b]	133.109	133.771	*133.440*	1.227
9	2-thienyl[c]	134.040	133.971	134.006	1.793
10	ethyl	134.029	134.028	134.029	1.815
11	$CH_2CH_2C_6H_4$	133.811	133.959	133.885	1.672
12	cyclopentyl	134.158	134.095	134.127	1.913
13	$C(CF_3)_3$	131.546	131.494	131.520	−0.693
14	3-BrC_6H_4	133.749	133.731	133.740	1.527
15	4-BrC_6H_4	133.847	133.841	133.844	1.631
16	3-ClC_6H_4	133.743	133.724	133.734	1.520
17	4-ClC_6H_4	133.850	133.856	133.853	1.640
18	3-FC_6H_4	133.745	133.744	133.745	1.532
19	3-IC_6H_4[d]	133.970	133.951	133.961	1.747
20	4-$NO_2C_6H_4$	133.248	133.248	133.248	1.035
21	4-EtC_6H_4	134.109	134.109	134.109	1.896
22	4-IC_6H_4 [d]	134.035	134.035	134.035	1.822
23	C_6Cl_5	132.716	132.717	132.717	0.503
24	3-acetylC_6H_4[b]	133.708	133.817	*133.763*	1.550

(continued)

Table 6.20 (continued)

Entry	Substrate	$r(B–F)_1$/pm	$r(B–F)_2$/pm	$r(B–F)_{av}$/pm[a]	$\Delta r(B–F)$/pm
25	4-$CH_2OHC_6H_4$	133.960	133.953	133.957	1.743
26	4-CNC_6H_4	133.565	133.565	133.565	1.352
27	4-acetylC_6H_4	133.696	133.735	133.716	1.503
28	C_6F_5[c]	132.889	132.889	132.889	0.676
29	mesityl[c]	134.321	134.318	134.320	2.107
30	CC	133.136	133.136	133.136	0.923
31	$CCCF_3$	132.476	132.476	132.476	0.263
32	$CCCH_3$	133.638	133.637	133.638	1.424

[a] This value used for normalisation of all "normal" substrates
[b] "Asymmetric" substrate; value in italics used for normalisation
[c] "Unusual" substrate
[d] DGDZVP basis set used

Table 6.21 σ_m and σ_p for substrates where available, and calculated $\Re_{MOD}$ and $\Re_{SL}$

Substrate		σ_m	σ_p	$\Re_{MOD}$	$\Re_{SL}$
4-Fluorophenyl	**1a**	0.12	0.06	−0.11	−0.09
2-Furanyl	**1ar**	0.06	0.02	−0.08	−0.07
Vinyl	**1 k**	0.06	−0.04	−0.17	−0.16
Cyclopropyl	**1x**	−0.07	−0.21	−0.23	−0.23
Alkynyl	**1c**	0.14	0.16	0.01	0.02
Cyclobutyl	**1y**	−0.05	−0.14	−0.16	−0.16
Isopropyl	**1at**	−0.04	−0.15	−0.19	−0.19
Benzyl	**1au**	−0.079	−0.106	−0.08	−0.08
1,3-Diphenylpropyl	**1av**				
Cyclohexyl	**1w**	−0.05	−0.15	−0.18	−0.17
Phenylethenyl	**1 l**	0.03	−0.07	−0.17	−0.16
4-Methoxyphenyl	**1o**	0.05	−0.08	−0.21	−0.20
4-Methylphenyl	**1z**	0.06	−0.03	−0.15	−0.14
Phenyl	**1d**	0.06	−0.01	−0.12	−0.12
1-Naphthyl	**1p**				
2-Naphthyl	**1aw**				
4-CF_3phenyl	**1ax**				
3-Nitrophenyl	**1aa**	0.21	0.2	−0.03	−0.01
3,5 bisCF_3phenyl	**1q**				

Table 6.22 Charton modification of $\Re_{SL}$ to improve fit to rate data

Substrate		Charton v	$\Re_{SL} - 0.09\ v$
Cyclopropyl	**1x**	1.06	−0.33
Cyclobutyl	**1y**	0.51	−0.21
Isopropyl	**1at**	0.76	−0.25
Benzyl	**1au**	0.70	−0.14
Phenyl	**1d**	0.57	−0.17
Cyclopentyl		0.72	−0.23
Cyclohexyl	**1w**	0.87	−0.25

Table 6.23 σ_m and σ_p for substrates where available, and calculated $\Re_{MOD}$ and $\Re_{SL}$

Entry	Substrate	σ_m	σ_p	$\Re_{MOD}$	$\Re_{SL}$
1	3-pyridyl	0.23	0.25	0.01	0.03
2	4-pyridyl	0.27	0.44	0.23	0.24
3	2-pyrimidyl	0.23	0.53	0.40	0.41
4	4-pyrimidyl	0.30	0.63	0.45	0.46
5	5-pyrimidyl	0.28	0.39	0.14	0.16
6	3-pyridazyl	0.28	0.48	0.27	0.29
7	Pyrrole	0.47	0.37	−0.13	−0.09
8	2-pyridyl	0.33	0.17	−0.23	−0.19
9	2-thienyl	0.09	0.05	−0.08	−0.07
10	Ethyl	−0.07	−0.15	−0.15	−0.15
11	$CH_2CH_2C_6H_4$	−0.07	−0.12	−0.11	−0.11
12	Cyclopentyl	−0.05	−0.14	−0.16	−0.16
13	$C(CF_3)_3$	0.55	0.55	0.02	0.06
14	3-BrC_6H_4	0.09	0.08	−0.04	−0.03
15	4-BrC_6H_4	0.15	0.12	−0.06	−0.05
16	3-ClC_6H_4	0.15	0.10	−0.09	−0.07
17	4-ClC_6H_4	0.15	0.12	−0.06	−0.05
18	3-FC_6H_4	0.15	0.10	−0.09	−0.07
19	3-IC_6H_4	0.13	0.06	−0.12	−0.10
20	4-$NO_2C_6H_4$	0.25	0.26	0.00	0.02
21	4-EtC_6H_4	0.07	−0.02	−0.15	−0.14
22	4-IC_6H_4	0.14	0.10	−0.08	−0.06
23	C_6Cl_5	0.25	0.24	−0.03	0.00
24	3-acetylC_6H_4				
25	4-$CH_2OHC_6H_4$				
26	4-CNC_6H_4				
27	4-acetylC_6H_4				
28	C_6F_5	0.26	0.27	0.00	0.02
29	Mesityl				
30	CC	0.21	0.23	0.01	0.03
31	$CCCF_3$	0.41	0.51	0.14	0.17
32	$CCCH_3$	0.21	0.03	−0.26	−0.24

6.4.6.2 Swain-Lupton $\Re$ values

Modified Swain-Lupton parameters, $\Re_{MOD}$, which are composed of Hammett values, σ_p and σ_m, were sourced from the literature [36] for all substrates where values existed. $\Re_{MOD}$ is calculated as $\Re_{MOD} = 1.385\ \sigma_p - 1.297\ \sigma_m - 0.033$ by the authors, Hansch, Leo and Taft. However, the original Swain-Lupton parameter, $\Re_{SL,}$ which is calculated as $\Re_{SL} = 1.355\sigma_p - 1.19\ \sigma_m - 0.03$, was found to correlate better with experimentally determined rate data. (Tables 6.21 and 6.23)

Charton steric parameters (ν) were sourced from the literature [37, 38] for all substrates where values existed (Table 6.22).

References

1. R.A. Oliveira, R.O. Silva, G.A. Molander, P.H. Menezes, Magn. Reson. Chem. **47**, 873–878 (2009)
2. G.A. Molander, M.R. Rivero, Org. Lett. **4**, 107–109 (2002)
3. G.A. Molander, B. Biolatto, Org. Lett. **4**, 1867–1870 (2002)
4. E.F. Santos-Filho, J.C. Sousa, N.M.M. Bezerra, P.H. Menezes, R.A. Oliveira, Tetrahedron Lett. **52**, 5288–5291 (2011)
5. G.A. Molander, S.L.J. Trice, S.D. Dreher, J. Am. Chem. Soc. **132**, 17701–17703 (2010)
6. L. Navarre, S. Darses, J.-P. Genet, Eur. J. Org. Chem. 2004, 69–73 (2004)
7. G.A. Molander, D.E. Petrillo, J. Am. Chem. Soc. **128**, 9634–9635 (2006)
8. G.A. Molander, P.E. Gormisky, J. Org. Chem. **73**, 7481–7485 (2008)
9. S.L. Buchwald, T.E. Barder, Org. Lett. **6**, 2649–2652 (2004)
10. G.A. Molander, B. Canturk, L.E. Kennedy, J. Org. Chem. **74**, 973–980 (2009)
11. G.A. Molander, B. Biolatto, J. Org. Chem. **68**, 4302–4314 (2003)
12. D.C. Ebner, J.T. Bagdanoff, E.M. Ferreira, R.M. McFadden, D.D. Caspi, R.M. Trend, B.M. Stoltz, Chem. Eur. J. **15**, 12978–12992 (2009)
13. F. Mo, Y. Jiang, D. Qiu, Y. Zhang, J. Wang, Angew. Chem. Int. Ed. **49**, 1846–1849 (2010)
14. T. Yamamoto, T. Morita, J. Takagi, T. Yamakawa, Org. Lett. **13**, 5766–5769 (2011)
15. J.M. Murphy, C.C. Tzschucke, J.F. Hartwig, Org. Lett. **9**, 757–760 (2007)
16. S.D. Dreher, P.G. Dormer, D.L. Sandrock, G.A. Molander, J. Am. Chem. Soc. **130**, 9257–9259 (2008)
17. J. Lindh, J. Sävmarker, P. Nilsson, P.J.R. Sjöberg, M. Larhed, Chem. Eur. J. **15**, 4630–4636 (2009)
18. G.A. Molander, R. Figueroa, Org. Lett. **8**, 75–78 (2006)
19. J.-P. Genet, S. Darses, G. Michaud, Eur. J. Org. Chem. 1999, 1875–1883 (1999)
20. W.A. Herrmann, A. Salzer, *Synthetic Methods of Organometallic and Inorganic Chemistry* (THIEME, Stuttgart, 1996)
21. M. Wong, X. Zhang, Tetrahedron Lett. **42**, 4087–4089 (2001)
22. I. Colon, D.R. Kelsey, J. Org. Chem. **51**, 2627–2637 (1986)
23. X. Xu, D. Cheng, W. Pei, J. Org. Chem. **71**, 6637–6639 (2006)
24. Á. Proszenyák, B. Ágai, G. Tárkányi, L. Vida, F. Faigl, J. Label Compd, Radiopharm **48**, 421–427 (2005)
25. J. Bromilow, R.T.C. Brownlee, D.J. Craik, M. Sadek, R.W. Taft, J. Org. Chem. **45**, 2429–2438 (1980)
26. W. Li, D.P. Nelson, M.S. Jensen, R.S. Hoerrner, D. Cai, R.D. Larsen, P.J. Reider, J. Org. Chem. **67**, 5394–5397 (2002)
27. G.A. Molander, L.N. Cavalcanti, B. Canturk, P.-S. Pan, L.E. Kennedy, J. Org. Chem. **74**, 7364–7369 (2009)
28. T. Hayashi, M. Konishi, Y. Kobori, M. Kumada, T. Higuchi, K. Hirotsu, J. Am. Chem. Soc. **106**, 158–163 (1984)
29. T.E. Cole, R. Quintanilla, S. Rodewald, Synth. React. Inorg. Met.-Org. Chem. **20**, 55–63 (1990)
30. I.J. Bruno, J.C. Cole, P.R. Edgington, M. Kessler, C.F. Macrae, P. McCabe, J. Pearson, R. Taylor, Acta Cryst. **B58**, 389–397 (2002)
31. H. Teng, L. Lou, K. Koike, Y. Koike, Y. Okamoto, Polymer **52**, 949–953 (2011)
32. T.K. Dougherty, K.S.Y. Lau, F.L. Hedberg, J. Org. Chem. **48**, 5273–5280 (1983)
33. Y. Wang, B. Huang, S. Sheng, M. Cai, J. Chem. Res. 2007, 728–732 (2007)
34. G.A. Molander, B.W. Katona, F. Machrouhi, J. Org. Chem. **67**, 8416–8423 (2002)
35. X.-F. Wu, H. Neumann, M. Beller, Chem. Commun. **47**, 7959–7961 (2011)
36. C. Hansch, A. Leo, R.W. Taft, Chem. Rev. **91**, 165–195 (1991)
37. M. Charton, J. Org. Chem. **41**, 2217–2220 (1976)
38. M. Charton, J. Am. Chem. Soc. **97**, 1552–1556 (1975)